Leibniz-Institut
für Festkörper- und
Werkstoffforschung
Dresden

Annual Report 2009

Contents

Flashback to 2009

The Annual Report 2009 of the IFW presents a typical cross section of our scientific activities in the past year, highlighting main results in the first part and giving a somewhat more systematic overview of results obtained in our five Research Areas in its second part. It finally informs on the materialized and personalized output and activities, and on how the IFW is organized. The very first pages of the Annual Report we want to use for a flashback to the institutes life in 2009: highlights, events and important developments beyond scientific results.

The IFW Winter School takes place every year in January to foster the scientific communication among all IFW groups and to train young scientists in special topics of IFW's Research Program. In 2009 the topical focus was put on low dimensions – a topic broad enough to gather a large number of scientists that could contribute with talks and discussions. The program of the four-day event included tutorial lectures of experts and short contributions of senior and young scientists as well as some time for skiing and social gathering. All participants agreed that the IFW Winter School is a very useful event to strengthen the internal cooperation and to train the skills of senior and young scientists.

On March 2, 2009, the IFW invited its partners, friends and sponsors to the Annual Reception. On this occasion Dr. Kathrin Doerr was awarded the IFW Research Prize for her excellent work on ferroic materials. The Deutsche Bank Junior Award was given to Dr. Jayanta Das for his outstanding PhD thesis on metallic glasses. A further highlight of this evening was the decoration of the Leibniz President Prof. Dr. Ernst Th. Rietschel with the Leibniz Medal of the IFW Dresden.

In March 2009 Dresden hosted the worldwide second largest physicists' meeting: The third time after 2003 and 2006 the Spring Meeting of the Condensed Matter Division of the German Physical Society was held in Dresden. The enthusiasm of the organizing team around Prof. Dr. Ludwig Schultz made it a big success with a record participation of more than 5300 scientists. Prior to the conference a week-long satellite event "Physics in the shopping Mall" brought physics to the public, in particular to children and young people. The overwhelming success of this event was based on the fascinating spirit of young scientists presenting physics in an every day environment both with competence and enthusiasm.

Prof. Dr. Ludwig Schultz und Dr. h. c. Rolf Pfrengle try the new model to demonstrate superconducting levitation for the Hannover Fair 2009

Prof. Dr. Jürgen Eckert (second from left in the front row) is among the winners of the prestigious Leibniz Prize 2009

Dr. Kathrin Dörr is awarded the IFW Research Award during the Annual Reception 2009




Further large conferences organized in 2009 by the IFW were the 9th European Conference on Applied Superconductivity (EUCAS) in September, the meeting of single crystal growers in March and the Workshop Spin Caloritronics in May. Furthermore we hosted two Kick-off-meetings of networks coordinated by the IFW: the Kick-Off Meeting of the EU network DIVERSITY in January and the Kick-off meeting of the Priority Program of the German Research Foundation on high temperature superconductivity in Fe Pnictides in July. The IFW is quite active in getting conferences to Dresden and organizing them. A full list of conferences organized by the IFW in 2009 is given on page 110. All these conferences demonstrate that Dresden has developed to an attractive place for the scientific community. The IFW as one of the key players in this regional network of university and non-university research institutes takes much effort to improve further the collaboration between Dresden institutes to have a good starting position for the next call in the German excellence initiative.

Prof. Dr. Helmut Eschrig, the founding director of the IFW and Scientific Director from 1998 to 2008 retired at the end of September 2009 and handed over the position of the Director of the Institute for Theoretical Solid State Physics to Prof. Dr. Jeroen van den Brink. The Institute for Theoretical Solid State Physics is the smallest in the concert of five IFW's institutes and was founded 2004 out of the theory group. It has its core competence in density functional theory and cooperates closely with experimentally working groups inside and outside the IFW. With Jeroen van den Brink the IFW could win an internationally recognised expert in the field of theory of correlated systems. His previous work on molecular crystals, multiferroics and superconductivity provides lots of opportunities for cooperation not only within the IFW but also with the university and other institutes in Dresden. A further bargain for the Institute for Theoretical Solid State Physics and for the IFW as a whole was the grant of an Emmy Noether Research Group on the simulation of spin-orbital systems from 2010 on to Dr. Maria Daghofer.

The training of students and young scientists is a very important concern of IFW's work. PhD and diploma students are involved in nearly all scientific projects and in the resulting publications. The number of PhD students working at the Institute has been increased in the last two years to about 150 on average. Also the number of diploma and master students doing their theses at the IFW has increased significantly during the last years resulting in the record number of 23 diploma or master theses in 2009.

In August 2009 we welcomed seven new apprentices

These young men finished their vocational training at IFW

The Dresden Long Night of Sciences attracted many curious people to the IFW's laboratories




The large efforts for project funding produced a good crop of fruit in 2009. The level of third party funding has significantly increased in 2009 to more than 16 Mio. Euro - twice as high as the target level and due to a special situation in funding and economic programs not being typical for the future. Nevertheless a large amount of that funding was acquired in competitive mode from the DFG and the EU. In particular the grant of a second Emmy Noether Research Group by the DFG and the new DFG Priority Program on Fe-pnictides which starts in 2010 coordinated by the IFW are a nice success. As in the years before the IFW is very successful in initiating EU projects and participating in them. Five of the 24 running EU-projects in 2010 in the IFW are coordinated by the IFW. Concerning the "Pakt für Forschung" the IFW was successful with all five applications for projects so far starting in 2006 and continuing in 2007, 2008, 2009 and 2010. There are very few institutes in the Leibniz Association equally successful.

Due to the increasing project funding and to the increasing number of PhD, master and diploma students the overall number of persons working in the IFW has grown to more than 600. The resulting severe shortage of office space is met – apart from improvising and moving closer - by plans for an annex building which has made further progress in 2009. We are looking forward to the start of construction and the appearance of the first excavators in 2010. Two other infrastructural projects came to a successful completion in 2009: The installation of a Helium liquefaction facility that makes the supply of liquid Helium independent from external influences (see pages 48-49) and the establishment of the IFW's Chemnitz research site. The latter is going to strengthen the cooperation with the Chemnitz University of Technology where Prof. Dr. Oliver G. Schmidt holds a chair. The IFW rented 260 square meter laboratory area in a start-up building within the "Smart System Campus" and equipped it for the development of 3D rolled-up nanomembranes.

2009 was again a yielding year with respect to prizes and honours awarded to members of the IFW. A complete list is included at the end of this Report. The most prestigious of the prizes won in 2009 by IFW members is the Gottfried-Wilhelm-Leibniz-Prize of the German Research Foundation, which has been awarded to Prof. Dr. Jürgen Eckert. The Federation of European Materials Societies (FEMS) awarded the FEMS Materials Gold Medal 2009 to Prof. Dr. Ludwig Schultz in recognition of his merits in materials science. The Technical University of Bratislava acknowledged the efforts of the IFW Dresden for close cooperation with an honorary doctorate for our Administrative Director, Dr. h. c. Rolf Pfrengle.

Women high school students try the work in a chemical lab during the Autumn School "Theoria cum Praxi"

The event "Physics in the shopping Mall" brought physics to the public, in particular to children and young people

Participants of the Kick-off meeting of the EU-project DIVERSITY in January 2009

Our team at IFW's Chemnitz research site headed by Prof. Dr. Oliver Schmidt (forth from right) who held a Chair at TU Chemnitz




A crucial part of the IFW's identity is its vivid life including the cultivation of the scientific dialogue, family-friendly working conditions and the support of sportive, creative and cultural activities. The IFW organizes a series of workshops, colloquia and talks to foster the scientific dialogue and, along the way, allow for social and communication aspects of cooperation. An important meeting for all scientists of the IFW is the yearly two-day program session where all scientists discuss and adjust the research program for the following year.

In 2009 the IFW continued its large efforts to make scientific work accessible for the general public and to inspire young people to study science or engineering. The IFW took part in many joint actions as the Summer University of the TU Dresden and the lecture series "Physics on Saturday". The IFW is one of the initiators of the Dresden Long Night on Sciences which took place for the seventh time in 2009. The greatest attraction in the IFW's program seemed to be the special offers for kids to try experiments themselves and to play with the superconducting train. Besides these big events we almost weekly organize lab-tours for various visitor groups, from school classes through official representatives to guests from foreign organizations.

So we are looking back to a successful year 2009 in the Institute's development. We are quite aware that this is due to the sustainable network of colleagues and partners in universities, research institutes and industry, both on the regional and the international scale. We thank all of them for constructive cooperation and are looking forward to taking up future challenges together. Special tribute is paid to the members of the Scientific Advisory Board and of the Board of Trustees as well as the funding organizations that continuously support and foster the positive development of the IFW.

Dresden, January 2010

Prof. Ludwig Schultz
Scientific Director

Dr. h. c. Rolf Pfrengle
Administrative Director

Prof. Dr. Ludwig Schultz is awarded the FEMS Gold Medal 2009

The TU Bratislava awarded Rolf Pfrengle an honorary doctorate

Dr. Christian Kramberger (second from right) is awarded the Prize of the "Dresdner Gesprächskreis der Wirtschaft und Wissenschaft e.V." for his excellent PhD Thesis

Part of the new Helium liquefaction facility completed in 2009

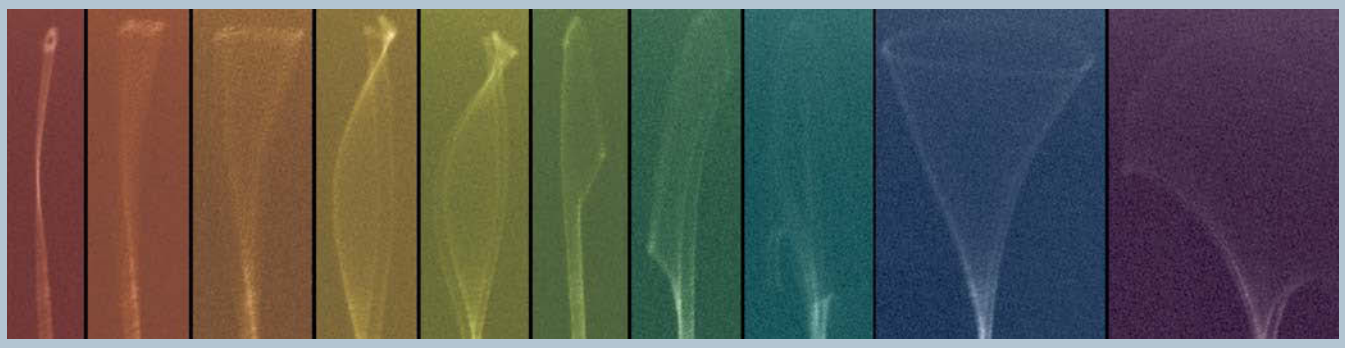

Highlights 2009

The picture “Nano-Dancer” by Franziska Wolny and Uhland Weissker was awarded the 1. Prize of the Nano&Arts Competition 2009. It shows induced vibrations of a Carbon nanotube in various stages.

Highlights

Electrons in cuprates: view by ARPES

A. A. Kordyuk, V. B. Zabolotnyy, D. V. Evtushinsky, S. V. Borisenko, B. Büchner

Angle resolved photoemission spectroscopy (ARPES) has been playing a crucial role in understanding of physics behind high temperature superconductivity. Our ARPES investigation of superconducting cuprates, performed over a decade and accomplished by very recent results [1, 2], suggests a consistent view of electronic interactions in cuprates which provides natural explanation of both the origin of the pseudogap state and the mechanism for high temperature superconductivity. Within this scenario, the spin-fluctuations play a decisive role in formation of the fermionic excitation spectrum in the normal state and are sufficient to explain the high transition temperatures to the superconducting state [1] while the pseudogap phenomenon is a consequence of a Peierls-type intrinsic instability of electronic system to formation of an incommensurate density wave [2]. In view of these results and their projection to numerous other materials [3-8], two general questions are arising: is the normal state in 2D metals ever stable and how does this intrinsic instability interplay with superconductivity?

For many years now, the search for the mechanism of high temperature superconductivity has been mostly reduced to a simple dilemma: phonons vs. spin-fluctuations [9]. Our commitment to the "spin-fluctuations camp" had started with the observation of strong doping dependence of the renormalization of the fermionic spectrum of Bi-2212 in the antinodal region of the Brillouin zone, known as a peak-dip-hump lineshape [10]. Such a dependence, the vanishing with overdoping and strong increase with underdoping, had suggested its magnetic origin due to "proximity to antiferromagnet" but had been difficult to reconcile with phonons. Later, the careful self-energy analysis of the nodal direction [11, 12] had revealed the same strong trend with doping. This, together with the other peculiarities of the fermionic spectrum [13, 14], forced us to conclude that the spin-fluctuations provide the main contribution to the scattering of the electrons and are, therefore, the main candidate for the superconducting pairing.

However, despite similar results of other groups, the spin-fluctuations scenario had not became generally accepted. On one hand, there were some open questions left. Among the most important was the 'kink puzzle', namely, why the nodal and antinodal renormalizations exhibit essentially different temperature dependence: the latter disappears just above T_c while the former, the 'kink', persists at much higher temperatures? On the other hand, the newly developed models for the electron-phonon coupling in HTSC [15] had a potential to adopt any particular property of the fermionic spectrum observed in experiment. This had called forth the necessity of a detailed comparison of the entire fermionic and bosonic excitation spectra measured for the same sample and search for distinctive fingerprints of one in another.

Since we have managed to disentangle the surface and bulk fermionic spectra in YBCO [16], a suitable material for inelastic neutron scattering (INS) experiments, we have been able to analyse the charge- and spin-excitation spectra determined by ARPES and INS, respectively, on the same crystals of $YBa_2Cu_3O_{6.6}$ [1]. In simple, these spectra are related by the Dyson equation: $G^{-1} = G_0^{-1} + U^2\chi \star G$, where $G_0(\mathbf{k}, \omega)$ and $G(\mathbf{k}, \omega)$ are the bare and renormalized fermionic Green's functions, respectively (the fermionic or charge-excitation spectrum is represented by the spectral function $A = \mathrm{Im}G$), $\chi(\mathbf{Q}, \Omega)$ is the spin susceptibility (the spin-excitation spectrum measured by INS is $\mathrm{Im}\chi$), U is the spin-fermion coupling constant, and the "correlation" $U^2\chi \star G$ gives the fermionic self-energy. The detailed description of the "correlation" procedure can be found in Ref. 1. Fig. 1a shows the Fermi surface, the Fermi level cut of the fermionic spectrum modelled based on ARPES data. Fig. 1b shows the intensity of spin excitations along $Q = q(2\pi,2\pi)$

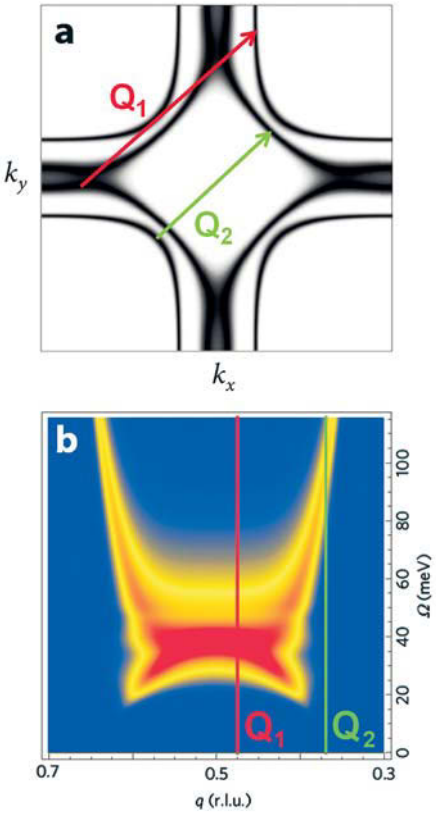

Fig. 1: The Fermi surface of YBCO in the 1st BZ derived from ARPES data [18] represents the fermionic Green's function (a). The intensity of spin excitations along $Q = q(2\pi,2\pi)$ resulting from numerical fits to the INS spectra measured by V. Hinkov and B. Keimer (MPI, Stuttgart) [1] (b).

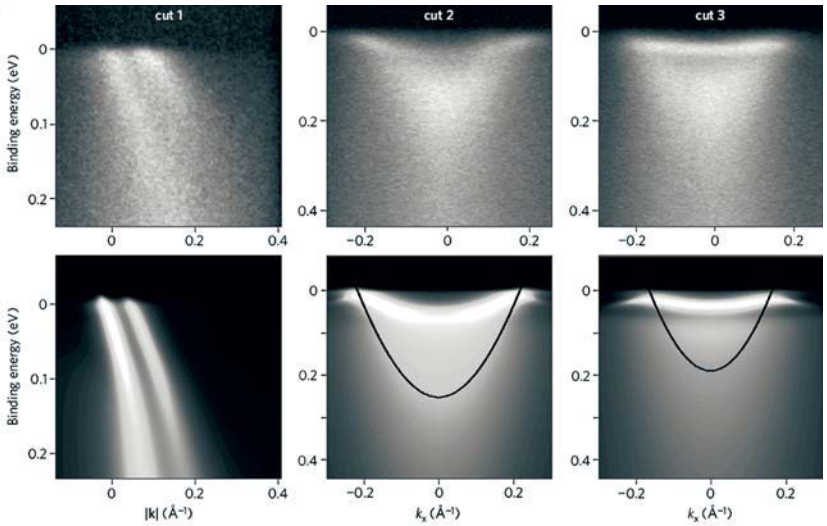

Fig. 2: Comparison of experimental (upper row) and theoretical (lower row) fermionic spectra (see Ref. 1 for details), by T. Dahm (University of Tübingen).

that represents Im$\chi(\mathbf{Q}, \Omega)$ and is derived from numerical fits to the INS spectra [1]. As we have found, a self-consistent description of both spectra can be obtained by adjusting a single parameter, U.

The comparison between the spectral functions, calculated in this way by T. Dahm and measured experimentally is presented in Fig. 2. The overall similarity demonstrates clearly that the spin fluctuations can explain all the peculiarities of the electronic scattering in cuprates. In particular, they provide natural explanation of different temperature dependence of the nodal and antinodal renormalizations. As illustrated in Fig. 1, the nodal 'kink' in fermionic dispersion is a result of the interband scattering on the spin-fluctuations from the upper, universal, weakly temperature-dependent branch of the spectrum (Q_1 vector), while the scattering between the antinodal regions (Q_2 vector) is determined by the middle of the spin-fluctuation spectrum where a large peak, known as a 'resonance mode' [9], appears just below T_c.

The determined value of the spin-fermion coupling constant, U = 1.59 eV, gives an estimate of T_c which exceeds 150 K [1]. This demonstrates that spin fluctuations have sufficient strength to mediate high-temperature superconductivity.

The actual T_c can be reduced by a variety of effects. Two of them, the phase fluctuations of the order parameter and competition with other types of order make a link to the pseudogap phenomenon, not considered in this analysis. In Ref. 2 we have shown that the electronic density ordering is the most probable origin of the pseudogap in cuprates.

Performing careful temperature- and momentum-resolved photoemission experiments [2], we have found that the depletion of the spectral weight in slightly underdoped Bi(Tb)-2212 superconductor, usually called the "pseudogap," exhibits an unexpected nonmonotonic temperature dependence: decreases linearly approaching T^* at which it reveals a sharp transition but does not vanish and starts to increase gradually again at higher temperature.

Fig. 3 illustrates the temperature evolution of the pseudogap presenting a temperature map (panel a) and momentum integrated energy distribution curves (EDCs) measured

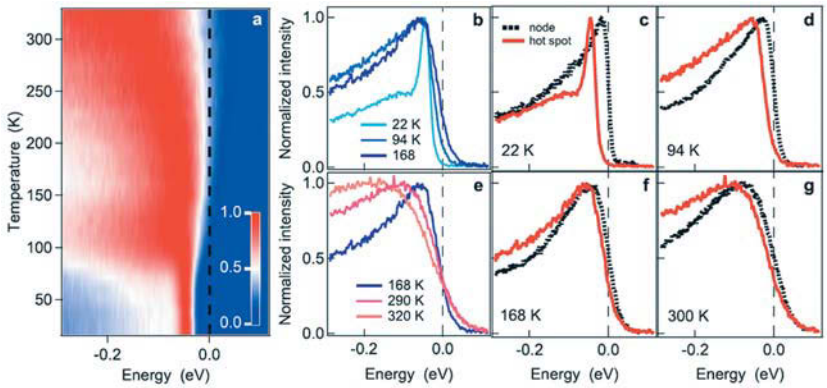

Fig. 3: The temperature map. (a) The temperature map which consists of a number of momentum integrated energy distribution curves (EDCs) measured at different temperatures at a 'hot spot'. Separate EDCs are shown in panels (b-g): as compared to each other (panels b and e) and to the similar EDCs measured each for the same temperature but along the nodal direction (panels c, d, f, g). The gap is seen as a shift of the leading edge midpoint (LEM). In terms of the colorscale of panel a, the LEM corresponds to white color close to the Fermi level [2].

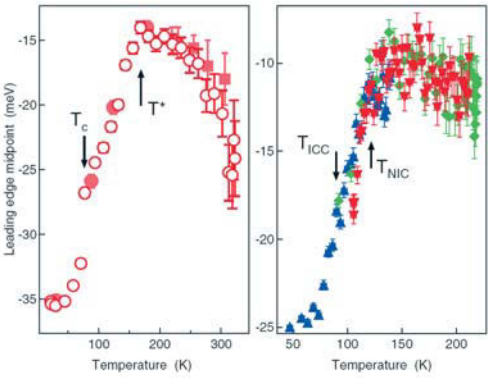

Fig. 4: Non-monotonic gap function. The position of the leading edge midpoint (LEM) of the integrated k_F EDCs (averaged for two Fermi-crossings), as function of temperature for an underdoped Tb-BSCCO (left) [2] with $T_c = 77$ K and $T^* = 170$ K is remarkably similar to the pseudo-gap in a transition-metal dichalcogenide $TaSe_2$ (right) [7] with the transitions to the commensurate and incommensurate CDW phases at $T_{ICC} = 90$ K and $T_{NIC} = 122$ K, respectively.

at different temperatures and compared to each other (panels b and e) as well as to the similar EDCs but measured for each temperature along the nodal direction (panels c, d, f, g). The gap is seen as a shift of the leading edge midpoint (LEM) of a gapped EDC. Since the momentum integrated EDC of the non-gapped spectrum is expected to stay at zero binding energy for any temperature, as it is observed for the nodal EDCs (Fig. 2 c, d, f, g), the finite shift of the LEM is a good empirical measure for a gap of unknown origin. From the temperature map presented in Fig. 2a one can easily see an unusual temperature evolution of the gap (in terms of the colorscale, the LEM corresponds to the white color): first it decreases with increasing temperature up to about 170 K, then it starts to increase again.

The temperature dependence of the LEM is summarized Fig. 4 (left panel) where it is compared to the similar quantity measured for $TaSe_2$ (right panel), for which it is known that the pseudogap results from the incommensurate charge density wave [7]. The observed one-to-one correspondence between the temperature dependences of the pseudogap for Bi-2212 and $TaSe_2$, which is discussed in details in Ref. 2, suggests that density wave ordering also appears in cuprates and, reducing the electron density of states at the Fermi level, competes with superconductivity. While the evidence for such a competition is also reported by other groups [17, 18], the exact nature of the ordering remains unclear. One may assume that the spin-fluctuations, being a dominant mediator for electronic interactions in cuprate, play also the role of the main driving force for the electronic instability resulting in the spin density wave formation. This assumption, however, requires future experimental verification.

We acknowledge discussions with P. Bourges, A. Chubukov, T. Dahm, T. P. Devereaux, I. Eremin, J. Fink, A. M. Gabovich, W. Hanke, V. Hinkov, D. S. Inosov, B. Keimer, T. K. Kim, M. Knupfer, Yu. V. Kopaev, E. E. Krasovskii, I. I. Mazin, E. A. Pashitskii, M. V. Sadovskii, D. J. Scalapino, R. Schuster, A. Semenov, V. N. Strocov, T. Valla, and technical support from R. Hübel.

References

[1] T. Dahm, et al., Nature Physics **5**, 217 (2009).
[2] A. A. Kordyuk, et al., Phys. Rev. B **79**, 020504(R) (2009).
[3] V. B. Zabolotnyy, et al., Nature **457**, 569 (2009).
[4] D. V. Evtushinsky, et al., Phys. Rev. B **79**, 054517 (2009).
[5] V. B. Zabolotnyy, et al., EPL **86**, 47005 (2009).
[6] S. V. Borisenko, et al., Phys. Rev. Lett. **102**, 166402 (2009).
[7] S. V. Borisenko, et al., Phys. Rev. Lett. **100**, 196402 (2008).
[8] D. V. Evtushinsky, et al., Phys. Rev. Lett. **100**, 236402 (2008).
[9] M. Eschrig, Adv. Phys. **55**, 47 (2006).
[10] S. V. Borisenko, et al., Phys. Rev. Lett. **90**, 207001 (2003).
[11] A. A. Kordyuk, et al., Phys. Rev. Lett. **92**, 257006 (2004).
[12] A. A. Kordyuk, et al., Phys. Rev. Lett. **97**, 017002 (2006).
[13] S. V. Borisenko, et al., Phys. Rev. Lett. **96**, 067001 (2006)
[14] S. V. Borisenko, et al., Phys. Rev. Lett. **96**, 117004 (2006).
[15] S. Johnston, et al., arXiv:0909.5489
[16] V. B. Zabolotnyy, et al., Phys. Rev. B **76**, 064519 (2007).
[17] K. Tanaka, et al., Science **314**, 1910 (2006)
[18] T. Kondo, et al., Nature **457**, 296 (2009).

Cooperation Univ. of Tübingen, Max-Planck-Institute for Solid State Research Stuttgart, EPFL Lausanne, BESSY Berlin, Swiss Light Source Villigen, Univ. of California, Univ. of Würzburg

Funded by DFG (Forschergruppe FOR538), BMBF

Nanoscale electronic order and the effect of smart impurities: nuclear magnetic and quadrupole resonance studies of the new iron pnictide superconductors

H.-J. Grafe, G. Lang, F. Hammerath, D. Paar, K. Manthey, S.-L. Drechsler, G. Fuchs, J. Werner, G. Behr, B. Büchner

Nanoscale electronic order in iron pnictides

The strong electronic correlations present in several transition metal oxides give rise to a broad range of exotic electronic states, notably high-temperature superconductivity. Observation of the latter in iron pnictides has ignited strong interest [1], especially as it requires doping a magnetically-ordered parent phase as in cuprate superconductors. This has led to question the interplay or competition between the magnetic ordering and superconductivity ground states, and the possible presence of intrinsic electronic inhomogeneities [2-7]. Therefore, we investigated the charge distribution in $LaO_{1-x}F_xFeAs$ and $SmO_{1-x}F_xFeAs$ using nuclear quadrupole resonance (NQR) measurements [8]. Our study shows the presence of an electronic inhomogeneity in the underdoped region of the phase diagram ($0.04 \le x \le 0.08$), ascribed to a nanoscale electronic order.

NQR takes advantage from the fact that a nucleus with a nuclear spin $I > 1/2$ features an electric quadrupole moment. In the presence of a finite electric field gradient (EFG) at the nuclear site, the degeneracy of the corresponding nuclear energy levels is lifted. Since $I = 1/2$ for iron, the ^{75}As nuclei ($I = 3/2$) were used as NQR probes. Their proximity to the iron layers helps to retain high sensitivity to electronic changes, which may be further helped by their large polarizability [9]. Probing by radiofrequency irradiation yields the quadrupole frequency $\nu_Q \propto V_{zz}(1+\eta^2/3)^{1/2}$, where V_{zz} and η are respectively the highest eigenvalue and the asymmetry of the EFG tensor. As the EFG stems from the surrounding charge distribution, peculiarities of the latter can be inferred from the determination of the histogram of quadrupole frequencies in the sample that is shown on Fig. 1. On doping, the frequency distribution shifts to higher values. In the undoped limit, the single narrow line agrees with a single well-defined charge environment for all As nuclei. The line is broadened in the optimally-doped/overdoped limit (La 10%/15%, Sm 10%), likely reflecting structural disorder of fluorine dopants and moderate fluorine concentration inhomogeneities. While LDA calculations are in agreement with the experimental NQR frequency in the undoped sample, they could not reproduce the shift to higher frequency upon doping [10]. However, in the underdoped region (La 5%/7.5%, Sm 4%/6%/8%), two fairly broad peaks are observed, with further structuring of the high frequency peak for Sm samples.

A direct explanation would be phase separation on a macroscopic or mesoscopic scale, with the difference in peak positions indicating low and high doping regions. Beyond incompatibility with initial X-ray characterization, this can be tested using T_1^{-1} spin-lattice relaxation rate measurements for each spectral peak in the La samples which are shown on Fig. 2. While $(T_1T)^{-1}$ in the undoped material tends to diverge on approaching the magnetic transition, all other peaks show no signature of magnetic ordering. They reflect however a superconducting transition at low temperature as seen from the rapid decrease of the relaxation, with a T_1^{-1} behavior broadly consistent with observed

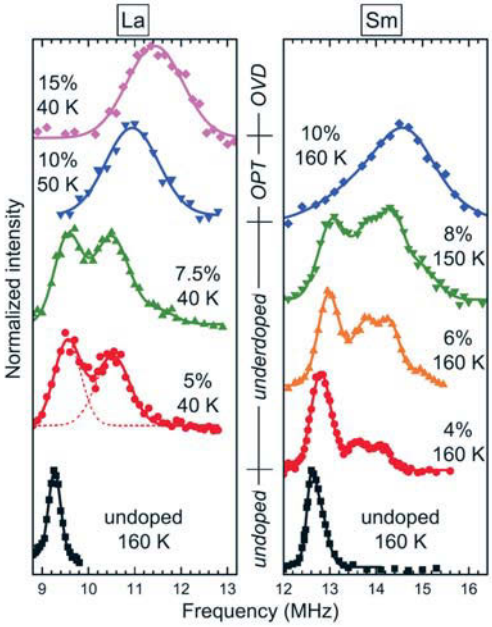

Fig. 1: ^{75}As NQR spectra of $LaFeAsO_{1-x}F_x$ and $SmFeAsO_{1-x}F_x$. "OPT" and "OVD" refer to optimally-doped and overdoped samples. Fits including up to three (La) or four (Sm) Gaussians are shown as full lines, with the two-Gaussian fit for x = 0.05 (La) detailed as an example.

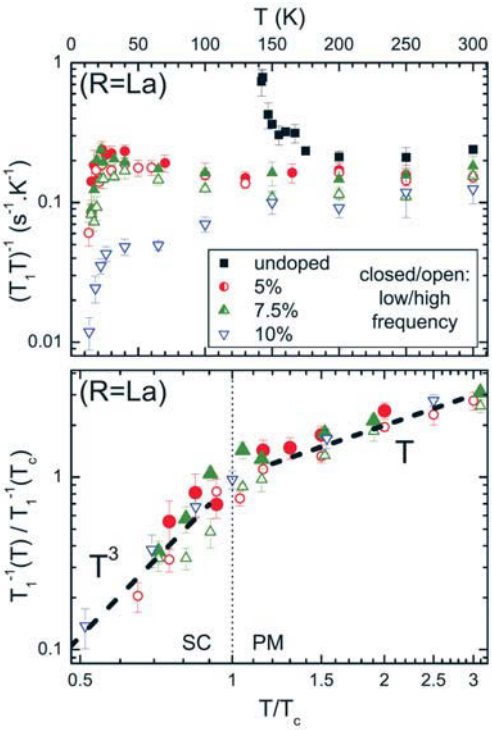

Fig. 2: ^{75}As spin lattice relaxation in $LaFeAsO_{1-x}F_x$. Note that the contribution of the Sm magnetic moments to T_1^{-1} in the Sm samples prohibits a comparison. (Upper panel) Temperature-dependence of $(T_1T)^{-1}$ with T_1^{-1} the spin-lattice relaxation rate as measured on each peak of Fig. 1, with closed/open symbols corresponding to low/high frequencies. The measurements are done at the T-dependent peak frequency (undoped), 9.7 and 10.6 MHz (both 5% and 7.5%), and 11 MHz (10%). (Lower panel) Temperature-dependence of T_1^{-1} at low temperature, with horizontal scaling by T_c (as determined from initial characterization) and vertical scaling to obtain coincidence about T_c.

power laws [11,12]. For the underdoped samples in the paramagnetic state, the two spectral peaks feature similar $(T_1T)^{-1}$ behaviors, very different from the progressive suppression of low-energy excitations observed at optimal doping. If phase separation would occur even on a rather small scale (several nanometers or more), the volume fraction corresponding to each peak would exhibit fluctuations specific to the then necessarily different doping levels. In light of the spectra, the relaxation contrast should then be much larger, with the high-frequency peak relaxation closer to developing a decrease similar to that at optimal doping. Here, the similar weak Curie-Weiss behavior above T_c and the moderate difference in amplitude show a sharing of electronic properties, i.e., coexistence of the two charge environments at the nanoscale.

However, a direct electrostatic effect of the fluorine ions such as the effect of Sr^{2+} on adjacent Cu ions in $La_{2-x}Sr_xCuO_4$ [13] can be excluded here. In this case, each fluorine must influence on average roughly nine As ions to properly account for the weights of the peak. The linear growth of the high frequency weight with doping would then suggest that no sizeable overlap of these patches of nine As ions develops as the doping rises, i.e. fluorine ordering must occur in the underdoped samples for which there is no experimental hint in iron pnictides. Therefore, the inhomogeneity likely arises not from the dopants but from an electronic order in the FeAs layers, due to competing interactions.

The resolved spectral features and their smooth doping dependence indicate a rather well-defined and reproducible topology, static on the slow (microsecond) timescale of NQR. The low and high frequency weights in the spectra would then correspond to low (closer to undoped) and high (closer to optimally-doped) doping situations. Expected to feature larger intrinsic magnetic fluctuations, the low-doping regions would account for the relaxation response of the whole system. Since doping corresponds to changes in the iron 3*d* orbital occupancies, it must however be noted that what appears to be a difference in total occupancy (charge ordering) around As sites may also have an orbital character (orbital ordering). The presence of a local electronic order is reminiscent of the situation observed for instance in cuprates [14] and manganates [15,16], such as stripe or checkerboard order, static or dynamic. This supports the widespread presence of electronic inhomogeneities in correlated systems, even in presence of a homogeneous ground state.

As for the different phase diagrams proposed for the iron pnictides, the electronic inhomogeneity of the underdoped region certainly influences the transition from static magnetism to superconductivity. Starting from high doping, superconductivity is unhindered if not helped by the local order and disappears [2,6,7] only at its low-doping end, where the high proportion of low-doping regions would allow static magnetism to shoot up, before recovering electronic homogeneity close to the undoped limit. At low-doping, the tight link between the structural and magnetic transitions has been argued to reflect orbital ordering [17]. The local order observed here could then suggest that a primary factor in the phase diagram of pnictides is realspace competition involving orbital physics, where sensitivity to structural details would yield seemingly different phase diagrams. In light of the reported importance of the Fermi surface topology [18], this would represent a significant change of perspective for future studies.

Smart impurities and the symmetry of the order parameter

Another intriguing aspect of the new iron pnictide superconductors is the symmetry of the order parameter and the underlying Cooper-pairing mechanism. The presence or absence of the Hebel-Slichter peak [19] together with the *T*-dependence of the nuclear spin lattice relaxation rate, T_1^{-1}, below T_c are frequently used to discriminate tentatively conventional from unconventional pairing. For a single Fermi surface sheet and superconductivity in the clean limit T^3- and T^5-dependencies would be regarded as evidence for line- and point-node superconducting order parameters, respectively,

which for singlet pairing correspond to the *d*- and a special *s*+*g*-wave state. Recently it has been realized that the situation in multiband superconductors to which the iron pnictides do belong is far from being that simple. In addition, the influence of defects such as impurities and partial chemical substitutions might be crucial for the symmetry of the order parameter and many physical properties in the superconducting state. In this context the experimentally observed non-universal behavior for the growing number of related compounds is challenging. Among various unconventional scenarios the $s_{\pm}$-symmetry proposed [20-22] at the early stages of the iron pnictide research at present is still the most popular one but other cases including conventional s_{++}-symmetry should be considered, too.

In this unclear situation we report ^{75}As NMR measurements of the nuclear spin lattice relaxation rate in $LaFeAsO_{0.9}F_{0.1}$ and As-deficient $LaFeAs_{1-\delta}O_{0.9}F_{0.1}$. [23] Surprisingly we observe a drastic change of the $T_1^{-1}(T)$ dependence below T_c from T^3 for the clean sample $LaFeAsO_{0.9}F_{0.1}$ to T^5 for the disordered $LaFeAs_{1-\delta}O_{0.9}F_{0.1}$ (see Fig. 3). In principle, our observation of an unusual transition from T^3 to T^5 with increasing disorder is not necessarily inconsistent with a $s_{\pm}$-wave superconducting gap though alternative scenarios should be invoked, too. Starting from the clean limit it has been shown [24-26] that within the generalized $s_{\pm}$-wave scenario both node-less and nodal superconducting gaps might occur depending on the proximity of the doped sample to the antiferromagnetic instability. In this regard, naively our finding can be interpreted in favor of a transition from a nodal to a nodeless unconventional superconducting gap upon adding As defects which for some reason should drive the system closer to the antiferromagnetism, in accord with the slightly enhanced normal state T_1^{-1} of the As deficient sample (see Fig. 3).

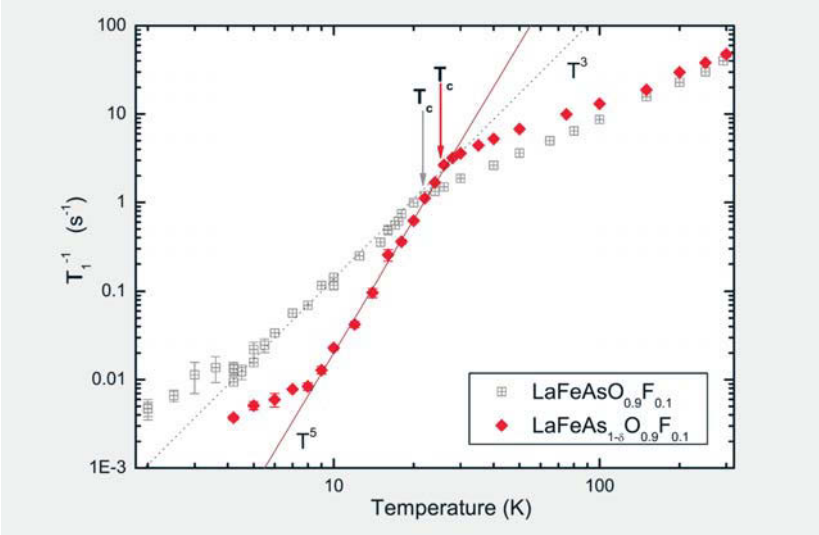

Fig. 3: ^{75}As T_1^{-1} for $LaFeAs_{1-\delta}O_{0.9}F_{0.1}$ (red diamonds) compared to $LaFeAsO_{0.9}F_{0.1}$ (grey crossed squares [12], new data points for $T \leq 4.2$ K). The dotted line illustrates the T^3 behaviour of T_1^{-1} for $LaFeAsO_{0.9}F_{0.1}$, the solid line indicates the T^5 behaviour observed for $LaFeAs_{1-\delta}O_{0.9}F_{0.1}$. The low-$T$ features with a nearly linear slope below $T \sim 0.3\,T_c$ are probably related to vortices.

However, such a simplistic point of view cannot be easily applied to pnictides as it is also known that the $s_{\pm}$-wave ground state is sensitive to non-magnetic impurities. Most importantly, the intraband impurity scattering does not affect the superconductivity, since the superconducting gap does not change its sign within each of the bands. At the same time the scattering with large momenta which connects electron and hole pockets (interband scattering) is pair-weakening and thus yields a decrease of T_c and simultaneously introduces power laws in the thermodynamics and T_1^{-1} at intermediate temperatures. Therefore, if for some reason As vacancies act as 'smart' impurities which change the ratio between the intra- and interband scattering, our observations could be also explained. The above-mentioned scenario is based on the assumption that $s_{\pm}$-wave order is stable and adding As vacancies either changes the proximity to the competing antiferromagnetism or/and the ratio of intra- to interband non-magnetic impurity scattering in pnictides.

There is, however, another intriguing possibility. Let us assume that there is a substantial electron-boson interaction which provides an attractive intraband potential for Cooper-pairing. In this case a (weak) repulsive interband Coulomb scattering will still lead to the $s_{\pm}$- wave superconducting order in the clean limit though the attractive electron-boson interaction dominates. However, once the As vacancies change the ratio between intra- and interband impurity scattering, a transition from $s_{\pm}$-wave to conventional s_{++}-wave superconducting order may be induced. This scenario, however, still needs further experimental clarification.

For example, despite the transition from T^3 to T^5 behavior we do not find any sign of the Hebel-Slichter peak in the latter case close to T_c. Moreover, current experimental data on the importance of the electron-phonon coupling are not very conclusive. Therefore, the intriguing possibility of high-energy charge fluctuations as well as weak electron-phonon interactions with orbital fluctuations [27,28] deserve more detailed studies. Another interesting point would be a detailed comparison with $FeSe_{0.92}$, which exhibits a T^3-law for T_1^{-1} [29] and other Fe-based superconductors with vacancies in the polarisable subsystem. We believe that a future quantitative realistic theoretical description of our data within unconventional $s_{\pm}$- or conventional, but unusual s_{++}-superconductivity scenarios will stimulate the further development of these approaches and this way is finally helpful for the elucidation of the underlying but yet unsettled mechanism.

References

[1] Y. Kamihara *et al.*, J. Am. Chem. Soc. **130**, 3296 (2008).
[2] A. J. Drew *et al.*, Nature Mater., **8**, 310 (2009).
[3] Y. Laplace *et al.*, Phys. Rev. B, **80**, 140501(R) (2009).
[4] J. T. Park *et al.*, Phys. Rev. Lett., **102**, 117006, (2009).
[5] M.-H. Julien *et al.*, Europhys. Lett., **87**, 37001, (2009).
[6] Jun Zhao *et al.*, Nature Mater., **7**, 953, (2008).
[7] H. Luetkens et al., Nature Mater., **8**, 305, (2009).
[8] G. Lang *et al.*, preprint, arxiv 09125495.
[9] M. Berciu *et al.*, Phys. Rev. B, **79**, 214507, (2009).
[10] H.-J. Grafe *et al.*, New J. Phys., **11**, 035002, (2009).
[11] Y. Nakai *et al.*, J. Phys. Soc. Jpn., **77**, 073701, (2008).
[12] H.-J. Grafe *et al.*, Phys. Rev. Lett., **101**, 047003, (2008).
[13] P. M. Singer *et al.*, Phys. Rev. Lett., **88**, 047602, (2002).
[14] J. M. Tranquada *et al.*, Nature, **375**, 561, (1995).
[15] J. van den Brink *et al.*, Phys. Rev. Lett., **83**, 5118, (1999).
[16] F. Weber *et al.*, Nature Mater., **8**, 798, (2009).
[17] K. Kubo and P. Thalmeier. J. Phys. Soc. Jpn., **78**, 083704, (2009).
[18] M. M. Korshunov and I. Eremin. Phys. Rev. B, **78**, 140509(R), (2008).
[19] L. C. Hebel and C. P. Slichter, Phys. Rev. **113**, 1504 (1959).
[20] I.I. Mazin *et al.*, Phys. Rev. Lett. **101**, 057003 (2008).
[21] K. Kuroki *et al.*, Phys. Rev. Lett. **101**, 087004 (2008).
[22] A.V. Chubukov, D.V. Efremov, and I. Eremin, Phys. Rev. B **78**, 134512 (2008).
[23] F. Hammerath et al., preprint, arXiv:0912.3682.
[24] K. Kuroki *et al.*, Phys. Rev. B **79**, 224511 (2009).
[25] T.A. Maier *et al.*, Phys. Rev. B **79**, 224510 (2009).
[26] A.V. Chubukov *et al.*, Phys. Rev. B **80**, 140515(R) (2009).
[27] H. Kontani and S. Onari, arXiv:0912.1975.
[28] Y. Yanagi, Y. Yamakawa and Y. Ono, arXiv:0912.2392v2.
[29] H. Kotegawa *et al.*, J. Phys. Soc. Jpn. **77**, 113703 (2008).

Cooperation Max-Planck-Institut für Physik komplexer Systeme Dresden, Germany
Max Planck Institute for Chemical Physics of Solids Dresden, Germany
Univ. of California, Davis, USA

Funded by DFG, Forschergruppe 538, SPP 1458, Alexander von Humboldt Stiftung

Iron pnictide thin films

S. Haindl, M. Kidszun, K. Iida, F. Kurth, J. Hänisch, A. Kauffmann, N. Kozlova, J. Freudenberger, E. Reich, T. Thersleff, R. Hühne, J. Werner, S. Baunack, L. Schultz, B. Holzapfel

Research on superconductivity in the iron pnictides continuously expands nearly two years after its discovery. In addition to the material synthesis and single crystal growth thin film fabrication received an important stimulus. On the one hand, epitaxial thin films support fundamental experiments in superconductivity like phase sensitive tests using Josephson contacts, current transport in bicrystals and tests of mesoscopic limits. On the other hand, the aspect of application of iron pnictides may open new and exciting pathways in material science.

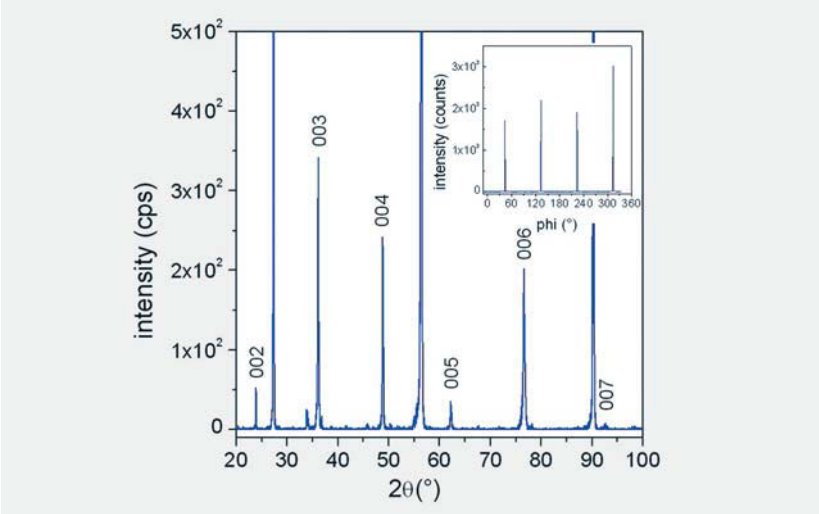

Fig. 1: *c*-axis orientation in a θ-2θ scan of an epitaxial $LaFeAsO_{1-x}F_x$ thin film. The inset shows a phi-scan of the (112) pole with a FWHM = 1°.

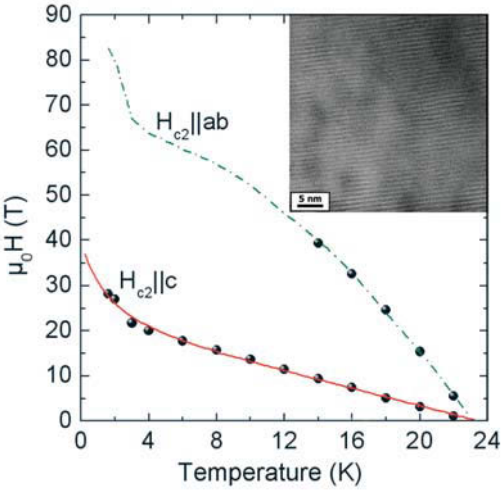

Fig. 2: Magnetic phase diagram of an epitaxial $LaFeAsO_{1-x}F_x$ thin film with fits from the two-band model. The inset shows a HRTEM micrograph of the La-1111 phase after noise reduction (filtered inverse FFT).

Successful growth of thin films has been reported only by a small number of research groups worldwide. Superconducting oxypnictide (1111-phase) thin films have been reported by IFW Dresden [1] using pulsed laser deposition (PLD) and recently by Nagoya University [2] using molecular beam epitaxy (MBE). However, a controlled growth of the oxypnictides is a challenging task. Epitaxy and the reduction of the LaOF impurity turned out to be the main goals in the preparation of thin films mainly governed by post annealing conditions [3]. A careful analysis of selected films was carried out by transmission electron microscopy which proved the LaOF impurity restricted at the surface of the film and at the substrate-to-film interface. Nevertheless, epitaxial $LaFeAsO_{1-x}F_x$ thin films (Fig. 1) have been grown by room-temperature deposition with subsequent post annealing at temperatures of 940 °C for 4 hours ('ex-situ' process) [4]. A two-band behaviour has been observed in pulsed field measurements of the upper critical field, $\mu_0 H_{c2}$ (Fig. 2). Attempts to fit the data after Gurevich [5, 6] with a set of coupling constants, λ_{ij} with $i,j = 1,2$, show that solutions with $\det(\lambda_{ij}) > 0$ and $(\lambda_{ij}) < 0$ for $i \neq j$ are possible. Therefore, a definitive conclusion about the symmetry of the order parameter (s++ and s+- respectively) cannot be made yet. In comparison, polycrystalline thin films exhibit a Pauli limit behaviour of the upper critical field (Fig. 3), which is still controversially discussed today [7, 8]. The same films brought also evidence for a weak link behaviour of the grain boundaries in this material for the first time [9].

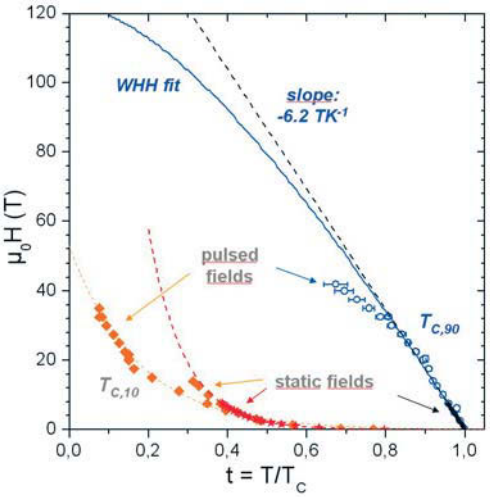

Fig. 3: Magnetic phase diagram of the polycrystalline $LaFeAsO_{1-x}F_x$ thin film. The upper critical field increases with a large slope of -6.2 TK^{-1}. The deviation from the Werthamer-Helfand-Hohenberg (WHH) fit indicates Pauli limit behaviour.

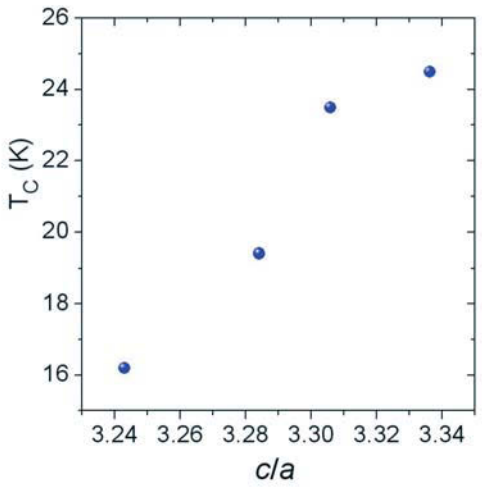

Fig. 4: Variation of the critical temperature of Co-doped $BaFe_2As_2$ thin films with lattice distortion of the film given by the ratio of the lattice parameters.

In collaboration with the University of Jena, first tunnelling contacts have been fabricated on La-1111 thin films and are currently under investigation. Both, tunnelling and optical experiments, will give new information about the coupling constant and, therefore, will provide a better understanding of the mechanism of superconductivity in the iron pnictides.

In addition to the 1111 thin films, the growth of Co-doped $BaFe_2As_2$ (122-phase) thin films has been started at IFW Dresden by ultra high vacuum (UHV) PLD. Co-doped $BaFe_2As_2$ and $SrFe_2As_2$ epitaxial films have been reported since 2008 [10, 11]. Epitaxial $Ba(Fe_{0.9}Co_{0.1})_2As_2$ thin films have been grown at IFW on various substrates (LAO, STO, LSAT, YAO, MgO) to investigate the influence of the lattice misfit on the superconductive properties [12]. As a result, an increase of the superconductive transition temperature, T_c, was observed with increasing lattice parameter ratio, c/a (Fig 4). Tunability of the transition temperature by lattice distortions has been suggested in accordance with observations with respect to the As-Fe-As bond angle [13]. Recently, optical investigations of the $Ba(Fe_{0.9}Co_{0.1})_2As_2$ thin films have found a nodeless superconducting gap [14]. Despite the fact that the measured value of $2\Delta/k_BT_c = 2.1$ is below the BCS universal value of 3.5, the electrodynamics of the superconductor agree with the BCS theory. However, the scattering mechanisms and their influence on superconductivity in the iron pnictides still remain an unsolved puzzle.

References

[1] E. Backen, et al., Supercond. Sci. Technol. **21**, 122001 (2008)
[2] T. Kawaguchi, et al., Appl. Phys. Express **2**, 093002 (2009)
[3] M. Kidszun, et al., submitted to Supercond. Sci. Technol. (EUCAS special issue)
[4] M. Kidszun, S. Haindl, E. Reich, J. Hänisch, L. Schultz, B. Holzapfel, Supercond. Sci. Technol. **23**, 022002 (2010)
[5] A. Gurevich, Phys. Rev. B **67**, 184515 (2003)
[6] J. Jaroszynski, et al., Phys. Rev. B **78**, 174523 (2008)
[7] G. Fuchs, et al., New Journal of Physics **11**, 075007 (2009)
[8] Y. Kohama, et al., Phys. Rev. B **79**, 144527 (2008)
[9] S. Haindl, et al., Phys. Rev. Lett. (accepted) *arXiv:* 0907.2271
[10] H. Hiramatsu, T. Katase, T. Kamiya, M. Hirano, H. Hosono, Appl. Phys. Express **1**, 101702 (2008)
[11] S. Baily et al., Phys. Rev. Lett. **102**, 117004 (2009)
[12] K. Iida, et al., Appl. Phys. Lett. **95**, 192501 (2009)
[13] C. H. Lee, et al., J. Phys. Soc. Jpn. **77**, 083704 (2008)
[14] B. Gorshunov, et al., *arXiv:* 0912.1256

Cooperation Univ. of Jena, Univ. of Stuttgart

Funded by DFG

Recent progress in the preparation of Ironpnictide Superconductors

S. Aswartham, C. Nacke, M. Schulze, L. Harnagea, S. Singh, I. Morozov, M. Deutschmann, J. Werner, S. Wurmehl, G. Behr, R. Klingeler, N. Leps, S. Gaß, K. Leger, G. Friemel, A. Kondrat, C. Hess, J. E. Hamann-Borrero, U. Stockert, M. Abdel-Hafez, B. Büchner

In February 2008, superconductivity was found in $LaO_{1-x}F_xFeAs$ with a T_C of 26 K [1]. The critical temperature in the oxypnictides, the so called '1111' compounds, can be increased by e.g. application of high pressure or by exchange of the rare earth element (e.g. *R*= Sm, T_C = 55 K [2]). Soon after the discovery of superconductivity in '1111'-compounds, superconductivity was also found in the $ThCr_2Si_2$-type '122'- and the Cu_2Sb-type '111'-materials. (Ba,K)Fe_2As_2 was the first superconductor found in the 122-system; its superconducting critical temperature T_C can be as high as 38 K [3]. Co-doping at Fe site in Ba122 leading to SC with T_C up to 22 K soon followed this report [4]. The parent (non-superconducting) AFe_2As_2 compounds are characterized by their first-order-like simultaneous structural and magnetic transitions at temperature T_0 = 130, 170 and 205 K for A = Ba, Ca and Sr, respectively [5-7]. In LiFeAs ('111') superconductivity was found at temperatures as high as 18 K [8]. The compound ß-$Fe_{1.01}Se$ ('11') consisting of FeSe layers shows superconductivity at 8.5 K, the maximum critical temperature enhances under pressure up to 37 K [9]. While each of these systems causes its specific challenges when growing crystals, crystal growth in general proceeds in a layered manner, i.e. single crystalline layers grow on top of each other, the plane of layers being perpendicular to the crystallographic c-axis. Crystals are, therefore, fragile and prone to exfoliation.

In the following, we will enlighten the materials and synthesis aspects of the new Ironpnictide superconductors.

We were successful in the growth of Ba, Sr, Eu and Ca 122 compounds and their doping variants. (Eu,K)Fe_2As_2 single crystals are also successfully grown. For the Ba and Ca series, different growth routes have been applied.
The Bridgman technique and growth from self-flux was employed to grow cm-size high-quality single crystals of pristine $BaFe_2As_2$ (Ba122) compound and several of its Co-, Ni- and K-doped superconducting variants; spanning almost the entire phase diagram [10]. Two different approaches for growing these single crystals were followed. In the first approach, self-flux $(Fe_{1-x}Co_x)As$ is used to obtain a homogeneous melt of the composition $Ba(Fe_{1-x}Co_x)_{3.1}As_{3.1}$. The melt composition was chosen to lower the melting temperature of $Ba(Fe_{1-x}Co_x)_2As_2$ to near T = 1463 K, which is the upper practical limit of using an evacuated silica ampoule. In such a case, the use of minimal quantity of self-flux helps increasing the single-crystal yield. A slow cool down in a temperature gradient of about 10 K/cm, in a specially designed crucible assembly, resulted in large flux-free single-

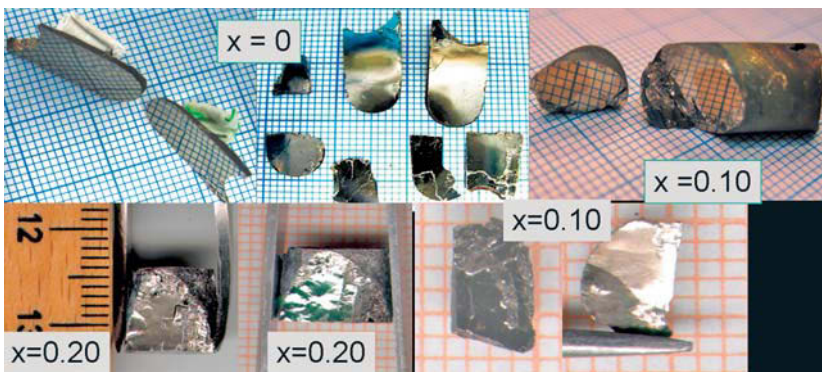

Fig. 1: Pictures of $Ba(Fe_{1-x}Co_x)_2As_2$ crystals with different Co doping level. The top row shows crystals obtained from self-flux, the bottom row displays crystals grown by the conventional Bridgman method.

crystals of the phase $Ba(Fe_{1-x}Co_x)_2As_2$. In the second approach, single-crystals were grown from a stoichiometric melt of composition $Ba(Fe_{1-x}Co_x)_2As_2$ using the Bridgman method in a vertical tube furnace in tapered alumina crucibles. Using both techniques, single-crystals with lateral dimensions up to 25x10 mm^2 and thickness up to 1 mm were obtained (see Fig. 1).

Single crystals of Ironpnictides $Ca(Fe_{1-x}Co_x)_2As_2$ ($0 \leq x \leq 0.2$) were grown from Sn-flux using the conventional high temperature solution growth technique, resulting in phase pure and flux free crystals. Figure 2 shows the crystals, which are plate-like exhibiting lateral dimensions up to 15 mm and 0.5 mm thickness.

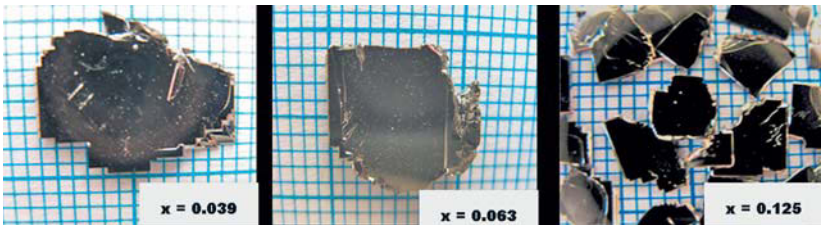

Fig. 2: Single crystals of $Ba(Fe_{1-x}Co_x)_2As_2$ grown by high temperature solution growth using Sn-flux.

For both the Ca and Ba system, the crystallographic c-axis of the tetragonal unit cell decreases upon Co-doping, while the a-axis shows a less significant variation. The microstructure and the actual Co-content for each grown crystal is by default examined in detail in an electron microscope equipped with energy dispersive x-ray (EDX) and wavelength dispersive x-ray (WDX) probe at several points of the crystals. In case of the Ca 122 samples, actual Co-contents are about 15 - 35 % smaller than the nominal values. The Ba crystals obtained from the vertical Bridgman method exhibit a higher Co-content than the nominal values, while the Co-contents of Ba crystals from self-flux are in good agreement with the nominal values.

In particular, the high quality of the $Ba(Fe_{1-x}Co_x)_2As_2$ obtained by the vertical Bridgman method was confirmed by ZF-μSR studies [11], demonstrating a pure Gaussian-like relaxation (Fig. 3). Measurements of magnetic susceptibility and electrical resistivity reveal superconducting properties of the Co-doped crystals. Narrow superconducting transition widths (≈ 0.5 K) and large residual resistivity ratios (≈ 7) indicate the high-quality of our single crystals. Figure 4 shows the electronic phase diagram of the 122 series comparing the results from crystals obtained by growth from self-flux and by a conventional Bridgman growth. The electronic phase diagram of the Ca 122 series as derived from magnetization, resistivity, specific heat, μSR data reveals a similar shape (not shown here).

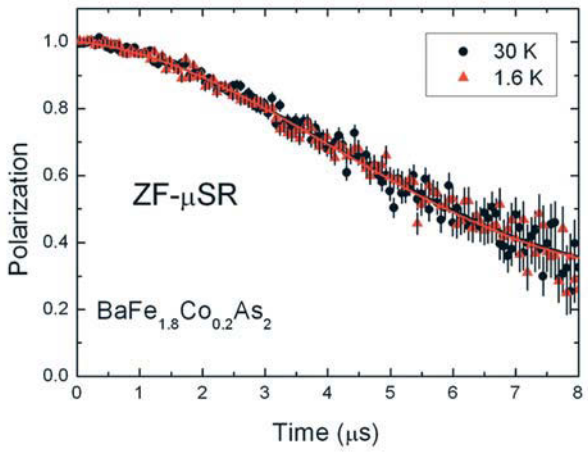

Fig. 3: ZF - μSR measurement of a $BaFe_{1.8}Co_{0.2}As_2$ sample grown via the vertical Bridgman technique. A pure Gaussian like relaxation confirms the very high quality of the crystal.

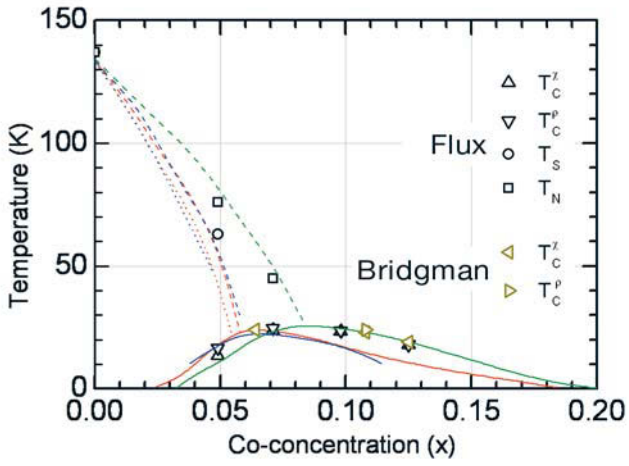

Fig. 4: Electronic phase diagram of the sample series $Ba(Fe_{1-x}Co_x)_2As_2$ comparing the results from crystals obtained by growth from self-flux and by vertical Bridgman growth.

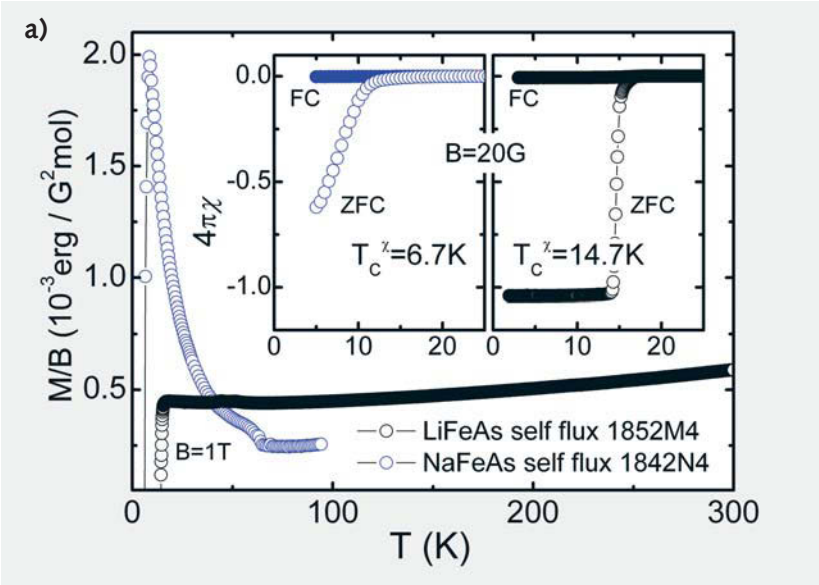

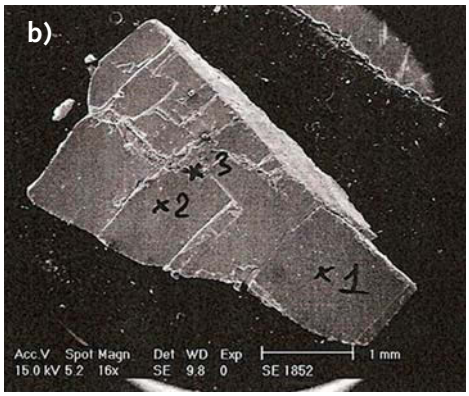

Fig. 5: (a) Measurement of the magnetization as a function of temperature for LiFeAs and NaFeAs single crystals. The inset shows the superconducting transitions. (b) SEM picture of a LiFeAs crystal obtained from self-flux.

Single crystals of LiFeAs and NaFeAs were obtained from self-flux in sealed Nb crucibles. For LiFeAs, a Li:Fe:As ratio of 3:2:3 was mixed and sealed in an Al_2O_3 crucible under 1.5 atm Ar. The resulting crystals have dimensions of maximum 10×8×0.2 mm and the LiFeAs phase was confirmed by EDX and X-ray diffraction (XRD). We also made LiFeAs single crystals with Sn-flux. Here, excess Sn was removed by decantation and centrifugation. The synthesis of LiFeAs single crystals has not been reported yet elsewhere, neither from self-flux nor Sn-flux. As displayed in Fig. 5, the material becomes bulk superconducting below ~16 K. Our susceptibility data prove the absence of magnetic impurities and the slope dM/dT at 300 K is in a good agreement with 122- single crystals, La 1111 samples and theoretical predictions [13]. In addition, ARPES measurements on LiFeAs crystals from self-flux are in agreement with the correct stoichiometry. Remarkably, the ARPES data exclude Fermi surface nesting indicating that superconductivity is not associated with a certain nesting condition [12].

NaFeAs single crystals have been made very similarly from self-flux, starting with Na:Fe:As = 1.6:1:1. The resulting crystals are slightly smaller than LiFeAs with a maximum size of 3×2×0.05 mm. The phase was confirmed by EDX and XRD, and the self-flux consists mainly of Na_3As. Superconductivity is found with $T_C \sim 7$ K (see Fig. 5). For NaFeAs, a single crystal has already been achieved in Ref. [14] by a slightly different procedure. Note, that in [14] $T_C = 23$ K is reported (onset temperature in $\rho(T)$) while the resistivity becomes zero clearly below 10 K. This agrees to the onset temperature of SC as derived from our susceptibility data, i.e. ~24 K. In addition, signatures of the structural and the magnetic phase transitions are reported in [14] at 52 K and 41 K while our sample exhibits only one but much more pronounced anomaly at 64 K.

Crystals with a nominal composition of $FeTe_{0.5}Se_{0.5}$ have been grown using a vertical Bridgman method in a vertical tube furnace and by a Bridgman-like growth in a horizontal setup. The material was put under 0.3 bar Ar into double walled quartz tubes. The temperature profiles are based as well on the extrapolation of the binary phase diagrams as on Ref. [15] but our studies suggest significantly lower temperatures. The samples show dendrite-like structures within a homogeneous single-crystalline matrix (see Fig. 6) which is Te rich as shown by EDX analysis, i.e. $Fe_{1.05}Te_{0.67}Se_{0.33}$. In particular, deviations in the ratio Te:Se are observed in the dendrites. The presence of the correct phase is corroborated by the observation of superconductivity at T_C = 11 K (Fig. 6). Samples with 2% of S doping also exhibit superconductivity with critical temperature of 11 K.

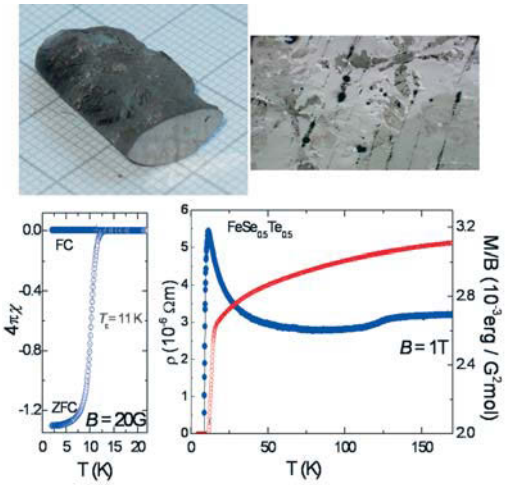

Fig. 6: Crystal with nominal $FeTe_{0.5}Se_{0.5}$ composition and the microstructure obtained by optical microscopy. Here, the formation of dendritic phases within the matrix is observed. The measurement of the magnetization as a function of temperature demonstrates the superconducting properties of the $FeTe_{0.5}Se_{0.5}$ with T_C = 11 K.

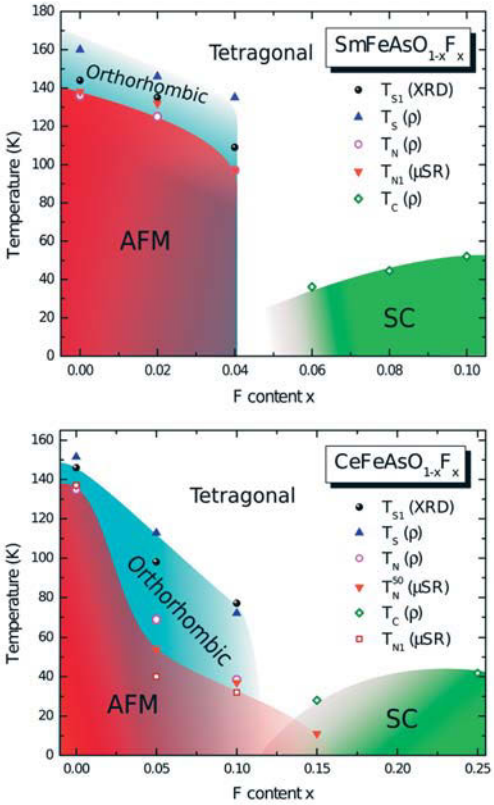

Fig. 7: Electronic phase diagram of the $SmFeAsO_{1-x}F_x$ and $CeFeAsO_{1-x}F_x$ series.

Polycrystalline samples of the rare earth Ironoxypnictides have been prepared and applied to study the electronic phase diagrams (see Fig. 7 for the Sm and Ce series [16]) and to provide materials for NMR, μSR, transport, magnetization, thermal expansion, specific heat, Andreev spectroscopy, optics, XAS, photoemission spectroscopy, pulsed magnetic field, and neutron studies. Sample optimization yielded highest quality polycrystals. The materials show superconductivity with critical temperatures comparable to those found in literature but with improved smaller widths of the superconducting transition. Among the successfully synthesized polycrystalline samples are the doping series $LaO_{1-x}F_xFeAs$ with $0 \leq x \leq 0.2$ and $La_{1-x}Sr_xOFeAs$ with $0 \leq x \leq 0.2$ and doping samples containing other rare earth elements such as Ce, Nd, Gd and Sm. New synthesis routes have been exploited to further enhance the sample quality e.g. by ball milling of the educts. All samples have been comprehensively studied regarding their physical properties, their structural perfection, their doping level and their microstructure.

The normal state magnetization of Ironpnictides exhibits a universal increase upon heating. In $LaO_{1-x}F_xFeAs$, both the slope and the absolute value of the susceptibility at elevated temperatures are independent on doping, irrespectively whether long range antiferromagnetic order or the non-magnetic superconducting ground state appears. Our data on LiFeAs (Fig. 5), NaFeAs (Fig. 5), $Ba(Fe_{1-x}Co_x)_2As_2$ and $Ca(Fe_{1-x}Co_x)_2As_2$ single crystals imply the generic nature of this feature. Remarkably, there is quantitative agreement of the slope well above the ground states.

The sample characteristics have a high impact on the experimental results and their interpretation. This implies that the confirmation of the results hitherto by means of high-quality samples is mandatory. In the last year, we had considerable progress in the successful synthesis of the new Ironpnictide superconductors. The high quality of our samples opens a route to study the underlying physics and to address the open questions related to this in this new and fascinating class of materials.

References

[1] Y. Kamihara et al., J. Am. Chem. Soc. **130** (2008) 3296.
[2] Margadonna et al., Phys. Rev. B **79** (2009) 014503.
[3] M. Rotter et al. Phys. Rev. Lett. **101** (2008) 107006.
[4] A. S. Sefat, et al. Phys. Rev. Lett. **101** (2008) 117004.
[5] F. Ronning et al. J. Phys.: Condens. Matter **20** (2008) 322201.
[6] M. Rotter et al. Phys. Rev. B **78** (2008) 020503.
[7] J.-Q. Yan et al. Phys. Rev. B **78** (2008) 024516.
[8] J. H. Tapp et al., Phys. Rev. B **78** (2008) 060505.
[9] S. Medvedev, Nature Materials **8** (2009) 630.
[10] S. Aswartham et al. submitted to J. Cryst. Growth (2009).
[11] H-H. Klauss in preparation (2009).
[12] S. Borisenko et al. in preparation (2009).
[13] I. Mozorov et al. in preparation (2009).
[14] H.-H. Wen et al., Europhys. Lett. **82** (2008) 17009
[15] K. Morinaga et al., Jpn. J. Appl. Phys. **48** (2009) 013004.
[16] J. E. Hamann-Borrero in preparation (2009).

Cooperation TU Dresden, Univ. Köln, HZ Berlin, TU Braunschweig, PSI Villigen

Funded by DFG (BE1749/12)

Skyrmions and chirality selection in noncentrosymmetric magnets

U. K. Rößler, A. A. Leonov, A. B. Butenko, A. N. Bogdanov

In noncentrosymmetric magnetic materials chiral Dzyaloshinskii-Moriya exchange stabilizes non-collinear twisted magnetization structures with a fixed sense of rotation. As an alternative to one-dimensional long period spirals, Skyrmion-strings can arise, which may condense into multiply modulated states. The extended Skyrmionic textures are determined by the stability of the localized solitonic Skyrmion cores and their geometrical incompatibility which frustrates regular space-filling. Similar solitonic states can exist in chiral liquid crystals, ferroelectrics, multiferroics and in confined systems (e.g. nanolayers of magnetic metals). Our recent results on the basic phenomenological models of chiral magnets reveal rich temperature-field phase diagrams that include different Skyrmionic lattices and confinement of Skyrmions.

Introduction

Smooth, multidimensional localized structures (Skyrmions) are intensively investigated in many areas of physics [1,2]. In the majority of nonlinear field models, Skyrmionic states appear only as dynamic excitations, but static configurations are generally unstable and collapse spontaneously into topological singularities [3]. These instabilities can be overcome if the energy functionals contain (i) contributions with higher-order spatial derivatives (*Skyrme mechanism*), [4] or (ii) terms linear with respect to spatial derivatives of the order parameters (so called Lifshitz invariants) [2,5].

In most condensed matter systems there are no physical interactions underlying energy contributions with higher order spatial derivatives. On the contrary, Lifshitz invariants arise in different condensed matter systems with intrinsic and induced chirality [5,6]. They stabilize two- and three-dimensional modulations of the order parameters with long period and fixed sense of rotation. Such solitonic textures can arise in different classes of noncentrosymmetric magnetic crystals [2,5,7], chiral liquid crystals, ferroelectrics, and multiferroics [7,8].

Effects of chiral couplings in magnetic systems

In magnetism, the chiral couplings rely on the asymmetric Dzyaloshinskii-Moriya (DM) exchange. In confined systems as magnetic nanolayers, nanowires, and nanodots surface/interface-induced DM couplings influence magnetic states. These surface-induced couplings favour one sense of rotation in conventional non-collinear micromagnetic structures as domain walls or vortices. Micromagnetic analysis of this chirality selection for the vortex ground states of magnetic nanodisks shows that the sign and the strength of the DM coupling strongly influence their structures, magnetization profiles and core sizes [9]. The calculated relations between strength of the DM interactions and vortex-core sizes provide a method to determine the magnitude of surface-induced DM couplings in ultrathin magnetic films/film elements.

As a genuine consequence of surface-induced DM couplings different types of chiral modulations may occur and have been observed [10]. Therefore, thin film systems are candidate structures to study chiral magnetic Skyrmions. Low temperature properties of Skyrmionic states have been comprehensively studied earlier [2,5-7]. Our recent results are concerned with nucleation processes of Skyrmions, their condensation into extended textures, and their further evolution under the influence of magnetic fields and temperature. By brute force energy minimization of the phenomenological (Dzyaloshinskii) models of chiral ferromagnets we have derived numerically exact solutions for isolated and bound Skyrmions and Skyrmion lattices that apply to different classes of uniaxial and cubic noncentrosymmetric ferromagnets [11,12,13].

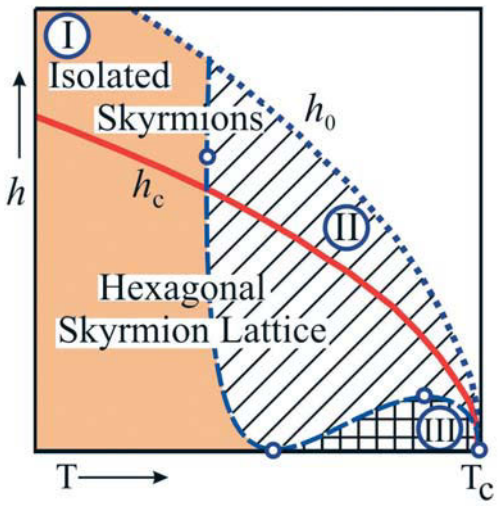

Fig. 2: Temperature (T) - magnetic field (h) phase diagram of an isotropic helimagnet includes regions with *repulsive* (I) and *alternating* (II) inter-Skyrmion interactions. In confinement pocket (III) Skyrmions exist only as bound states. Solitary Skyrmions condense into a hexagonal lattice at critical field h_c (T) (red solid line) and collapse at h_0 (T) (dotted line).

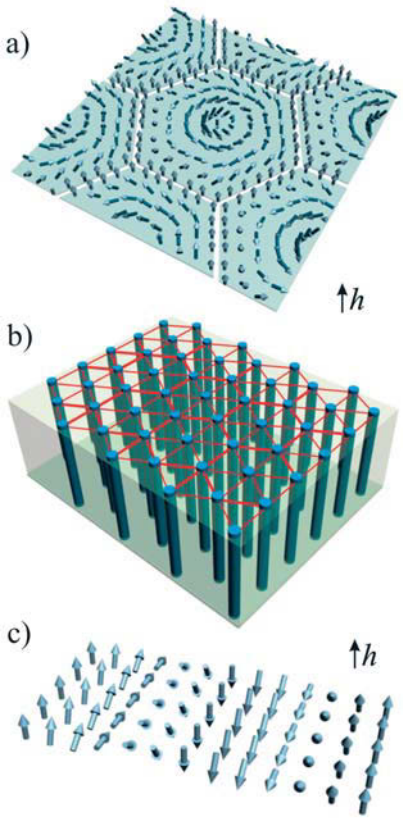

Fig. 3: A cross-section of a cell (a) in a hexagonal Skyrmion lattice (b) and a one-dimensional chiral texture (*helicoid*) (c).

Chiral flux-lines as the building blocks of Skyrmionic matter

The micromagnetic equations for chiral systems include solutions for axisymmetric localized states, *isolated Skyrmions*. They can be thought of as isolated topologically stable filaments within spatially homogeneous phases (Fig. 1 a, b). Being proportional to the strength of DM coupling their sizes reduce to zero in centrosymmetric systems.

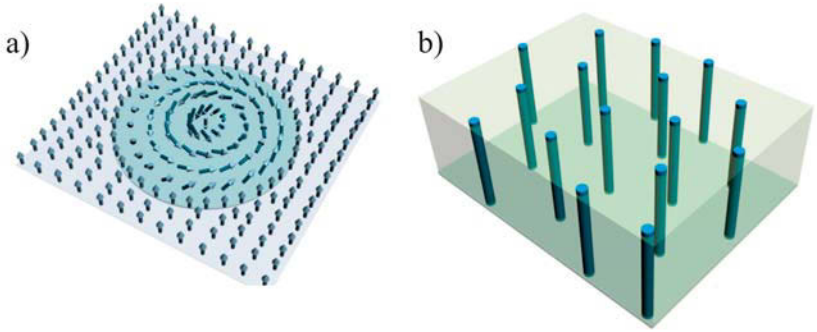

Fig. 1: Cross-section through an isolated Skyrmion in chiral magnets with D_n and cubic symmetry (a) and a set of isolated Skyrmion lines (b).

Hence, the chiral coupling supplies the unique mechanism to stabilize Skyrmionic textures. This singles out chiral condensed matter systems with Lifshitz-type invariants into a particular class of materials with Skyrmionic states. Isolated Skyrmions remind Abrikosov vortices in type II superconductors or thread-like textures in nematic liquid crystals. Contrary to these defected patterns with singularities in the core, the distribution of the order parameter in Skyrmions is smooth. In the phase diagram of the solutions (Fig. 2) the isolated Skyrmions exist below a certain critical field h_0 (Fig. 2) and are characterized by weak variation of the magnetization modulus m and strong localization of their cores (Fig. 1). Near the critical field h_0 the magnetization modulus at the Skyrmion axis approaches zero. This destroys topological stability of Skyrmions and leads to their collapse.

Skyrmion lattices and helicoids: double-twist versus ideal compatibility

Below another critical field h_c solitary Skyrmion lines condense into hexagonal Skyrmion lattices (Fig. 3 a, b). These 2D modulated textures compete with the common one-dimensional (helical) modulations (Fig. 3 c). Skyrmion lattices are characterized by a strong variation of the cell sizes and transformation of their structures near cell boundaries. However, they preserve axisymmetric distribution of the magnetization near the cell center. This remarkable property is due to the specific balance of energy contributions in the Skyrmions. "Double-twist" rotation of the magnetization near the Skyrmion core leads to larger energy reduction than in "single-twisted" spiral phases. Conversely, the energy density is larger at the outskirt of the Skrymion than in the helical states. This explains the unusual axial symmetry of the cell cores and the stability of their cores. There is an inherent frustration built into models with chiral couplings that prevents to fill the whole space with the ideal, energetically most favoured double-twist motif. The condensation of Skyrmions, therefore, creates spatially inhomogeneous twisted phases which can form lattice-like or amorphous assemblies of these multi-dimensional solitonic objects.

Skyrmion-Skyrmion interactions and confinement phenomenon

The phase diagram (Fig. 2) includes three distinct regions with different character of inter-Skyrmion coupling. *Repulsive* interactions are found in a broad temperature range extending to low temperatures. At higher temperatures, the interactions become *oscillatory* with alternating sign. Depending on the distance between Skyrmions, their interaction can be either attractive or repulsive. In this region, Skyrmions are energetically *confined*, because pairs or clusters of free Skyrmions can achieve lower

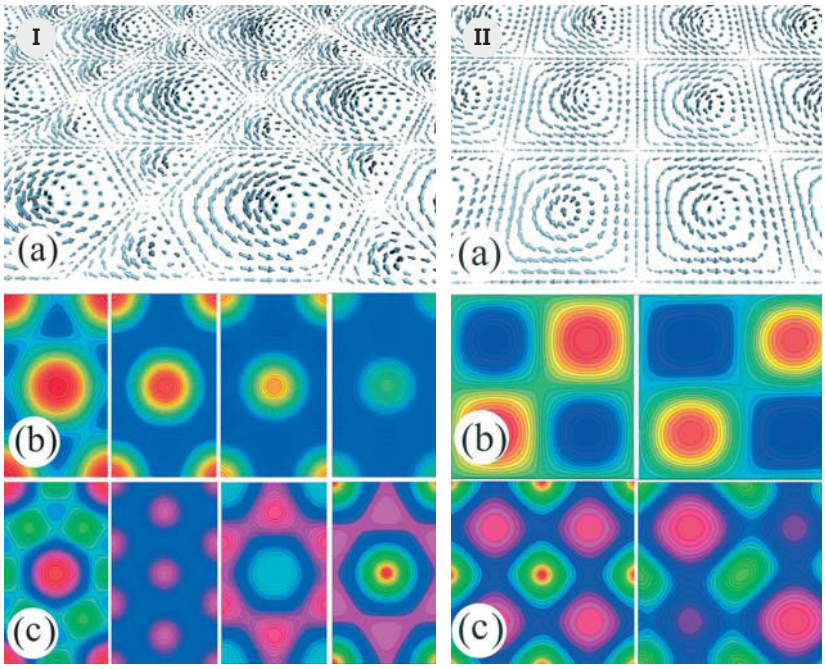

Fig. 4: Structure of hexagonal (column I) and square (column II) Skyrmion lattices near the ordering temperature (a) and contour plots for the magnetization modulus m (b) and the magnetization component along the magnetization field (c) for increasing magnetic fields.

energies by a suitable arrangement than the same number of free Skyrmions. Thus, Skyrmions may form bound agglomerations and extended textures to fill the whole space, if they can exist in this region of the phase diagram. Finally near the ordering point Skyrmions are strictly *confined*, because there cannot exist solutions for asymptotically free Skyrmions within this confinement pocket (area (III) in Fig. 2). These bound Skyrmions exist as hexagonal or half-Skyrmion (square) lattices (Fig. 4). As the magnetization modulus m is "soft" near the ordering temperature, the magnetic-field-driven evolution of such confined Skyrmions causes a strong variation of the modulus within Skyrmion cores, while the equilibrium lattice periods varies little with the applied field (Figs. 4, 5).

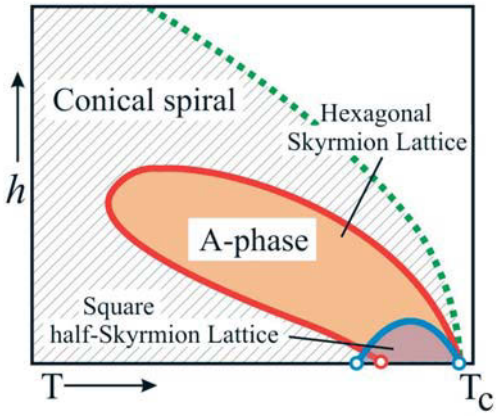

Fig. 5: In cubic helimagnets like MnSi magnetic anisotropy stabilizes hexagonal and square Skyrmion lattices near the ordering temperature T_c.

Physical nature of precursor states in chiral magnets

The confinement of Skyrmions is responsible for anomalous magnetic properties in chiral magnets. The formation of extended Skyrmionic textures at elevated temperatures belongs to a rare class of instability-type nucleation transitions [14]. The lattices composed of confined localized Skyrmion units disappear at the transition temperature continuously as the amplitude of the modulus variation in the lattice vanishes [11]. However, there exists still a multitude of possible arrangements of Skyrmions as they are nucleated in an extended texture. Evidence for these anomalous transitions into multiply modulated magnetic states has been found in experiments on chiral magnets as precursor phases that precede the formation of the helical ground state [15,16]. Our results show that these precursor phenomena are a general effect related to the confinement of localized Skyrmionic excitations.

We also find that magnetic anisotropy plays a crucial role to stabilize Skyrmionic states as thermodynamic phases in cubic helimagnets [11,13]. The magnetic phase diagram in Fig. 5 includes two regions with Skyrmionic states that are thermodynamically stabilized by exchange magnetic anisotropy. At zero field the precursor phase is a staggered half-Skyrmion square lattice, and at higher field a hexagonal Skyrmion lattice is formed in the so-called A-phase.

References

[1]. C. Bäuerle et al. Nature 382 (1996) 332; L. Brey et al. Phys. Rev. Lett. 75 (1995) 2562.
[2] U.K. Rößler et al., Nature 442 (2006) 797; A.N. Bogdanov et al., Physica B 359 (2005) 1162.
[3] G. H. Derrick, J. Math. Phys. 5 (1964) 1252.
[4] T. H. R. Skyrme, Proc. Roy. Soc. Lon. 260 (1961) 127.
[5] A.N. Bogdanov and D.A. Yablonsky, Sov. Phys. JETP 68 (1989) 101; A. Bogdanov, JETP Lett. 62 (1995) 247.
[6] I. E. Dzyaloshinskii, Sov. Phys. JETP 19 (1964) 960.
[7] A. N. Bogdanov et al. Phys. Rev. B 66 (2002) 214410; H. Murakawa et al., Phys. Rev. Lett. 103 (2009) 14701.
[8] D. C. Wright, N. D. Mermin, Rev. Mod. Phys. 61 (1989) 385.
[9] A. B. Butenko et al. Phys. Rev. B 80 (2009) 134410.
[10] M. Bode et al. Nature 447 (2007) 190; A. N. Bogdanov, U. K. Rößler, Phys. Rev. Lett. 87 (2001) 037203.
[11] A. N. Leonov et al. Phys. Rev. Lett. submitted.
[12] U. K. Rößler et al., arXiv:0907.3651v2 (2009).
[13] A. B. Butenko et al. Phys. Rev. B, submitted, arXiv://0904.4842.
[14] J. W. Felix et al., Phys. Rev. Lett. 57 (1986) 2180.
[15] C. Pfleiderer et al., Nature 427 (2004) 227; C. Pappas et al., Phys. Rev. Lett. 102 (2009) 197202.
[16] C. I. Gregory et al., J. Magn. Magn. Mater. 104-107 (1992) 689 (1992); B. Lebech et al. J. Magn. Magn. Mater. 140 (1995) 119; S. Mühlbauer et al., Science, 323 (2009) 915.

Cooperation Donetsk Institute of Physics and Technology

Funded by DFG

Direct observation of superconducting vortex clusters pinned by a periodic array of magnetic dots in ferromagnetic/superconducting hybrid structures

T. Shapoval, V. Metlushko[1], M. Wolf, B. Holzapfel, V. Neu and L. Schultz

Strong pinning of superconducting flux quanta by a square array of 1 µm-sized ferromagnetic dots in a magnetic-vortex state was visualized by low-temperature magnetic force microscopy (LT-MFM). A direct correlation of the superconducting flux lines with the position of the dots was observed. The force that the MFM tip exerts on the individual vortex in the depinning process was used to estimate the spatial modulation of the pinning potential. It was found, that the superconducting vortices which are preferably located on top of the ferromagnetic dots experience a pinning force about 15 times stronger as compared to the pinning force in the pure niobium film. This strong pinning exceeds the repulsive interaction between the superconducting vortices and allows vortex clusters to be located at each dot. Our microscopic studies are consistent with global magnetoresistance measurements on the hybrid structures, but suggest a modified picture of the pinning mechanism.

Controlling the distribution of magnetic flux quanta (superconducting vortices) in superconducting materials by introducing artificial pinning centers is a challenge, both in basic and in applied research. Whereas randomly distributed defects act as strong local pinning centers which significantly improve the in-field critical parameters of superconducting films, ordered pinning potentials give rise to collective pinning mechanisms and thus lead to commensurate pinning effects. In comparison to simple structurally ordered pinning sites, magnetic pinning centers provide additional degrees of freedom, which lead to several pronounced effects, such as domain-wall superconductivity, field induced superconductivity, proximity effect, magnetostatic interaction, and local suppression of superconductivity by strong out-of-plane field components.

Until now the scientific community concentrates on the investigation of the vortex behaviour in superconducting/ferromagnetic (SC/FM) hybrid structures where the magnetic dots are in a multi domain or single domain state with homogeneous in-plane or out-of-plane (for strong perpendicular anisotropy) magnetization. But depending on their shape and aspect ratio, the so called magnetic vortex state can be energetically stable in circular dots at remanence. Here, the magnetization curls continuously around the center while staying purely in-plane in a large area of the dot and turns perpendicular to the surface in the center of the dot creating a small magnetization swirl.

It was shown recently in Hoffmann *et al.* [1] that the nature of pinning of SC vortices in such hybrid systems should crucially differ from that where the dots are in the single domain state. The strong drop of the magnetoresistance curve of the SC film was clearly correlated to the presence of the magnetic-vortex state of the underlying FM dots. To look deeper into the nature of this enhanced pinning, local investigations of the distribution of SC vortices and there behaviour are indispensable.

In our work we have performed the first local imaging of SC vortices in the vicinity of such magnetic dots in the magnetic-vortex state.

The techniques we used, low temperature magnetic force microscopy (LT-MFM), is a powerful method to probe the spatial variation of the pinning landscape, as it allows combining the non-invasive imaging of individual vortices with the direct manipulation and depinning of vortices from their positions.

The following hybrid structure was studied: a square array of permalloy (Py = $Ni_{80}Fe_{20}$) dots with 1 µm diameter, 25 nm height and 2 µm periodicity was prepared on a Si (100) substrate using standard e-beam lithography, e-beam evaporation, and lift-off processes; a 100 nm thick SC niobium (Nb) film (T_c = 8.32 K) was deposited on top of the Py

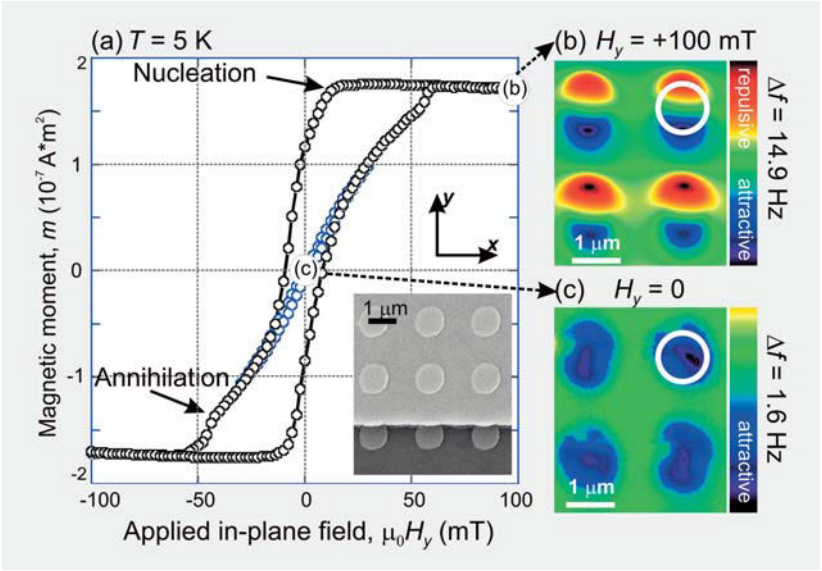

Fig. 1: Magnetic hysteresis loop of the Py array measured at 5 K using a superconducting quantum interference device (SQUID) displays magnetic vortex behaviour with vortex nucleation and annihilation fields. For the inner loop in the field range from −30 mT to +30 mT, the magnetization process occurs only by vortex propagation and, thus, is reversible (vortex branch). The inset shows a SEM image of Py dots covered with a 100 nm thick Nb layer. The in-plane field H_y was varied along the hysteresis loop starting from saturation at +100 mT (b), through applying a negative field less than the magnetic-vortex annihilation field (−25 mT) to the magnetic-vortex state at zero field (c). Color bars give the measured Δf signal which strongly differs between the saturated (b) and the vortex state (c). A small out-of-plane field of +10 mT was permanently applied to insure a positive polarity of the magnetic vortex. Scanning distance was 75 nm, T = 14.6 K. The white circles represent the location of the Py dot.

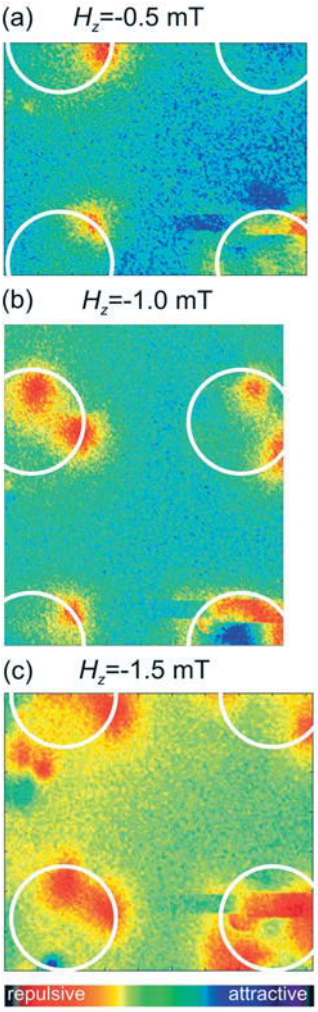

Fig. 2: Visualization of superconducting vortices pinned by Py dots at 6.1 K (72% T_c). An area where one dot is not fully switched to the magnetic-vortex state and has a residual in-plane component was chosen for LT-MFM imaging to ensure that the same dots are imaged at different fields and to correct a small thermal drift during experiments. It was established that the vertical coil of the microscope has a shift of zero point in the range of −0.5 mT. This justifies to consider the +0.5 mT image, where only magnetic contrast from the Py dots is observed, as a "background", and to subtract it from the other ones. In the lower right dot, the residual in-plane component of the Py magnetization leads to a slightly disturbed difference image. The frozen effective fields H_z are: (a) −0.5 mT, (b) −1 mT and (c) −1.5 mT. SC vortices are visualized as red spots.

dot array by sputter deposition [1]. A SEM scan of this Py/Nb hybrid structure is shown in Fig. 1 (a) (inset). The magnetic in-plane hysteresis loop [Fig. 1 (a)] of the Py clearly reveals magnetic vortex behaviour with vortex nucleation and annihilation fields.

As the first step we have generated magnetic vortices in the Py dots with a defined polarity, such that the magnetic-vortex core and the MFM tip experience an attractive interaction that shows up as a dark contrast in the center of the dot [Fig. 1 (c)]. Then, the sample was cooled down to a temperature below T_c of the Nb film (T = 6.1 K = 72% T_c) in perpendicular fields H_z = − 0.5 mT, − 1 mT, − 1.5 mT that are close to the matching fields, H_m, for this hybrid structure ($H_m = m\phi_0/S$, with $\phi_0 = h/2e$ being the magnetic flux quantum and S = 4 μm^2). The imaged vortex distributions are shown in Fig. 2 (a)–(c), respectively. The orientation of H_z is negative, so that SC vortices and the MFM tip exhibit repulsive interaction and SC vortices show up as confined circular objects with positive frequency shift (red color). Hence, the SC vortices in Nb film have a polarity opposite to that of the magnetic-vortex core in Py dots. Thus the magnetostatic interaction between magnetic and SC vortices turns out to be repulsive. Such a configuration is selected to differentiate the magnetostatic pinning mechanism from the non-magnetic one.

Figure 2 (a) corresponds to the first matching field H_1. Here one SC vortex is visualized per unit area of the dot array, as expected. The SC vortices are located on top of Py dots (white circles), showing that the dots act as preferable pinning centers. Nevertheless, they do not concentrate at the center of the dot, but occupy the *edges* of the dot. Furthermore, no SC vortices are found in the interstitial positions between Py dots. This effect becomes more pronounced when the second matching field H_2 has been applied during cooling [Fig. 2 (b)]. Also here, despite of the long-range repulsive interaction between SC vortices, they are not distributed homogeneously, but are strongly pinned by the Py dots, so that two vortices are located on each dot. A further increase of the field to H_3 leads to an enhanced magnetic contrast on top of the Py dots, which corresponds

to multiple flux quanta (*vortex cluster*) pinned by the dots [Fig. 2 (c)]. Here the expected three SC vortices could not be separately resolved due to overlapping of their magnetic stray fields at small vortex-vortex distances. The discussion of the nature of the imaged vortex distribution can be found in Shapoval *et al.* [2].

A first estimation of the pinning force is based on the fact that two SC vortices are situated close to each other on top of the Py dot rather than being organized in a homogeneous Abrikosov lattice. Consequently, the pinning force due to these artificial defects (F_p) is higher than the repulsive force between vortices F_{v-v}. The repulsive force between two SC vortices in thin films with a thickness below the penetration depth, λ, has been approximated in the Pearl model [3] as: $F_{v-v} = \phi_0^2/\pi\mu_0 a^2$, where a is the distance between the vortices. For H_2, where the distance between two vortices was measured to be about $a = 750$ nm [Fig. 2 (b)], the vortex-vortex repulsion force normalized by the Nb film thickness was estimated to be $f_{v-v} = 19 \pm 0.3$ pN/µm. Due to the long-range character of this interaction, the formation of SC vortex clusters in thin films is energetically unfavorable [3]. Consequently, the presence of a strong pinning potential is required to ensure the visualized distribution of SC vortices. As it was shown recently by Brandt [4], according to the finite-size of the film the real vortex-vortex interaction is weaker than the value calculated from the Pearl model for an infinite thin SC layer.

While scanning with the MFM tip, an additional lateral force, F_{lat}, that acts on the SC vortices arises. Thus, a non-invasive imaging of vortices by MFM is possible only if the vortices are pinned. The tip-vortex interaction force can be accurately tuned during scanning by varying the tip-sample separation h and F_{lat} can be estimated from the monopole-monopole model [5] as $\max(F_{lat}) = 0.38\,\tilde{m}\,\frac{\phi_0}{2\pi}\,(h + 1.27\lambda + \delta)^{-2}$, where $\tilde{m}$ is the monopole moment per unit length of the tip and δ is its position within the tip as sketched in Fig. 3 (e). If this force exceeds the pinning force of an individual vortex at a natural or artificial defect the vortex can be dragged from its position.

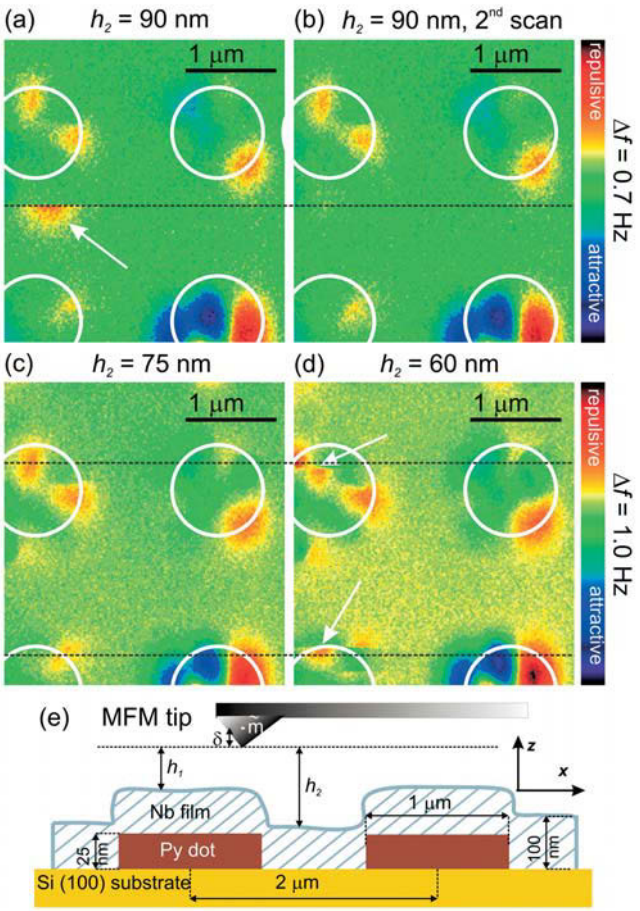

Fig. 3: Distribution of the SC vortices in a Nb film in the presence of the Py dots in the magnetic-vortex state measured at $T = 6.1$ K and the second matching field. The tip-sample distance was varied. As long as the tip-sample distance h_2 is larger than 90 nm, the vortices are not dragged by the tip. As soon as h_2 reaches 90 nm **(a)**, the interstitial vortex (marked by the arrow) is depinned and moved completely out of the scanned area. This is apparent from the second scan at the same distance **(b)**, where this vortex between the Py dots is no longer visible. The presence of the 25 nm thick Py dots underneath the Nb film leads to a surface modulation of the SC film, as it is sketched in **(e)**. The AFM profile (not presented here) shows that the modulation $h_2 - h_1 = 30$ nm is on the scale of the Py dot thickness. Consequently, the SC vortices imaged on top of the Py dots have a lower tip-sample distance and experience a stronger lateral force from the MFM tip. Despite the decreased distance, the vortices on the Py dots are not dragged by the tip at $h_2 = 90$ nm and also $h_2 = 75$ nm **(c)**. Only when h_2 decreases to 60 nm ($h_1 = 30$ nm) and the lateral depinning force that acts additionally to the existing repulsive interaction, F_{v-v}, reaches 2.3 pN/µm, the vortices on top of the Py dots also start to move **(d)**. Panel **(e)** sketches a cross-sectional cut of the FM/SC hybrid structure and the MFM tip scanning above the surface.

In order to probe this effect, MFM scans have been performed on the same sample position at different tip-sample distances in order to depin the SC vortices located on the Py dots and in the interstitial positions under the influence of the stray field of the tip (Fig. 3). From these images using the monopole-monopole model we have estimated the lateral force that acts between the MFM tip and a SC vortex in the interstitial position and on the dot. This force normalized by the Nb film thickness was found to be 1.5 pN/µm for an interstitial vortex that is located in the pure Nb film and 2.3 pN/µm for the vortices on top of the Py dots. As the vortices on the top of the dots already undergo strong repulsive interaction (f_{v-v}) the effect of the MFM tip should be added to f_{v-v} in order to find the real force needed to depin the vortices from the dots. As a result, the total pinning force at the Py dots is estimated to be 21 pN/µm, which is about 15 times stronger as compared to the pinning force in the pure Nb film estimated above. The details of the local pinning analysis can be found in Shapoval *et al.* [6].

On the one hand, our microscopic observations support the conclusion made from the magnetoresistance measurement that the Py dots in the magnetic-vortex state act as highly preferable pinning sites [1], on the other hand they show that a more detailed explanation of the pinning mechanism is essential for understanding the visualized arrangement of SC vortices in such FM/SC hybrid structures.

References

[1] A. Hoffmann *et al.*, Phys. Rev. B. **77**, 060506(R) (2008)
[2] T. Shapoval *et al.*, arXiv:0907.2821v1, submitted to PRB(R)
[3] J. Pearl, Appl. Phys. Lett. **5**, 65 (1964)
[4] E. H. Brandt, Phys. Rev. B. **79**, 134526 (2009)
[5] E. W. J. Straver *et al.*, Appl. Phys. Lett. **93**, 172514 (2008)
O. M. Auslaender *et al.*, Nature Physics **5**, 35 (2009)
[6] T. Shapoval *et al.*, Physica C, accepted (2009)

Cooperation [1]Department of Electrical and Computer Engineering, University of Illinois at Chicago, USA.

Structuring Graphene

M. Rümmeli, J. H. Warner[1], A. Bachmatiuk, F. Schäffel, B. Büchner

Graphene is a remarkable material with incredible electrical and mechanical properties. However, it has only recently been isolated. This has made graphene the "new rising star" in nano-carbon based materials due to its exciting properties at the nanoscale, e.g. high charge carrier mobility. In addition, when existing as narrow strips or ribbons (ca. 10 nm wide) a band gap opens making them excellent candidates for field effect transistors. Hence, apart from the exciting possibilities in discovering new physics from these 2D structures, they offer tantalizing opportunities for the development of high speed (and even flexible) molecular electronics. However, one of the major barriers impeding their progress on this front relates to difficulties in their fabrication. In order to integrate them in to electronics they need to be fabricated in large areas or in highly defined ways (e.g. nanoribbons), better still, in a manner suited to current complimentary metal oxide semiconductor (CMOS) technology. This latter point is important because the semiconducting industry has invested billions in its current technology and so its use for the large-scale manufacture of graphene based high speed electronic devices and circuitry will make it economically viable.

Various routes exist to synthesize graphene and the number of routes is ever increasing. However, the primary routes are through graphite exfoliation, epitaxial graphene, graphene oxide and chemical vapour deposition. Most techniques, with the exception of epitaxial growth on SiC, have a serious draw back because one needs to transfer the graphene to a semiconducting support such as SiO_2 for further processing. Within our research here at the IFW we are developing a carbothermal reduction route which reduces SiO_2 to SiC and then forms graphene layers in a standard CVD reaction. Carbothermal reduction of silica is usually performed by placing silica in contact with solid carbon material. Our newly developed CVD carbothermal route does not utilize solid carbon but takes advantage of carbon species produced by the decomposition of hydrocarbons in a CVD reaction. Initial studies [1], show the reaction is possible at temperatures of 900°C using ethanol as the feedstock and amorphous SiO_2 as the source for crystalline SiO_2. An interesting aspect of this reaction is that sp^2 carbon layers form on the surface of the SiC (from the reduced SiO_2). The mechanism involved in this sp^2 layer formation is not clear at this stage. Our initial studies the bottom graphene layer's basal plane lies parallel to the underlying SiC surface. The data suggest precipitation processes may be occurring. Hence, it is conceivable if one can prepare a flat SiO_2 surface to reduce to SiC and form flat sp^2 layers, control of the layer formation will provide a simple route to form graphene and few layer graphene using CVD directly on a semiconducting surface. Figure 1 presents a simple illustration of the aim. Essentially an oxide layer is formed on a silicon wafer, for example poly-silicon which is often used in CMOS technology. The route potentially can be used for patterning graphene structures directly on silicon wafers.

We are also exploring the structural transformation or engineering of graphene via catalytic hydrogenation. This nano-engineering approach involves the dispersion of metallic nanoparticles onto a graphene or graphite sheet and their exposure to hydro-

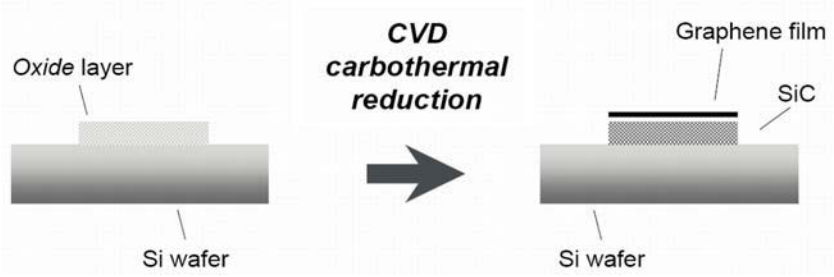

Fig. 1: Schematic representation of a patterned SiO_2 oxide structure on Si (right side) undergoing a carbothermal reduction process yielding SiC with graphene (or few lazer graphene) on its surface (right side).

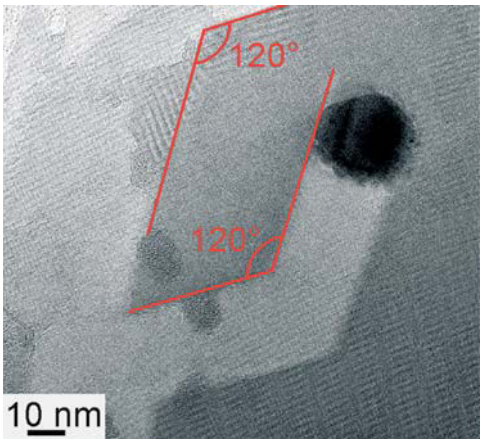

Fig. 2: Co catalyst particle residing at the head of an etch track in few layer graphene after having undergone a hydrogenation reaction.

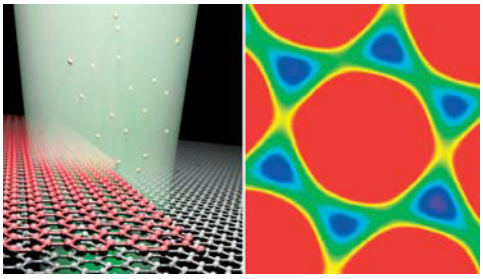

Fig. 3: *Left panel*: Schematic representation of carbon atoms being selectively sputtered off the edge of a graphene layer residing on another graphene layer. The process allows graphene restructuring. *Right panel*: False colour image of a single benzene ring from a graphene sheet. The image was acquired using an aberration corrected transmission electron microscope operating at 80 kV. Sub Ångstrom resolution is possible. The image clearly resolves the six carbon atoms forming the benzene ring. The inter-carbon atom spacing is 1.4 Å.

gen at elevated temperatures. In this process the catalyst helps to dissociate molecular hydrogen which then reacts with carbon (from the graphene) to form methane, leaving an etch track behind (see Fig. 2). From previous studies it is well known that methane is the only reaction product from this reaction. Catalytic hydrogenation has great advantages since it provides a means for the controlled cutting of graphene sheets with atomic precision to create structures of different shapes and sizes with defined edge structures. In contrast to scanning tunnelling microscope lithography technique it is intrinsic to the hydrogenation process to accurately etch along specific crystallographic directions. It also allows for greater angular precision at bends. Although catalytic hydrogenation reactions have been investigated for a long time the hydrogenation mechanism itself remains controversial. However, in order to be able to effectively utilize catalytic hydrogenation as a tool to design the desired graphene nanostructures, an improved understanding of the underlying mechanisms at the nanoscale is crucial. In our studies [2], etch active Co particles revealed an asymmetric hemispherical shape at the etch front and were faceted at the graphite-particle interface. This is a result of maintaining maximum surface contact with the graphite edges at the etching front. The particles where either hcp cobalt or cobalt oxides. Further we were able to directly image the etch tracks and identify the crystallographic etch direction from HRTEM to predominantly be [1010]. Additional studies in which a post-annealing step was introduced showed etch inactive Co particles encapsulated with graphitic shells. These findings point to an additional source of carbon, probably surface carbon species which can be mopped up by mobile catalyst particles. The data suggests that all catalysts, whether etch active or not, are actively producing methane and that this occurs at or near the surface of the catalyst particles. The results point against carbon dissolution mechanisms in the catalytic hydrogenation process and provide new insight into the catalytic hydrogenation of graphite at an atomic level.

Another attractive route to tailor the edges of patterned graphene structures or simply etch large areas of graphene is through electron beam etching. With the emergence of aberration corrected electron lenses, atomically accurate electron beam etching of graphene is now truly feasible. Recent studies of ours show the edge states of graphene can be etched in a controlled manner using low voltage e-beam irradiation in TEM [3]. This is illustrated in Fig. 3 (left panel). Indeed using low voltage high resolution TEM we are able to examine the structural reconstruction at the atomic level with sub Ångstrom resolution (see Fig. 3, right panel). We find preferential termination for graphene layers along the zigzag orientation for large hole sizes. The temporal resolution can also be reduced to a record breaking 80 ms, enabling real-time observation of the reconstruction of carbon atoms during the sputtering process. In addition, the electron-beam induces rapid displacement of monolayers, fast elastic distortions and flexible bending at the edges of graphene sheets. These results disclose how energy transfer from the electron beam to few-layer graphene sheets leads to unique structural transformations.

References

[1] A. Bachmatiuk, F. Börrnert, M. Grobosch, F. Schäffel, U. Wolff, A. Scott, M. Zaka, J.H. Warner, R. Klingeler, M. Knupfer, B. Büchner, M.H. Rümmeli, ACS Nano, 3 (2009) 4098

[2] F. Schäffel, J.H. Warner, A. Bachmatiuk, B. Rellinghaus, B. Büchner, L. Schultz, M.H. Rümmeli, Nano Research 2 (2009) 695

[3] J.H. Warner, M.H. Rümmeli, L. Ge, T. Gemming, B. Montanari, N.M. Harrison, B. Büchner, G.A.D. Briggs, Nature nanotechnology 4 (2009) 500

Cooperation

[1] Oxford Univ., UK; West Pomeranian Univ. of Technology, Szczecin, Poland; TU Dresden, Dresden, Germany

Funded by DFG, EU

Magnetic resonance excitations in the heavy fermion compound $YbRh_2Si_2$

V. Kataev, U. Schaufuß, A. A. Zvyagin[1], J. Sichelschmidt[2], J. Wykhoff[2], C. Krellner[2], C. Geibel[2], F. Steglich[2], B. Büchner

In $YbRh_2Si_2$ conduction band electrons have a strongy enhanced effective mass due to the Kondo effect. The electronic properties of this heavy fermion system can be tuned by magnetic field *B* and temperature *T*. By studying the high-field electron spin resonance response across a (*B*,*T*)-crossover line that separates different electronic regimes in $YbRh_2Si_2$ we have found that the signal is given essentially by the resonance of heavy fermions, providing thus direct experimental access to the dynamics of heavy quasiparticles in the Kondo state.

In intermetallic compounds comprising a lattice of magnetic rare-earth or actinide ions quantum interactions between the local $4f(5f)$ magnetic moments and conduction electrons may lead to a formation of so-called heavy fermions at low temperatures, i.e. conduction electrons with a strongly enhance effective mass. This is the result of the so-called Kondo effect. It yields the screening of local magnetic moments by conduction electrons thereby "dissolving" the *f*-spins into the sea of conduction electrons and hence transforming conducting electrons into heavy fermion quasiparticles. Heavy fermion compounds may exhibit a variety of phases and behaviors such as, e.g., exotic superconducting or magnetic states, unusual metal-insulator transitions, and strong deviations of electronic properties from a conventional Fermi liquid (FL) metal known as a non Fermi liquid (NFL) behavior. In these materials magnetic instability may arise due to a competition of the Kondo effect and the so-called RKKY-interaction between the *f*-states and conduction electrons that favors a magnetically ordered ground state. A prominent example of such class of systems is the intermetallic compound $YbRh_2Si_2$ (see, e.g., Ref. [1] and references therein). Here the competition between these two interactions can be tuned by a magnetic field *B* and temperature *T*. In $YbRh_2Si_2$ the heavy fermion state is confined to temperatures and fields $T < T_0 \approx 25$ K and $B < B^* \approx 10$ T, respectively (Fig. 1). In this regime the local 4*f*-spins should be quenched due to the Kondo effect rendering the electron spin resonance (ESR) of Yb^{3+} ions unobservable. Yet, surprisingly, a sharp anisotropic ESR signal resembling the ESR of well localized Yb^{3+} spin states has been experimentally observed [4].

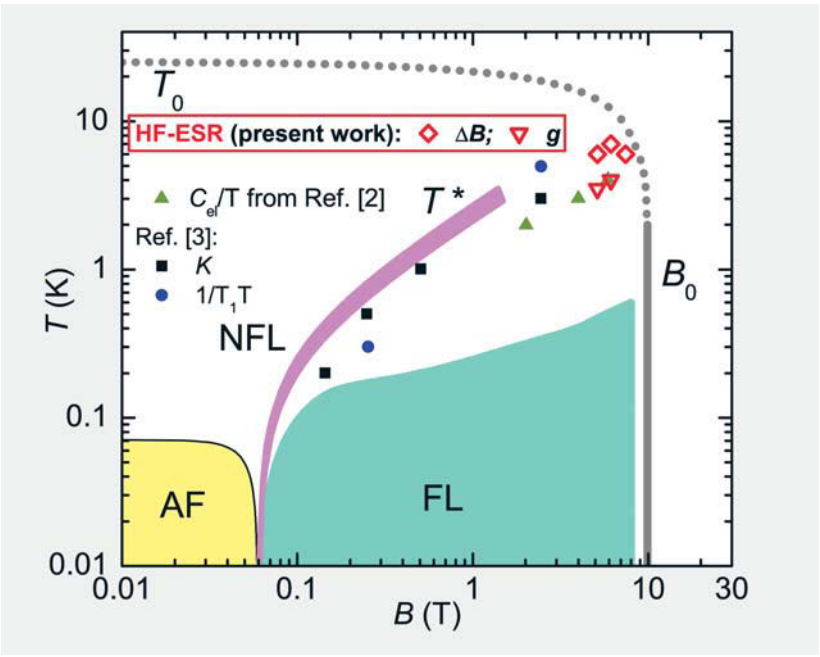

Fig. 1: Schematic phase diagram of $YbRh_2Si_2$ for $B \perp c$-axis from Refs. [1,5]. Dash and solid gray lines delineate the heavy fermion state confined to the region $T < T_0 \approx 25$ K and $B < B^* \approx 10$ T. The FL region denotes the $T - B$ domain where the electrical resistivity follows the Fermi liquid behavior $\sim T^2$. The broad (pink) line depicts the thermodynamic and Hall effect FL-NFL crossover line. Closed symbols depict $T(B)$-crossover temperatures below which specific heat (C_{el}/T) [2] and ^{29}Si-NMR Knight shift K and relaxation rate $1/(T_1T)$ [3] become temperature independent as expected in the FL regime. Open red symbols display crossover temperatures from the HF-ESR $g(T,B)$- and $\Delta B(T,B)$ dependences (see the text and Ref. [5]).

To unravel the nature of this unexpected resonance excitation we have studied the ESR response in that part of the $T(B)$ phase diagram of $YbRh_2Si_2$ where a remarkable crossover between the NFL regime at low temperatures and small fields to the FL state at higher temperatures and stronger fields close to the breakdown of the heavy fermion behavior takes place (Fig. 1). Detailed presentation of our work can be found in Ref. [5]. These experiments have become possible in the high-field ESR (HF-ESR) laboratory recently built at the IFW Dresden. In contrast to standard commercial ESR spectrometers our instrumentation enables high sensitive measurements in a very broad frequency range $\nu = 10$ GHz – 1 THz in magnetic fields up to 17 T.

In agreement with previous low-frequency ($\nu < 34$ GHz) low field ($B < 1$ T) ESR studies [4], at high fields a strongly anisotropic ESR line can be observed below $T \sim 25$ K. In Figs. 2 and 3 we show the T-dependences of the g-factor $g = h\nu/(\mu_B B_{res})$ and the width ΔB of this line, respectively, for the frequencies $\nu =$ 93, 249, 297, and 360 GHz. Here B_{res}, h and μ_B are the resonance field, the Planck constant and the Bohr magneton, respectively. The corresponding resonance fields amount to $B_{res} \approx 1.85$, 5.15, 6.15, and 7.45 T, respectively. At a fixed frequency ν, the g-factor (Fig. 2) increases approximately as $\ln(T)$ at high temperatures for all frequencies. The rate of this increase is smaller for the higher frequency/magnetic field and the $g(T)$ dependence shows a saturation tendency below ~ 4 – 5 K for $B_{res} \sim 5.15$ T and 6.15 T (marked by arrows in Fig. 2).

The $\Delta B(T)$-dependence [Fig. 3(a)] can be described as a sum of three contributions $\Delta B(T) = a + bT + c/(\exp(\Delta_{ex}/T)-1)$. Here a depicts a T-independent contribution due to various kinds of inhomogeneities, bT stands for the relaxation broadening via electronic degrees of freedom, and the last term has been assigned to a relaxation channel via an excited doublet state of Yb^{3+} ions at an energy Δ_{ex} above the ground state. At $\nu = 93$ GHz and $B_{res} \approx 1.85$ T the data points closely follow this dependence in the entire temperature range of study [solid lines in Fig. 3(a)]. However, further increase of the frequency and magnetic field gives rise to a deviation from this dependence at $T \sim 7$ K, namely ΔB begins to decrease more rapidly. This feature is more clearly seen in the plot representation ΔB vs. T^2 [Fig. 3(b)]. Note that such a hump in the $\Delta B(T)$-dependence occurs closely to the temperature region where the g-factor begins to saturate (Fig. 2).

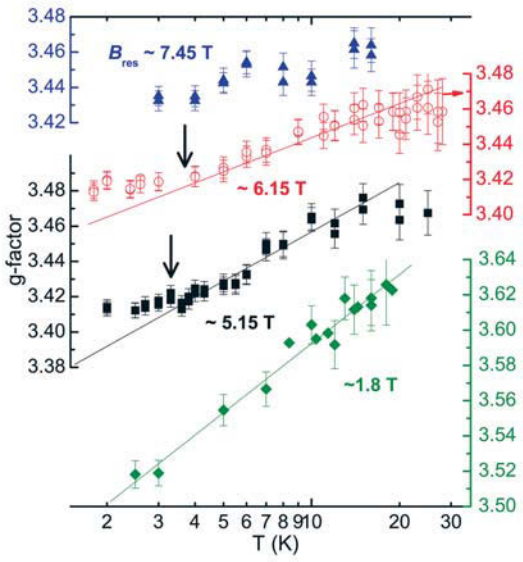

Fig. 2: Temperature dependence of the g-factor for $B \perp c$-axis at ν = 93, 249, 297, and 360 GHz (from bottom to top), which correspond to resonance fields as indicated. Arrows indicate a crossover from a -ln$T$ to g = const behavior (see also Ref. [5]).

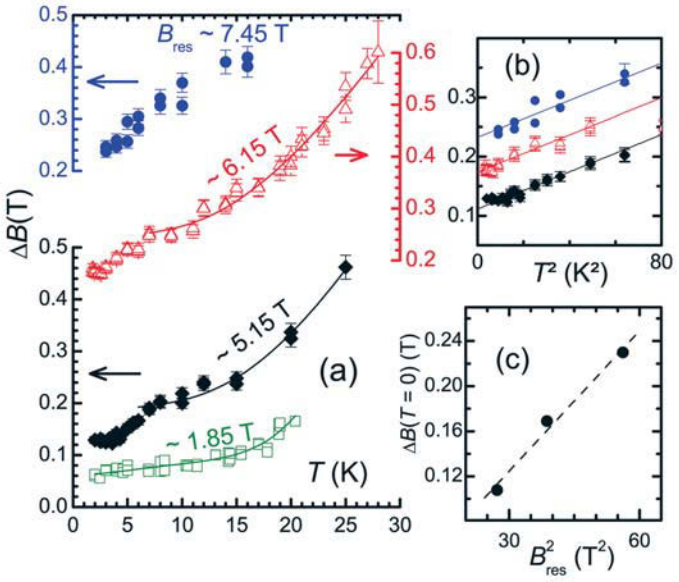

Fig. 3: (a) Temperature dependence of the HF-ESR linewidth ΔB for $B \perp c$-axis at ν = 93, 249, 297, and 360 GHz (from bottom to top), which correspond to resonance fields as indicated. Solid lines are fits (see the text and Ref. [5]); **(b)** Corresponding low temperature data in the representation ΔB vs T^2. Solid lines are fits to the T^2 dependence; **(c)** Residual HF-ESR linewidth at $T = 0$ vs. B^2 in the FL regime of $YbRh_2Si_2$ obtained from the T^2 fits in panel (b).

Remarkably, as can be seen in Fig. 1, the characteristic crossover temperatures in the behavior of the g–factor and the linewidth ΔB fall into the crossover line that separates the electronic regime of the development of the heavy fermion state below the Kondo temperature $T_0 \approx 25$ K followed by the formation of the NFL behavior at higher T from the FL regime at lower T and higher B (pink line and data points in Fig. 1). Furthermore, the HF-ESR data points continue this line towards the crossover line for the breakdown of the heavy fermion state (gray dash line in Fig. 1). The fact that characteristic changes in the HF-ESR observables occur at the crossover between the NFL and FL regimes in the Kondo state strongly suggests that ESR in $YbRh_2Si_2$ is given by the resonance response of the heavy electrons to microwaves and as such it has distinct properties in the FL and NFL regimes. (For a detailed discussion see Ref. [5]).

Strong experimental indications for the occurrence of a novel kind of ESR excitation in a correlated quantum metal obtained in our HF-ESR experiments on $YbRh_2Si_2$ have stimulated intensive theoretical work [6-9]. We refer here briefly to just the two pioneering works on this subject [6-7] that treat the ESR response of a Kondo lattice system in the framework of the Anderson lattice model. In both theories the ESR is considered as the response due to the collective excitations, i.e., quasiparticles, which appear owing to the hybridization of the f-electron (localized levels) with the conduction band electrons. In particular, both theories predict for the Fermi liquid phase with ferromagnetic interactions a sharp ESR line only slightly shifted from the position expected for the local $4f$ resonance of Yb^{3+} ions. The narrowing of the signal takes place by a factor of the heavy fermion mass enhancement m/m^* [6], or is due to the action of only the anisotropic part of the electron-electron interaction [7]. Remarkably, both theories predict for the FL regime a T^2 and B^2 dependence of the linewidth ΔB and a temperature independent g-factor. Indeed, these signatures have been observed in the HF-ESR experiment: The g-factor tends to a T-independent value in the FL phase (Fig. 2) where the ΔB closely follows a T^2-dependence [Fig. 3(b)]; The B^2-behavior appears in the dependence of the extrapolated residual linewidth at $T = 0$ [Fig. 3(c)]. Moreover, the theory in Ref. [7], which considers also the non Fermi liquid regime, predicts a logarithmic in T dependence of the g-factor in the NFL phase, in a nice agreement with our experimental observation (Fig. 2).

References

[1] P. Gegenwart *et al.*, Nature Phys. **4** (2008) 186
[2] O. Trovarelli *et al.*, Phys. Rev. Lett. **85** (200) 626
[3] K. Ishida *et al.*, 2002 Phys. Rev. Lett. **89** (2002) 107202
[4] J. Sichelschmidt *et al.*, Phys. Rev. Lett. **91** (2003) 156401; J. Wykhoff *et al.*, Physica C **460-462** (2007) 686
[5] U. Schaufuß *et al.*, Phys. Rev. Lett. **102** (2009) 076405
[6] E. Abrahams and P. Wölfle, Phys. Rev. B **78** (2008)104423 (2008).
[7] A. Zvyagin *et al.*, Phys. Rev. B. **80** (2009) 024412
[8] P. Schlottmann, Phys. Rev. B **79** (2009) 045104
[9] B. Kochelaev *et al.*, Eur. Phys. J. B **72** (2009) 1434-6028

Cooperation

[1]B.I. Verkin Institute for Low Temperature Physics and Engineering, Kharkov, Ukraine
[2]Max Planck Institute for Chemical Physics of Solids, Dresden, Germany

Funded by DFG

Shape memory effect in CuZr-based bulk metallic glass matrix composites

S. Pauly, G. Wang, U. Kühn, N. Mattern, T. Gemming, A. Gebert, L. Schultz and J. Eckert

Bulk metallic glasses (BMGs) are interesting from both scientific and engineering aspects because of their high yield strength and large elastic limit, which are certainly desirable characteristics for many applications. However, if the catastrophic fracture behaviour of bulk metallic glasses cannot be overcome their potential to be used in structural parts will never be exploited. We report here on CuZr-based BMG matrix composites, which contain shape memory crystals, leading to an exceptional deformation behaviour and a significant improvement of the mechanical properties.

Plastic deformation in BMGs is highly localised in shear bands with a thickness of only a few nanometres, which severely limits the plastic deformability [1]. There are different approaches how to introduce a somewhat more homogeneous plastic strain in glassy materials among them the synthesis of BMG matrix composites [2]. However, the increase in plasticity does not necessarily go along with work hardening, another necessity from an engineering point of view [3, 4].

Among the diversity of BMGs [5], CuZr-based alloys are peculiar under two aspects: Firstly, their melts have a relatively strong tendency to solidify into a glassy structure. Even binary and ternary glassy alloys can be obtained in the Cu-Zr system [6]. Secondly, crystalline B2 CuZr (P*m*-3*m*) shows the shape memory effect [7]. The cubic primitive B2 structure can undergo a reversible transformation to a monoclinic B19' (C*m* and $P2_1/m$) structure [8]. Both peculiarities can be made use of by synthesising BMG matrix composites in CuZr-based alloy systems, e.g. $Cu_{47.5}Zr_{47.5}Al_5$. Even tough B2 CuZr is only stable at temperatures above 988 K proper alloy composition and cooling rates allow for precipitation of B2 CuZr in a glassy matrix. In order to understand and model the mechanical properties of BMG matrix composites containing the B2 phase it is vital to also prepare and analyse the response of this crystalline phase to mechanical loading, which was conducted in this work.

Fig. 1 shows the true stress-strain curves of selected $Cu_{47.5}Zr_{47.5}Al_5$ specimens with different crystalline volume fractions. The inset to Fig. 1 shows three typical microstructures of the composites with different crystalline volume fractions. The larger the amount of the crystalline phase in the composites (i) the lower the yield stress, (ii) the larger the plasticity and (iii) the more pronounced the work hardening. This behaviour becomes obvious when the yield stress (Fig. 2(a)) and the fracture strain (Fig. 2(b)) are plotted as a function of the crystalline volume fraction. At crystalline volume fractions up to 10 vol.% the BMG matrix composite can be described by the rule of mixtures (ROM) since the matrix has a yield strength much higher than that of the second phase. Yielding of the composite is therefore controlled by yielding of the relatively harder glassy $Cu_{47.5}Zr_{47.5}Al_5$ phase:

$$\sigma^c = f_\alpha \sigma^\alpha + f_\beta \sigma^\beta, \quad (1)$$

where f and σ are the volume fraction and the yield strength of the constituent phases, and subscript/superscript α and β refer to B2 CuZr and the BMG, respectively.

At crystalline volume fractions exceeding 50 vol.% the composite can be modelled as a crystalline matrix reinforced with glassy $Cu_{47.5}Zr_{47.5}Al_5$. In this case, the load-bearing model captures the yield stress [9]:

$$\sigma^c = \sigma^\alpha (1 + 0.5 f_\beta). \quad (2)$$

Between those two limiting cases there is a transition determined by a critical crystalline volume fraction (v_{crit}), which has a physical meaning similar to the percolation threshold used to quantify the formation of long-range connectivity in random systems [10].

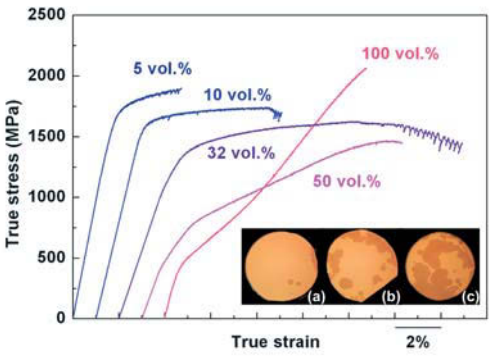

Fig. 1: True stress-strain curves of $Cu_{47.5}Zr_{47.5}Al_5$ BMG matrix composites with different crystalline volume fractions. The inset shows the microstructures of rods with a diameter of 2 mm and crystalline volume fractions of (a) 5 vol.%, (b) 30 vol.% and (c) 50 vol.%.

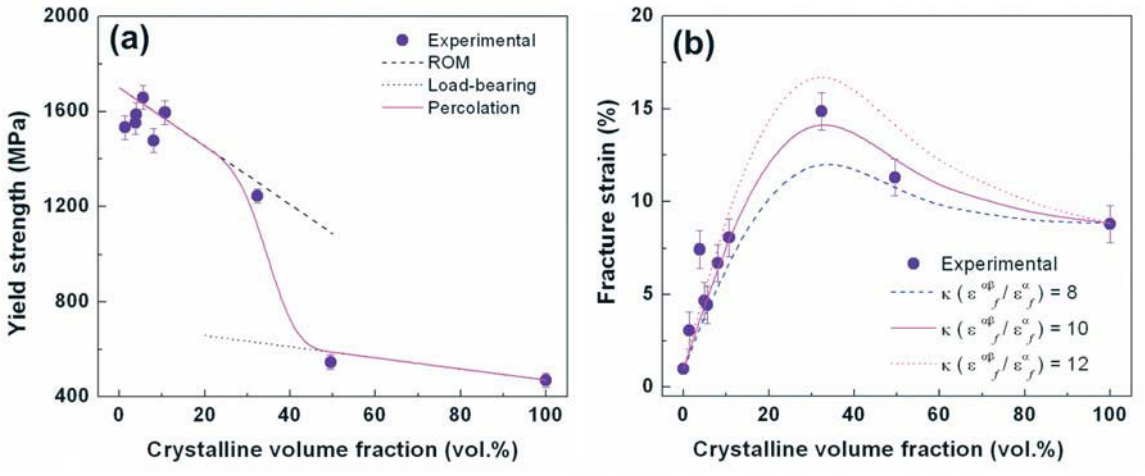

Fig. 2: (a) Experimental and calculated values for the fracture strain as a function of the crystalline volume fraction and (b) yield strength versus crystalline volume fraction of the $Cu_{47.5}Zr_{47.5}Al_5$ BMG matrix composites.

In the present case, v_{crit} lies between 30 and 50 vol.%. At the critical volume fraction the crystals interconnect and form a structural framework. This can be readily seen in the micrographs of the rods (inset to Fig. 1).

The fracture strain versus crystalline volume fraction is displayed in Fig. 2(b). We adapt the empirical approach developed by Fan and Miodownik to model the dependence of fracture strain on the crystalline volume fraction [11]. The composite is topologically transformed into a three-microstructural-element body, viz. the B2 phase (α), the glassy phase (β) and phase consisting to equal parts of α and β ($\alpha\beta$). Physically, the $\alpha\beta$-element can be regarded as effective interface between the α and the β phase. The fracture strain can then be described by:

$$\varepsilon_f^c = f_{\alpha c}\,\varepsilon_f^{\alpha} + f_{\beta c}\,\varepsilon_f^{\beta} + \kappa f_{\alpha\beta}\,\varepsilon_f^{\alpha\beta}, \qquad (3)$$

where $f_{\alpha c}$, $f_{\beta c}$, and $f_{\alpha\beta}$ are the corrected volume fraction of element α, β, and $\alpha+\beta$, ε_f^{α}, ε_f^{β}, and $\varepsilon_f^{\alpha\beta}$ are the fracture strain of α phase, β phase, and homogenous $\alpha+\beta$ composite, respectively, and κ is a dimensionless constant accounting for the constraint effect of the element α and/or element β on the element $\alpha+\beta$ [12]. Regardless of the value for $\kappa(\varepsilon_f^{\alpha\beta}/\varepsilon_f^{\alpha})$ equation (3) is capable to capture the measured fracture strains. The best fit is obtained with $\kappa(\varepsilon_f^{\alpha\beta}/\varepsilon_f^{\alpha}) = 10$.

The pure B2 CuZr phase exhibits a pronounced hardening behaviour and a surprisingly large plasticity for an intermetallic compound reminiscent of TRIP (transformation-induced plasticity) materials (Fig. 1). The deformation of the crystalline specimens was monitored *in-situ* with high energy X-rays to follow the evolution of structural changes. Fig. 3 shows a 2D diffraction image of the undeformed (left half) and deformed sample at a stress of 1100 MPa (right half). The integrated 2D diffraction data is shown in the inset to Fig. 3. At a stress of 0 MPa the Bragg reflections correspond to B2 CuZr, when the stress reaches 1100 MPa new Bragg peaks can be detected, which are allocated to B19′ CuZr (martensite). Obviously, the work hardening of the B2 phase must be attributed to the martensitic transformation from B2 CuZr to B19′ in the fully crystalline sample. Remarkably, even for low volume fractions the work hardening of the B2 crystals leaves its fingerprints in the stress-strain curves of the composite material.

The elastic properties of the glassy and the B2 phase were furthermore analysed by ultrasonic measurements. Surprisingly, all three, Young's, shear and bulk modulus of the glassy and the crystalline B2 phase are nearly identical (Table I). In other words: though being structurally completely different the glassy and crystalline phases are highly compatible. We believe that the good match of the shear moduli facilitates the slip transfer from the matrix to the B2 crystals. The glassy matrix deforms by shear banding and

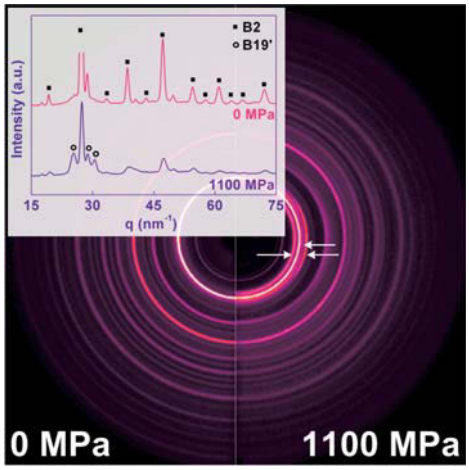

Fig. 3: 2D diffraction image of the fully crystalline $Cu_{47.5}Zr_{47.5}Al_5$ sample unstressed (left half) and at 1100 MPa. The arrows show the strongest peaks of the new phase (B19'), which forms induced by plastic deformation. The inset shows the integrated 2D diffraction images in the undeformed (upper pattern) and deformed (lower pattern) state. Note, that the strongest reflection of B2 CuZr has been cut off in the upper diffraction pattern.

the shear is imposed on the crystalline phase when a shear band reaches the interface with a crystal. The propagation of shear band will be inhibited by the deformation and work-hardenability of the B2 phase, which results in the nucleation of more shear bands.

Table I: Elastic properties of B2 CuZr and the glassy phase in $Cu_{47.5}Zr_{47.5}Al_5$.

Phase	E [GPa]	ν	G [GPa]	B [GPa]
B2 CuZr	82 ± 2	0.385 ± 0.004	29 ± 1	118 ± 3
Glass	89 ± 2	0.373 ± 0.003	33 ± 2	117 ± 3

References

[1] E. Pekarskaya, C.P. Kim, W.L. Johnson. *J. Mater. Res.* 16 (2001) 2513.
[2] J. Eckert, J. Das, S. Pauly, C. Duhamel. *J. Mater. Res.* 22 (2007) 285.
[3] H. Li, G. Subhash, L.J. Kecskes, R.J. Dowding. *Mater. Sci. Eng. A.* 403 (2005) 134.
[4] Y.C. Kim, E. Fleury, J.C. Lee, D.H. Kim. *J. Mater. Res.* 20 (2005) 2474.
[5] A. Inoue. *Acta Mater.* 48 (2000) 279.
[6] A. Inoue, W. Zhang. *Mater. Trans.* 43 (2002) 2921.
[7] Y.N. Koval, G.S. Firstov, A.V. Kotko. *Scripta Metall. Mater.* 27 (1992) 1611.
[8] D. Schryvers, G.S. Firstov, J.W. Seo, J. van Humbeeck, Y.N. Koval. *Scripta Mater.* 36 (1997) 1119.
[9] V.C. Nardone, K.M. Prewo. *Scripta Metall.* 20 (1986) 43.
[10] D. Stauffer and A. Aharony, *Introduction to percolation theory* (Taylor and Francis, London, 1992).
[11] Z. Fan, A.P. Miodownik. *Scripta Metall. Mater.* 28 (1993) 895.
[12] G. Liu, J. Sun, C.W. Nan, K.H. Chen. *Acta Mater.* 53 (2005) 3459.

Cooperation Xi'an Jiaotong University (China), Yonsei Univ. and Sejong Univ. (South Korea), HASYLAB at DESY Hamburg.

Funded by The Global Research Laboratory Program of the Korean Ministry of Education, Science and Technology and the program "Promotionsförderung des Cusanuswerks".

High strength conductors: Non-destructive pulsed field CuAg-solenoids

J. Freudenberger, M. Frey, A. Gaganov, H. Klauß, J. Lyubimova, L. Schultz, D. Seifert, T. Wolf

Ultra strong CuAgZr conductors were developed and tested in pulsed high field magnets. Based on the materials properties a coil featuring additional internal reinforcement layers was designed and tested. In combination with refined computer simulation techniques significant progress was made concerning pulsed magnet applications. The coil generated a flux density of 66 T without being destroyed.

Introduction

The development of non-destructive pulsed high-field solenoids is crucial for reproducible studies under extreme conditions involving high external magnetic fields. The maximum flux density that is presently available with these kinds of magnets is in the order of 90 T. However, there are numerous activities to increase this value.

Commonly, high field solenoids are wound from a highly strengthened conductor material, which is insulated and reinforced. The conductor-reinforcement composite is required to have a high strength to withstand the Lorentz forces during the pulse. The conductor is required to possess a high electrical conductivity in order to minimise ohmic heating and energy losses. A high fatigue strength of the wire helps to guarantee a long lifetime of the coil. These material properties have to be met at the same time in a single conductor material to make it suitable for pulsed high field applications. The present CuAgZr (i.e. Cu-Ag7-Zr0.05 in wt.%) alloys meet these requirements. For details concerning the preparation process and microstructural features please refer to [1].

The coil design is naturally affected by the desired magnet specifications, such as the peak field, pulse duration and inner bore. Pulsed magnets with a relatively short pulse duration (less than 100 ms) and magnetic fields up to 70 T are usually designed as a solenoid. Longer pulses and higher fields result in large magnets with several sections.

Coil winding

The coil was initially designed using PMDS 2.1 and further refined using finite element simulations; the commercial programs COMSOL and ANSYS. The coil is wound from a CuAgZr wire with a cross section of 3.69 mm x 2.46 mm; corner radius: 0.62 mm. The bore of the coil is 9 mm, which means that about 8 mm are available for experiments. The length of the winding section is 75 mm. The wire is insulated with Kapton™. The first five layers of conductor are reinforced using Zylon. The thickness of the reinforcement layer is adjusted to reduce the peak stress in the conductor at peak field below the ultimate tensile strength. The last layer of the coil is reinforced using carbon fibre. After winding, the coil was vacuum impregnated. An axial pre-stress of about 100 MPa has been applied, which is beneficial for the pulsed magnets in the sense of stress development during the pulse.

Coil modelling

The temperature and current density distribution during the discharge is evaluated using an FEA model. An axisymmetric model is used to increase accuracy and reduce the simulation time. In principle, the FEA model solves for the magnetic diffusion and thermal diffusion equations:

$$\sigma \frac{\partial \vec{A}}{\partial t} + \nabla \times \mu_0^{-1} \nabla \times \vec{A} + \sigma \nabla V = 0$$

$$\rho \cdot C \frac{\partial T}{\partial t} - \nabla \cdot (k \nabla T) = \frac{J^2}{\sigma}$$

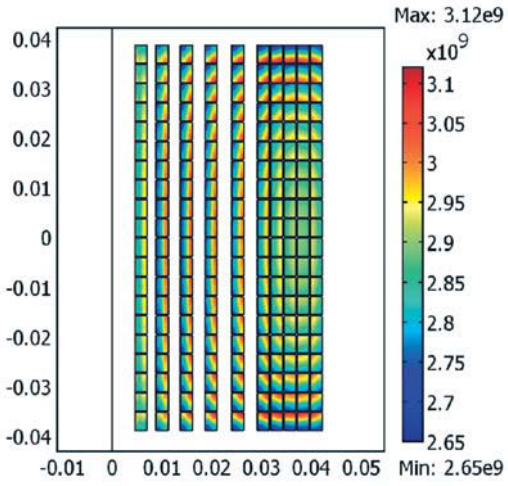

Fig. 1: Cross section of the coil showing the current density distribution within the conductor material at peak field. The current density (right colour map) is in A/m^2.

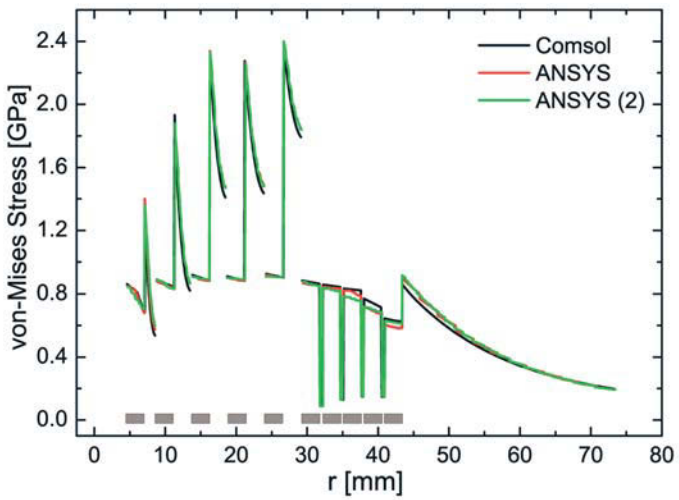

Fig. 2: Von-Mises stress across the radius at the centre of the coil. Results were obtained with COMSOL and ANSYS using a bi-linear (index 1) and multi-linear stress-strain model (index 2).

σ is the electrical conductivity, $\vec{A}$ the magnetic vector potential, V the voltage applied to a turn, J the current density, k the heat conductivity, C the heat capacity, ρ the density and T the temperature. The heating Q in the model is calculated by

$$Q = \frac{J^2}{\sigma}$$

The material properties are modelled as functions of the temperature. The electrical conductivity of the conductor was determined to be 70% and 210% IACS at room temperature and 77K, respectively.

An advantage of the FEA simulation is that the current density distribution can be evaluated for the entire cross-sectional area of the coil, which is shown at 4.8 ms at peak field in Figure 1. The current density varies by about 15% at peak field.

It can be seen that the current density distribution is similar for all turns in shape and magnitude. Equally steep gradients in the current density can be observed, though the gradients arise in a different direction for the outer turns. Whereas for turns close to the centre plane the gradients are in the radial direction, for turns further away an axial gradient exists. This is particularly pronounced for the turns close to the end flanges.

The mechanical stresses in the coil are evaluated using an elasto-plastic axisymmetric model of the coil. The centre plane of the coil is assumed to be a symmetry plane. The body force $\vec{F} = \vec{J} \times \vec{B}$ is applied as a body load to the individual turns of the coil. Stresses occurring because of different temperatures and different thermal expansion coefficients are considered as well.

It was verified that the highest stresses occur at peak field, which is not immediately obvious due to the fact that the changes in current density distribution across a turn lead to changes in the body force. Figure 2 shows the von-Mises stress plotted along the centre plane of the coil, which is where the stresses are highest. The stresses were calculated for a peak field of 70 T using a multi-linear stress-strain model (ANSYS) and by using a bilinear stress-strain model (COMSOL). The result illustrates that both models yield a similar approximation.

The thickness of the individual reinforcement layers was adjusted to lower the stress in the conductor below the ultimate tensile strength, which was measured to be 1.1 GPa in the case of CuAgZr. For safety reasons 900 MPa were used in the model. The stress in the reinforcement fibre is still fairly moderate in comparison to the reported UTS of the fibre composite (i.e. 4 GPa at 77 K). In order to achieve a good load transfer between

conductor and fibre a minimum strain at break of about 3% is necessary. Simple FEA simulations show that for achieving the highest possible stress in both, the conductor and the reinforcement, the conductor needs to be able to tolerate this strain.

Coil test

The coil is energised by a 0.8 MJ capacitor bank at the Clarendon Laboratory in Oxford, UK. The coil was tested carefully over 44 pulses. The maximum field obtained during the coil test was 66 T at a peak voltage of 6500 V using 24 mF (i.e. a total energy of 507 kJ). This constitutes a new high field record for the Clarendon Laboratory. The rise time of the pulse is about 4.4 ms and the total pulse length about 12.6 ms, which is shown in Figure 3.

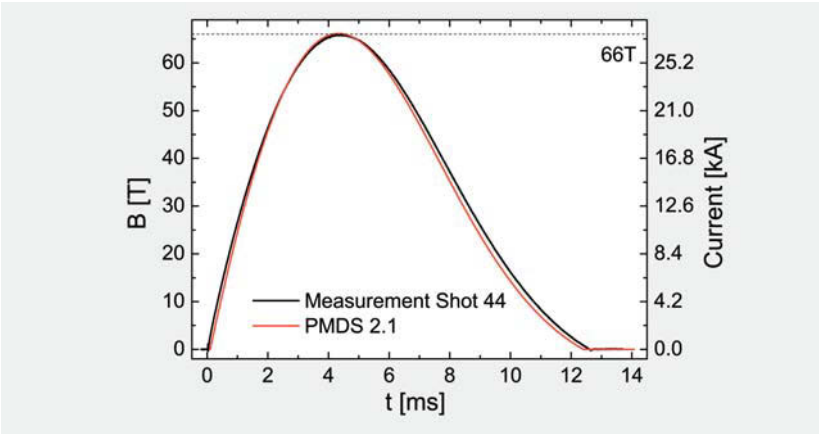

Fig. 3: 66 T discharge

The inductance of the coil measured after each pulse showed an irreversible change of 1.85 %. It was verified in subsequent pulses that the inductance is stable.

Coil performance

High field pulsed solenoids can benefit from highly optimised materials. The characterisation of the materials is a key issue to support modelling of pulsed high field solenoids. Not every conductor is compatible with every reinforcement. Soft materials and conductors with intermediate strength possess enough margin in terms of strain to be combined with any type of reinforcement. High strength conductors are more challenging, as little is gained when reinforcing them using a high strength fibre. Despite this, a coil has been designed and tested successfully using a high strength CuAgZr conductor. The coil relies on optimally placed internal reinforcement layers; at peak field the conductor is stressed to its mechanical limit. The coil generated a record field of 66 T. Finite element calculations suggest that the coil design can generate fields up to 70 T and is therefore in good agreement with the experimental findings. The results show that even a high strength conductor such as CuAgZr can be reinforced using high strength fibres.
Although the results are promising there are still big challenges to be faced. Future work should concentrate on reducing the electrical resistivity of CuAgZr, which would flatten the path to higher fields. Alternatively, the load in the fibre could be increased, which would require a conductor with a larger plastic strain. Both aspects can be addressed by the optimisation of the thermo-mechanical treatment of the CuAgZr alloy, which is under progress. We believe that a material with a conductivity of about 70 % IACS and the highest possible ultimate tensile strength at a plastic strain of 3 % may be the ideal compromise for pulsed high field applications.

References

[1] A. Gaganov et al., Mat. Sci. Eng. A 437 (2006) 313
[2] U. F. Kocks et al., Prog. Mater. Sci 19 (1975) 1

Cooperation Univ. of Oxford, UK; Univ. of Ottawa, Canada
Funded by DFG, FR 1714/2

Rolled-Up Metamaterials

E. J. Smith, Y. F. Mei, and O. G. Schmidt

By combining the idea of creating metamaterials through alternating stacked layers of a metal and an oxide with rolled-up technology, we explore different realizable devices. By releasing strained nanomembrane bi-layers grown on photoresist-patterned Si wafers, three dimensional, rolled-up, optically plasmonic metamaterials can be created. The resulting stacked metal-oxide bi-layers allow for the guidance and coupling of surface plasmons which leads to the transmission of sub-wavelength information in such devices as the hyperlens and metamaterial fiber optics.

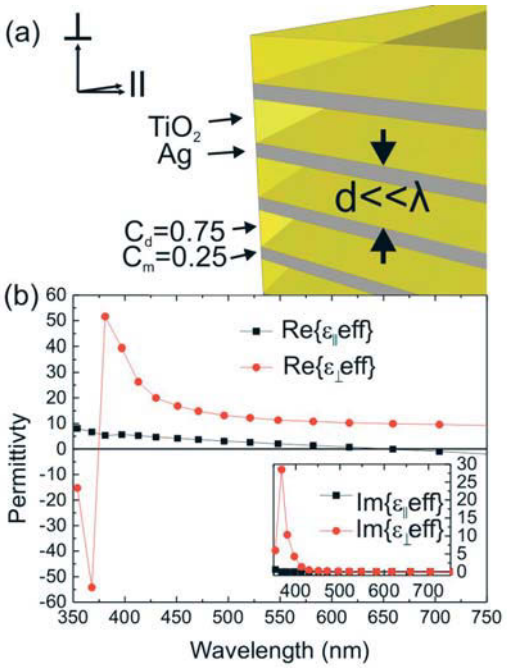

Fig. 1: (a) A plasmonic metamaterial can be created by stacking alternating layers of a metal and an oxide whose overall bi-layer thickness is much smaller than the incident wavelength ($d << \lambda$). This lattice structure allows for the manipulation of the material's permittivity, leading to an anisotropic plasmonic metamaterial (differing in the parallel and perpendicular axis). (b) This is illustrated by using the effective media theory to calculate the permittivities of a stacked system comprised of a 3:1 ratio of TiO_2:Ag.

Introduction

Metamaterials are man-made materials which exhibit optical effects that are naturally nonexistent. By combining two unlike materials on a sub-wavelength lattice, one is able to create new materials which can lead to the development of devices with negative index of refraction [1], "invisibility" cloaking devices [2], sub-wavelength imaging devices (hyperlens) [3-5], and new ways of guiding light (metamaterial fiber optics) [6] to name a few. Plasmonic metamaterials function through the manipulation of the permittivity (ε) of a material and are achievable by growing alternating layers of oxides and plasmonic metals with a bi-layer thickness much smaller than the working wavelength of light ($d << \lambda$). These materials are of interest because of their ability to transmit sub-wavelength information; which in turn can lead to the miniaturization and increased sensitivity of communication and biological sensing devices. In this highlight we discuss our recent work on the investigation and realization of rolled-up metamaterials.

Stacking bi-layers of a metal and an oxide leads to an anisotropic metamaterial media as shown in Fig. 1(a). The result is a different permittivity in the tangential and parallel plane of the stacked layers which allow for plasmons to couple through or propagate along the metal and oxide layers. The resulting permittivity of these stacked bi-layers can be calculated by using an effective media theory [7] $\varepsilon_{||} = (c_m\varepsilon_m + c_d\varepsilon_d)/(c_m + c_d)$ and $\varepsilon_{\perp} = [(c_m + c_d)\varepsilon_m\varepsilon_d]/(c_d\varepsilon_m + c_m\varepsilon_d)$, where ε_m is the permittivity of the metal, ε_d is the permittivity of the dielectric, c_m and c_d are the relative ratios of the metal and dielectric for a single bi-layer ($c_m + c_d = 1$). In Fig. 1(b), the effective permittivity for a 3:1 ratio of a TiO_2:Ag stacked lattice is given for the perpendicular and parallel plane of the metamaterial. The inset of Fig. 1(b) shows the imaginary part of the permittivities which accounts for loss in the system. One way of creating these metamaterials is by simply growing layer after layer on top of one another, which leads to a well-established planer configuration. However, if we grow a single strained bi-layer of metal and oxide on a sacrificial layer, upon releasing of the sacrificial layer, we can obtain a rolled-up metamaterial whose overall permittivity can be expressed simply by the coordinate change:

$$[\varepsilon^{eff}] = \begin{bmatrix} \varepsilon_{\perp}\cos^2(\theta) + \varepsilon_{||}\sin^2(\theta) & (\varepsilon_{\perp} - \varepsilon_{||})\sin(\theta)\cos(\theta) & 0 \\ (\varepsilon_{\perp} - \varepsilon_{||})\sin(\theta)\cos(\theta) & \varepsilon_{\perp}\sin^2(\theta) + \varepsilon_{||}\cos^2(\theta) & 0 \\ 0 & 0 & \varepsilon_{||} \end{bmatrix}$$

Rolled-Up Hyperlens

One of the devices which was investigated and can be realized from such a rolled-up metamaterial is the hyperlens. The hyperlens works by coupling surface plasmons to the near field, evanescent waves of an object. The coupling of the surface plasmons through alternating layers of metal and oxide converts these evanescent waves into propagating waves which can then be picked up through classical microscopy techniques[3], visually described in Fig. 2(a). The mathematical explanation comes from the dispersion relation for transverse magnetic (TM) modes $k_o^2 = (k_r^2/\varepsilon_\theta) + (k_\theta^2/\varepsilon_r)$, where k_r is the wave vector in the radial direction and k_θ is the wave vector in the tangential direction of the tube, ε_θ and ε_r are the effective tangential and radial permittivities of the material (note

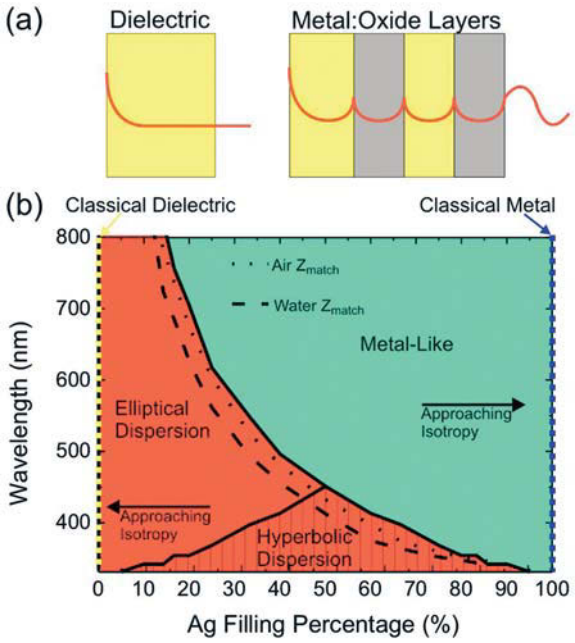

Fig. 2: (a) The evanescent near-field of an object dies off exponentially as is travels away from the source. However, through alternating stacked layers of a metal and an oxide, the evanescent waves couple with surface plasmons which convert them to propagating waves that can be picked up in the far-field with classical optics. (b) The dispersion relation for TM modes for a metamaterial can take on many forms as seen here for a TiO_2/Ag combination showing the effects of using a different wavelength and filling percentage of Ag. The dotted and dashed lines represent the impedance matching of a hyperlens, to the surrounding medium of air or water respectively, as a function of wavelength vs. Ag filling percentage.

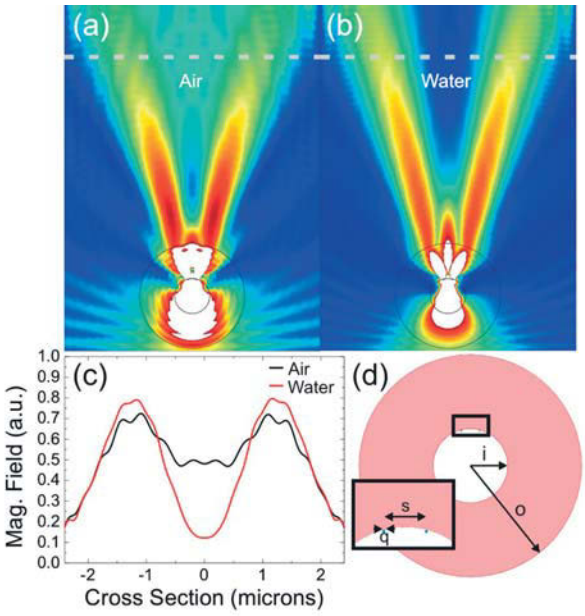

Fig. 3: (Copyright AIP) Impedance matching the lens to the surrounding medium becomes important for higher transmission and can give way to higher resolution than unmatched systems. This condition is met with sqrt(ε_θ) = n_{medium}, and results in suppressed Fresnel reflection at the outer interface of the hyperlens for a higher output and better resolution. The normalized magnetic field distribution for air (a) and water(b) are shown. (c) A cross section of the magnetic field profile taken at 3.5microns [dotted line in (a) and (b)] from the outer surface is shown to have higher resolution in water than in air. For this particular simulation, the effective permittivity is used for a 2:1 ratio of Al_2O_3:Ag at λ = 342 nm leading to a sqrt(ε_θ) = 1.32 and a index of refraction for water used was 1.33. (d) The geometry used is as follows; an inner diameter i = λ, outer diameter o = 3λ, a separation of dots s = λ/2 and a dot size q = λ/30.

the shift to polar coordinates for simplicity). This shows that when $Re\{\varepsilon_r\} < 0$ and $Re\{\varepsilon_\theta\} > 0$, leading to a hyperbolic dispersion, or when $Re\{\varepsilon_r\} >> Re\{\varepsilon_\theta\}$, leading to an elliptical dispersion, the transmission of high order spatial information is possible[5]. The k_θ governs the smallest size limit of an object, the larger the k_θ the smaller the object. When there is an elliptical dispersion relation, a higher k_θ is obtainable, and when there is hyperbolic dispersion, k_θ becomes unbound, allowing for the resolution of objects with limitless size. As one can see in Fig. 2(b), by changing the bi-layer composition or the working wavelength, it is possible to control the level of anisotropy of the material and how the light is mediated inside the metamaterial. In this figure the dispersion of a rolled bi-layer of TiO_2 and Ag is looked at by adjusting the filling percentage of Ag. As the Ag is increased, the metamaterial can take on many types of dispersion until it finally approaches classical Ag behavior. Likewise, as the filling percentage of Ag is lowered, the metamaterial approaches classical TiO_2 behavior.

The hyperlens is of particular interest because of the prospect of being able to image sub-wavelength information of molecules or objects within living cells. Existing conventional microscopy techniques for seeing such small details cannot look at a living object. With this in mind we studied how to optimize the rolled-up hyperlens to work with such objects. We studied how to better improve the output signal of the lens to allow for larger magnification and higher resolution. One way of doing this is by using the hyperlens as an immersion lens; by impedance matching (Z_{match}) the lens to the surrounding system, the output is much higher. In order to impedance match, the square root of the tangential permittivity must be equal to the index of refraction of the surrounding medium (sqrt(ε_θ) = n_{medium}). The impedance matching conditions for a surrounding media of air and water are shown in Fig. 2(a). The improved resolution can be seen in Fig. 3 when comparing how a hyperlens, that is impedance matched to water, performs in air (Fig. 3(a)) and water (Fig. 3(b)). The far field cross section of the magnetic field shows much better resolution for the properly impedance-matched lens Fig. 3(c).

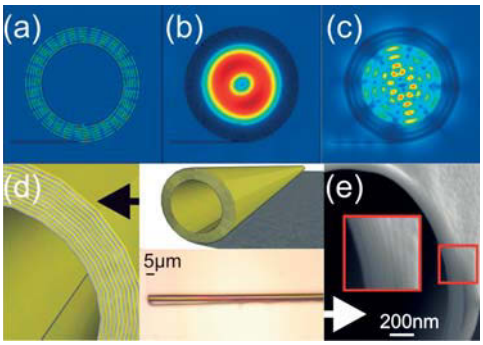

Fig 4: By changing the metamaterial makeup or the incident wavelength of light, rolled-up MFOs are able to propagate light via: (a) plasmonic means in the cladding, (b) classically through the hollow core, (c) as well as coupling the plasmonic modes of the cladding with the classical core of a higher index medium which could give way to higher sensitivity sensors. (d) A close-up figure of the geometry of the MFOs used for the simulations can be compared to (e) the recent results in our progress towards experimental realization. The SEM image of a FIB-cut tube shows the compactness achieved by rolling a single bi-layer of SiO_2 (9nm) and Ag (3nm).

Metamaterial Fiber Optics

The second rolled-up metamaterial device that can be created by using the same material combination and geometry [but by turning the propagation direction of light parallel to the tube rather than perpendicular and switching to Hybrid waves (HE)] is what we call metamaterial fiber optics (MFOs) [6]. There are a number of reasons and advantages for studying and developing MFOs. There currently exist two main forms of guiding light, either via classical core propagation or via surface plasmon (SP) guidance. Classical guidance is obviously practical in light guidance on a large scale but for on-chip electro-optics, they fall short because of there large size, on the order of 100 μm; this is one reason to turn to SP waveguides. SP waveguides allow for the miniaturization of devices and can be developed for faster on-chip communication. MFOs combine both technologies into a single device due to their unique 3-fold anisotropy [ε^{eff}]. Light can be guided either plasmonically (Fig. 4(a)), or classically (Fig. 4(b)), or can allow for a coupling between plasmonic and classical guidance, Fig. 4(c), which could lead to sub-wavelength information transmission. The other advantages include the small compact size, a few microns or smaller, and the ability to guide light using a cladding thinner than the incident wavelength.

The type of guidance is determined by the material makeup and the incident wavelength. There are a number of regions in which the permittivities of our system have unique values, each leading to a unique form of guidance; ($\varepsilon_{||}^{eff} < 0 / \varepsilon_{\perp}^{eff} > 0$) ($\varepsilon_{||}^{eff} > 0 / \varepsilon_{\perp}^{eff} < 0$) ($\varepsilon_{||}^{eff} > 0 / \varepsilon_{\perp}^{eff} > 0$), all of which cater to plasmonic guidance in the cladding and ($0 < \{\varepsilon_{||}^{eff}, \varepsilon_{\perp}^{eff}\} < 1$) ($\varepsilon_{||}^{eff} / \varepsilon_{\perp}^{eff} = 0$) which allow for classical core guidance. The region where $\varepsilon_{||}^{eff}$ and $\varepsilon_{\perp}^{eff}$ are both negative arises from guides made of metal and lead to core guidance via total internal reflection [Some of these regions can be seen in the single material composition of TiO_2 and Ag calculated for Fig 1(b)]. As mentioned before, the plasmonic modes can be coupled into the core when a higher index medium is introduced, which could lead to higher sensitivity sensors. Fig. 4(d) shows a close-up of the cladding layers of a metamaterial optical fiber in order to highlight the recent development which has been made to experimentally realize our devices shown in an SEM image in Fig. 4(e). Taking a FIB cut of one of our tubes, the inset of Fig. 4(e) reveals the level of compactness (which is necessary for plasmonic coupling) obtainable by rolling a nanomembrane bi-layer of SiO_2 (9nm) and Ag (3nm) grown on a photoresist sacrificial layer.

In conclusion, we have explored various metamaterials which can be realized experimentally through rolled-up technology. One device which can go beyond the diffraction limit and image nano-objects optically, and another device which can combine classical and plasmonic guidance through means of a sub-wavelength cladding and an overall miniaturized structure. Both devices can be grown and implemented into existing and future on-chip technology through self assembly. The experimental progress which has been made to develop these devices was also presented.

Acknowledgements: We would like to thank Suwit Kiravittaya, Peter Cendula, and R. J. Smith for fruitful discussions as well as Ronny Engelhard and Dominic Thurmer for help in the experimental progress of making our devices.

References

[1] V.G. Veselago, Sov. Phys. Usp. **10** (1968) 509
[2] W. Cai et al., Nat. Photonics **1** (2007) 224
[3] B. Wood et al., Phys. Rev. B **74** (2006) 115116
[4] Z. Liu et al., Science **315** (2007) 1686
[5] E. Smith et al., Appl. Phys. Lett. **95** (2009) 083104
[6] E. Smith et al., Nano Lett. **10** (2010) DOI:NL900550J (2009)
[7] S. M. Rytov, Sov. Phys. JETP **29** (1955) 605

Cooperation Zhaowei Liu, Electrical & Computer Engineering, Univ. of California, San Diego, US.
Funded by Volkswagen Foundation (I/84 072); Multidisciplinary University Research Initiative (MURI) sponsored by the U.S. Air Force Office of Scientific Research (AFOSR) Grant No. FA9550-09-1-0550.

Self-assembled quantum dots in stretchable nanomembranes

F. Ding, J. D. Plumhof, V. Křápek, M. Benyoucef, K. Dörr, A. Rastelli, and O. G. Schmidt

Strain is one of the key parameters in nanoscience. We fabricated a piezoelectric-based electro-mechanical device to study the effect of external biaxial stress on the light emission of single InGaAs/GaAs (001) quantum dots embedded in a 200 nm-thick GaAs nanomembrane. Reversible and bi-directional spectral tuning of quantum dot excitonic emission is demonstrated. The most intriguing finding is that biaxial strain is a reliable tool to engineer the quantum dot electronic structure and reach color coincidence between exciton and biexciton emission, providing a vital prerequisite for the generation of polarization entangled photon pairs through a time reordering strategy. The physical origin of this new phenomenon is discussed based on empirical pseudopotential calculations.

To possibly make use of quantum phenomena in the field of quantum information processing and communication, a key tool is entanglement - the spooky, distance-defying link that can form between objects such as photons even when they are completely shielded from one another. It's a link that Einstein went to his grave denying, yet its existence is now beyond dispute [1-3]. One of the research interests in our institute (IIN) is the generation of entangled photon pairs from semiconductor quantum dots (QDs) [2]. Polarization-entangled photons can be produced by the radiative cascade: biexciton (XX) → exciton (X) → ground state (G), where the polarization of a photon pair is determined by the spin of the intermediate X state [see Fig. 1(a)]. However, in real self-assembled semiconductor QDs the intermediate X states split into two states by an energy δ called fine structure splitting (FSS) [4, 5]. This non-vanishing FSS makes the two decay paths distinguishable and destroys the polarization entanglement. A number of post-growth techniques have been used to reduce δ, such as in-plane magnetic fields, lateral electric fields, uniaxial stress [6] and rapid thermal annealing.

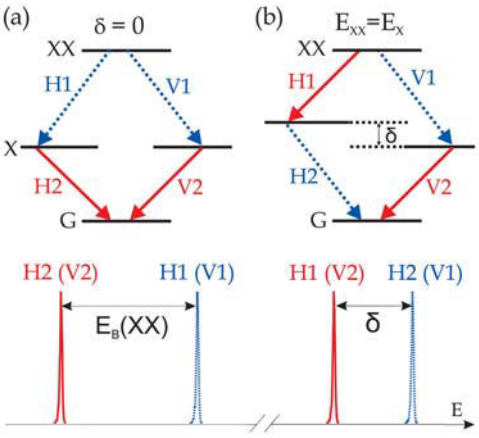

Fig. 1: Level schemes showing the biexciton-exciton cascade. The solid (dashed) line represents the decay channel that yields H (V) polarized photons.
(a) Entangled photon pairs are obtained by reducing the FSS δ to zero. Two lines (X and XX) with energy splitting E_B(XX) can be seen in a PL spectrum.
(b) An alternative consists in engineering the system so as to reduce E_B(XX) to zero, thus to obtain color coincidence across generation. Now two lines with splitting δ are present in the PL spectrum.

Inspired by a recent proposal, we focus on an alternative approach which does not require the FSS to be below radiative linewidth [7]. In this so-called "time-reordering scheme" the emission energies of X (E_X) and XX (E_{XX}) are tuned into resonance. Now, one matches the red photons H1 (V2) and the blue photons V1 (H2) [see Fig. 1(b)] across generations in a QD. The entanglement is then accomplished by performing a unitary time reordering on the two-photon state.

The experimental challenge is that the emission energies E_X and E_{XX} in as-grown QDs are usually different, i.e. the energy of two excitons (XX) is not simply twice the energy of a single exciton (X), because of interactions. We have demonstrated that an external biaxial tensile (T) or compressive (C) stress, provided by a piezoelectric actuator, can be used to achieve $E_X \approx E_{XX}$, one step towards the generation of polarization entangled photon pairs through the time reordering strategy.

The sample used here was grown on a GaAs(001) substrate in a solid-source molecular beam epitaxy (MBE) machine [see Fig. 2]. A layer of self-assembled In(Ga)As QDs sandwiched between 150 nm and 50 nm GaAs layers was grown on top of a 1 µm thick $Al_{0.7}Ga_{0.3}As$ sacrificial layer. By means of optical lithography we defined square patterns on the sample followed by a non-selective wet chemical etching step. The $Al_{0.7}Ga_{0.3}As$ sacrificial layer was completely removed in HF (5% vol.), leaving the square-shape nano-membranes on the GaAs substrate. The membranes were then transferred onto a 300 µm-thick $[Pb(Mg_{1/3}Nb_{2/3})O_3]_{0.72}-[PbTiO_3]_{0.28}$ (PMN-PT) actuator via PMMA resist. A bias voltage V applied to the PMN-PT results in an in-plane strain $\varepsilon_{//}$ in the GaAs membrane and the QD structure. The PMN-PT was poled so that $V > 0$ (< 0) corresponds to in-plane compressive (tensile) strain $\varepsilon_{//} < 0$ (> 0). The choice of PMN-PT is due to its large in-plane strain capabilities and negligible drop of strain at low temperature.

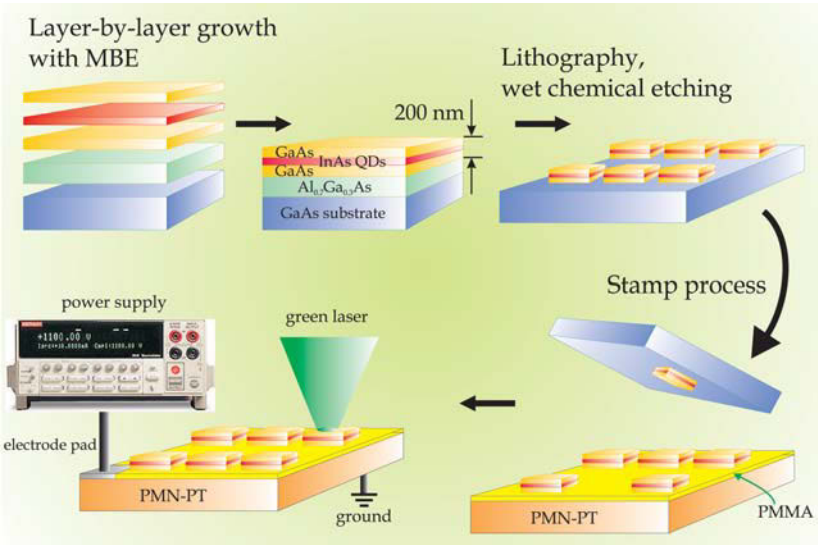

Fig. 2: Fabrication process of the 200-nm-thick GaAs membrane containing the In(Ga)As QDs. The membranes were then transferred, using a thin layer of PMMA as glue, onto a PMN-PT piezoelectric actuator. A bias voltage *V* applied to the PMN-PT results in an in-plane strain $\varepsilon_{//}$ in the GaAs membrane and the QD structure.

Fig. 3(a) shows photoluminescence (PL) spectra of a single In(Ga)As QD under different strain states. With increasing in-plane compression (C), the emission energies of different lines shift to higher energy (blue shift), while under tensile (T) stress the QD emission lines shift to lower energy (red shift). More interestingly, the binding energy E_B of XX, defined as $E_B(XX) = E_X - E_{XX}$, is also modified by external biaxial stress. A clear demonstration is given in Fig. 3(b), where the grayscale-coded PL intensity of X and XX are plotted as a function of linear polarization angle and energy for various values of *V*. As expected, X and XX show anti-correlated shifts as we rotate the analyzer. The FSS for this QD, i.e., the energy separation δ between the H and V components of X or XX can be well resolved, and we obtain δ = 48 ± 5 μeV, see left inset of Fig. 3(b). As the voltage increases the magnitude of $E_B(XX)$ decreases, while δ (FSS) stays constant within the measurement uncertainties. At 1100 V (the maximum voltage available at present) $E_B(XX) \rightarrow 0$ and δ dominates the energy scale in the problem: only two peaks with the splitting of δ can be observed. We have now practically reached the color coincidence of (V2, H1) and (H2, V1), an ideal condition for the time reordering entanglement measurement as described in Fig. 1(b).

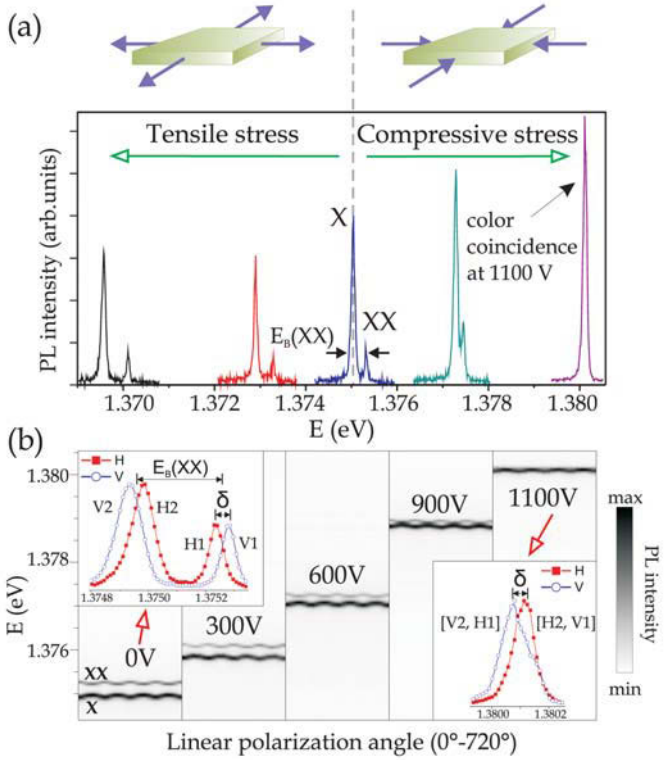

Fig. 3: (a) Low-temperature (6 K) PL spectra of a single QD under different strain states. The excitonic lines can be either blue shifted or red shifted, depending on the external stress. Under compressive stress the color coincidence of X and XX is reached at *V*~1100 V.
(b) Polarization-resolved PL map for the X and XX lines at several voltages. At 0 V $E_B(XX)$ is much larger than δ, while $E_B(XX)$ vanishes (limited by the system resolution) and δ dominates at 1100 V, in accordance with Figure 1.

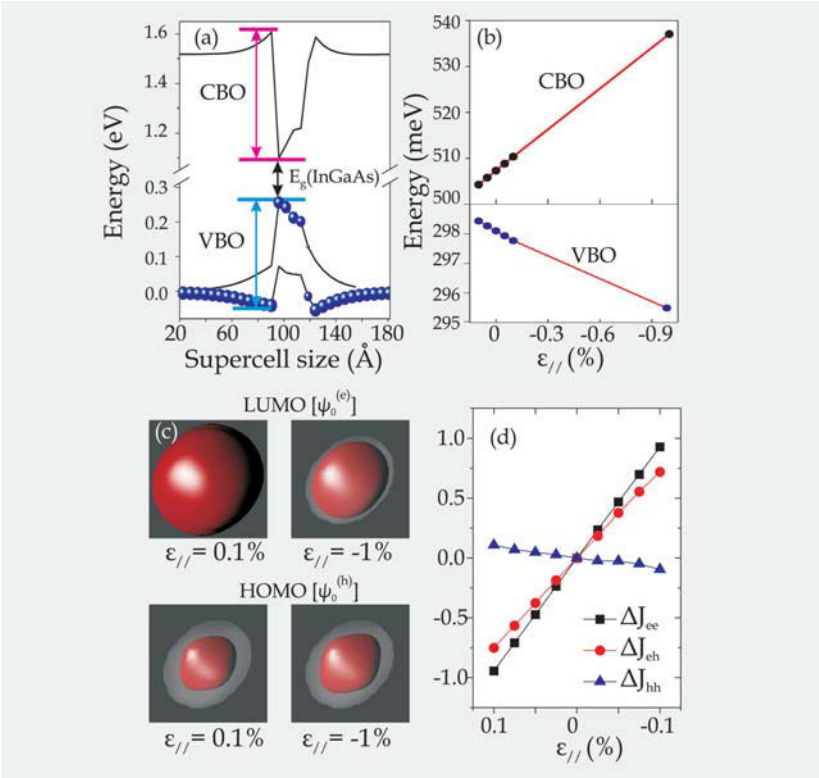

Fig. 4: (a) Calculated band diagram at $\varepsilon_{//} = 0$; for the valence band, the size of the circles is proportional to the heavy hole character of the bands.
(b) Changes in CBO (VBO) with strain $\varepsilon_{//}$.
(c) HOMO and LUMO wave function of QD at $\varepsilon_{//} = 0.1\%$ and -1%. The red color encloses 75% of the charge density, while light gray color represents the outline of the QD.
(d) Changes in Coulomb integrals with biaxial strain.

In order to understand the experimental results, calculations on realistic InGaAs/GaAs QDs containing 3 million atoms were performed using the empirical pseudopotential and the configuration interaction (CI) approaches [8] at the Max-Planck-Institute for Solid State Research in Stuttgart. The QD was modeled as a lens shaped $In_{0.8}Ga_{0.2}As$ structure with a height of 2.5 nm and elliptical base of major (minor) axis of 10 (7.5) nm along the [1-10] ([110]) crystal direction. We plot in Fig. 4(a) the strain modified conduction band minimum and the upper two valence bands. For the latter bands we used circles proportional in size to the fraction of heavy hole character. In the unstrained region, far from the dot, heavy- and light-hole bands are degenerate; close to the dot (inside the dot), the light (heavy)-hole band forms the valence band maximum. The valence band offset (VBO) and the conduction band offset (CBO) are also defined. In Fig. 4(b) we show a linear increase by ~35 meV for the CBO upon change in biaxial strain $\varepsilon_{//}$ from 0.1% to -1%. This represents an increased confinement and localization of electron wave function. For the VBO, however, we find a decrease by ~3 meV for the same range of strains. Upon compression, the hole wave functions tend to become more delocalized. This, rather counterintuitive behavior can be observed directly on the wave functions in Fig. 4(c), where we display the lowest electron state (LUMO) and highest hole state (HOMO) at two different strains. This localization/delocalization gives rise to changes in the Coulomb integrals between lowest electron (e) and hole (h) states, as shown in Fig. 4(d).

From the calculations, we find that the effect of biaxial strain on the correlation energy is very small. The main changes in the binding energy of XX are due to changes in the direct Coulomb interactions between electron and holes under biaxial strain. In this case, changes in binding energy can be approximated by:

$$\Delta E_B(XX) \approx [\Delta J_{eh} - \Delta J_{hh}] - [\Delta J_{ee} - \Delta J_{eh}],$$

where J_{ee}, J_{hh}, and J_{eh} are the Coulomb integrals. Figure 4(d) shows that ΔJ_{eh} and ΔJ_{ee} increase with compressive strain, with only small deviations from each other. Interestingly, ΔJ_{hh} shows the opposite behavior, but its magnitude is substantially smaller than those of ΔJ_{eh} and ΔJ_{ee}. We thus conclude that the increase in binding energy of XX upon compression is mainly a consequence of the increase in the electron-hole attraction term.

In conclusion, we have developed a promising technique to investigate the effect of external stress on the optical properties of single QDs. Stress is provided by a piezoelectric actuator at low temperatures and allow us to engineer the properties of QDs embedded in nanomembranes or optical microcavities [9]. We find that biaxial strain is a reliable tool to engineer the QD electronic structure and reach color coincidence between exciton and biexciton emission. This represents the first, but a critical step towards the generation of entangled photon pairs via the newly proposed time reordering scheme.

References

[1] R. J. Young et al., Phys. Rev. Lett. 102, 030406 (2009)
[2] R. Hafenbrak et al., New J. Phys. 9, 315 (2007)
[3] O. Benson et al., Phys. Rev. Lett. 84, 2513 (2000)
[4] D. Gammon et al., Phys. Rev. Lett. 76, 3005 (1996)
[5] M. Bayer et al., Phys. Rev. B 65, 195315 (2002)
[6] S. Seidl et al., Appl. Phys. Lett. 88, 203113 (2006)
[7] J. E. Avron et al., Phys. Rev. Lett. 100, 120501 (2008)
[8] L.-W. Wang and A. Zunger, Phys. Rev. B 59, 15806 (1999)
[9] T. Zander et al., Optics Express 17, 22452 (2009)

Cooperation R. Singh, G. Bester, T. Zander, Max Max-Planck-Institut für Festkörperforschung, Stuttgart, Germany; N. Akopian, U. Perinetti, V. Zwiller, Delft University of Technology, The Netherlands; Y.H. Chen, Institute of Semiconductor, Chinese Academy of Sciences, Beijing, China; We acknowledge Andreas Herklotz, Jong-Woo Kim, C. C. Bof Bufon, R. Hafenbrak and P. Michler for fruitful discussions

Funded by DFG (FOR730), BMBF (No. 01BM459), NWO (VIDI), CAS-MPG Joint Scholarship and NSFC China (60625402)

Technological impact

New facility for Helium liquefaction in the IFW

D. Lindackers

The installation of new scientific instruments and medical devices operating under cryogenic conditions are the major reasons for a worldwide increase of Liquid Helium (LHe) consumption in the last two decades. At the same time the few natural gas sources from which Helium gas can be extracted under economical conditions are going to deplete. Both constraints are causing the shortage of LHe and the steady price increase being observed since a couple of years. Under these general conditions the specific situation in the IFW is indicated by a dramatic increase of the LHe-demand from 15.000 l in 1995 to 80.000 l in 2009 together with a painful lack of reliable supply from the gas industries. During the last years the amount of LHe delivered by the gas industries did not cover the demand of the operating cryostats causing unplanned shut downs of quite a number of cryogenic experiments. This situation causes hard impact to the scientific work and increases the Helium consumption again, because the restart procedures require large quantities of LHe during the cool down phase. In order to have LHe permanently available the IFW decided to install its own liquefaction facilities and to organise the delivery of LHe into the labs as well as the recovery of the gaseous match.

Setting up the project the new Helium plant should meet highest standards regarding energy efficiency and helium loss. At the same time it has to be compatible to the existing recovery system which was installed in the mid nineties. Fig. 1 shows a scheme of the entire plant. On the left side the existing recovery system is shown. It consists of a piping net collecting the gaseous Helium which boils off the cryostats and transfers the gas from all labs to a balloon of 20 m^3 capacity. From there the gas is compressed into transport cylinders at 200 bars and returned to the gas industries.

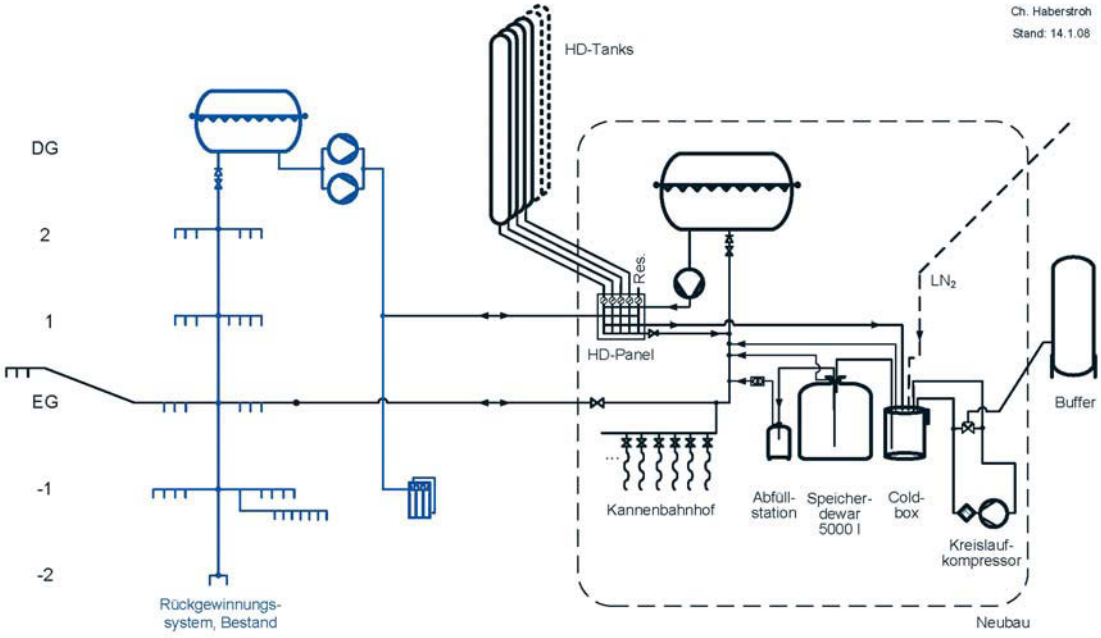

Fig. 1: Scheme of IFW Helium plant (source: C. Haberstroh, TU Dresden)

At the right side of Fig. 1 the new part of the Helium facilities are shown by its main components. The transportable high pressure cylinders are replaced by ten stationary mounted cylinders with a total geometrical volume of 25 m^3. Their operation pressure is again 200 bars, providing enough storage capacity to cope with 2-3 weeks of shut down of the liquefier, e.g. for maintenance reasons. The operation of the ten cylinders is controlled by a system of high pressure valves which are controlled by a central PLC,

allowing their filling for gas recovery and their unloading for liquefaction at the same time. Together with a number of gas sensors measuring the He quality the high pressure control system allows the separation the raw gas in different cylinders according to the impurity content. By blending the gas inside the different cylinders, the liquefier can be provided with an optimized feed gas quality for the achievement of maximum efficiency.

The coldbox liquefies the gaseous helium with a regular send-out of 39 l/h which can be doubled by pre-cooling the feed gas with LN_2. The liquid is transferred into a storage dewar of 5000 l capacity from which it can be filled into transport dewars of 100 l capacity each, further used for the delivery of LHe into the IFW labs. The filling is performed by a cryogenic rotary pump which is mounted inside the storage dewar. Together with a feedback line the transfer system introduces LHe into the transport dewars and replaces the volume loss in the storage dewar by the cold GHe which is displaced by the liquid. By these means the liquid can be stored and filled under atmospheric conditions, keeping its temperature at 4.2 K thus avoiding the occurrence of flash gas. This technology saves 30% of primary energy and more than 80% of filling time.

The components framed by the dashed square in Fig. 1 are installed inside a new building, which was erected on an open place between two laboratory buildings, which were already existent in the IFW premises. Fig. 2 shows the arrangement of equipment in the main liquefaction hall.

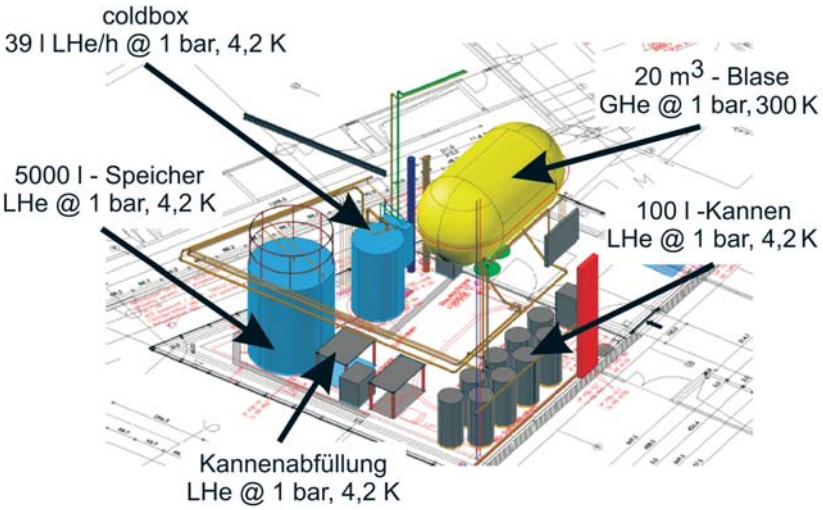

Fig. 2: Arrangement of liquefaction components inside the new building between Haus B and Haus C (Source: DERU, Blum & Schultze Architekten)

The plot plan is optimized for the handling of transport dewars during the filling campaigns. Therefore the coldbox, storage dewar, and filling station are gathered on one side and the docking station, where the transport dewars are connected to the recovery system, on the opposite side. The boil off gas occurring in the liquefaction hall is collected by a balloon of 20 m^3 volume which is attached to the existing recovery system in order to enlarge the entire low pressure buffer. The machinery equipment which is depicted in Fig. 1 is installed in the basement underneath the liquefaction hall and is not depicted in Fig. 2.

Fig. 3: New IFW Helium plant in operation

After one year of planning the construction and installation works could be completed within ten month. The IFW planning team was supported by the Technical University Dresden Dept. of Cryogenics, DERU Planungsgesellschaft für Reinraumtechnik Dresden, and Blum & Schultze Architekten Dresden. Since December 2009 the Helium cycle in the IFW is closed and the institute is now able to provide its cryogenic experiments with the needed coolant. Fig. 3 shows the new helium facility in operation.

"Rhone"- New high-performance hardware for scientific computing

U. Nitzsche

It is our aim to explain experimental findings, to get insight into the mechanisms behind the measured properties and, last but not least, to predict unexpected properties or new materials. This aim not only requires appropriate analytical theories but, in most cases, also numerical methods and high-performance computer facilities. Accordingly, there exists a long-time experience at ITF to build up and operate computer clusters based on standard PC technology and on Linux operating systems. Our previous cluster named "mulde" was designed six years ago as a cost-efficient system fitting to the needs at that time. The end of its lifetime is foreseeable and a new cluster had to be acquired. Our intention was that the new machine should not simply replace the old one. Rather, it should be better in those points that meanwhile had turned out as bottlenecks. After a long series of performance tests, not only concerning the computing speed but also the I/O rate for the hard disk access, comparison of different racks and finally different manufacturers, we decided to order a system consisting of

- 32 nodes, each equipped with 8 Intel Nehalem processor cores, 2.93 GHz clock rate, and 24 GB of DDR3 RAM; this combination yields a doubled memory access bandwidth;
- a working file space of 1.7TB realized with fast SAS hard disks and with a 10 Gbit/s connection to the nodes;
- a very fast interprocess connection network between the nodes, based on the InfiniBand IV technology as a prerequisite for parallel computing.

The high power density of current Quadcore-processors requires water-cooling: under full load, the new system has a power draw comparable with 25 averaged 4-persons households. This posed a new challenge, excellently mastered by our facility management.

On December 8, the cluster was delivered and started. First tests already confirm the concept. In particular, processes with high traffic between CPU and RAM like band structure codes profit from the new design. For this kind of processes we really achieved a speedup of 100% compared with the former cluster "mulde". Additionally, network dropouts caused by high I/O traffic to the hard disks could even not be produced on the new system. The system went productive on December 23. Many thanks to the members of the IT department and of the facility management, especially to Thomas and Jan Fichte, to Mr Ulrich from the plumber service, and to Mr Effenberg and Dr. Zimmermann for their straightforward support.

Cooperation MEGWARE Computer GmbH Chemnitz

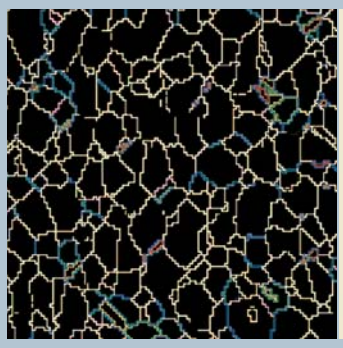
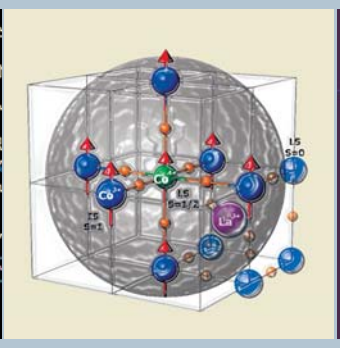
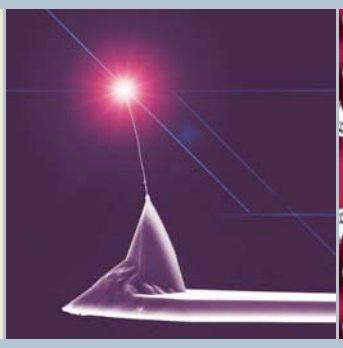
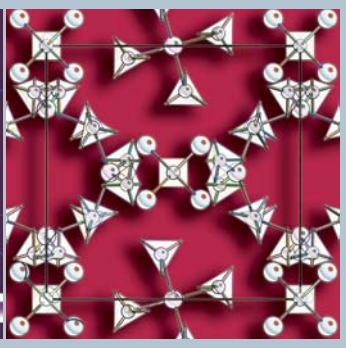

Reports from Research Areas

Highly textured Nickel-Tungsten substrate for YBCO coated conductors (graphically altered EBSD image)

Visualization of the spin polaron in $LaCoO_3$

Iron filled carbon nanotube attached to a conventional AFM cantilever

Unit cell of $Al_3Li_4(BH_4)_{13}$

Research Area 1
Superconductivity and superconductors

Cu NQR Evidence for a Different Effect of Zn and Ni Doping on the Pseudogap in $(Eu,Nd)Ba_2(Cu,Zn,Ni)_3O_7$

H.-J. Grafe, F. Hammerath, T. Wolf[1], G. Khaliullin[2], V. Kataev, B. Büchner

The origin of the pseudogap in the cuprates and its relation to high temperature (high-T_c) superconductivity is still under debate. Theoretically, it has been related either to a precursor superconducting state without macroscopic phase coherence or to a kind of order that may even compete with superconductivity such as a stripe order or spin and charge density waves. Experimentally, measurements of the optical conductivity [1] that probe the *charge* excitations in $(Eu,Nd)Ba_2(Cu,Zn,Ni)_3O_7$ show that large Zn impurity doping suppresses the charge pseudogap, whereas large amounts of Ni enhances its energy scale. Therefore we have investigated the *spin* dynamics by means of nuclear quadrupole resonance (NQR) measurements on the Cu nucleus in these compounds [2]. Whereas our previous measurements were somewhat affected by the additional magnetic moment of the Nd, we could now measure single crystals of $EuBa_2(Cu,Zn,Ni)_3O_7$ where the Eu is non-magnetic [3]. We find that Ni doping enhances the nuclear spin lattice relaxation rate, $(T_1T)^{-1}$, leading to a Curie Weiss like temperature dependence (see Fig.). In contrast, large amounts of Zn reduces $(T_1T)^{-1}$. At low temperatures, this effect is even more pronounced, and the opening of a spin pseudogap in the Zn doped samples is clearly visible. Since $(T_1T)^{-1}$ probes the low frequency dynamic spin susceptibility of the CuO_2 planes at the antiferromagnetic wave vector, $\boldsymbol{Q}_{af}$, we conclude that Ni enhances antiferromagnetic correlations, and thereby the hole localization and the charge pseudogap. In contrast, large amounts of Zn dilute the spin system, and thus the low energy spin collective modes are suppressed, resulting in a (spin) pseudogap like decrease of $(T_1T)^{-1}$ at low temperatures. Our results reveal hence an intimate relationship between magnetic correlations and the charge pseudogap phenomenon in high-T_c cuprates.

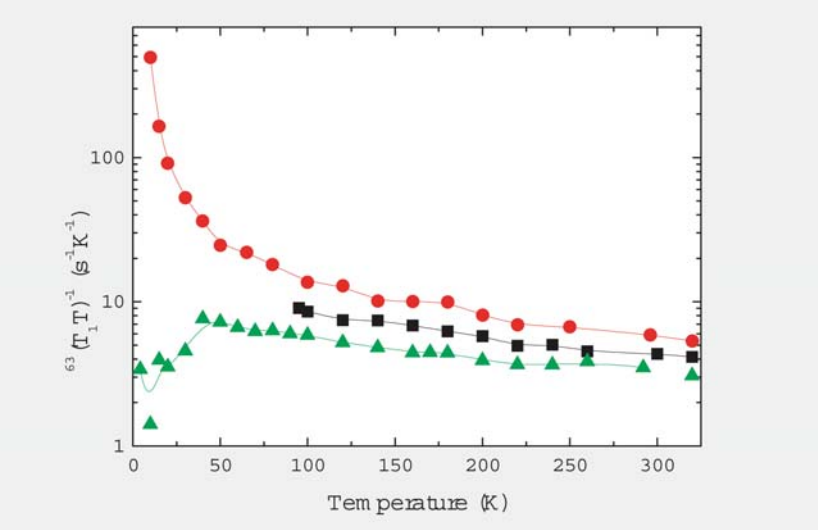

Fig.: Cu spin lattice relaxation rate divided by temperature, $(T_1T)^{-1}$, for undoped (black squares), Zn doped (green triangles) and Ni doped (red dots) $EuBa_2(Cu,Zn,Ni)_3O_7$. Ni doping enhances $(T_1T)^{-1}$, while Zn doping reduces $(T_1T)^{-1}$ leading to a pseudogap like decrease below ~40 K.

[1] A. V. Pimenov *et al.*, Phys. Rev. Lett. **94**, 227003 (2005)
[2] H.-J. Grafe *et al.*, Phys. Rev. B **77**, 014522 (2008)
[3] H.-J. Grafe *et al.*, preprint

Cooperation [1]Forschungszentrum Karlsruhe, Germany; [2]Max-Planck-Institut für Festkörperforschung, Stuttgart, Germany
Funded by DFG, Forschergruppe 538

YBCO coated conductor architectures

B. Holzapfel, R. Hühne, J. Eickemeyer, U. Gaitzsch, A. Güth, C. Rodig, H. Klauß, J. Freudenberger, J. Hänisch, M. Sparing, B. Rellinghaus, R. Gärtner, T. Thersleff, A. Kirchner, T. Freudenberg, M. Erbe, M. Schubert, L. Schultz

The preparation of coated conductor architectures for high-performance superconducting tapes based on YBCO films was continued last year in the framework of an IFW project. A major part of the work was dedicated to the development of improved textured metal substrates showing a reduced ferromagnetism at 77 K and higher mechanical strength compared to the standard Ni-5at%W tape. For the first time, highly textured Ni-9at%W tapes were realized using specific homogenisation and stress relief treatments leading to a cube orientated fraction of more than 94 % [1]. Simultaneously, the preparation of Ni-7.5at%W substrates was optimised resulting in an improved texture with a cube oriented fraction of more than 97 %. A standard Y_2O_3/YSZ/CeO_2 coated conductor architecture was prepared on these substrates using pulsed laser deposition. The final YBCO layers showed an in-plane alignment below 8° and a critical current density of 1.1 MA/cm^2 on Ni-9at%W and 1.25 MA/cm^2 on Ni-7.5at%W, respectively (see Fig.).

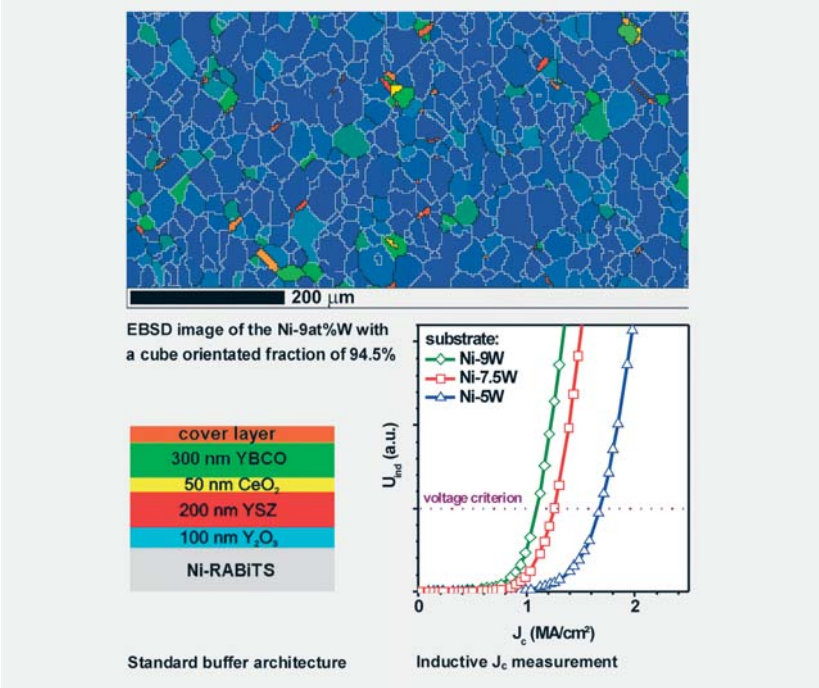

Fig.: Newly developed highly textured Ni-9at%W substrates as templates for YBCO coated conductors [1].

Furthermore, the work was focused on the improvement of the critical current density of the superconducting layer in magnetic fields by the incorporation of artificial pinning centres. Pulsed laser deposition as well as chemical solution deposition was used to implement different second phase materials, as for example $Y_2Ba_4Cu(Nb,Zr)O_y$ [2], $BaZrO_3$ or $BaHfO_3$ in the YBCO matrix. The influence of these nanoparticles on the local structure of the grown film was investigated in detail using high resolution transmission electron microscopy in order to correlate the defect structures to the measured electrical properties of the YBCO layer. As a result, it was found that the J_c anisotropy of the superconducting layer can be tuned by adapting deposition parameters like temperature or deposition rate.

[1] R. Hühne et al., Supercond. Sci. Technol. 23 (2010) accepted.
[2] E. Reich et al., Supercond. Sci. Technol. 22 (2009) 105004.

Cooperation evico GmbH, Univ. Cambridge, Gent Univ., Zenergy GmbH, ICMAB Barcelona, Shanghai Univ., Bruker HTS GmbH
Funded by BMBF, EU, DAAD

Plasmon Dispersion vs. Charge Order in Transition-Metal Dichalcogenides?

R. Schuster, M. Knupfer, B. Büchner

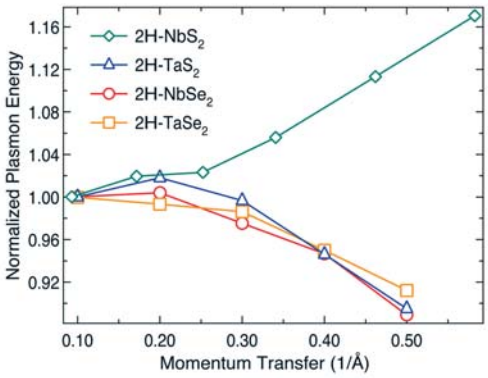

Fig.: Dispersion of the charge carrier plasmon for different representatives of the transition-metal dichalcogenides measured at room temperature. The curves are normalized to their onset values at 0.1Å^{-1}.

The transition-metal dichalcogenides are quasi-2D metallic systems that are known to exhibit different electronic instabilities as a function of temperature. Prominent representatives are 2*H*-$TaSe_2$, 2*H*-TaS_2 and 2*H*-$NbSe_2$ all undergoing a charge-density wave (CDW) transition followed by the onset of superconductivity at lower temperatures. Another very similar member of this class is 2*H*-NbS_2 which, however, does not show any signs of charge order. In addition to the above mentioned phase transitions, the conduction electrons, derived mainly from the transition-metal ions, can also perform collective density oscillations – so called plasmons – that can be probed with the help of electron energy-loss spectroscopy. Such experiments have been done on 2*H*-NbS_2 in the past and revealed conventional quadratic plasmon dispersion with a positive slope that is theoretically predicted for ordinary metals. We performed similar investigations on the other three above given members of the family and found a remarkably different behavior that is summarized in the figure. All the compounds which are known to undergo the CDW transition show a negative dispersion of the plasmon which contradicts not only the behaviour found in 2*H*-NbS_2 but also the prediction of a positive dispersion for conventional metallic systems. This behavior points to a possible – yet unknown – interference between the plasmon and the CDW. But even if the coexistence of negative plasmon dispersion and the charge order is purely accidental the negative dispersion poses considerable theoretical questions.

Cooperation Institut de Physique de la Matière Complexe, Ecole Polytechnique Féderale de Lausanne, Switzerland
Funded by DFG

MgB_2 – Preparation of first 1000 m long multifilamentary wire

M. Herrmann, W. Häßler, A. Kario, C. Rodig, D. Seifert, T. Wolf, H.-P. Trinks, J. Scheiter, M. Schubert, K. Nenkov, G. Fuchs, B. Holzapfel, L. Schultz

Fig.: First 1000 m multifilamentary MgB_2 wire using mechanically alloyed in-situ powder manufactured under industrial production conditions

The collaboration with Bruker HTS succeeded in the preparation of a single piece multifilamentary wire exceeding a 1000 m in length with a J_e of up to 91 A/mm^2 at 4.2 K and 5 T. This conductor, using a mechanically alloyed in-situ MgB_2 precursor prepared at IFW was manufactured under industrial production conditions at Bruker HTS. Only a reasonable interplay of both key parameters, an appropriate preparation route and high current carrying capability, will allow for a widespread use of MgB_2 conductors.
Detailed studies on the influence of the milling parameters, e.g. time and speed of processing has been done and showed, that the morphology of the powder is strongly affected. With increasing milling energy, a refined particle size down to several nanometer, improved homogeneity of the powder and subsequently improved critical current densities in the wires are observed. At the same time the decreasing flowability of the precursor changes the deformability of the conductor when used in the powder-in-tube approach. In order to allow for an easy and reliable production of MgB_2 wires on the kilometer scale, it was essential to prepare a precursor which could be deformed properly within the sophisticated architecture of the conductor as required for all different aspects of the application.

Cooperation Bruker HTS GmbH Alzenau, Slovak Academy of Science - Institute of Electrical Engineering Bratislava, Karlsruhe Institute of Technology
Funded by EAS Bruker GmbH, DAAD, NESPA

Research Area 2
Magnetism and magnetic materials

Hole induced spin polarons in $LaCoO_3$

A. Alfonsov, E. Vavilova[1], A. Podlesnyak[2], D.I. Khomskii[3], V. Kataev, B. Büchner

$LaCoO_3$ is nonmagnetic at low temperatures and shows a temperature activated magnetism due to a change of the Co^{3+} spin state. Surprisingly, a very small hole doping (< 0.5 %) via Sr^{2+} or Ca^{2+} substitution for La^{3+} yields a strong magnetization already at low temperatures. The expected saturation magnetic moment should not exceed 5 μ_B per doped hole, which is the maximum possible value for the Co ion transformed into the 4+ oxidation state due to the heterovalent Sr/Ca substitution at the La site. In fact, the magnetic field dependence of the magnetization yields a much higher value of ~ 15 μ_B/hole. To uncover the nature of this effect we have measured electron spin resonance (ESR) on $La_{0.998}Sr_{0.002}CoO_3$ and $La_{0.998}Ca_{0.002}CoO_3$ samples using the unique possibilities of the high field ESR laboratory at the IFW Dresden. The home made setup enables high sensitive measurements in the frequency range from 10 GHz to 1 THz, in the magnetic fields up to 17 T and at temperatures from 300 K down to 2 K. The low temperature ESR experiments reveal multiple resonance excitations indicating the occurrence of extended clusters (spin polarons) with a high spin value and substantial orbital contribution to the magnetism (Fig.). We have found out that the crucial role in the formation of the spin polaron is played by the introduced hole: It turns the oxidation state of the central Co ion to 4+, changes the spin states of 6 neighbouring Co^{3+} ions and couples them ferromagnetically through the double exchange mechanism (Fig.). Details of the ESR experiments, supporting nuclear magnetic resonance and inelastic neutron scattering measurements, as well as the discussion of the spin polaron model can be found in Ref. [1].

[1] A. Podlesnyak et al., Phys. Rev. Lett. 101, 247603 (2008)

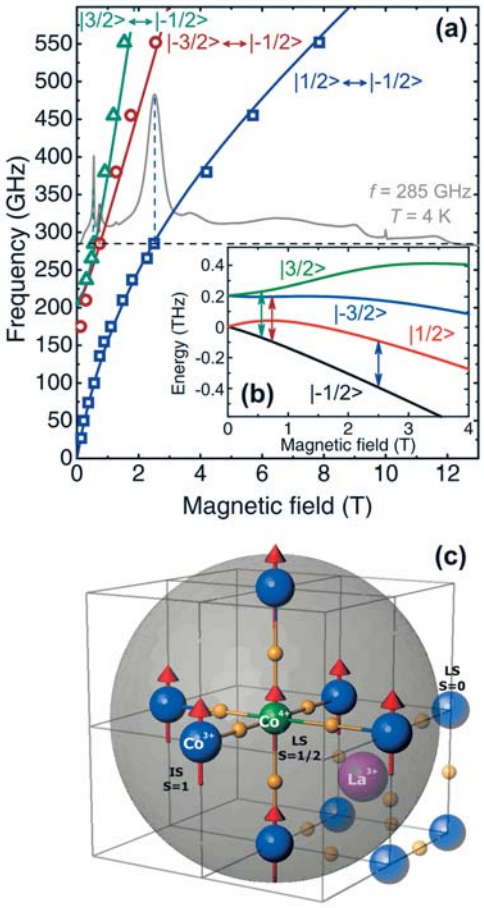

Fig. a) The ESR spectrum measured at a frequency $f = 285$ GHz and a temperature $T = 4$ K (gray line); the frequency dependence of the three most intense resonance lines at $T = 4$ K (cyan triangles, brown circles and blue squares). Solid lines (cyan, brown and blue) represent a calculated frequency dependence of the ESR absorption lines of the spin polaron with the spin $S = 13/2$, g-factor of ~2.6 and the anisotropy energy gap of ~100 GHz (~0.4 meV).
b) Calculated energy levels diagram of the spin polaron with $S = 13/2$ (high energy S_z states $|\pm 5/2>$ to $|\pm 13/2>$ are not shown). Arrows represent the three most intense ESR transitions between the S_z states $|3/2> \Leftrightarrow |-1/2>$, $|-3/2> \Leftrightarrow |-1/2>$ and $|1/2> \Leftrightarrow |-1/2>$ at a frequency $f = 285$ GHz and a temperature $T = 4$ K [see panel (a)].
c) Visualization of the spin polaron in $LaCoO_3$. A central Co^{4+} ion in the low spin (LS) $S = 1/2$ state is surrounded by 6 Co^{3+} ions in the intermediate spin (IS) $S = 1$ state. The hole is dynamically distributed over the cluster providing a ferromagnetic coupling of spins via the double-exchange mechanism.

Cooperations [1]Zavoisky Physical Technical Institute, RAS, Kazan, Russia; [2]Oak Ridge National Laboratory, Oak Ridge, USA; [3]II. Physikalisches Institut, Universität zu Köln, Köln, Germany
Funded by DFG, IMPRS

LSDA+U revisited

K. Koepernik, W. E. Pickett[1], E. R. Ylvisaker[1]

Density functional theory (DFT) is an amazingly successful tool to quantitatively describe many properties of solids, surfaces and molecules in the limit of "weak" correlation. In its practical implementation DFT is based on the local spin density approximation (LSDA) or gradient corrected schemes (GGA), which includes the full correlation

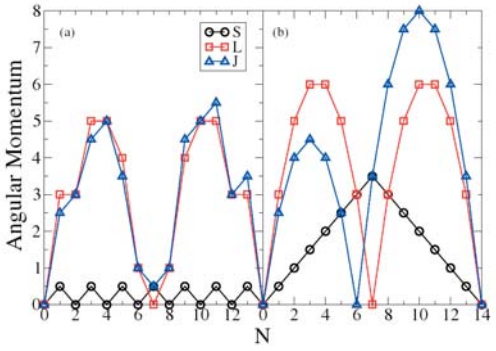

Fig.: Spin (S), orbital (L) and total (J) angular momentum for an isolated 4f-shell as a function of the total 4f-shell occupation. The left panel shows the results for the AMF functional and clearly violates Hund's first rule, while the right panel (AL/FLL functional) follows Hund's rules.

energy of the homogeneous electron liquid. This approach is lacking effects of the energy dependence of the electronic self-energy and contains spurious self-interactions, which becomes important in strongly correlated systems. One commonly used simplistic remedy for these problems is the LSDA+U scheme, which incorporates an ad-hoc occupation number dependent term to the functional. There are many heuristic arguments involved in its construction and consequently several different flavors of the theory exist. We investigated the physical implications of the various flavors of LSDA+U, based both on a theoretical analysis and on numerical calculations. It turns out that among the two commonly used flavors one exhibits a very strange behavior with respect to predicted ground state properties, which leads to a violation of Hund's first rule for isolated atoms. Our analytical results increase the understanding of the physical effects of these kinds of functionals and may lead to improved functionals. It is conceivable that this kind of discussion will also have implications for the LSDA+dynamical mean-field (DMFT) theory, since it is based on a similar ad-hoc Hamiltonian.

Cooperation [1]Univ. of California Davis, USA

Angle-resolved Photoemission Spectroscopy of Spin – Ladder Compounds

A. Koitzsch, D. S. Inosov[1], H. Shiozawa[2], V. B. Zabolotnyy, S. V. Borisenko, A. Varykhalov[3], C. Hess, M. Knupfer, U. Ammerahl[4], A. Revcolevschi[4], and B. Büchner

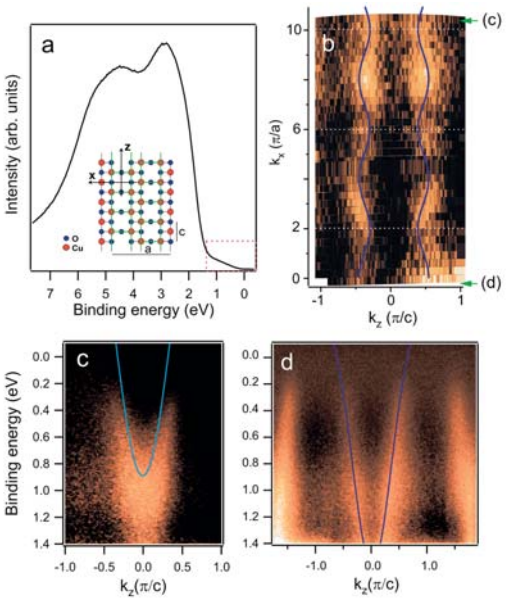

Fig.: Photoemission spectra of $Sr_{14}Cu_{24}O_{41}$. (a) k- integrated valence band. Inset: Crystal structure of the ladder plane. (b) Map of photoemission intensity at E_B = 0.4 eV integrated over ΔE = 0.08 eV. The blue line corresponds to the tight binding fit of bandstructure calculations for the bonding band [5]. Green arrows mark the k_x positions of the measurements in (c+d). (c) Intensity map with perpendicular polarization. The light blue line corresponds to the antibonding band of [5]. (d) Intensity map taken with parallel polarization.

One of the peculiar properties of the cuprates is their ability to form sophisticated crystal structures where copper-oxygen networks with a dimensionality between one and two can occur – so called ladder compounds. Cuprate two-leg ladder compounds of the type $Sr_{14-x}Ca_xCu_{24}O_{41}$ have been in the focus of intense research for many reasons: i) they are believed to be relevant for the cuprate high-T_c problem, both as simpler paradigm of t-J models [1] and due to the known affinity of the two-dimensional cuprates to one-dimensional (stripe) phenomena [2], ii) as quasi one-dimensional materials they are subject to strong quantum fluctuations and complex density wave order, giving rise to exotic ground states [3], iii) they are superconductors in their own right with an unresolved pairing mechanism [4]. We have investigated the electronic structure of $Sr_{14-x}Ca_xCu_{24}O_{41}$ (x = 0; 11.5) single crystals by angle-resolved photoemission spectroscopy. Remarkable agreement with bandstructure calculations is found. The Fermi surface is observed for $Sr_{2.5}Ca_{11.5}Cu_{24}O_{41}$ from which we derive a charge carrier concentration between 0.15 and 0.2 holes per Cu atom at T = 25 K in the ladder substructure. The chain substructures, on the other hand, act as diffraction grating for the ladder photoelectrons giving rise to incommensurate replicas of the ladder bands. A low energy band renormalization, a kink, is observed at E = 70 meV for $Sr_{2.5}Ca_{11.5}Cu_{24}O_{41}$. The kink is similar to the one found in two-dimensional cuprates, suggesting a close relationship between the latter and ladder compounds with high internal pressure.

[1] E. Dagotto et al., Phys. Rev. B **45**, 5744 (1992)
[2] J. M. Tranquada et al., Nature **375**, 561 (1995)
[3] T. Vuletic et al., Phys. Rep. **428**, 169 (2006)
[4] M. Uehara et al., J. Phys. Soc. Jpn. **65**, 2764 (1996)
[5] M. Arai et al., Phys. Rev. B **56**, R4305 (1997)

Cooperation [1]Max-Planck-Institute for Solid State Research, Stuttgart, Germany; [2]Univ. of Surrey, Guildford, United Kingdom; [3]BESSY, Berlin, Germany; [4]Univ. Paris-Sud, France

Non-existence of exact Kohn-Sham-equations in semi-relativistic current density functional theory

M. Taut, P. Machon, and H. Eschrig

One of the basic theorems for the widely used Kohn-Sham (KS) equations in density functional theory (DFT) is that for any *interacting* electron system in an external scalar potential $v^{ext}(\mathbf{r})$ there is a *non-interacting* model system, which provides the exact density $n(\mathbf{r})$ and energy E_{tot} of the ground state. This follows from the fact that the external potential is a unique functional of the density. If additionally a magnetic field (or vector potential $\mathbf{A}^{ext}(\mathbf{r})$) is involved, then semi-relativistic current density functional theory (CDFT) applies, but the external potentials $v^{ext}(\mathbf{r})$ and $\mathbf{A}^{ext}(\mathbf{r})$ are no more unique functionals of the densities $n(\mathbf{r})$ and $\mathbf{j}^{p}(\mathbf{r})$. Consequently, the existence of exact Kohn-Sham equations for the ground state cannot be proven. In standard CDFT implementations, the exsistence of exact KS equations is nevertheless presupposed. However, we have shown [1] using the exact analytical solutions of a two-electron quantum dot in a magnetic field [2] that in this system exact KS equations can exist only for certain orbital angular momenta. Consequently, the existence of exact KS equations is neither guaranteed for - nor restricted to ground states (see also Fig.), a result important for the application of KS theory to orbital magnetism.

[2] M. Taut, et al. Phys. Rev. A **80**, 022517 (2009)
[1] M.Taut, J. Phys. A**27**, 1045 (1994)

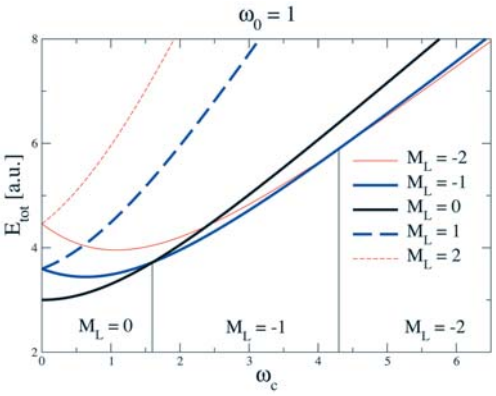

Fig.: Total energy of the harmonic two-electron quantum dot for fixed confinement frequency $\omega_0 = 1$ versus cyclotron frequency ω_c. The orbital angular momentum M_L is varied. Thick lines indicate states for which an exact Kohn-Sham system exists. The vertical lines indicate where the angular momentum of the ground state changes.

Electrodeposition of structured layers using defined magnetic field gradients

K. Tschulik, M. Uhlemann, J. Koza, K. Hennig, I. Mönch, V. Hoffmann, A. Gebert

Structuring of deposits has been demonstrated in ∇B-fields superimposed during the electrodeposition process in presence of paramagnetic ions as Cu^{2+}, Fe^{2+} or Co^{2+}. Defined ∇B -fields at disc-electrodes have been generated by a magnetic field template prepared from Fe wires (∅ = 1 mm, l = 3 mm) embedded in PVC (Fig. a) placed directly behind the electrode. The wire axes have been aligned perpendicularly to the horizontal electrode and magnetized by a homogeneous magnetic field B_{ex} of 0.5 T.

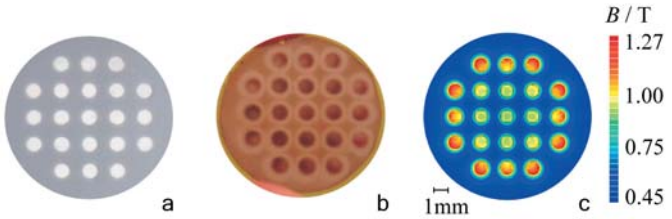

Fig.: Optical images of magnetic field template (a), structured Cu deposit (b), and simulated flux density distribution (c).

Obtained deposits show a direct correlation of the distribution of magnetic flux density B at the electrode and the morphology and thickness of the deposit. Maxima of deposit thickness correlate with maxima of B∇B, so evidently ∇B -fields can alter the current distribution at the electrode (Fig. b,c). As the depositions have been performed in the mass-controlled regime this observation indicates enhanced mass-transport of paramagnetic ions to these regions, leading to locally increased deposition rates. In contrast to that no structuring effect has been achieved for deposition of Bi from electrolytes containing diamagnetic Bi^{3+} ions. The structuring mechanism is mainly based on a sufficient influence of the field gradient force which attracts paramagnetic ions to regions of high field gradients. This force is overlapped by the Lorentzforce inducing a local MHD-convection.

Cooperation TU Dresden, Forschungszentrum Dresden-Rossendorf
Funded by DFG / SFB 609, Studienstiftung des deutschen Volkes

Highly ordered, half-metallic Co_2FeSi single crystals

C. G. F. Blum, S. Wurmehl, G. Friemel, C. Hess, G. Behr, B. Büchner, C. A. Jenkins[1], J. Barth[1], C. Felser[1], A. Reller[2], S. Riegg[2], S. G. Ebbinghaus[3], T. Ellis[4], P. J. Jacobs[4], J. T. Kohlhepp[4], and H. J. M. Swagten[4]

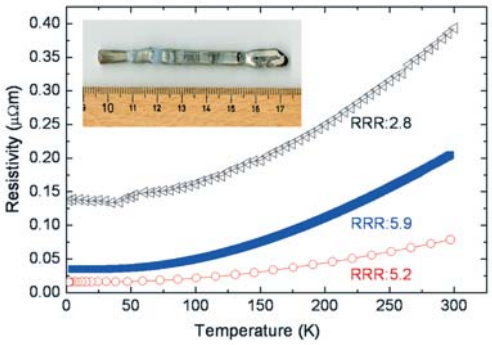

Fig.: Resistivity as a function of temperature for the Czochralski grown single crystal (triangles), the polycrystal (squares) and the zone molten single crystal (dots).The inset shows a rod obtained from the floating zone method containing large and high quality Co_2FeSi single crystals.

A wide variety of properties such as half-metallicity is found among Heusler compounds. In order to separate intrinsic and extrinsic properties, high quality single crystals are required. Here, we report on differently grown crystals (by arc-melting, floating zone and Czochralski method) of the half-metallic ferromagnet Co_2FeSi [1]. All crystals show excellent ordering, confirmed by Laue diffraction and nuclear magnetic resonance spectroscopy, resulting in outstanding electrical behaviour with low residual resistivity and high residual-resistivity-ratio. All Co_2FeSi crystals show a plateau in the resistivity below 50 K, which might point to half-metallic ferromagnetism. The cross-over from this unusual to more conventional transport (T^2 dependence) around 50 K indicates the onset of spin flip scattering and thus is indispensable for understanding the strong temperature dependence of Co_2FeSi tunnelling magnetoresistance-devices.

[1] C. G. F. Blum *et al.*, Appl. Phys. Lett. **95** (2009) 161903.

Cooperation [1]Johannes Gutenberg-Univ. Mainz, Germany; [2]Univ. Augsburg, Germany; [3]Martin-Luther-Univ. Halle-Wittenberg, Germany; [4]Eindhoven Univ. of Technology, The Netherlands

Funded by DFG (Research Unit 559) and WU595/1-1.

Epitaxial thin $SmCo_5$ films with perpendicular anisotropy

M. Seifert, V. Neu, and L. Schultz

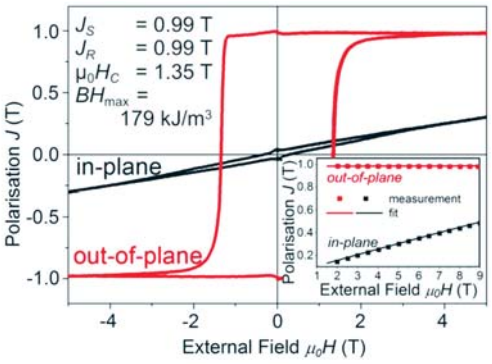

Fig.: Magnetic hysteresis of an epitaxial $SmCo_5$ film with perpendicular anisotropy. The flat and narrow hard axis loop can be fitted to a high uniaxial anisoptropy with K_u = 7.6 MJ/m³.

$SmCo_5$ is the hard magnetic material with the highest uniaxial magnetic anisotropy and is long established for bulk permanent magnet applications. As a thin film, epitaxial $SmCo_5$ has only been realized on Cr buffered MgO(110) with a perfect in-plane texture, where the c-axis is oriented along the MgO[001] direction [1]. Due to the interest in materials with strong perpendicular anisotropy, recently several groups investigated polycrystalline Sm-Co based thin films on Cu templates with a preferred orientation of the c-axis perpendicular to the film plane [2]. In contrast to this, we achieved epitaxial growth of $SmCo_5$ with a perpendicular anisotropy without the use of an additional copper layer, and with a largely improved anisotropy constant of $K_u = 7.6$ MJ/m³ [3].

The films have been prepared by UHV pulsed laser deposition (PLD) at 700°C in on-axis geometry (KrF excimer laser, 248 nm, base pressure $< 5 \times 10^{-9}$ mbar) on a Ru buffered Al_2O_3(0001) substrate. $SmCo_5$ $(10\bar{1}1)$ pole figure measurements result in two sets of poles with 6-fold symmetry which are rotated 30° with respect to each other in agreement with two rotated variants of hexagonal $SmCo_5$ growing with the c-axis perpendicular to the surface. For film reduced thicknesses the intensity of one variant decreases, leading to a single orientation of $SmCo_5$ on Al_2O_3. The figure shows the highly anisotropic magnetic behavior of a 20 nm thin $SmCo_5$ film when measuring out of the film plane (i.e. parallel to the uniaxial anisotropy axis) and perpendicular to it, together with the extrinsic magnetic properties.

[1] A. Singh, *et al.*, J. Appl. Phys. **99**, 08E917 (2006)
[2] J. Sayama *et al.* Appl. Phys. Lett. **85**, 5640 (2004); S. Takei *et al.* J. Magn. Magn. Mater. **272**, 1703 (2004)
[3] M. Seifert *et al.*, Appl. Phys. Lett. **94**, 022501 (2009)

Huge tetragonal distortion in epitaxial films

J. Buschbeck, I. Opahle, M. Richter, U. K. Rößler, L. Schultz, S. Fähler

Strained coherent film growth is commonly either limited to ultrathin films or low strains. Here, we present an approach to achieve high strains in thicker films, by using materials with inherent structural instabilities. As an example, 50 nm thick epitaxial films of the $Fe_{70}Pd_{30}$ magnetic shape memory alloy are examined. Strained coherent growth on various substrates allows us to adjust the tetragonal distortion from c/a_{bct} = 1.09 to 1.39, covering most of the Bain transformation path from *fcc* to *bcc* crystal structure.

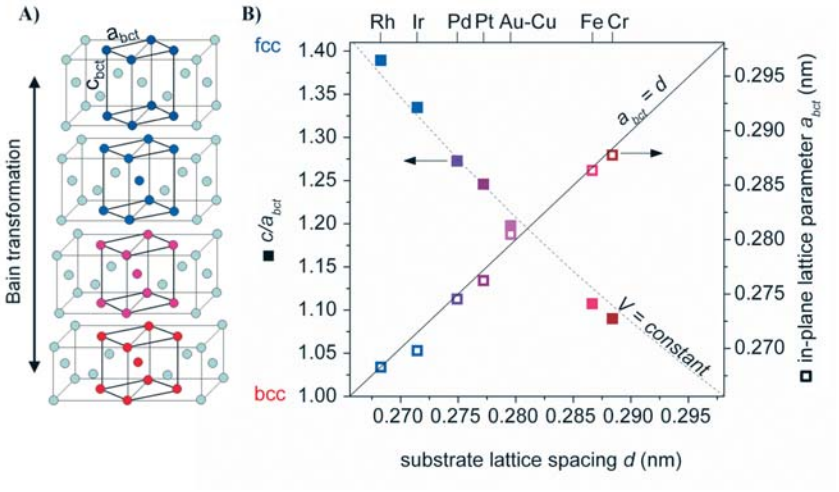

Fig.: A) Sketch of the Bain transformation between *fcc* (top) and *bcc* structure (bottom); B) *c*/*a* ratio (left scale) and in-plane lattice constants (right scale) of the Fe-Pd *bct* unit cell in dependence of the lattice spacings of the various buffer layers used (marked on top).

The magnetic properties of these films display considerable changes: The Curie temperature is increased more than 25% with respect to the value for $Fe_{70}Pd_{30}$ with *fcc* structure. This is accompanied by an increase of the magnetic anisotropy from near zero to values close to those of "*fct*" bulk $Fe_{70}Pd_{30}$.

Softening of the crystal lattice and a flat energy landscape along the Bain path are not a unique feature of this alloy. Similar lattice instabilities may be exploited in various functional materials including (magnetic) shape memory, ferroelectric, multiferroic, or magnetocaloric materials for extended adjustability of their crystal structure in strained epitaxial films.

Cooperation Univ. Frankfurt; Johannes Gutenberg-Univ.Mainz
Funded by DFG via SPP1239 (www.MagneticShape.de)

Domain models for ferromagnetic shape memory materials

A. T. Onisan, A. N. Bogdanov, U. K. Rößler

The twinned martensitic microstructure of ferromagnetic shape-memory materials is transformed by modest applied magnetic fields. A domain model for the twin-variant and magnetic domain distribution in bulk systems of ferromagnetic shape-memory materials has been developed. The approach combines crystal elasticity, compatibility between twins with a (pseudo)-tetragonal lattice structure, and micromagnetic domain theory. The model has been applied to calculate detailed phase diagrams under external magnetic fields and stresses for the archetypical ferromagnetic shape-memory material Ni-Mn-Ga as a magnetic system with easy-axis anisotropy and for Fe-Pd with easy-plane fourfold anisotropies. The example shown is a phase diagram for Ni-Mn-Ga with two-variant microstructure composed of x- and z-variants. The phase diagrams allow to analyse the anhysteretic transformation and magnetization processes under combined

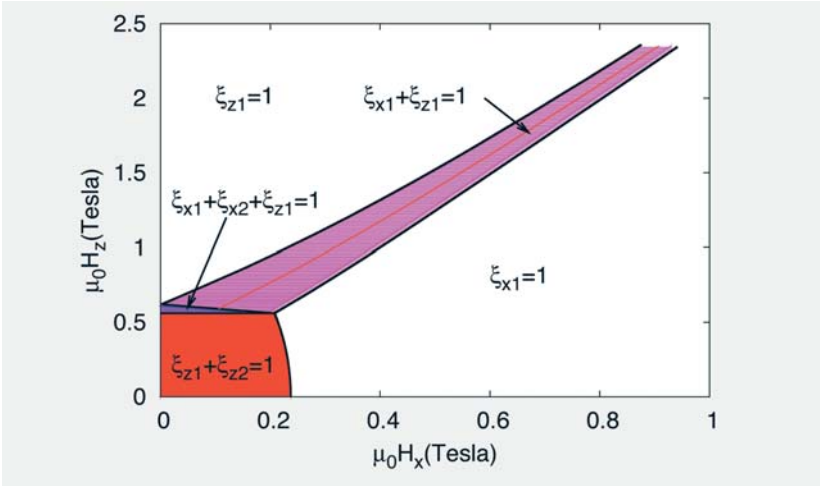

Fig.: Phase diagram for Ni-Mn-Ga under magnetic fields and compressive stress in z-direction in terms of volume fractions ξ of tetragonal x- and z-variants and internal magnetic domains 1 (2) with up (down) magnetization.

external magnetic fields and stresses. It is found that equilibrium domain and variant structures, caused by the depolarization, can own degrees of freedom in these systems that allow a rearrangement without energy cost.

Funded by DFG (SPP1239, A8)

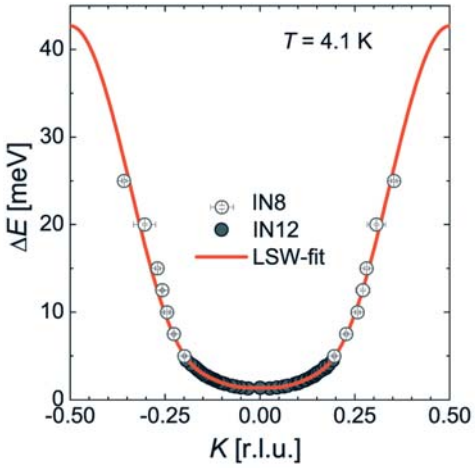

Fig. 1: The experimental magnon dispersion measured by various inelastic neutron scattering (INS) studies along the chain direction as compared with a linear spin wave (LSW)-fit.

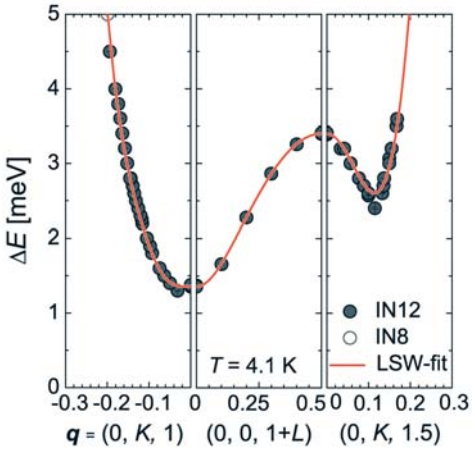

Fig. 2: The same as in Fig. 1 as measured by cold neutrons including also a direction perpendicular to the CuO_2-chains (central panel). For the low-energy minimum corresponding to incommensurate spiral excitations see right panel.

Highly dispersive and low-energy spiral magnetic excitations in the frustrated chain compound Li_2CuO_2

S. L. Drechsler, W. E. A. Lorenz, R. Klingeler, N. Wizent, G. Behr, U. Nitzsche, J. Málek, B. Büchner

Li_2CuO_2 is the first and the most frequently studied compound of the growing class of frustrated edge-shared spin-chain cuprates. Owing to its structural simplicity with ideally planar CuO_2 chains it can be considered as a model quasi-one-dimensional (1D) frustrated quantum spin system. We performed various inelastic neutron scattering (INS) investigations of Li_2CuO_2 and detected the long sought quasi-1D magnetic excitations with a large dispersion along the CuO_2-chains (Fig. 1). The total dispersion is governed by a surprisingly large ferromagnetic (FM) nearest-neighbor exchange integral $J_1 = -228$ K. An anomalous quartic dispersion near the zone center and a pronounced minimum corresponding to a low-energy spiral excitation over a commensurate collinear NÉEL ground state with a pitch angle of about 41° (Fig. 2) which points to the vicinity of a 3D FM-spiral critical point. The leading exchange couplings are obtained applying standard linear spin-wave theory. The 2nd neighbor inter-chain interaction suppresses a spiral state and drives the FM in-chain ordering below the NÉEL temperature. The obtained exchange parameters are in agreement with the exact diagonalization results for a realistic five-band extended HUBBARD Cu3dO2p model on Cu_nO2_{n+2} clusters (n = 2 - 6) and with predictions derived from total energy calculations for various magnetic structures using the L(S)DA+U scheme, if a moderate value of the COULOMB repulsion on Cu-sites $U = 5.6$ eV is employed. The achieved detailed knowledge of the main exchange couplings derived from the INS-data provides a good starting point for an improved general theoretical description of other CuO_2-chain systems.

[1] W.E.A. Lorenz et al., Europhysics Lett. **88**, 37002 (2009).

Cooperation R. Kuzian, Institute for Problems of Materials Science, Kiev, Ukraine; H. Rosner, Max Planck Institute for Chemical Physics of Solids, Dresden; A. Hiess, Institut Laue Langevin, Grenoble, France; M. Loewenhaupt, Institut für Festkörperphysik, TU Dresden

Funded by DFG, Emmy-Noether Gruppe

Permanent Magnets

O. Gutfleisch, T. G. Woodcock, J. Thielsch, K. Güth, J. Lyubina, L. Römhildt,
K. Skokov, R. Schäfer, K.-H. Müller, L. Schultz

New energy concepts are required for the future of our industrial society resulting in e.g. an ever increasing emphasis on improving the efficiency of electricity transmission and utilisation and in the progressive replacement of oil-based fuels in transportation by electric motors. Recently, there is a much revived interest in various types of high performance permanent magnets (RPMs) based on rare earth intermetallic compounds. This is triggered by e.g. the growing demand for energy efficient technologies in which magnets often play a pivotal part. One prominent example is found in automobiles, specifically for traction motors in hybrid electric vehicles (HEVs). In this context, advanced permanent magnets are being studied in our group in terms of their fundamentals, processing and applications. This includes the determination of intrinsic magnetic properties, investigation of high pulsed magnetic field-induced phase transitions, detailed microstructural and micromagnetic analysis as well as the development of novel processing routes.

Fig. 1: Highest resolution TEM image of the $Nd_2Fe_{14}B$ phase in a Dy-free sintered magnet with the c-axis perpendicular to the imaging plane.

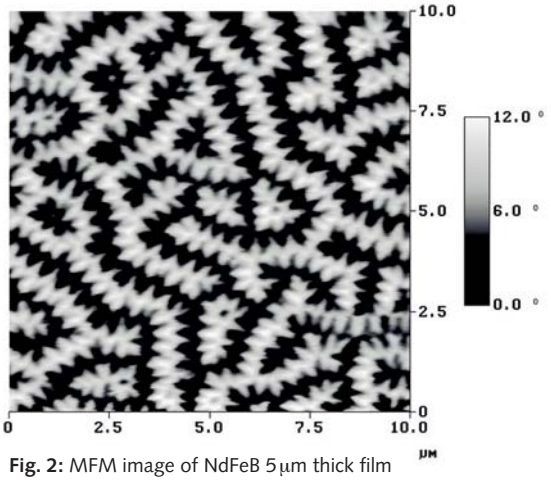

Fig. 2: MFM image of NdFeB 5 µm thick film deposited by triode sputtering (cooperation Institute Néel Grenoble).

Generally, the major driver for research and development of RPMs is the need for maximised energy densities at various operating temperatures. This includes $Pr_2Fe_{14}B$-type magnets for applications at 77 K together with high T_c superconductors, $Nd_2Fe_{14}B$-type magnets with reduced Dy content and much improved temperature stability for electromotor applications at around 450 K, and a new generation of SmCo 2:17-type magnets for applications exceeding 670 K. It also includes magnetic microelectromechanical systems (mag-MEMS) for e.g. high speed permanent magnetic generators which require highly textured thick RPM films.
The characterisation and engineering of internal interfaces on a (sub-)nano scale is aimed at improved temperature stability of the magnet for HEVs applications.

Cooperation CNRS Grenoble, France; Toyota Motor Corporation, Japan; Tohoku Univ. Sendai, Japan; Univ. of Texas, USA; Vacuumschmelze Hanau, Germany; National Institute of Materials Science, Tsukuba, Japan
Funded by Toyota, Hans L. Merkle Stiftung, Bosch, Aichi-Steel, Forschungsvereinigung Antriebstechnik (FVA)

Magnetocaloric Materials

O. Gutfleisch, K. Skokov, J. Lyubina, M. Krautz, N. Scheerbaum, J. Liu, M. Richter

Magnetic refrigeration offers a solid state alternative to standard gas compression-based cooling that would simultaneously eliminate the need for harmful refrigerant gases and reduce energy requirements and hence carbon dioxide emissions. About ten years have passed since the discovery of the giant magnetocaloric effect in $Gd_5(Si,Ge)_4$, the magnetic refrigerant that re-ignited interest in magnetic cooling around room temperature. Since then a number of alternative magnetic refrigerants have emerged, resulting in a field that is yielding fundamental discoveries regarding solid-solid phase transitions whilst opening the way to new applications in cooling and other magneto-thermal and magneto-mechanical areas.

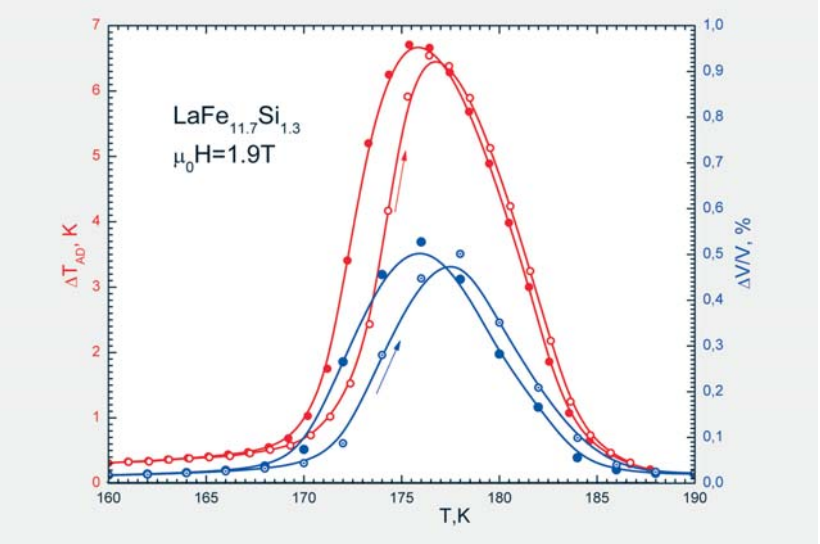

Fig.: An example for a solid-solid phase transition in $La(Fe,Si)_{13}$ correlating the resulting adiabatic temperature change with a strong magnetovolume effect, both in an applied magnetic field of 1.9 Tesla.

Our research focuses on the search for novel material systems, novel processing routes, and nano-architectures, the hysteresis properties, the time-dependency of magneto-structural and magnetoelastic transitions, the tailoring of operating temperature and of required magnetic fields, the engineering properties of magnetocaloric materials and ultimately the design of magnetic cooling devices. Systems of interest are the La-series alloy compounds, some transition-metal-based compounds, especially MnFePGe, as well as Heusler alloys.

Cooperation Imperial College London, UK; Vacuumschmelze Hanau, Germany; Istituto Nazionale di Ricerca Metrologica Torino, Italy; Univ. de Barcelona, Spain; Ames National Labs, USA; Univ. de Zaragoza, Spain; Camfridge Ltd., UK
Funded by EU (Solid State Energy Efficient Cooling - SSEEC), BASF Future Business

Research Area 3
Molecular nanostructures and molecular solids

Engineering of the energy level alignment at organic semiconductor interfaces by intramolecular degrees of freedom: transition metal phthalocyanines

M. Grobosch, V. Yu. Aristov, O. V. Molodtsova, C. Schmidt, and M. Knupfer

We have determined the energy level alignment at interfaces between various transition metal phthalocyanines (MnPc, FePc, CoPc, NiPc, CuPc) and gold using photoemission spectroscopy. Our results demonstrate that the transition metal center has a strong influence on the electronic properties of the phthalocyanine films as well as their interfaces with gold. This offers a route to adjust the hole injection barrier via the choice of otherwise equivalent molecular organic semiconductors. In particular, the interfaces MnPc/Au and CoPc/Au are characterized by a small hole injection barrier, which would be advantageous for applications. These are directly related to the presence of metal 3*d* states closest to the chemical potential. The nature of the molecular orbitals (metal 3*d* or ligandlike), that form the states closest to the chemical potential differ between MnPc and CoPc. In CoPc they are of predominantly metallic 3*d* character with a_{1g} symmetry and do not hybridize with the ligand π-system. Therefore, they are most likely to be highly localized due to the very small overlap between these orbitals of adjacent molecules and thus do not contribute to charge transport. Oppositely, the relevant states in MnPc strongly hybridize with the ligand, and thus, injection into these states with a small barrier from gold should also result in continuous charge transport across the interface. For details see: M. Grobosch *et al.*, J. Phys. Chem. C **113**, 13219 (2009).

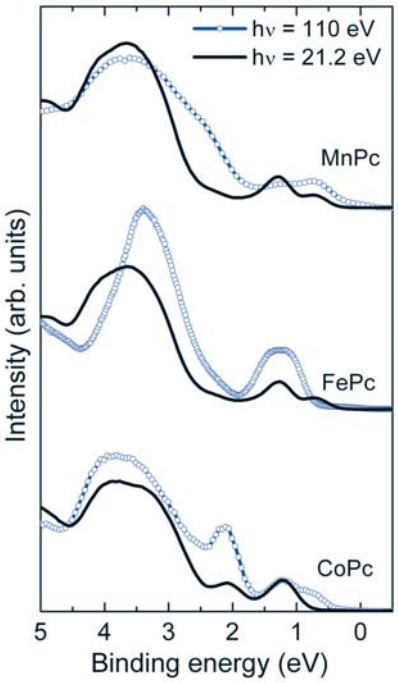

Fig.: Comparison of the valence band photoemission spectra of MnPc, FePc, and CoPc taken with photon energies of 21.2 and 110 eV (MnPc, CoPc) or 100 eV (FePc). Due to different cross sections, the data at 100/110 eV more strongly reflect metal 3d contributions.

Cooperation Institute of Solid State Physics, Russian Academy of Sciences; TASC-INFM Laboratory; Univ. of Johannesburg
Funded by DFG, RFBR

Time-delayed release of the cytostatic carboplatin from multiwalled carbon nanotubes

D. Haase, M. Arlt, K. Krämer, A. Leonhardt, S. Oswald, M. Ritschel, R. Klingeler, S. Hampel, B. Büchner

The ongoing progress in developing tailored nanoscaled materials opens novel perspectives in applying nanotechnological approaches for medical therapy. Here, we show the feasibility of carbon nanotubes (CNT) as casing and carrier for cytostatics and demonstrate time-delayed release which is preferable in actual chemotherapies.

CNT/Carboplatin-hybrids have been synthesized via a liquid phase method using different types of CNT (multiwalled CNT with tubular and with herringbone structure, respectively). The relevant difference between the starting materials concerns their inner diameter which amounts 10-20 nm for the tubular CNT and about 100 nm for the herringbone type CNT. Interestingly, the carboplatin filling content is the same for both types, i.e. around 0.13 mg Pt per mg total mass. The release of the drug from the CNT was investigated by dispersion of the hybrids in cell culture medium and quantification of the drug present in the medium. Concerning the release, the tubular CNT/Carboplatin-hybrid was found to be favourable from which after 7 days 30 % of the Pt-content have been released, thereby demonstrating the carrier function for drugs. In comparison, the herringbone CNT/Carboplatin-hybrid released only 10 % of the Pt after 7 days.

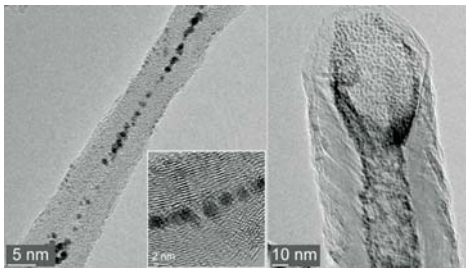

Fig. TEM images of two different types (tubular and herringbone) of CNT filled with Carboplatin.

Cytotoxicity of the hybrids as well as of the pure CNT was assessed *in vitro* using prostate carcinoma cells. CNT/Carboplatin-hybrids reduced cell viability with the same efficiency as pure Carboplatin at the same concentration. Carboplatin-loaded CNT effectively reduced colony formation of prostate cancer cell lines similar to Carboplatin solution. Our study highlights the potential of the use of CNT for biomedical applications.

Cooperation Department of Urology, TU Dresden University of Technology
Funded by DFG, EU

Iron filled carbon nanotubes – Novel high resolution high stability probes for quantitative magnetic force microscopy

F. Wolny, T. Mühl, U. Weissker, K. Lipert, A. Leonhardt, B. Büchner

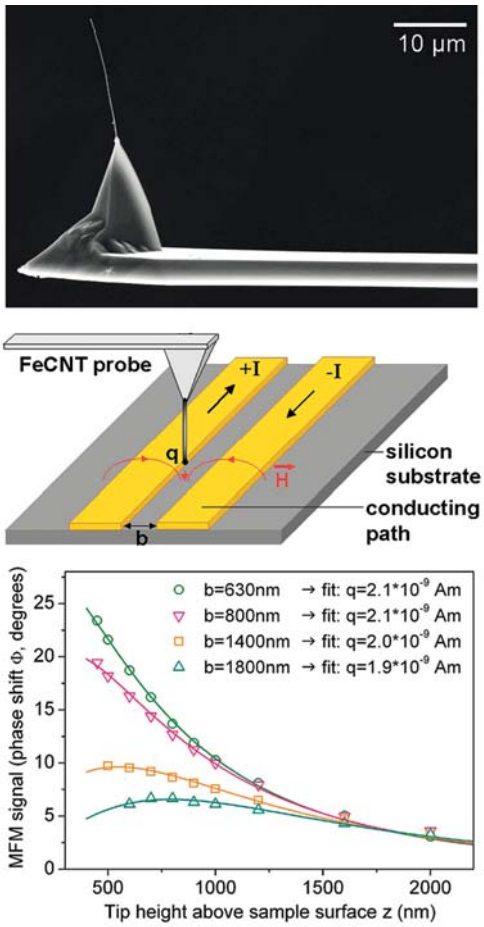

Magnetic force microscopy (MFM) is a popular scanning probe technique to qualitatively image magnetic stray fields. To obtain quantitative information on the magnetic stray field or its gradients at the specimen's surface it is necessary to know the magnetic characteristics of the applied MFM tip. However, due to the complex geometry of conventional magnetically coated MFM probes, the effective magnetic tip coating involved in the tip-sample interaction depends on the geometry of the sample stray field. We use an iron filled carbon nanotube (FeCNT) which contains a long single-crystal iron cylinder of defined geometry (several microns in length, 10-50 nm in diameter) as MFM probe. This probe possesses well defined magnetic properties and thus permits a straightforward, universal calibration. The enclosed ferromagnetic wire can be regarded as an extended dipole of which only the monopole close to the sample surface plays a role during the imaging process. An easy calibration routine involving two parallel conducting paths that produce a defined magnetic field can be used to determine the probe's magnetic monopole moment needed for quantitative MFM measurements. Furthermore, the FeCNT probe has many more advantages over a conventional MFM probe: the mechanical and oxidation stability of the FeCNT leads to an extraordinarily long probe lifetime, the small diameter enables a high magnetic resolution and the magnetic shape anisotropy of the elongated iron cylinder ensures a stable direction of the probe magnetization.

Fig.: Top: Iron filled carbon nanotube attached to a conventional AFM cantilever.
Middle: Setup for calibrating the FeCNT probe. The gold conducting paths of known geometry produce a defined magnetic field which is used to relate the MFM signal to actual magnetic field gradient values. Bottom: Calibration curves for a FeCNT probe. Conducting paths with different geometry (separation b between both paths) yield similar values of the corresponding probe magnetic monopole moment q.

Cooperation Ohio State Univ., USA
Funded by DFG

Space-charge-limited currents in organics with trap distributions

G. Paasch, S. Scheinert[1]

Analytical approximations for space-charge-limited currents (SCLCs) in systems with exponential or Gaussian trap distributions were widely used in analyzing organic diodes. The current follows a power law with a transition into the trap-free SCLC at high voltages and an ohmic low voltage limit. The power coefficient γ is connected with either the decay constant or the variance of the distributions. Within these formulations, it is not possible to check the relevance of the numerous approximations needed to derive them. This concerns especially the relations of the contact work functions and of the layer

thickness with the trap concentration, the position of the center of the trap distribution and its maximum value. Application of the analytical approximations to results of full numerical simulations allows one to set limits for the parameter ranges in which the approximations can be applied. In the case of the exponential distribution the analytical approximation is rather good for high trap concentrations and thicker layers. However, the simulations reveal a number of additional peculiarities. Such, the high voltage limit is usually not the trap-free SCLC but ohmic and determined only by the anode barrier, the low voltage limit leads to a diodelike dependence with a large ideality factor and scaling with layer thickness and position of the trap distribution is extremely limited. In the case of the Gaussian trap distribution the simulations show indeed that the formula together with the connection between the power coefficient and the variance of the distribution fails completely. *Thus, in principle, earlier analyzes of experimental data should be revised by using numerical simulations.*

[1] G. Paasch and S. Scheinert, JOURNAL OF APPLIED PHYSICS **106**, 084502 (2009)

Cooperation [1]Institute of Solid State Electronics, Ilmenau Technical Univ.
Funded by DFG

Co Dimers on Hexagonal Carbon Rings Proposed as Subnanometer Magnetic Storage Bits

R. Xiao, D. Fritsch, M. D. Kuz'min, K. Koepernik, H. Eschrig, M. Richter, K. Vietze[1], G. Seifert[1]

It is demonstrated by means of density functional and *ab initio* quantum chemical calculations [1], that transition-metal–carbon systems have the potential to enhance the presently available area density of magnetic recording by 3 orders of magnitude. As a model system, Co_2 benzene with a diameter of 0.5 nm is investigated. It shows a magnetic anisotropy of the order of 0.1 eV per molecule, large enough to store permanently one bit of information at temperatures considerably larger than 4 K. A similar performance can be expected, if cobalt dimers are deposited on graphene or on graphite.

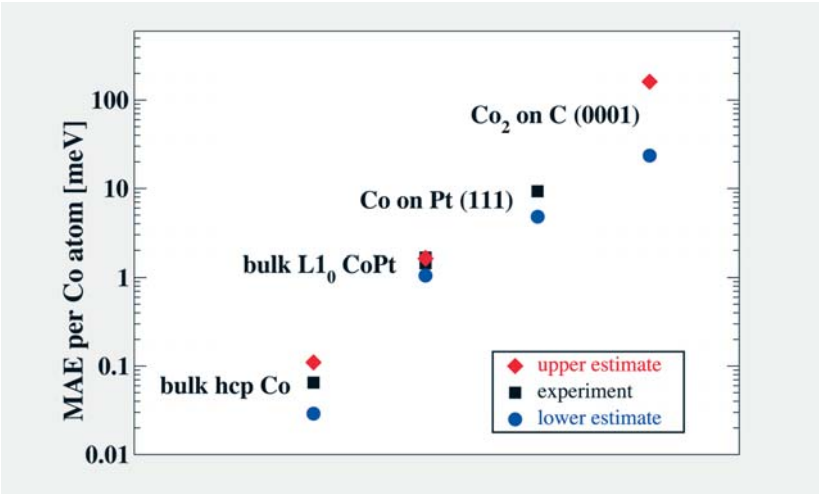

Fig. Magnetic anisotropy energy of Co atoms in different chemical and structural environments. Black squares denote experimental data, blue circles and red diamonds denote lower and upper estimate theoretical data. Bulk hcp Co, bulk $L1_0$ CoPt, Co atoms on the Pt (111) surface, and Co dimers on the graphite (0001) surface (our prediction) consecutively differ from each other by about 1 order of magnitude.

[1] R. Xiao et al. Phys. Rev. Lett. **103** (2009) 187201, selected for Virtual Journal of Nanoscale Science & Technology **20**, 2009.

Cooperation [1]TU Dresden
Funded by DFG, SPP 1145 and FOR 520.

The CVD synthesis of carbon coated magnetic nanoparticles

A. Leonhardt, V. Khavrus, E. M. M. Ibrahim, A. A. El-Gendy, S. Hampel, R. Klingeler, B. Büchner

Magnetic nanoparticles are receiving a lot of attention because this kind of heterostructure offers opportunities to develop devices and materials with new functions for different applications such as magnetic recording, tissue engineering, drug delivery/targeting, magnetic resonance imaging, magnetic bio-separation, and so on. The necessity of coating magnetic nanoparticles with protective shell like carbon is to achieve their stability against oxidation and corrosion and reduce their agglomeration.

Carbon coated Fe, Co and Ni nanoparticles (Fe@C, Co@C, and Ni@C, respectively) have been produced by high pressure chemical vapour deposition [1, 2]. The used method is based on the decomposition of a vapor consisting of metallocene ($Me(C_5H_5)_2$, Me = Fe, Co, or Ni) at a temperature in the range of 800–950 °C and a pressure of 10–30 bar in a horizontal steel reactor. A water-cooled finger is located in the cold zone of the reactor. The gas mixture is injected by using a nozzle-system. After the deposition process Me@C nanoparticles are concentrated on the cooled finger. Scanning and high resolution transmission electron microscopy images show that the nanoparticles have a size distribution from 2 to 100 nanometers and display the core/shell structure with one or more metal particles forming the core in a particular shell (see Fig.). The thickness of the protective carbon layers encapsulating the core particles amounts to 3–7 nm. The coated nanoparticles are ferromagnetic at least up to 400 K [1].

The proposed method can be extended for the synthesis various carbon coated alloys nanoparticles with different stochiometric ratio of the core composition using different volatile metalorganic compounds.

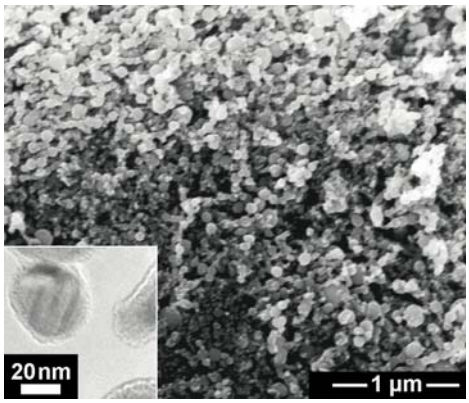

Fig.: SEM and TEM (inset) images of prepared Co@C nanoparticles.

[1] A.A. El-Gendy et al. Carbon 47 (2009) 2821-2828.
[2] V.O. Khavrus et al. J. Phys. Chem. C 2010, accepted.

Cooperation L.V. Pisarzhevsky Institute of Physical Chemistry, National Academy of Sciences of Ukraine, Kyiv, Ukraine; Sohag Univ. Egypt.
Funded by DFG, SMWK

Research Area 4
Metastable alloys

Liquid-liquid phase separation in binary Ti-Gd and Zr-Gd melts

W. Löser, S. Schmitz, H.-G. Lindenkreuz, N. Mattern, B. Schwarz, B. Büchner

Phase separated metallic glasses, as a new class of cluster materials, can be produced from complex alloys involving binary terminal systems with both negative and positive heats of mixing, respectively. It was shown that phase separation of the supercooled liquid state into two different glasses occurred in melt spun Zr-based metallic glass alloys due to the positive heat of mixing in the liquid state for Zr-R, where R is a Rare Earth element. Liquid phase separation below a critical temperature T_c can principally occur within either a stable or a metastable miscibility gap. While the former is an equilibrium phase diagram feature, the latter one lies beneath the liquidus curve ($T_c < T_L$). For thermodynamic modeling of glass forming systems experimental data are an urgent need. Liquid phase separation in two binary melt systems, Gd-Zr and Gd-Ti, related to phase separated metallic glasses are investigated by electromagnetic levitation experiments along with differential scanning calorimetric (DSC) studies. Gd-Ti samples quenched onto a copper chill substrate from temperatures below the binodal line exhibit typical coarse phase separated microstructures, assigning melt immiscibility. According to the undercooling experiments the miscibility gap of Gd-Ti melts extends at least from 10 to 80 at.% Gd (Fig.), much wider than reported previously [1]. The critical temperature is about 1580°C at $Gd_{20}Ti_{80}$. In the Gd-Zr system melt droplets quenched from the undercooled state exhibit concurrent coarse Gd and Zr primary phase constituents suggesting a metastable miscibility gap. The dissimilar phase separation features of the two binary systems investigated may imply different glass forming ability of the alloys.

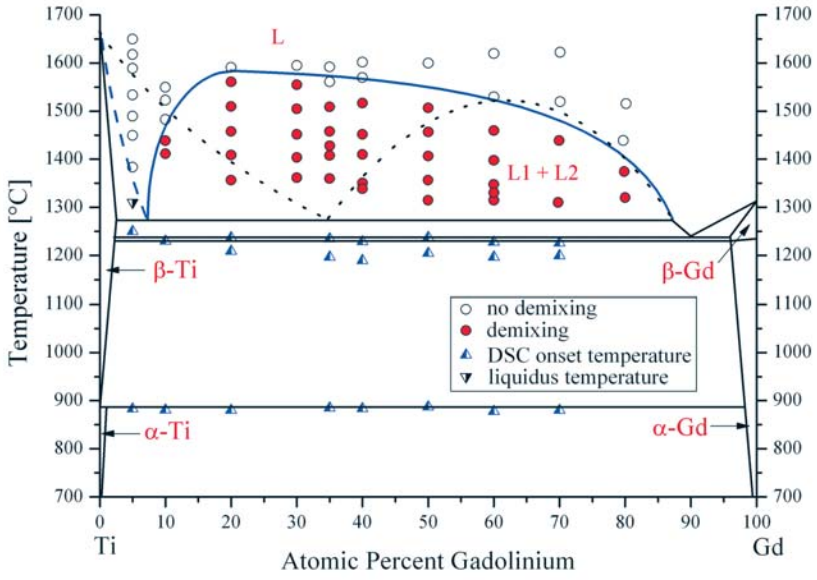

Fig.: Phase diagram of Gd-Ti with predicted liquidus and binodal line (dotted). Onset temperatures of the α-Ti to β-Ti solid state transformation, the eutectic/monotectic reaction and the liquidus temperature in case of Gd_5Ti_{95} from the DSC measurements are denoted by triangles. Different microstructures of samples quenched from the various temperatures are denoted by open dots (macroscopically homogeneous microstructure) and filled dots (coarse phase separated microstructure), respectively. Full line: binodal line fitted from microstructure analyses. Dashed line: tentative liquidus line.

[1] J.L. Murray. In: T.B. Massalski, editor. *Binary alloy phase diagrams*, ASM International, Materials Park (OH); 2nd Ed., 1990, p.1935.

Cooperation DLR Cologne, TU Bergakademie Freiberg
Funded by Pakt für Forschung 2008

Phase separation in $Cu_{46}Zr_{47-x}Al_7Gd_x$ metallic glasses

N. Mattern, J. M. Park, J. H. Han, J. Eckert

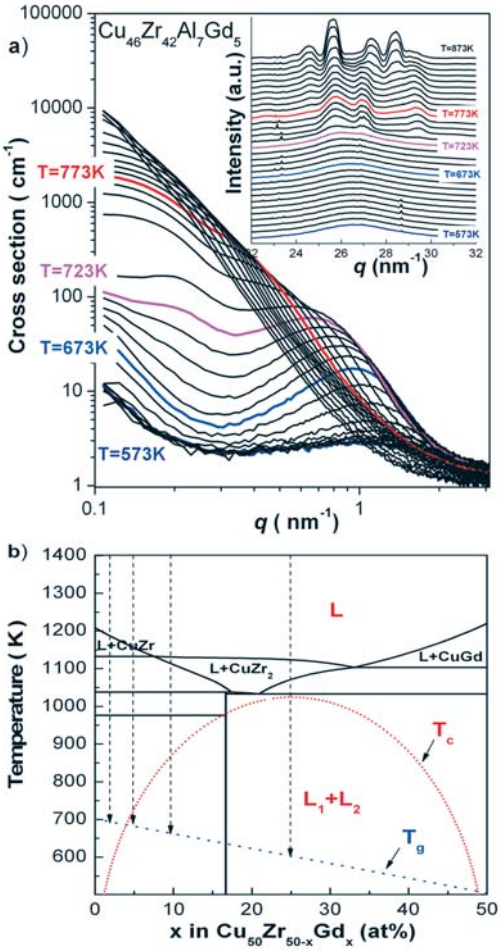

Phase separated metallic glasses can be prepared in the Cu-Zr-Gd system by rapid quenching the melt as a consequence of the large positive enthalpy of mixing between gadolinium and zirconium [1,2]. The influence of composition on phase separation and microstructure of $Cu_{46}Zr_{47-x}Al_7Gd_x$ glasses was studied by in-situ synchrotron small-angle scattering (SAXS) combined with simultaneous measurement of wide angle X-ray scattering (WAXS). The question viewed is to which extend phase separation occurs in the glasses if the concentration of gadolinium is low, because for such compositions improved glass forming ability and plasticity is observed [1]. Low SAXS intensities of $Cu_{46}Zr_{47-x}Al_7Gd_x$ alloys with $x \leq 5$ indicate a homogeneous glass for the as-quenched state. Fig. 1a shows the in situ scattering data of the $Cu_{46}Zr_{42}Al_7Gd_5$ glass at elevated temperatures. The increase of the SAXS intensities between T = 573 – 673 K give evidence of on-going phase separation by spinodal decomposition with a correlation length of about 6 nm prior to crystallisation as seen by WAXS at T_x = 723 K. For $x \geq 7$ at % the heterogeneities are already observed in the as-quenched glasses increasing in size for higher gadolinium contents. Fig. 1b shows the calculated pseudo-binary section along $Cu_{50}Zr_{50}$-$Cu_{50}Gd_{50}$ of the ternary phase diagram. The composition dependence of the miscibility gap of the under-cooled metastable liquid determines the structure formation of the glasses. Early stages of spinodal decomposition or an almost homogeneous glassy state is obtained if the critical temperature of liquid-liquid phase separation T_C is near to the glass transition temperature T_g. On the other side, if T_C is much larger then T_g, the microstructure becomes coarsened due to additional growth of the phase separated liquids during quenching.

Fig. 1a: SAXS and WAXS (inset) intensities of glassy $Cu_{46}Zr_{42}Al_7Gd_5$ at elevated temperatures. After measurement at T = 573 K the temperature was stepwise increased by 10 K and repeated for each temperature.
Fig. 1b: Calculated pseudo binary section of the Cu-Zr-Gd phase diagram with the miscibility gap in the undercooled metastable liquid (red dotted line). The glass transition temperature T_g is extrapolated from the binary glasses (blue dashed line).

[1] E. S. Park et al. Scripta Mater. 57 (2007) 49.
[2] I.V. Stasi et al. J. Optoelectronics and Advanced Materials 10 (2008) 2963.

Cooperation Yonsei Univ. Seoul, Hasylab at DESY Hamburg
Funded by DFG

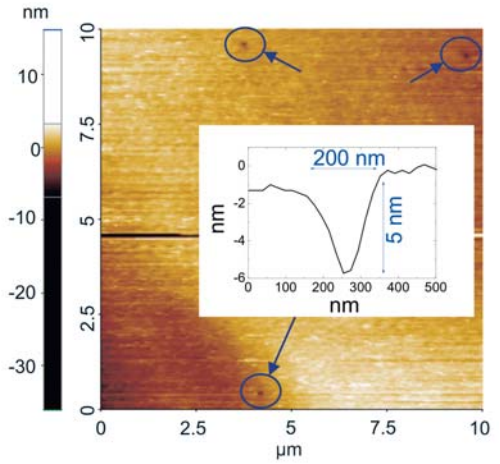

Fig.: In-situ AFM image of a corroding surface of a Fe-based BMG

In-situ AFM studies for corrosion analysis of Fe-based bulk metallic glasses

F. Gostin, A. Gebert, M. Uhlemann, U. Kühn, J. Eckert, L. Schultz

In-situ atomic force microscopy (AFM) is a powerful technique which offers the possibility of direct observation of surface topographical changes during electrochemical measurements. An in-house built set-up allows a three electrode configuration to be used and full capability of control with an external potentiostat. Studies concerning the particularities of corrosion damage morphologies of Fe-based glassy alloys have not been performed up to now. Corrosion morphologies of classical crystalline alloys are strongly dependent on their structural characteristics such as grain boundaries, secondary phases, different orientation of grains etc. However, glassy alloys are missing most of these. In consequence, initiation of corrosion on such alloys is expected to be stochastic in nature. In-situ AFM realizes the detection of very early corrosion morphology features due to two factors: one is the very good depth resolution and the

second is the advantage of monitoring the same area of the surface throughout the corrosion process. This in turn allows tracing back the features from the late stages where they are easily visible. The figure shows an in-situ AFM image of a bulk glassy $(Fe_{44.3}Cr_5Co_5Mo_{12.8}Mn_{11.2}C_{15.8}B_{5.9})_{98.5}Y_{1.5}$ alloy surface taken after 1 hour in 0.5 M H_2SO_4 under free corrosion conditions. The arrows indicate initial centres of dissolution on the nano-scale otherwise not observable by optical or electron microscopy. Their appearance can be correlated with the chemical short range order of the glassy state.

Cooperation TU Dresden, Univ. Politehnica Bucarest

Geometrical aspects of the glass-forming ability of binary metallic alloys

V. Kokotin, A. Elsner, H. Hermann

The glass forming ability of metallic alloys and the stability of bulk metallic glasses have been addressed in numerous publications. Experimental rules have been established summarizing the experimental knowledge of conditions required for good glass forming ability. The atomic size distribution is one of the important variables controlling the stability of non-crystalline states. It is obvious that in dense-packed systems the local symmetry of clusters of atoms and the character of the medium-range order are correlated. If, e.g., the local clusters have essentially five-fold symmetry the system which the clusters are embedded in can not be periodic with respect to translational operations. We characterize a system of atoms given by the coordinates and the size of each atom in the following way: The Voronoi/Laguerre mosaic of the system is generated. A mosaic cell describes the cluster formed by the central atom and its neighbours. Two neighbouring clusters have one common interface. The number of edges of this interface is used as a measure for the symmetry of the rotation axis linking both clusters. For three-, four- and six-fold symmetry (approximated by the edge number) the link between the clusters would favour crystalline arrangements. For all other edge numbers the link would promote non-crystalline medium-range order. The complete system of atoms is now described by the number, f_{nc}, of all cluster interfaces with 5, 7, ..., edges divided by the number of interfaces with 3, 4, or 6 edges. The figure shows the result for dense-packed binary systems. Parameter f_{nc} is plotted versus size ratio and composition. Clearly, there is a confined region where f_{nc} is comparatively high. This is the region where geometrical aspects contribute to preferred glass forming ability. The binary bulk metallic glasses known until now fit into this region. Probably, further alloys situated in the high f_{nc} region are waiting for their discovery as bulk metallic glasses.

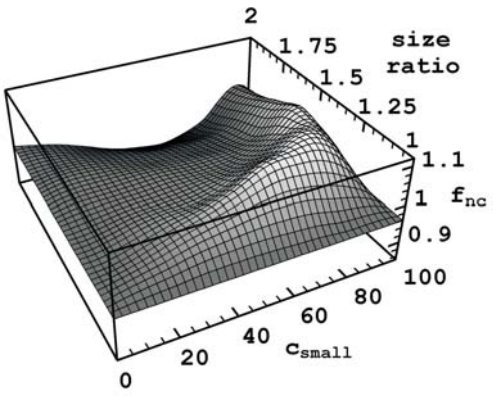

Fig.: Degree of non-crystalline local symmetry versus size ratio and fraction of small atoms for computer simulated dense packed binary mixtures of spherical atoms.

Cooperation Univ. of Appl. Sc. Darmstadt, Bergakademie Freiberg, RAN Novosibirsk
Funded by DFG

High-strength Al-based composites

S. Scudino, K. B. Surreddi, M. Sakaliyska, F. Ali, T. Gemming, U. Kühn, M. Stoica, N. Mattern, H. Ehrenberg, J. Eckert

As a result of the increasingly severe requirements for limiting fuel consumption and carbon dioxide emission, there is a growing trend to reduce the structural weight of vehicles in the transport sector. Among the advanced engineering materials for transport applications, Al-based metal matrix composites (MMCs) show the largest potential to reach this goal and to develop novel lightweight high-performance materials due to

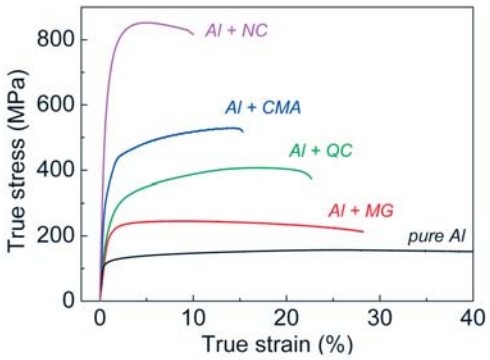

Fig.: Room temperature compression stress-strain curves for the Al-based metal matrix composites reinforced with different reinforcing particles: metallic glasses (MG), quasicrystals (QC) complex metallic alloys (CMA) and nanocrystals (NC).

their remarkable properties, including low density, high strength and good fatigue and wear resistance. In addition, MMCs offer the possibility to tailor their properties to meet specific requirements, which renders this type of materials quite unique in comparison to conventional unreinforced materials. In this project, several high-strength reinforcing phases, ranging from metallic glasses, complex metallic alloys and quasicrystals have been used to produce lightweight Al-based MMCs. The results indicate that the reinforcing particles are very effective for improving the mechanical properties of the metal matrix, revealing that the properties can be tuned within a wide range of strength and ductility as a function of size and volume fraction of the reinforcement.

Cooperation FZ Jülich; MPI Dresden; Univ. Frankfurt; Sejong Univ. Seoul/Korea; Univ. Torino, Italy; CNRS Grenoble, France; Slovak Univ. of Technology, Trnava, Slovak Republic

Funded by EU (NoE CMA), DAAD, BMBF, Pieas

High-strength martensitic Fe-base alloys

H. Wendrock, U. Kühn, H. Turnow, J. Stange, J. Hufenbach, C. Powik, U. Siegel, M. Kaiser, N. Mattern, H. Klauß, A. Güth, S. Roth, J. Eckert

Alloys of the type $Fe_{84.3}Cr_{4.3}Mo_{4.6}V_{2.2}C_{4.6}$ show outstanding mechanical properties when prepared by arc or induction melting under high purity conditions and cast into copper moulds. Compressive strength values of more than 4000 MPa combined with a compressive fracture strain of more than 20 % were achieved. Also tensile tests show large strength of about 1400 MPa already in the as-cast state of the material. A number of alloy variations with partial substitution of the carbide forming elements were investigated, and the mechanical properties of some promising compositions were studied at higher temperatures.

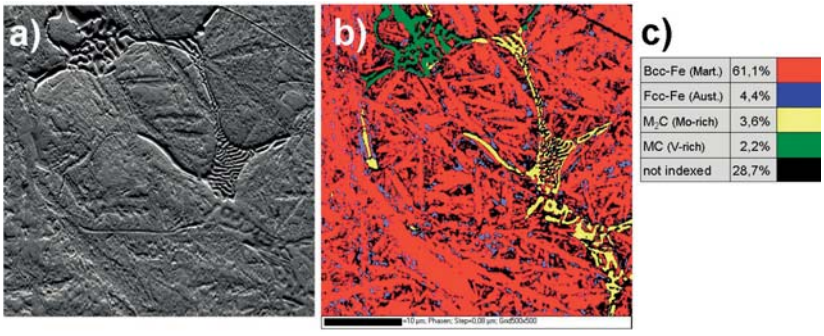

Fig.: a) SEM secondary electron micrograph showing a typical image of a specimen of $Fe_{84.3}Cr_{4.3}Mo_{4.6}V_{2.2}C_{4.6}$ polished for EBSD, FOV is 40 μm;
b) coloured EBSD+EDS map at the same location on a grid of 500x500 points with 80 nm distance showing 4 phases (black = not recognizable, grain/phase boundaries or zones of very high deformation);
c) colour legend of b) and numerical results of phase fractions

The complex microstructure (martensite, different complex carbides, residual austenite, see Fig. 1a for the initial alloy) was studied after appropriate metallographic preparation by highly resolved EBSD measurements combined with fast EDX mapping (Fig. 1b). The phase fractions and the typical grain size and shape could be determined in this way. Two main carbide types (MC and M_2C) were found forming a skeleton of lamellar primary carbides 0.2 to 1.5 μm thick. Austenite regions are nearly equiaxed with a size of 0.3 to 1 μm, situated mostly between the martensite needles.
Tensile tests in-situ in the SEM showed that the fracture surface is highly connected with the interface between the carbides and the martensitic matrix. Thus, confinement of the primary carbide network is expected to be advantageous for increasing the tensile strength of this material.

Cooperation TU BA Freiberg, MPI for Iron research Düsseldorf

Hybrid cathodes of $LiMPO_4$ (M = Mn, Fe, Co, Ni) and carbon nanofilaments (CNF) for Li-ion batteries

H. Ehrenberg, A. Sarapulova, D. Mikhailova, N. N. Bramnik, J. Eckert

Phosphoolivines $LiMPO_4$ are promising cathode materials, but suffer from a low electronic conductivity and, depending on the specific 3d-transition metal M, pronounced instabilities in the charged state. For M = Fe the fully charged state is very stable, and appropriate composite concepts, based on carbon coatings are well established with excellent performance but a rather low cell voltage of about 3.4 V. A much higher energy density would be possible for $LiCoPO_4$, which offers cell voltages of about 4.9 V, but with a different working mechanism [1]. The charged state Li_xCoPO_4 is intrinsically unstable at elevated temperatures and suffers from oxygen release, especially in the presence of fine carbon particles [3]. To overcome limitations from low electronic conductivity and oxygen release in the charged state we have proposed a hybrid concept, based on an ordered array of carbon nanofilaments (CNF), which is in contact with a graphite current collector and coated with the electrochemically active phosphoolivines. Different processes have been established for the coating of the CNFs, e.g. for M = Fe [4] or Mn [5]. Most promising results are obtained for M = Co by the so-called triethylphosphite method, which allows a complete coverage of the CNFs with $LiCoPO_4$, see the top figure for a single nanofibre and the bottom one for an ordered array of CNFs. The ongoing work is focused on building a demonstrator battery to determine the actual performance parameters for such hybrid cathodes in real devices.

[1] Bramnik et al. Chem. Mater. 19 (2007) 908-915.
[2] Ehrenberg et al. Solid State Sciences 11 (2009) 18-23.
[3] Bramnik et al. Electrochem. Solid-State Lett. 11 (2008) A89-A93
[4] Sivakumar et al. J. Power Sources 180 (2008) 553-560.
[5] Bramnik et al. J. Alloys Compd. 464 (2008) 259-264.

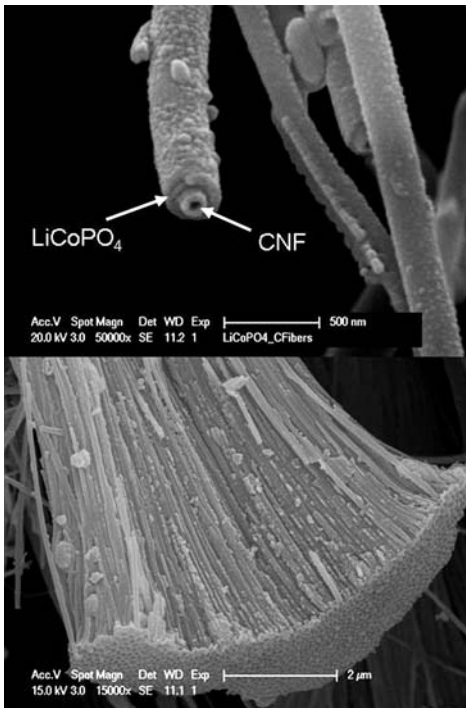

Fig.: (top) CNFs, coated with $LiCoPO_4$ by the triethylphosphite method, (bottom) an ordered array of CNFs, all coated with $LiCoPO_4$.

Cooperation Materials Science and Inorganic Chemistry at TU Darmstadt
Funded by DFG, SPP 1181 "NanoMat"

New Hydrides

O. Gutfleisch, C. Rongeat, I. Lindemann, C. Bonatto-Minella,
R. Domènech Ferrer, C. Geipel, B. Gebel, M. Herrich, L. Dunsch,
S. Oswald, M. Uhlemann, A. Gebert, L. Schultz

Human development has caused a depletion of natural energy resources and climate changes with non-predictable consequences. New energy concepts are required for the future of our industrial society. The only known energy carrier with a high energy density and no emission of greenhouse gas is hydrogen.
Research of solid-state storage of hydrogen – for e.g. zero-emission vehicle propulsion and other mobile applications – is pursued by exploring functional complex hydrides such as alanates and borohydrides. These materials offer several advantages over conventional metal hydrides provided thermodynamics, kinetics decomposition pathways and the reabsorption of hydrogen in modest conditions can be controlled and mastered. Our work includes the characterisation with high-pressure differential scanning calorimetry, gravimetric and pressure-composition-temperature analysis as well as the study of hydrogen dynamics using in-situ XPS, XRD and Raman in order to understand details of the complex sequence of transformations, to identify intermediate reaction products and rate determining steps in complex hydrides and reactive hydride composites.

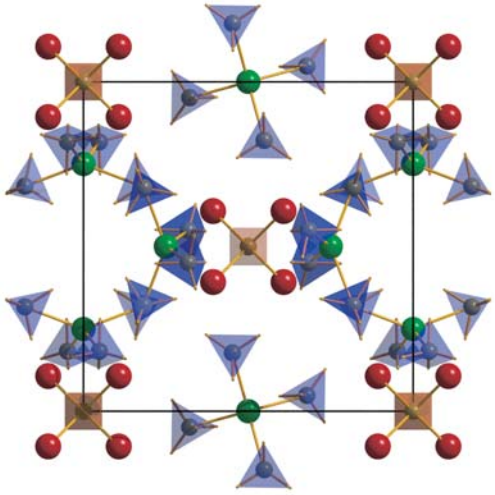

Fig.: Unit cell of $Al_3Li_4(BH_4)_{13}$. Four $(BH_4)^-$ tetrahedrons (blue) and one Al^{3+} cation (green) form the complex anion $[Al(BH_4)_4]^-$. Four Li^+ cations (red) bonded to one $(BH_4)^-$ tetrahedron (brown) in the centre form the complex cation $[Li_4(BH_4)]^{3+}$.

Novel processing techniques such as high hydrogen pressure reactive milling and high pressure annealing are used in order to identify new materials with high reversible hydrogen contents.

Recently we focused on the double-cation system Li-Al-borohydride, which shows a desorption temperature suitable for applications (~70°C) combined with an high gravimetric (17.2 wt.%) as well as volumetric (117 kg/m^3) hydrogen density. The material was synthesised via high energy ball milling of $AlCl_3$ and $LiBH_4$ in different molar ratios to find the adequate stoichiometry of the metathesis reaction. The structure of the compound was determined from high-resolution synchrotron powder diffraction and shows a unique complex structure within the borohydrides with the chemical formula $Li_4(BH_4)[Al(BH_4)_4]_3$. The compound forms a cubic unit cell containing a complex cation $[Li_4(BH_4)]^{3+}$ and a complex anion $[Al(BH_4)_4]^-$. Both are observed for the first time in solid state.

Cooperation EMPA, Switzerland; GKSS Research Centre Geesthacht, Germany; FZ Karlsruhe, Germany; Univ. of Amsterdam, Netherlands; Univ. of Geneva, Switzerland; Swiss-Norwegian Beam Line at ESRF, France; Univ. of Utrecht, Netherlands; Interdisciplinary Nanoscience Center, Univ. of Aarhus, Denmark

Funded by EU (NESSHY, COSY), HGF (FuncHy), ECEMP (Sächsische Exzellenzinitiative)

Research Area 5
Stress-driven architectures and phenomena

Spectral tunability of rolled-up microtube resonators on glass

V. A. Bolaños Quiñones, G. S. Huang, J. D. Plumhof, S. Kiravittaya, A. Rastelli, Y. F. Mei, and O. G. Schmidt

Microtubular resonators fabricated by the release and roll-up of strained nanomembranes guide light along the tube wall in the azimuthal direction. After a few rotations performed by the pre-stressed nanomembranes, the wall thickness of the final tube is smaller than the resonant wavelengths (or modes) supported by the resonator. As a consequence, the evanescent field of the resonant modes interacts with the media surrounding the microresonator, suggesting potential applications for on-chip components like filters and sensors. In order to fine tune the resonant modes, stepwise one-by-one monolayer (ML) Al_2O_3 coating on a SiO/SiO_2 rolled-up microtube with atomic layer deposition is carried out. As shown in Fig. 1a, rolled-up microtubes are fabricated on a transparent glass substrate, and their scanning electron microscopy (SEM) image is presented in Fig. 1b. By ALD coating, a controllable red shift of TM polarized resonant modes (labelled by solid circles and empty triangles in Fig. 1c) measured by photoluminescence (PL) is obtained over a wide spectral range. The measurements are well reproduced by finite-difference-time-domain (FDTD) simulations. In addition, a new group of resonant modes emerge when the Al_2O_3 coating is thicker than 200 ML (~ 20 nm). These modes are TE polarized (labelled by solid triangles) perpendicular to the previous group. Therefore, as the wall thickness increases, the diffraction loss of the TE modes decrease, allowing the microresonator to simultaneously support both TM and TE resonant modes. FDTD simulations reveal a progressive increase of the microtube refractive index after the consecutive Al_2O_3 coating, which cause a higher contrast between the microtube and the surrounding media resulting in the observed mode shifts.

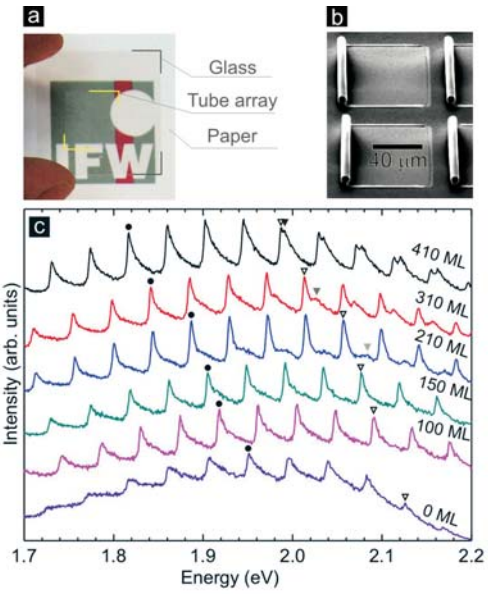

Fig.: (a) Rolled-up microtubular cavity array fabricated on a transparent glass substrate; (b) SEM image of microtubes rolled up from a square pattern. (c) Photoluminescence (PL) spectra of an ~7 µm diameter tube after coating with Al_2O_3 layers with increasing thicknesses (in MLs). Symbols mark the evolution of two TM modes (solid circles and empty triangles) and one TE mode (solid triangles).

Funded by Volkswagen Foundation (I/84 072) and a Multidisciplinary University Research Initiative (MURI) sponsored by the U.S. Air Force Office of Scientific Research (AFOSR) Grant No. FA9550-09-1-0550

Characterization of promising piezoelectric single crystals

A. Sotnikov, E. Smirnova, H. Schmidt, and M. Weihnacht

Hexagonal aluminum nitride (AlN) as a single crystal is of great interest due to its extreme physical and chemical properties. Attractive piezoelectric properties, very high values of sound velocity and the possibility to operate in harsh environment make AlN a very promising material for surface acoustic wave (SAW) applications. As expected, piezoelectric response in AlN can be observed up to very high temperatures.

Tetragonal $LiAlO_2$ crystal is attracting much attention as a promising substrate for growing III-nitrides like GaN/(Al,Ga)N which are technologically very important materials. Since $LiAlO_2$ shows high sound velocities and piezoelectric response, it might also be a potential candidate for SAW applications.

Material parameters including the elastic, piezoelectric and dielectric constants of AlN and $LiAlO_2$ piezoelectric single crystals, respectively, have been evaluated at room temperature by different methods: ultrasonic pulse-echo method, electromechanical resonance-antiresonance method and traditional dielectric method. Temperature dependences of the dielectric constant ε_{33}, the piezoelectric stress constant e_{33} as well as the elastic constants C_{33} and C_{44} of AlN have been measured at temperatures up to 500°C.

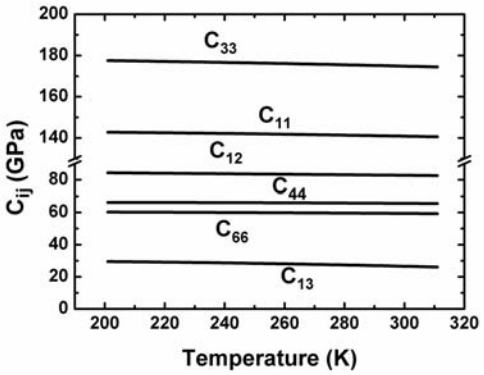

Fig.: Elastic constants of $LiAlO_2$ single crystal as a function of temperature.

The full set of the dielectric, elastic and piezoelectric constants for $LiAlO_2$ single crystal has been obtained in the temperature range from -70°C to +50°C for the first time (see Fig.). Using the experimental data, temperature coefficients of material parameters of $LiAlO_2$ have been calculated. The experimental results show that both materials, AlN and $LiAlO_2$ crystals are promising for surface- and bulk acoustic wave applications.

Cooperation Nitride Crystals Group, St. Petersburg, Russia; Tohoku University, Sendai, Japan.
Funded by BMBF (InnoProfile), SMWK

Wireless Control of Tubular Catalytic Microbots for the Transportation, Assembly and Delivery of Microobjects

A. A. Solovev, S. Sanchez[1], Y. F. Mei, O. G. Schmidt

Recently significant attention has been dedicated towards the development of man-made synthetic catalytic micro- and nanomotors which can mimic biological counterparts in terms of propulsion power, motion control and speed. However, only few applications of such self-propelled vehicles have been described. Here we show wireless control of self-propelled catalytic Ti/Fe/Pt rolled-up microtubes (microbots). Magnetically directed movement of tubular microbots was accomplished through the incorporation of a ferromagnetic (Fe) layer. The extraordinary easy control over microbots movement by changing the direction of an external magnetic field during motion helps to specifically load and deliver cargo at the desired place. Microbots self-propel by ejecting microbubbles via platinum catalytic decomposition of hydrogen peroxide into oxygen and water. Furthermore, the physical characteristics of tubular microbots lead to high propulsion power achieving the absorption and delivering of up to sixty polymeric particles to a desired location as shown in Fig. 1A. As expected, their speeds slow down with more loaded particles. Our presented results are very promising for future drug delivery systems, biomedical applications require the use of biocompatible fuels for powering autonomous micromachines. Furthermore, one exciting direction could be a "microfactory" for nanoscience, which is illustrated in Fig. 1B. We are investigating on microbots powered by glucose fuels, their integration into Lab-On-a-Chip technologies, communication and self-organization.

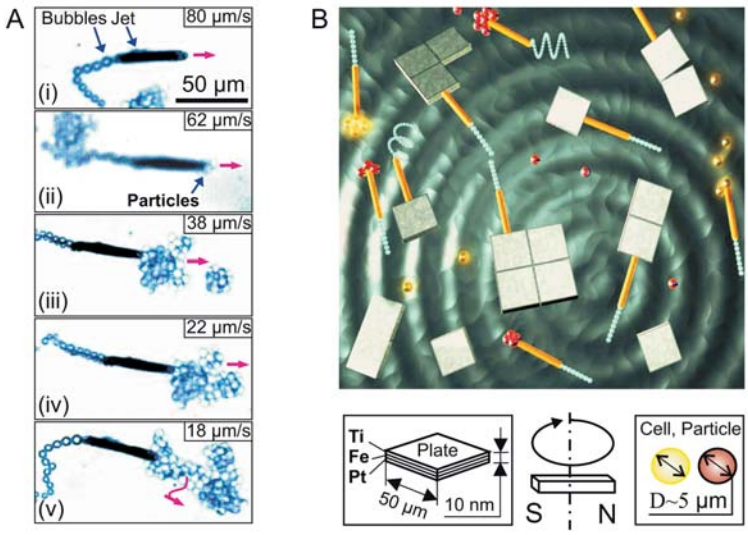

Fig.: A) Transportation of polystyrene microparticles of 5 µm diameter. A) Optical microscope images of microbot loading and transporting 3 (ii), 27 (iii), 44 (i) and 58 (iv) particles. Insets show microbot's average speeds. B) Schematic representation of "microfactory" where wireless control of microbots by an external magnet, assisted load, transport, delivery and assembly of microparticles and nanoplates in fuel solution.

Cooperation [1]National Institute for Materials Science, Tsukuba, Ibaraki, Japan; School of Physical & Mathematical Sciences, Nanyang Technological Univ., Singapore

Multiferroic Oxide Film Structures

K. Dörr, O. Bilani, K. Boldyreva, M. C. Dekker, C. Deneke, E. Wild, A. Herklotz, J.-W. Kim, K. Nenkov, A. Rastelli, A. D. Rata, O. G. Schmidt, L. Schultz

Multiferroic $HoMnO_3$ films of thicknesses ≤ 1 μm were prepared by pulsed laser deposition (PLD) and have been investigated by optical Second Harmonic Generation (SHG) [1] and SQUID magnetometry in order to reveal the ferroic phases present in the thin films (thesis of J.-W. Kim). While $HoMnO_3$ is a single-phase low-temperature multiferroic, magnetic films epitaxially grown on piezoelectric substrates of PMN-PT(001) ($Pb(Mg_{1/3}Nb_{2/3})_{0.72}Ti_{0.28}O_3$) provide a model system for strain-coupled two-phase multiferroics [2] comprising of a ferroelectric and a magnetic component. For the magnetic films, phase-separated manganites [3] and $La_{1-x}Sr_xCoO_3$ with a potentially strain-controllable spin state of the Co ions have been investigated. Cobaltite films reveal spin-state control by strain for x = 0 [4], and a tendency for defect formation resulting from spin-state-related enhanced thermal expansion. In User projects at the CNMS, ORNL the reversible strain induced in coherent superlattices of $[La_{0.7}Sr_{0.3}MnO_3/SrTiO_3]_n$ (Fig.) and in buffer layers of $LaAl_{1-x}Sc_xO_3$ offering an adjustable in-plane lattice parameter of 3.8 – 4 Å has been demonstrated using four-circle x-ray diffraction. Strain application in thin film membranes is promising through the approach of rolled-up epitaxial oxide layers.

The light emission from InGaAs quantum dots embedded in GaAs microring resonators has been efficiently tuned employing the reversible compressive or expansive strain from PMN-PT crystals at 10 K [5], indicating a promising potential of the strain tuning for establishing resonances which are required to achieve entangled photon states. Light-control of the metal or insulator state has been demonstrated for epitaxial electron-doped films of $La_{0.7}Ce_{0.3}MnO_3/SrTiO_3$(001) [6].

[1] T. Kordel et al., Phys. Rev. B **80**, 045409 (2009)
[2] K. Dörr et al., Eur. J. Phys. B **71**, 361 (2009)
[3] M. C. Dekker et al., Phys. Rev. B **80**, 144402 (2009)
[4] A. Herklotz et al., Phys. Rev. B **79**, 092409 (2009)
[5] T. Zander et al., Optics Express **17**, 22452 (2009)
[6] E. Beyreuther et al., Phys. Rev. B **80**, 075106 (2009)

Cooperation TU Dresden, Univ. of Bonn, Oak Ridge National Laboratory, TN, USA
Funded by DFG, DAAD, IMPRS

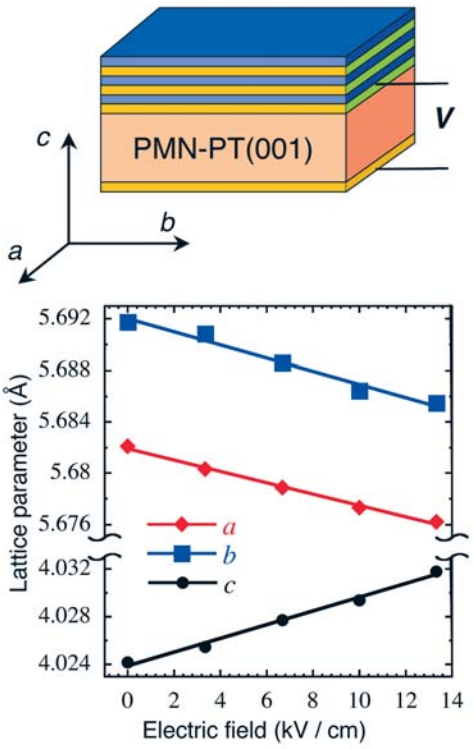

Fig.: Scheme of a reversibly strainable oxide superlattice on a piezoelectric substrate of PMN-PT (top) and electrically controlled lattice parameters of PMN-PT measured by x-ray diffraction (bottom).

Rolled-up Cr microtubes alignment in microfluidic systems by standing surface acoustic waves

X. H. Kong, H. Schmidt, C. Deneke, H. X. Ji, D. J. Thurmer, M. Bauer, S. Menzel, and O. G. Schmidt

Recently, surface acoustic waves (SAW) have been established as a promising approach for fast, reliable manipulation and alignment of micro- and nanostructures in microfluidic systems. Here, the alignment of rolled-up Cr microtubes dispersed in propylene carbonate solvent by standing surface acoustic waves (SSAW) is demonstrated. For our experiments, a pair of electrically optimized, opposing interdigital transducers (IDTs) is fabricated on top of a 128° rotated *Y*-cut $LiNbO_3$ substrate. Each IDT launches a SAW with a wavelength of 130 μm at a corresponding frequency of about 30 MHz, to form a SSAW pattern in the area of a fluidic channel between the substrate and a glass cover. For the alignment experiment, the capillary is filled with Cr tube suspension. In the start, the rolled-up microtubes are randomly dispersed in the fluidic channel (see Fig. inset). When two rf power signals (here: 6 dBm) are simultaneously applied to both IDT ports in equal portions, a standing wave pattern accompanied by an appropriate electric field

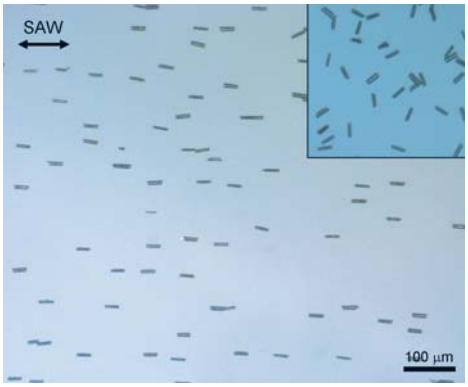

Fig.: Typical optical micrograph of Cr microtube alignment by standing surface acoustic waves on a $LiNbO_3$ substrate. The 30 μm long Cr microtubes are orderly aligned in parallel to the SAW propagation direction (denoted by the double arrows). The inset shows the initial random dispersion of the microtubes before starting of SAW excitation.

pattern forms in the capillary. Due to these patterns, the rolled-up Cr microtubes are aligned into one direction, with their axis parallel to the propagation direction of the SAWs. Such an aligned tube area is depicted in the figure. The proportion of microtube alignment by SSAWs at a certain frequency depends on the length of the tubes and the applied signal power. In a setup with two IDT pairs, arranged perpendicularly to each other, the alignment of the Cr microtubes can be switched by this method between the two main directions.

Funded by BMBF (InnoProfile)

Optical microcavity tuning by local laser processing

H. S. Lee, S. Kiravittaya, S. Kumar, J. D. Plumhof, A. Rastelli, O. G. Schmidt

Photonic crystal (PhC) optical microcavities are attracting much interest for their potential application in advanced optical devices such as switches, filters, multiplexers, low-threshold lasers, and cavity quantum electrodynamics. For such applications, it is necessary to control and tune the resonant wavelength of the PhC cavity modes. The PhC cavity resonances (or modes) can be tuned by adjusting the PhC lattice and defect geometries. However, the exact spectral position of the modes can not be predicted with the accuracy required for some applications, because the modes are highly sensitive to fabrication parameters. Therefore, postprocessing tuning techniques able to compensate for fabrication imperfections are particularly demanded. Most of tuning techniques presented so far either modify the properties of the whole sample, which prevents the local tuning of a single nanocavity, or need extra materials and processing tools.

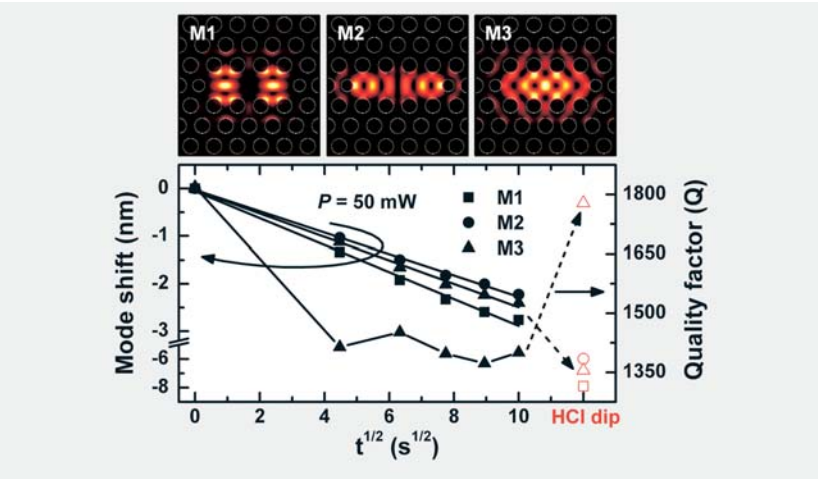

Fig.: Top: FDTD-calculated electric field intensity profiles for the TE modes M1, M2, and M3 confined in a PhC nanocavity. Bottom: mode wavelength shift for three modes and quality factor for M3 as a function of the square root of the oxidation time at a laser power $P = 50$ mW. The open symbols indicate the values after a dip in HCl for 5 s.

In this work, we investigated the local tuning of optical modes in GaAs PhC microcavities by continuous wave laser-assisted oxidation in air atmosphere. The oxide growth leads to controllable shifts of the cavity modes to shorter wavelengths. By irradiation with a focused laser beam at power levels of a few tens mW, PhC nanocavity modes blueshift by up to 2.5 nm. The mode shifts, which are different for different modes of the same cavity, can be controlled by varying the irradiation conditions and are well explained by finite-element-method (FEM) and finite-difference time-domain (FDTD) simulations.

[1] H. S. Lee et al. Appl. Phys. Lett. 95, 191109 (2009).

Cooperation EPFL Institute of Photonics and Quantum Electronics, Switzerland; Institute of Photonics and Nanotechnology, Italy; COBRA Research Institute, Netherlands

Funded by DFG (FOR 730), Korea Research Foundation (KRF-2008-357-C00035)

Publications 2009

Monographs and Editorships

1) A.V. Granato , G. Gremaud, F.M. Mazzolai, J. Eckert (eds.) *15th International Conference on Internal Friction and Mechanical Spectroscopy, Perugia/ Italien, 20.-25.7.08*, Elsevier Science, Amsterdam. Sonderband Materials Science and Engineering A 521-522, 2009, 426 S.
2) L. Schultz , J. Eckert, L. Battezzati, M. Stoica (eds.) *The 13th International Conference on Rapidly Quenched and Metastable Materials: Proceedings*, IoP Publishing, Journal of Physics: Conference Series, 144, 2009, 1101 S.

Journal Papers

1) A. Alfonsov, E. Vavilova, V. Kataev, B. Buechner, A. Podlesnyak, M. Russina, A. Furrer, T. Straessle, E. Pomjakushina, K. Conder, D.I. Khomskii, *Origin of a spin-state polaron in lightly hole doped LaCoO3*, Journal of Physics: Conference Series 150 (2009), S. 42003/1-4.
2) B. Antonioli, B. Buechner, J.K. Clegg, K. Gloe, K. Gloe, L. Goetzke, A. Heine, A. Jaeger, K.A. Jolliffe, O. Kataeva, V. Kataev, R. Klingeler, T. Krause, L.F. Lindoy, A. Popa, W. Seichter, M. Wenzel, *Interaction of an extended series of N-substituted di(2-picolyl)amine derivatives with copper(II). Synthetic, structural, magnetic and solution studies*, Dalton Transactions (7) (2009), S. 4795-4805.
3) V.Y. Aristov, O.V. Molodtsova, Y.A. Ossipyan, B.P. Doyle, S. Nannarone, M. Knupfer, *Chemistry and electronic properties of ferromagnetic metal-organic semiconductor interfaces: Fe on CuPc*, physica status solidi (a) 206 (2009) Nr. 12, S. 2763-2770.
4) V.Y. Aristov, O.V. Molodtsova, Y.A. Ossipyan, B.P. Doyle, S. Nannarone, M. Knupfer, *Ferromagnetic cobalt and iron top contacts on an organic semiconductor: Evidence for a reacted interface*, Organic Electronics 10 (2009) Nr. 1, S. 8-11.
5) M.E. Arroyo y de Dompablo, U. Amador, J.M. Gallardo-Amores, E. Moran, H. Ehrenberg, L. Dupont, R. Dominko, *Polymorphs of Li3PO4 and Li2MSiO4 (M = Mn, Co): The role of pressure*, Journal of Power Sources 189 (2009) Nr. 1, S. 638-642.
6) P. Atkinson, O.G. Schmidt, *Gallium-assisted deoxidation of patterned substrates for site-controlled growth of InAs quantum dots*, Journal of Crystal Growth 311 (2009) Nr. 7, S. 1815-1818.
7) A. Bachmatiuk, F. Boerrnert, M. Grobosch, F. Schaeffel, U. Wolff, A. Scott, M. Zaka, J.H. Warner, R. Klingeler, M. Knupfer, B. Buechner, M.H. Ruemmeli, *Investigating the graphitization mechanism of SiO2 nanoparticles in chemical vapor deposition*, ACS nano 3 (2009) Nr. 12, S. 4098-4104.
8) A. Bachmatiuk, M. Bystrzejewski, F. Schaeffel, P. Ayala, U. Wolff, C. Mickel, T. Gemming, T. Pichler, E. Borowiak-Palen, R. Klingeler, H.-W. Huebers, M. Ulbrich, M. Knupfer, D. Haberer, B. Buechner, M.H. Ruemmeli, *Carbon nanotube synthesis via ceramic catalysts*, Physica Status Solidi B 246 (2009) Nr. 11-12, S. 2486-2489.
9) N. Balchev, K. Nenkov, G. Mihova, B. Kunev, J. Pirov, D.A. Dimitrov, *Structure, magnetic and superconducting properties of MoSr2HoCu2O8-delta*, Journal of Magnetism and Magnetic Materials 321 (2009) Nr. 5, S. 388-391.
10) L. Balsanova, D. Mikhailova, A. Senyshyn, D. Trots, H. Fuess, W. Lottermoser, H. Ehrenberg, *Structure and properties of a-AgFe2(MoO4)3*, Solid State Sciences 11 (2009) Nr. 6, S. 1137-1143.
11) M. Baricco, T.A. Baser, J. Das, J. Eckert, *Correlation between Poisson ratio and Mohr-Coulomb coefficient in metallic glasses*, Journal of Alloys and Compounds 483 (2009) Nr. 1-2, S. 125-131.
12) S. Barnoss, H. Shanak, C.C. Bof Bufon, T. Heinzel, *Piezoresistance in chemically synthesized polypyrrole thin films*, Sensors and Actuators A 154 (2009), S. 79-84.
13) T.A. Baser, J. Das, J. Eckert, M. Baricco, *Glass formation and mechanical properties of (Cu50Zr50)100-xAlx (x = 0, 4, 5, 7) bulk metallic glasses*, Journal of Alloys and Compounds 483 (2009) Nr. 1-2, S. 146-149.
14) M. Behulova, M. Liptak, P. Grgac, W. Loeser, H.-G. Lindenkreuz, *Comparison of microstructures developed during solidification of undercooled tool steel in levitation and on a substrate*, Journal of Physics: Conference Series 144 (2009) Nr. 1, S. 12099/1-4.
15) M. Benyoucef, H.S. Lee, J. Gabel, T.W. Kim, H.L. Park, A. Rastelli, O.G. Schmidt, *Wavelength tunable triggered single-photon source from a single CdTe quantum dot on silicon substrate*, Nano Letters 9 (2009) Nr. 1, S. 304-307.
16) M. Benyoucef, L. Wang, A. Rastelli, O.G. Schmidt, *Toward quantum interference of photons from independent quantum dots*, Applied Physics Letters 95 (2009) Nr. 26, S. 261908/1-3.
17) B. Bergk, V. Petzold, H. Rosner, S.-L. Drechsler, M. Bartkowiak, O. Ignatchik, I. Sheikin, P.C. Canfield, J. Wosnitza, *Many-body effects in LuNi2B2C*, Journal of Physics: Conference Series 150 (2009) Nr. Part 5, S. 52021/1-4.
18) H. Bih, I. Saadoune, H. Ehrenberg, H. Fuess, *Crystal structure, magnetic and infrared spectroscopy studies of the LiCryFe1-yP2O7 solid solution, Journal of Solid State Chemistry 182 (2009), S. 821-826.*
19) S.V. Biryukov, H. Schmidt, A.V. Sotnikov, M. Weihnacht, T.Y. Chemekova, Y.N. Makarov, Ring waveguide resonator on surface acoustic waves: First experiments, Journal of Applied Physics 106 (2009) Nr. 12, S. 126103/1-2.

20) *K. Biswas, R. Hermann, H. Wendrock, J. Priede, G. Gerbeth, B. Buechner, Effect of melt convection on the secondary dendritic arm spacing in peritectic Nd–Fe–B alloy, Journal of Alloys and Compounds 480 (2009) Nr. 2, S. 295-298.*

21) *G. Bo, L. Ying, J. Liu, Y. Lu, Z. Liu, C. Cai, R. Huehne, B. Holzapfel, Crystallization and magneto-transport characteristics in mod YBa2Cu3O7-d films, International Journal of Modern Physics B 23 (2009) Nr. 17, S. 3470-3475.*

22) *V.A. Bolanos Quinones, G. Huang, J.D. Plumhof, S. Kiravittaya, A. Rastelli, Y. Mei, O.G. Schmidt, Optical resonance tuning and polarization of thin-walled tubular microcavities, Optics Letters 34 (2009) Nr. 15, S. 2345-2347.*

23) *E. Bonera, F. Pezzoli, A. Picco, G. Vastola, M. Stoffel, E. Grilli, M. Guzzi, QA. Rastelli, O.G. Schmidt, L. Miglio, Strain in a single ultrathin silicon layer on top of SiGe islands: Raman spectroscopy and simulations, Physical Review B 79 (2009) Nr. 7, S. 75321/1-5.*

24) *S.V. Borisenko, A.A. Kordyuk, V.B. Zabolotnyy, D.S. Inosov, D. Evtushinsky, B. Buechner, A.N. Yaresko, A. Varykhalov, R. Follath, W. Eberhardt, L. Patthey, H. Berger, Two energy gaps and fermi-surface ìArcsî in NbSe2, Physical Review Letters 102 (2009) Nr. 16, S. 166402/1-4.*

25) *E. Borowiak-Palen, M.H. Ruemmeli, Activated Cu catalysts for alcohol CVD synthesized non-magnetic bamboo-like carbon nanotubes and branched bamboo-like carbon nanotubes, Superlattices and Microstructures 46 (2009), S. 374-378.*

26) *E. Borowiak-Palen, A. Steplewska, M.H. Ruemmeli, On the use of Cu catalysts for tailoring carbon nanostructures in alcohol-CVD, Physica Status Solidi B 246 (2009) Nr. 11-12, S. 2448-2452.*

27) *B. Braeuer, M. Grobosch, M. Knupfer, F. Weigend, Y. Vaynzof, A. Kahn, T. Rueffer, G. Salvan, How photoelectron spectroscopy and quantum chemical studies can help understanding the magnetic properties of molecules: An example from the class of Cu(II)-Bis(oxamato) complexes, The Journal of Physical Chemistry B 113 (2009), S. 10051-10054.*

28) *N.N. Bramnik, D.M. Trots, H.J. Hofmann, H. Ehrenberg, Mixed LiCo0.6M0.4P04 (M = Mn, Fe, Ni) phosphates: cycling mechanism and thermal stability, Physical Chemistry Chemical Physics 11 (2009) Nr. 17, S. 3271-3277.*

29) *C. Bran, A.B. Butenko, N.S. Kiselev, U. Wolff, L. Schultz, O. Hellwig, U.K. Roessler, A.N. Bogdanov, V. Neu, Evolution of stripe and bubble domains in antiferromagnetically coupled [(Co/Pt)8/Co/Ru]18 multilayers, Physical Review B 79 (2009) Nr. 2, S. 24430/1-7.*

30) *J. Brandenburg, R. Huehne, L. Schultz, V. Neu, Domain structure of epitaxial Co films with perpendicular anisotropy, Physical Review B 79 (2009) Nr. 5, S. 54429/1-7.*

31) *B. Buechner, C. Hess, Iron-based superconductors: Vital clues from a basic compound, Nature materials- news and views 8 (2009) Nr. 8, S. 615-616.*

32) *J. Buschbeck, R. Niemann, O. Heczko, M. Thomas, L. Schultz, S. Faehler, In situ studies of the martensitic transformation in epitaxial Ni–Mn–Ga films, Acta Materialia 57 (2009) Nr. 8, S. 2516-2526.*

33) *J. Buschbeck, I. Opahle, M. Richter, U.K. Roessler, P. Klaer, M. Kallmayer, H.J. Elmers, G. Jakob, L. Schultz, S. Faehler, Full tunability of strain along the fcc-bcc bain path in epitaxial films and consequences for magnetic properties, Physical Review Letters 103 (2009) Nr. 21, S. 216101/1-4.*

34) *M. Bystrzejewski, A. Bachmatiuk, J. Thomas, P. Ayala, H.-W. Huebers, T. Gemming, E. Borowiak-Palen, T. Pichler, R.J. Kalenczuk, B. Buechner, M.H. Ruemmeli, Boron doped carbon nanotubes via ceramic catalysts, Physica Status Solidi (RRL) 3 (2009) Nr. 6, S. 193-195.*

35) *M. Bystrzejewski, A. Huczko, P. Byszewski, M. Domanska, M.H. Ruemmeli, T. Gemming, H. Lange, Systematic studies on carbon nanotubes synthesis from aliphatic alcohols by the CVD floating catalyst method, Fullerenes, Nanotubes and Carbon Nanostructures 17 (2009) Nr. 3, S. 298-307.*

36) *M. Bystrzejewski, A. Huczko, M. Soszynski, S. Cudzilo, W. Kaszuwara, T. Gemming, M.H. Ruemmeli, H. Lange, An easy one-step route to carbon-encapsulated magnetic nanoparticles, Fullerenes, Nanotubes and Carbon Nanostructures 17 (2009), S. 600-615.*

37) *M. Bystrzejewski, H.W. Huebers, A. Huczko, T. Gemming, B. Buechner, M.H. Ruemmeli, Bulk synthesis of carbon nanocapsules and nanotubes containing magnetic nanoparticles via low energy laser pyrolysis of ferrocene, Materials Letters 63 (2009) Nr. 21, S. 1767-1770.*

38) *M. Bystrzejewski, M.H. Ruemmeli, T. Gemming, T. Pichler, A. Huczko, H. Lange, Functionalizing single-wall carbon nanotubes in hollow cathode glow discharges, Plasma Chemistry and Plasma Processing 29 (2009) Nr. 2, S. 79-90.*

39) *J.-S. Caux, A. Klauser, J. van den Brink, Polarization suppression and nonmonotonic local two-body correlations in the two-component Bose gas in one dimension, Physical Review A 80 (2009) Nr. 6, S. 61605/1-4.*

40) *P. Cendula, S. Kiravittaya, Y.F. Mei, C. Deneke, O.G. Schmidt, Bending and wrinkling as competing relaxation pathways for strained free-hanging films, Physical Review B 79 (2009) Nr. 8, S. 85429/1-4.*

41) *I. Chaplygin, Ensemble interpretation of L(S)DA+U, Physical Review B 80 (2009) Nr. 24, S. 245111/1-11.*

42) *P. Chaudhuri, V. Kataev, B. Buechner, H.-H. Klauss, B. Kersting, F. Meyer, Tetranuclear complexes in molecular magnetism: Targeted synthesis, high-field EPR and pulsed-field magnetization, Coordination Chemistry Reviews 253 (2009) Nr. 19-21, S. 2261-2285.*

43) *L.F. Chazaro-Ruiz, A. Kellenberger, L. Dunsch, In situ ESR/UV-vis-NIR and ATR-FTIR spectroelectrochemical studies on the p-Doping of copolymers of 3-Methylthiophene and 3-Hexylthiophene, Journal of Physical Chemistry B 113 (2009) Nr. 8, S. 2310-2316.*

44) *J. Chen, C.J. Lee, E. Louis, F. Bijkerk, R. Kunze, H. Schmidt, D. Schneider, R. Moors, Characterization of EUV induced carbon films using laser - generated surface acoustic waves, Diamond and Related Materials 18 (2009) Nr. 5-8, S. 768-771.*

45) *J. Chen, E. Louis, C.J. Lee, H. Wormeester, R. Kunze, H. Schmidt, D. Schneider, R. Moors, W. van Schaik, M. Lubomska, F. Bijkerk, Detection and characterization of carbon contamination on EUV multilayer mirrors, Optics Express 17 (2009) Nr. 19, S. 16969-16979.*

46) *Y.F. Chen, J. McCord, J. Freudenberger, R. Kaltofen, O.G. Schmidt, Effects of strain on magnetic and transport properties of Co films on plastic substrates, Journal of Applied Physics 105 (2009) Nr. 7, S. 7C302/1-3.*

47) *V. Cloet, J. Feys, R. Huehne, S. Engel, B. Holzapfel, S. Hoste, I. Van Driessche, A water-based sol-gel precursor for deposition of thin La2Zr2O7 layers on Ni-W substrates, IEEE Transactions on Applied Superconductivity 19 (2009) Nr. 3, S. 3467-3470.*

48) *V. Cloet, J. Feys, R. Huehne, S. Hoste, I. Van Driessche, Thin La2Zr2O7 films made from a water-based solution, Journal of Solid State Chemistry 182 (2009) Nr. 1, S. 37-42.*

49) *J. Coll, J. Gazquez, R. Huehne, B. Holzapfel, Y. Morilla, J. Garcia-Lopez, A. Pomar, F. Sandiumenge, T. Puig, X. Obradors, All chemical YBa2Cu3O7 superconducting multilayers: Critical role of CeO2 cap layer flatness, Journal of Materials Research 24 (2009) Nr. 4, S. 1446-1455.*

50) *A. Concustell, J. Sort, J. Fornell, E. Rossinyol, S. Surinach, A. Gebert, J. Eckert, M.D. Baro, Work-hardening mechanisms of the Ti60Cu14Ni12Sn4Nb10 nanocomposite alloy, Journal of Materials Research 24 (2009) Nr. 10, S. 3146-3153.*

51) *S. Costa, B. Scheibe, M.H. Ruemmeli, E. Borowiak-Palen, Raman spectroscopy study on concentrated acid treated carbon nanotubes, Physica Status Solidi B 246 (2009) Nr. 11-12, S. 2717-2720.*

52) *R.M. Costescu, C. Deneke, D.J. Thurmer, O.G. Schmidt, Rolled-up nanotech: Illumination-controlled hydrofluoric acid etching of AlAs sacrificial layers, Nanoscale Research Letters 4 (2009) Nr. 12, S. 1463-1468.*

53) *J. Cwik, T. Palewski, K. Nenkov, J. Lyubina, J. Warchulska, J. Klamut, O. Gutfleisch, Magnetic properties and specific heat of Dy1-xLaxNi2 compounds, Journal of Magnetism and Magnetic Materials 321 (2009) Nr. 18, S. 2821-2826.*

54) *T. Dahm, V. Hinkov, S.V. Borisenko, A.A. Kordyuk, V.B. Zabolotnyy, J. Fink, B. Buechner, D.J. Scalapino, W. Hanke, B. Keimer, Strength of the spin-fluctuation-mediated pairing interaction in a high-temperature superconductor, Nature physics 5 (2009) Nr. 3, S. 217-221.*

55) *A.N. Darinskii, M. Weihnacht, H. Schmidt, Rayleigh wave reflection from single surface imperfections on isotropic substrates, Journal of Applied Physics 106 (2009) Nr. 3, S. 34914/1-8.*

56) *J. Das, S. Pauly, M. Bostroem, K. Durst, M. Goeken, J. Eckert, Designing bulk metallic glass and glass matrix composites in martensitic alloys, Journal of Alloys and Compounds 483 (2009) Nr. 1-2, S. 97-101.*

57) *L. de Abreu Vieira, M. Doebeli, A. Dommann, E. Kalchbrenner, A. Neels, J. Ramm, H. Rudigier, J. Thomas, B. Widrig, Approaches to influence the microstructure and the properties of Al–Cr–O layers synthesized by cathodic arc evaporation, Surface and Coatings Technology, online first (2009).*

58) *M.C. Dekker, A.D. Rata, K. Boldyreva, S. Oswald, L. Schultz, K. Doerr, Colossal elastoresistance and strain-dependent magnetization of phase-separated (Pr1-yLay)0.7Ca0.3MnO3 thin films, Physical Review B 80 (2009) Nr. 14, S. 144402/1-7.*

59) *C. Deneke, J. Schumann, R. Engelhard, J. Thomas, C. Mueller, M.S. Khatri, A. Malachias, M. Weisser, T.H. Metzger, O.G. Schmidt, Structural and magnetic properties of an InGaAs/Fe3Si superlattice in cylindrical geometry, Nanotechnology 20 (2009) Nr. 4, S. 45703/1-5.*

60) *C. Deneke, R. Songmuang, N.Y. Jin-Phillipp, O.G. Schmidt, The structure of hybrid radial superlattices, Journal of Physics D 42 (2009) Nr. 10, S. 103001/1-16.*

61) *D.H.N. Dias, E.S. Motta, G.G. Sotelo, R. deAndrade, R.M. Stephan, L. Kuehn, O. de Haas, L. Schultz, Simulations and tests of superconductivity linear bearings for a MAGLEV prototype, IEEE Transactions on Applied Superconductivity 19 (2009) Nr. 3, S. 2120-2123.*

62) *K. Doerr, O. Bilani-Zeneli, A. Herklotz, A.D. Rata, K. Boldyreva, J.-W. Kim, M.C. Dekker, K. Nenkov, L. Schultz, M. Reibold, A model system for strain effects: epitaxial magnetic films on a piezoelectric substrate, The European Physical Journal B 71 (2009) Nr. 3, S. 361-366.*

63) *S.-L. Drechsler, J. Malek, S. Nishimoto, U. Nitzsche, R. Kuzian, H. Eschrig, H. Rosner, Peculiar temperature-dependent charge response of frustrated chain cuprates near a critical point, Journal of Physics: Conference Series 145 (2009) Nr. 1, S. 12060/1-4.*

64) *S.-L. Drechsler, J. Malek, S. Nishimoto, J. Richter, R. Kuzian, H. Rosner, H. Eschrig, Low-temperature pecularities of the optical response in undoped cuprates, Journal of Physics: Conference Series 150 (2009) Nr. Part 4, S. 42026/1-4.*

65) *S.-L. Drechsler, J. Maleka, R.O. Kuziana, S. Nishimotoa, U. Nitzsche, W.E.A. Lorenz, R. Klingeler, B. Buechner, M. Knupfer, Intersite Coulomb interactions in edge-shared CuO2 chains: Optics and EELS, Physica C, online first (2009).*

66) *S.-L. Drechsler, F. Roth, M. Grobosch, R. Schuster, K. Koepernik, H. Rosner, G. Behr, M. Rotter, D. Johrendt, B. Buechner, M. Knupfer, Insight into the physics of Fe-pnictides from optical and T = 0 penetration depth data, Physica C, online first (2009).*

67) *H. Ehrenberg, N.N. Bramnik, A. Senyshyn, H. Fuess, Crystal and magnetic structures of electrochemically delithiated Li1-xCoPO4 phases, Solid State Sciences 11 (2009), S. 18-23.*

68) *M. Eisterer, W. Haessler, P. Kovac, Critical currents in weakly textured MgB2: Nonlinear transport in anisotropic heterogeneous media, Physical Review B 80 (2009) Nr. 17, S. 174516/1-4.*

69) *A.A. El-Gendy, E.M.M. Ibrahim, V.O. Khavrus, Y. Krupskaya, S. Hampel, A. Leonhardt, B. Buechner, R. Klingeler, The synthesis of carbon coated Fe, Co and Ni nanoparticles and an examination of their magnetic properties, Carbon 47 (2009) Nr. 12, S. 2821-2828.*

70) *A. Elsner, A. Wagner, T. Aste, H. Hermann, D. Stoyan, Specific surface area and volume fraction of the cherry-pit model with packed pits, Journal of Physical Chemistry B 113 (2009), S. 7780-7784.*

71) *J.M. Engel, H. Ahsbahs, H. Fuess, H. Ehrenberg, Polymorphism of K2Co2Mo3O12: variations in the packing schemes and changes in molybdenum coordination under high pressure, Acta Crystallographica Section B 65 (2009), S. 29-35.*

72) *H. Eschrig, K. Koepernik, Tight-binding models for the iron-based superconductors, Physical Review B 80 (2009) Nr. 10, S. 104503/1-14.*

73) *R. Essehli, B. El Bali, H. Ehrenberg, I. Svoboda, N. Bramnik, H. Fuess, Co0.5TiOPO4: Crystal structure, magnetic and electrochemical properties, Materials Research Bulletin 44 (2009) Nr. 4, S. 817-821.*

74) *D. V. Evtushinsky, D.S. Inosov, V.B. Zabolotnyy, A. Koitzsch, M. Knupfer, B. Buechner, M.S. Viazovska, G.L. Sun, V. Hinkov, A.V. Boris, C.T. Lin, B. Keimer, A. Varykhalov, A.A. Kordyuk, S.V. Borisenko, Momentum dependence of the superconducting gap in Ba1-xKxFe2As2, Physical Review B 79 (2009) Nr. 5, S. 54517/1-13.*

75) *D.V. Evtushinsky, D.S. Inosov, V.B. Zabolotnyy, M.S. Viazovska, R. Khasanov, A. Amato, H.H. Klauss, H. Luetkens, C. Niedermayer, G.L. Sun, V. Hinkov, C.T. Lin, A. Varykhalov, A. Koitzsch, M. Knupfer, B. Buechner, A.A. Kordyuk, S.V. Borisenko, Momentum-resolved superconducting gap in the bulk of Ba1.xKxFe2As2 from combined ARPES and my-SR measurements, New Journal of Physics 11 (2009) Nr. 5, S. 550069/1-13.*

76) *J.T. Fan, Z.F. Zhang, S.X. Mao, B.L. Shen, J. Eckert, Serrated flow behavior induced by blunt mechanism of shear crack propagation in metallic glass, Journal of Materials Research 24 (2009) Nr. 2, S. 436-440.*

77) *J. Fassbender, T. Strache, M.O. Liedke, D. Marko, S. Wintz, K. Lenz, A. Keller, S. Facsko, I. Moench, J. McCord, Introducing artificial length scales to tailor magnetic properties, New Journal of Physics 11 (2009) Nr. 12, S. 125002/1-19.*

78) *A. Feldhoff, J. Martynczuk, M. Arnold, M. Myndyk, I. Bergmann, V. Sepelak, W. Gruner, U. Vogt, A. Haehnel, J. Woltersdorf, Spin-state transition of iron in (Ba0.5Sr0.5)(Fe0.8Zn0.2)O3-delta perovskite, Journal of Solid State Chemistry 182 (2009), S. 2961-2971.*

79) *P. Feng, I. Moench, S. Harazim, G. Huang, Y. Mei, O.G. Schmidt, Giant persistent photoconductivity in rough silicon nanomembranes, Nanoletters 9 (2009) Nr. 10, S. 3453-3459.*

80) *J. Fink, E. Schierle, E. Weschke, J. Geck, D. Hawthorn, V. Soltwisch, H. Wadati, H.-H. Wu, H.A. Duerr, N. Wizent, B. Buechner, G.A. Sawatzky, Charge ordering in La1.8-xEu0.2SrxCuO4 studied by resonant soft x-ray diffraction, Physical Review B 79 (2009) Nr. 10, S. 100502(R)/1-4.*

81) *J. Fink, S. Thirupathaiah, R. Ovsyannikov, H.A. Duerr, R. Follath, Y. Huang, S. de Jong, M.S. Golden, Y.-Z. Zhang, H.O. Jeschke, R. Valenti, C. Felser, S. Dastjani Farahani, M. Rotter, D. Johrendt, Electronic structure studies of BaFe2As2 by angle-resolved photoemission spectroscopy, Physical Review B 79 (2009) Nr. 15, S. 155118/1-10.*

82) *K. Flatz, M. Grobosch, M. Knupfer, The electronic excitation spectrum of CuPcF16 films, Applied Physics /A 94 (2009) Nr. 1, S. 179-183.*

83) *J. Fornell, A. Concustell, S. Surinach, W.H. Li, N. Cuadrado, A. Gebert, M.D. Baro, J. Sort, Yielding and intrinsic plasticity of Ti–Zr–Ni–Cu–Be bulk metallic glass, International Journal of Plasticity 25 (2009) Nr. 8, S. 1540-1559.*

84) *M. Fronk, B. Braeuer, J. Kortus, O.G. Schmidt, D.R.T. Zahn, G. Salvan, Determination of the Voigt constant of phthalocyanines by magneto-optical Kerr-effect spectroscopy, Physical Review B 79 (2009) Nr. 23, S. 235305/1-7.*

85) *G. Fuchs, S.-L. Drechsler, N. Kozlova, M. Bartkowiak, G. Behr, K. Nenkov, H.-H. Klauss, J. Freudenberger, M. Knupfer, F. Hammerath, G. Lang, H.-J. Grafe, B. Buechner, L. Schultz, Evidence for Pauli-limiting behaviour at high fields and enhanced upper critical fields near Tc in several disordered FeAs based superconductors, Physica C, online first (2009).*

86) *G. Fuchs, S.-L. Drechsler, N. Kozlova, M. Bartkowiak, J.E. Hamann-Borrero, G. Behr, K. Nenkov, H.-H. Klauss, H. Maeter, A. Amato, H. Luetkens, A. Kwadrin, R. Khasanov, J. Freudenberger, A. Koehler, M. Knupfer, E. Arushanov, H. Rosner, B. Buechner, L. Schultz, Orbital and spin effects for the upper critical field in As-deficient disordered Fe pnictide superconductors, New Journal of Physics 11 (2009) Nr. 7, S. 75007/1-26.*

87) *J. Fuezer, P. Kollar, D. Oleksakova, S. Roth, AC magnetic properties of the bulk Fe–Ni and Fe–Ni–Mo soft magnetic alloys prepared by warm compaction, Journal of Alloys and Compounds 483 (2009) Nr. 1-2, S. 557-559.*

88) *U. Gaitzsch, M. Poetschke, S. Roth, B. Rellinghaus, L. Schultz, A 1% magnetostrain in polycrystalline 5M Ni–Mn–Ga, Acta Materialia 57 (2009) Nr. 2, S. 365-370.*

89) *A. Gebert, F. Gostin, U. Kuehn, L. Schultz, Corrosion of a Zr-based bulk metallic glass with different surface finishing states, ECS Transactions 16 (2009) Nr. 32, S. 1-7.*

90) *A. Gebert, S. Roth, S. Oswald, L. Schultz, Passivity of polycrystalline NiMnGa alloys for magnetic shape memory applications, Corrosion Science 51 (2009) Nr. 5, S. 1163-1171.*

91) *G. Giovannetti, S. Kumar, D. Khomskii, S. Picozzi, J. van den Brink, Multiferroicity in Rare-Earth nickelates RNiO3, Physical Review Letters 103 (2009) Nr. 15, S. 156401/1-4.*

92) *S. Girod, M. Gottwald, S. Andrieu, S. Mangin, J. McCord, E.E. Fullerton, J.-M.L. Beaujour, B.J. Krishnatreya, A.D. Kent, Strong perpendicular magnetic anisotropy in Ni/Co(111) single crystal superlattices, Applied Physics Letters 94 (2009), S. 262504/1-3.*

93) *R. Gopalan, K. Hono, A. Yan, O. Gutfleisch, Direct evidence for Cu concentration variation and its correlation to coercivity in Sm(Co0.74Fe0.1Cu0.12Zr.04)7.4 ribbons, Scripta Materialia 60 (2009) Nr. 9, S. 764-767.*

94) P.F. Gostin, R. Sueptitz, A. Gebert, U. Kuehn, L. Schultz, Comparing the corrosion behaviour of Zr66/Ti66–Nb13Cu8Ni6.8Al6.2 bulk nanostructure-dendrite composites, Intermetallics 16 (2008) Nr. 10, S. 1179-1184.

95) F. Gostin, U. Siegel, C. Mickel, S. Baunack, A. Gebert, L. Schultz, Corrosion behavior of the bulk glassy (Fe44.3Cr5Co5Mo12.8Mn11.2C15.8B5.9)98.5Y1.5 alloy, Journal of Materials Research 24 (2009) Nr. 4, S. 1471-1479.

96) H.-J. Grafe, G. Lang, F. Hammerath, D. Paar, K. Manthey, K. Koch, H. Rosner, N. J. Curro, G. Behr, J. Werner, N. Leps, R. Klingeler, H.-H. Klauss, F. J. Litterst, B. Buechner, Electronic properties of La01-xFxFeAs in the normal state probed by NMR/NQR, New Journal of Physics 11 (2009) Nr. 3, S. 35002/1-14.

97) M. Grobosch, V.Y. Aristov, O.V. Molodtsova, C. Schmidt, B.P. Doyle, S. Nannarone, M. Knupfer, Engineering of the energy level alignment at organic semiconductor interfaces by intramolecular degrees of freedom: Transition metal phthalocyanines, The Journal of Physical Chemistry C 113 (2009), S. 13219-13222.

98) M. Grobosch, K. Doerr, R.B. Gangineni, M. Knupfer, Energy level alignment and interactions at potential contacts for spin injection into organic semiconductors, Advanced Engineering Materials 11 (2009) Nr. 4, S. 285-290.

99) M. Grobosch, K. Doerr, R.B. Gangineni, M. Knupfer, Energy level alignment at interfaces between organic semiconductors and clean ferromagnetic La0.7Sr0.3MnO3 thin film contacts for spin injection, Applied Physics A 95 (2009), S. 95-99.

100) P. Gruendler, O. Frank, L. Kavan, L. Dunsch, Carbon nanotube electrodes for hot-wire electrochemistry, ChemPhysChem 10 (2009), S. 559-563.

101) P. Gruendler, A. Kirbs, L. Dunsch, Modern thermoelectrochemistry, ChemPhysChem 10 (2009) Nr. 11, S. 1722-1746.

102) A. Grueneis, C. Attaccalite, A. Rubio, D.V. Vyalikh, S.L. Molodtsov, J. Fink, R. Follath, W. Eberhardt, B. Buechner, T. Pichler, Angle-resolved photoemission study of the graphite intercalation compound KC8: A key to graphene, Physical Review B 80 (2009) Nr. 7, S. 75431/1-5.

103) A. Grueneis, C. Attaccalite, A. Rubio, D.V. Vyalikh, S.L. Molodtsov, J. Fink, R. Follath, W. Eberhardt, B. Buechner, T. Pichler, Electronic structure and electron-phonon coupling of doped graphene layers in KC8, Physical Review B 79 (2009) Nr. 20, S. 205106/1-9.

104) A. Grueneis, K. Kummer, D.V. Vyalikh, Dynamics of graphene growth on a metal surface: a time-dependent photoemission study, New Journal of Physics 11 (2009) Nr. 7, S. 73050/1-9.

105) A. Grueneis, J. Serrano, A. Bosak, M. Lazzeri, S.L. Molodtsov, L. Wirtz, C. Attaccalite, M. Krisch, A. Rubio, F. Mauri, T. Pichler, Phonon surface mapping of graphite: Disentangling quasi-degenerate phonon dispersions, Physical Review B 80 (2009) Nr. 8, S. 85423/1-5.

106) W. Gruner, J. Hassler, P. Barth, J. Behm, J. Sunderkoetter, The precise determination of nitrogen in boron nitride, Journal of the European Ceramic Society 29 (2009) Nr. 10, S. 2029-2035.

107) K. Gueth, R. Huehne, V. Matias, J. Rowley, T. Thersleff, L. Schultz, B. Holzapfel, Preparation of conductive buffer architectures based on IBAD-TiN, IEEE Transactions on Applied Superconductivity 19 (2009) Nr. 3, S. 3447-3450.

108) V.M. Gvozdikov, M. Taut, Magnetic quantum oscillations of diagonal conductivity in a two-dimensional conductor with a weak square superlattice modulation under conditions of the integer quantum Hall effect, New Journal of Physics 11 (2009) Nr. 6, S. 63005/1-12.

109) R. Hafenbrak, S.M. Ulrich, L. Wang, A. Rastelli, O.G. Schmidt, P. Michler, Single entangled photon pair emission from an InGaAs/GaAs quantum dot up to temperatures of 30 K , Physica Status Solidi (c) 6 (2009) Nr. 2, S. 389-394.

110) S. Harikrishnan, S. Roessler, C.M. Naveen Kumar, H.L. Bhat, U.K. Roessler, S. Wirth, F. Steglich, S. Elizabeth, Phase transitions and rare-earth magnetism in hexagonal and orthorhombic DyMnO3 single crystals, Journal of Physics / Condensed Matter 21 (2009) Nr. 9, S. 96002/1-10.

111) O. Heczko, M. Thomas, R. Niemann, L. Schultz, S. Faehler, Magnetically induced martensite transition in freestanding epitaxial Ni–Mn–Ga films, Applied Physics Letters 94 (2009) Nr. 15, S. 152513/1-3.

112) E. Heister, V. Neves, C. Tilmaciu, K. Lipert, V. Sanz Beltran, H.M. Coley, S.R.P. Silva, J. McFadden, Triple functionalisation of single-walled carbon nanotubes with doxorubicin, a monoclonal antibody, and a fluorescent marker for targeted cancer therapy, Carbon 47 (2009) Nr. 9, S. 2152-2160.

113) C. Hermannstaedter, M. Witzany, G.J. Beirne, W.-M. Schulz, M. Eichfelder, R. Rossbach, M. Jetter, P. Michler, L. Wang, A. Rastelli, O.G. Schmidt, Polarization fine structure and enhanced single-photon emission of self-assembled lateral InGaAs quantum dot molecules embedded in a planar microcavity, Journal of Applied Physics 105 (2009) Nr. 12, S. 122408/1-5.

114) A. Herrera-Gomez, J.T. Grant, P.J. Cumpson, M. Jenko, F.S. Aguirre-Tostado, C.R. Brundle, T. Conard, G. Conti, C.S. Fadley, J. Fulghum, K. Kobayashi, L. Koever, H. Nohira, R.L. Opila, S. Oswald, R.W. Paynter, R.M. Wallace, W.S.M. Werner, J. Wolstenholme, Report on the 47th IUVSTA Workshop Angle-Resolved XPS: the current status and future prospects for angle-resolved XPS of nano and subnano films, Surface and Interface Analysis 41 (2009) Nr. 11, S. 840-857.

115) M. Herrmann, W. Haessler, M. Schubert, B. Holzapfel, L. Schultz, Conflicting effects of SiC doping on the properties of mechanically alloyed bulk MgB2, IEEE Transactions on Applied Superconductivity 19 (2009) Nr. 3, S. 2726-2729.

116) C. Hess, A. Kondrat, A. Narduzzo, J.E. Hamann-Borrero, R. Klingeler, J. Werner, G. Behr, B. Buechner, The intrinsic electronic phase diagram of iron-oxypnictide superconductors, epl 87 (2009) Nr. 1, S. 17005/1-6.

117) S.G. Hickey, C. Waurisch, B. Rellinghaus, Demonstration of shape and size control of applications relevant colloidally synthesized IV-VI nanoparticulateTIN(II) Sulfide, Physics, Chemistry and Application of Nanostructures (2009), S. 321-324.

118) *C. Hossbach, S. Teichert, J. Thomas, L. Wilde, H. Wojcik, D. Schmidt, B. Adolphi, M. Bertram, U. Muehle, M. Albert, S. Menzel, B. Hintze, J.W. Bartha, Properties of plasma-enhanced atomic layer deposition-grown tantalum carbonitride thin films, Journal of The Electrochemical Society 156 (2009) Nr. 11, S. H 852-H 859.*

119) *N. Hrauda, J.J. Zhang, J. Stangl, A. Rehman-Khan, G. Bauer, M. Stoffel, O.G. Schmidt, V. Jovanovich, L.K. Nanver, X-ray investigation of buried SiGe islands for devices with strain-enhanced mobility, Journal of Vacuum Science and Technology / B 27 (2009) Nr. 2, S. 912-918.*

120) *N. Hrauda, J.J. Zhang, M. Stoffel, J. Stangl, G. Bauer, A. Rehman-Khan, V. Holy, O.G. Schmidt, V. Jovanovic, L.K. Nanver, X-ray diffraction study of the composition and strain fields in buried SIGe islands, The European Physical Journal - Special Topics 168 (2009), S. 41-46.*

121) *G. Huang, Y. Mei, D.J. Thurmer, E. Coric, O.G. Schmidt, Rolled-up transparent microtubes as two-dimensionally confined culture scaffolds of individual yeast cells, Lab on a chip 9 (2009) Nr. 2, S. 263-268.*

122) *G.S. Huang, S. Kiravittaya, V.A. Bolanos Quinones, F. Ding, M. Benyoucef, A. Rastelli, Y.F. Mei, O.G. Schmidt, Optical properties of rolled-up tubular microcavities from shaped nanomembranes, Applied Physics Letters 94 (2009) Nr. 14, S. 141901/1-3.*

123) *G.S. Huang, Y.F. Mei, F. Cavallo, S. Baunack, E. Coric, T. Gemming, F. Bertram, J. Christen, R.K.Y. Fu, P.K. Chu, O.G. Schmidt, Fabrication and optical properties of C/ beta-SiC/Si hybrid rolled-up microtubes , Journal of Applied Physics 105 (2009), S. 16103/1-3.*

124) *C. Huerrich, H. Wendrock, M. Poetschke, U. Gaitzsch, S. Roth, B. Rellinghaus, L. Schultz, Analysis of variant orientation before and after compression in polycrystalline Ni50Mn29Ga21 MSMA, Journal of Materials Engineering and Performance 18 (2009), S. 554-557.*

125) *K. Iida, J. Haenisch, R. Huehne, F. Kurth, M. Kidszun, S. Haindl, J. Werner, L. Schultz, B. Holzapfel, Strong Tc dependence for strained epitaxial Ba(Fe1-xCox)2As2 thin films, Applied Physics Letters 95 (2009) Nr. 19, S. 192501/1-3.*

126) *D.S. Inosov, D.V. Evtushinsky, A. Koitzsch, V.B. Zabolotnyy, S.V. Borisenko, A.A. Kordyuk, M. Frontzek, M. Loewenhaupt, W. Loeser, I. Mazilu, H. Bitterlich, G. Behr, J.-U. Hoffmann, R. Follath, B. Buechner, Electronic structure and nesting-driven enhancement of the RKKY interaction at the magnetic ordering propagation vector in Gd2PdSi3 and Tb2PdSi3, Physical Review Letters 102 (2009) Nr. 4, S. 46401/1-4.*

127) *D.S. Inosov, D.V. Evtushinsky, V.B. Zabolotnyy, A.A. Kordyuk, B. Buechner, R. Follath, H. Berger, S.V. Borisenko, Temperature-dependent fermi surface of 2H-TaSe2 driven by competing density wave order fluctuations, Physical Review B 79 (2009) Nr. 12, S. 125112/1-5.*

128) *N. Ismail, A.A. El-Meligi, M. Uhlemann, A. Gebert, J. Eckert, L. Schultz, Hydrogenation of Zr-Cu-Al-Ni-Pd metallic glasses by electrochemical means, Journal of Alloys and Compounds 480 (2009) Nr. 2, S. 321-324.*

129) *T.T. Jaervi, D. Pohl, K. Albe, B. Rellinghaus, L. Schultz, J. Fassbender, A. Kuronen, K. Nordlund, From multiply twinned to fcc nanoparticles via irradiation-induced transient amorphization, epl 85 (2009) Nr. 2, S. 26001/1-6.*

130) *O. Janson, W. Schnelle, M. Schmidt, Y. Prots, S.-L. Drechsler, S.K. Filatov, H. Rosner, Electronic structure and magnetic properties of the spin-1/2 Heisenberg system CuSe2O5, New Journal of Physics 11 (2009) Nr. 11, S. 113034/1-19.*

131) *J. Jayaraj, A. Gebert, L. Schultz, Passivation behaviour of structurally relaxed Zr48Cu36Ag8Al8 metallic glass, Journal of Alloys and Compounds 479 (2009) Nr. 1-2, S. 257-261.*

132) *J. Jayaraj, J.M. Park, P.F. Gostin, E. Fleury, A. Gebert, L. Schultz, Nano-porous surface states of Ti–Y–Al–Co phase separated metallic glass, Intermetallics 17 (2009), S. 1120-1123.*

133) *H.-J. Jun, K.S. Lee, U. Kuehn, J. Eckert, Y.W. Chang, Effect of crystalline phases on deformation and warm formability of a bulk metallic glass composite within supercooled liquid region, Materials Science and Engineering A 525 (2009), S. 62-68.*

134) *I. Kaban, P. Jovari, M. Stoica, J. Eckert, W. Hoyer, B. Beuneu, Topological and chemical ordering in Co43Fe20Ta5.5B31.5 metallic glass, Physical Review B 79 (2009) Nr. 21, S. 212201/1-4.*

135) *M. Kalbac, L. Kavan, L. Dunsch, Changes in the electronic states of single-walled carbon nanotubes as followed by a raman spectroelectrochemical analysis of the radial breathing mode, Journal of Physical Chemistry C 112 (2008) Nr. 43, S. 16759-16763.*

136) *M. Kalbac, L. Kavan, M. Zukalova, L. Dunsch, Doping of C60 fullerene peapods with lithium vapor: Raman spectroscopic and spectroelectrochemical studies, Chemistry - A European Journal 14 (2008) Nr. 20, S. 6231-6236.*

137) *M. Kalbac, L. Kavan, L. Dunsch, Controlled doping of double walled carbon nanotubes and conducting polymers in a composite: An in situ Raman spectroelectrochemical study, Composites Science and Technology 69 (2009), S. 1553-1557.*

138) *M. Kalbac, L. Kavan, L. Dunsch, In situ Raman spectroelectrochemistry of SWCNT bundles: Development of the tangential mode during electrochemical charging in different electrolyte solutions, Diamond and Related Materials 18 (2009) Nr. 5-8, S. 972-974.*

139) *M. Kalbac, L. Kavan, L. Dunsch, Selective etching of thin single-walled carbon nanotubes, Journal of the American Chemical Society 131 (2009), S. 4529-4534.*

140) *M. Kalbac, L. Kavan, L. Dunsch, Effect of bundling on the tangential displacement mode in the raman spectra of semiconducting single-walled carbon nanotubes during electrochemical charging, Journal of Physical Chemistry C 113 (2009) Nr. 4, S. 1340-1345.*

141) *M. Kalbac, L. Kavan, L. Dunsch, An in situ Raman spectroelectrochemical study of the controlled doping of semiconducting single walled carbon nanotubes in a conducting polymer matrix, Synthetic Metals 159 (2009) Nr. 21-22, S. 2245-2248.*

142) *A.E. Karkin, J. Werner, G. Behr, B.N. Goshchitskii, Neutron-irradiation effects in polycrystalline LaFeAs00.9F0.1 superconductors, Physical Review B 80 (2009) Nr. 17, S. 174512/1-6.*

143) V. Kataev, U. Schaufuss, B. Buechner, A.A. Zvyagin, J. Sichelschmidt, J. Wykhoff, C. Krellner, C. Geibel, F. Steglich, High-field ESR study of the Kondo lattice system YbRh2Si2, Journal of Physics: Conference Series 150 (2009), S. 42085/1-4.

144) V. Kataev, U. Schaufuss, F. Muranyi, A. Alfonsov, M. Doerr, M. Rotter, B. Buechner, Magnetic anisotropy of the spin-antiferromagnet GdNi2B2C probed by high-frequency ESR, Journal of Physics: Conference Series 150 (2009), S. 42086/1-4.

145) V. Kataev, M. Yehia, E. Vavilova, B. Buechner, A. Moeller, T. Taetz, N. Hollmann, J.A. Mydosh, Interplay between structure, transport and magnetism in the frustrated S = 1/2 system In2VO5, Journal of Physics: Conference Series 150 (2009), S. 42084/1-4.

146) L. Kavan, O. Frank, A.A. Green, M.C. Hersam, J. Koltai, V. Zolyomi, J. Kuerti, L. Dunsch, In situ raman spectroelectrochemistry of single-walled carbon nanotubes: Investigation of materials enriched with (6,5) tubes, Journal of Physical Chemistry C 112 (2008) Nr. 36, S. 14179-14187.

147) L. Kavan, O. Frank, M. Kalbac, L. Dunsch, Supramolecular assembly of single-walled carbon nanotubes with a ruthenium(II)-Bipyridine complex: An in situ raman spectroelectrochemical study, Journal of Physical Chemistry C 113 (2009), S. 2611-2617.

148) L. Kavan, P. Janda, M. Krause, F. Ziegs, L. Dunsch, Rotating cell for in situ raman spectroelectrochemical studies of photosensitive redox systems, Analytical Chemistry 81 (2009) Nr. 5, S. 2017-2021.

149) A. Kellenberger, E. Jaehne, H.-J. Adler, T. Khandelwal, L. Dunsch, In situ FTIR spectroelectrochemistry of poly[2-(3-thienyl)ethyl acetate] and its hydrolyzed derivatives, Electrochimica Acta 53 (2008) Nr. 24, S. 7054-7060.

150) M.S. Khatri, H. Schloerrb, S. Faehler, L. Schultz, B. Nandan, M. Boehme, R. Krenek, M. Stamm, *Electrodeposition of Co–Pt continuous films and nanowires within diblock copolymer template*, Electrochimica Acta 54 (2009), S. 2536-2539.

151) S. Kiravittaya, A. Rastelli, O.G. Schmidt, *Advanced quantum dot configurations*, Reports on Progress in Physics 72 (2009) Nr. 4, S. 46502/1-34.

152) D. Klemm, V. Hoffmann, C. Edelmann, *Controlling of material analysers of the GD-OES type with help of pump-down curves*, Vacuum 84 (2009) Nr. 2, S. 299-303.

153) D. Klemm, V. Hoffmann, K. Wetzig, J. Eckert, *DC-and RF-GD-OES measurements of adsorbed organic monolayers on copper*, Analytical and Bioanalytical Chemistry 395 (2009) Nr. 6, S. 1893-1900.

154) S. Klod, L. Dunsch, *The role of aprotic solvents in the dynamic behavior of fullerenes like C60 and C70: An NMR spin-lattice relaxation study*, Journal of Physical Chemistry C 113 (2009) Nr. 34, S. 15191-15195.

155) M. Knupfer, *Characterization of the electronic excitations in Alq3 using electron energy-loss spectroscopy*, Applied Physics /A 94 (2009) Nr. 1, S. 31-34.

156) K. Koch, R.O. Kuzian, K. Koepernik, I.V. Kondakova, H. Rosner, *Analysis of the electric field gradient in the perovskites SrTiO3 and BaTiO3: Density functional and model calculations*, Physical Review B 80 (2009) Nr. 12, S. 125113/1-9.

157) A. Koehler, G. Behr, G. Fuchs, K. Nenkov, L.C. Gupta, *Si-induced superconductivity and structural transformations in DyRh4B4*, Journal of Alloys and Compounds 482 (2009) Nr. 1-2, S. 5-9.

158) A. Koenig, F. Roth, R. Kraus, M. Knupfer, *Electronic properties of potassium doped FePc from electron energy-loss spectroscopy*, The Journal of Chemical Physics 130 (2009) Nr. 21, S. 214503/1-5.

159) A. Koitzsch, D. S. Inosov, D. V. Evtushinsky, V. B. Zabolotnyy, A. A. Kordyuk, A. Kondrat, C. Hess, M. Knupfer, B. Buechner, G. L. Sun, V. Hinkov, C. T. Lin, A. Varykhalov, S. V. Borisenko, *Temperature and doping-dependent renormalization effects of the low energy electronic structure of Ba1-xKxFe2As2 single crystals*, Physical Review Letters 102 (2009) Nr. 16, S. 167001/1-4.

160) A. Koitzsch, I. Opahle, S. Elgazzar, S.V. Borisenko, J. Geck, V.B. Zabolotnyy, D. Inosov, H. Shiozawa, M. Richter, M. Knupfer, J. Fink, B. Buechner, E.D. Bauer, J.L. Sarrao, R. Follath, *Electronic structure of CeCoIn5 from angle-resolved photoemission spectroscopy*, Physical Review B 79 (2009) Nr. 7, S. 75104/1-7.

161) V. Kokotin, H. Hermann, *Geometrical aspects of the glass-forming ability of dense binary hard-sphere mixtures*, Scripta Materialia 61 (2009) Nr. 3, S. 261-264.

162) A. Kondrat, J.E. Hamann-Borrero, N. Leps, M. Kosmala, O. Schumann, A. Koehler, J. Werner, G. Behr, M. Braden, R. Klingeler, B. Buechner, C. Hess, *Synthesis and physical properties of La01-xFxFeAs*, The European Physical Journal B 70 (2009), S. 461-468.

163) A.A. Kordyuk, S.V. Borisenko, V.B. Zabolotnyy, R. Schuster, D. S. Inosov, D.V. Evtushinsky, A.I. Plyushchay, R. Follath, A. Varykhalov, L. Patthey, H. Berger, *Nonmonotonic pseudogap in high-Tc cuprates*, Physical Review B 79 (2009) Nr. 2, S. 20504/1-4.

164) P. Kovac, I. Husek, E. Dobrocka, T. Melisek, W. Haessler, M. Herrmann, *MgB2 tapes made of mechanically alloyed precursor powder in different metallic sheaths*, Superconductor Science and Technology 21 (2008) Nr. 1, S. 15004/1-6.

165) J.A. Koza, S. Muehlenhoff, M. Uhlemann, K. Eckert, A. Gebert, L. Schultz, *Desorption of hydrogen from an electrode surface under influence of an external magnetic field – In-situ microscopic observations*, Electrochemistry Communications 11 (2009), S. 425-429.

166) J.A. Koza, M. Uhlemann, A. Gebert, C. Mickel, S. Baunack, L. Schultz, *The effect of magnetic fields on the electrodeposition of CoFe alloys*, Magnetohydrodynamics 45 (2009) Nr. 2, S. 259-266.

167) J.A. Koza, M. Uhlemann, C. Mickel, A. Gebert, L. Schultz, *The effect of magnetic field on the electrodeposition of CoFe alloys*, Journal of Magnetism and Magnetic Materials 321 (2009) Nr. 14, S. 2265-2268.

168) C. Kramberger, H. Rauf, M. Knupfer, H. Shiozawa, D. Batchelor, A. Rubio, H. Kataura, T. Pichler, *Potassium-intercalated single-wall carbon nanotube bundles: Archetypes for semiconductor/metal hybrid systems*, Physical Review B 79 (2009) Nr. 19, S. 195442/1-5.

169) R. Kraus, M. Grobosch, M. Knupfer, *Full electronic excitation spectrum of condensed manganese phthalocyanine*, Chemical Physics Letters 469 (2009), S. 121-124.

170) T. Kroll, V.Y. Aristov, O.V. Molodtsova, Y.A. Ossipyan, D.V. Vyalikh, B. Buechner, M. Knupfer, *Spin and Orbital Ground State of Co in Cobalt Phthalocyanine*, The Journal of Physical Chemistry A 113 (2009), S. 8917-8922.

171) T. Kroll, F. Roth, A. Koitzsch, R. Kraus, D.R. Batchelor, J. Werner, G. Behr, B. Buechner, M. Knupfer, *Absorption and photoemission spectroscopy of rare-earth oxypnictides*, New Journal of Physics 11 (2009) Nr. 2, S. 25019/1-11.

172) Y. Krupskaya, C. Mahn, A. Parameswaran, A. Taylor, K. Kraemer, S. Hampel, A. Leonhardt, M. Ritschel, B. Buechner, R. Klingeler, *Magnetic study of iron-containing carbon nanotubes: Feasibility for magnetic hyperthermia*, Journal of Magnetism and Magnetic Materials 321 (2009) Nr. 24, S. 4067-4071.

173) M.L. Kulic, S.-L. Drechsler, O.V. Dolgov, *Conventional superconductivity in Fe-based pnictides: The relevance of intra-band electron-boson scattering*, epl 85 (2009) Nr. 4, S. 47008/1-6.

174) M. Kulich, P. Kovac, M. Eisterer, I. Husek, T. Melisek, H.W. Weber, W. Haessler, *Effect of C and SiC additions into in situ or mechanically alloyed MgB2 deformed in Ti sheath*, Physica / C 469 (2009), S. 827-831.

175) N.V. Kuratieva, D. Mikhailova, H. Ehrenberg, *A new polymorph of Cu3B2O6*, Acta Crystallographica Section C 65 (2009), S. 185-186.

176) M.D. Kuzmin, M. Richter, A.M. Tishin, *Field dependence of magnetic entropy change: Whence comes an intercept?*, Journal of Magnetism and Magnetic Materials 321 (2009) Nr. 1, S. L1-L3.

177) A.R. Kwon, V. Neu, V. Matias, J. Haenisch, R. Huehne, J. Freudenberger, B. Holzapfel, L. Schultz, S. Faehler, *Tuning functional properties by plastic deformation*, New Journal of Physics 11 (2009) Nr. 8, S. 83013/1-10.

178) S. Laubach, S. Laubach, P.C. Schmidt, D. Ensling, S. Schmid, W. Jaegermann, A. Thissen, K. Nikolowski, H. Ehrenberg, *Changes in the crystal and electronic structure of LiCoO2 and LiNiO2 upon Li intercalation and de-intercalation*, Physical Chemistry Chemical Physics 11 (2009) Nr. 17, S. 3278-3289.

179) H. S. Lee, A. Rastelli, S. Kiravittaya, P. Atkinson, C. C. Bof Bufon, I. Moench, O.G. Schmidt, *Selective area wavelength tuning of InAs/GaAs quantum dots obtained by TiO2 and SiO2 layer patterning*, Applied Physics Letters 94 (2009) Nr. 16, S. 161906/1-3.

180) H.S. Lee, S. Kiravittaya, S. Kumar, J.D. Plumhof, L. Balet, L.H. Li, M. Francardi, A. Gerardino, A. Fiore, A. Rastelli, O.G. Schmidt, *Local tuning of photonic crystal nanocavity modes by laser-assisted oxidation*, Applied Physics Letters 95 (2009) Nr. 19, S. 191109/1-3.

181) H.S. Lee, A. Rastelli, M. Benyoucef, F. Ding, T.W. Kim, H.L. Park, O.G. Schmidt, *Microphotoluminescence spectroscopy of single CdTe/ZnTe quantum dots grown on Si(001) substrates*, Nanotechnology 20 (2009) Nr. 7, S. 75705/1-5.

182) J.K. Lee, K.B. Kim, M.H. Lee, T.S. Kim, J.C. Bae, *Microstructure and mechanical properties of metallic glass/metallic glass composites*, Journal of Alloys and Compounds 483 (2009) Nr. 1-2, S. 286-288.

183) K.S. Lee, H.-J. Jun, S. Pauly, B. Bartusch, Y.W. Chang, J. Eckert, *Thermomechanical characterization of Cu47.5Zr47.5Al5 bulk metallic glass within the homogeneous flow regime*, Intermetallics 17 (2009) Nr. 1, S. 65-71.

184) K.S. Lee, J.-H. Lee, J. Eckert, *On the structural relaxation of bulk metallic glass under warm deformation*, Intermetallics 17 (2009) Nr. 4, S. 222-226.

185) M.H., Lee, J.K. Lee, K.T. Kim, J. Thomas, J. Das, U. Kuehn, J. Eckert, *Deformation-induced microstructural heterogeneity in monolithic Zr44Ti11Cu9.8Ni10.2Be25 bulk metallic glass*, Physica Status Solidi RRL 3 (2009) Nr. 2-3, S. 46-48.

186) P.V. Leksin, R.I. Salikhov, I.A. Garifullin, H. Vinzelberg, V. Kataev, R. Klingeler, L.R. Tagirov, B. Buechner, *Observation of the "Inverse" spin valve effect in a Ni/V/Ni trilayer system*, JETP Letters 90 (2009) Nr. 1, S. 59-63.

187) A.A. Levin, T. Weissbach, A.I. Pommrich, O. Bilani-Zeneli, D.C. Meyer, *In situ X-ray investigation of lattice strain in SrTiO3/La0.7Sr0.3MnO3 thin films induced by piezoelectric 0.72Pb(Mg1/3Nb2/3)O3–0.28PbTiO3 substrate in an external electric field*, Applied Physics /A 96 (2009) Nr. 3, S. 575-580.

188) R. Li, S. Kumar, S. Ram, M. Stoica, S. Roth, J. Eckert, *Crystallization and magnetic properties of [(Fe,Co)0.75Si0.05B0.20]94Nb6 metallic glasses*, Journal of Physics D 42 (2009) Nr. 8, S. 85006/1-6.

189) R. Li, M. Stoica, J. Eckert, *Effect of minor Cu addition on phase evolution and magnetic properties of {[(Fe0.5Co0.5)0.75Si0.05B0.20]0.96Nb0.04}100-x Cux alloys*, Journal of Physics: Conference Series 144 (2009) Nr. 1, S. 12042/1-4.

190) X. Li, Y.J. Wei, H. Ehrenberg, D.L. Liu, S.Y. Zhan, C.Z. Wang, G. Chen, *X-ray diffraction and Raman scattering studies of Li+/e—extracted inverse spinel LiNiVO4*, Journal of Alloys and Compounds 471 (2009) Nr. 1-2, S. L26-L28.

191) K. Lipert, F. Kretzschmar, M. Ritschel, A. Leonhardt, R. Klingeler, B. Buechner, *Nonmagnetic carbon nanotubes*, Journal of Applied Physics 105 (2009) Nr. 6, S. 63906/1-4.

192) K.G. Lisunov, N. Wizent, A. Waske, J. Werner, N. Tristan, C. Sekar, G. Krabbes, G. Behr, E. Arushanov, B. Buechner, *Quasi-one-dimensional hopping conductivity of the spin-ladder CaCu2O3 single crystals: Influence of the cation and oxygen nonstoichiometry*, Journal of Applied Physics 103 (2008) Nr. 12, S. 123712/1-6.

193) J. Liu, S. Aksoy, N. Scheerbaum, M. Acet, O. Gutfleisch, *Large magnetostrain in polycrystalline Ni-Mn-In-Co*, Applied Physics Letters 95 (2009) Nr. 23, S. 232515/1-3.

194) J. Liu, N. Scheerbaum, S. Weiss, O. Gutfleisch, *Ni–Mn–In–Co single-crystalline particles for magnetic shape memory composites*, Applied Physics Letters 95 (2009) Nr. 15, S. 152503/1-3.

195) J. Liu, T.G. Woodcock, N. Scheerbaum, O. Gutfleisch, *Influence of annealing on magnetic field-induced structural transformation and magnetocaloric effect in Ni–Mn–In–Co ribbons*, Acta Materialia 57 (2009) Nr. 16, S. 4911-4920.

196) W.E.A. Lorenz, R.O. Kuzian, S.-L. Drechsler, W.-D. Stein, N. Wizent, G. Behr, J. Malek, U. Nitzsche, H. Rosner, A. Hiess, W. Schmidt, R. Klingeler, M. Loewenhaupt, B. Buechner, *Highly dispersive spin excitations in the chain cuprate Li2Cu02*, epl 88 (2009) Nr. 3, S. 37002/1-6.

197) H. Luetkens, H.-H. Klauss, M. Kraken, F. J. Litterst, T. Dellmann, R. Klingeler, C. Hess, R. Khasanov, A. Amato, C. Baines, M. Kosmala, O. J. Schumann, M. Braden, J. Hamann-Borrero, N. Leps, A. Kondrat, G. Behr, J. Werner, B. Buechner, *The electronic phase diagram of the LaO1-xFxFeAs superconductor*, Nature materials 8 (2009) Nr. 4, S. 305-309.

198) P. Lukaszczuk, E. Borowiak-Palen, M.H. Ruemmeli, R.J. Kalenczuk, *Single-walled carbon nanotubes modified by PFO: An optical absorption and Raman spectroscopic investigation*, Physica Status Solidi B 246 (2009) Nr. 11-12, S. 2699-2703.

199) J. Lyubina, O. Gutfleisch, O. Isnard, *Phase transformations and magnetic structure of nanocrystalline Fe–Pd and Co–Pt alloys studied by in situ neutron powder diffraction*, Journal of Applied Physics 105 (2009) Nr. 7, S. 7A717/1-3.

200) J. Lyubina, O. Gutfleisch, M.D. Kuzmin, M. Richter, *La(Fe,Si)13-based magnetic refrigerants obtained by novel processing routes*, Journal of Magnetism and Magnetic Materials 321 (2009), S. 3571-3577.

201) H. Maeter, H. Luetkens, Y.G. Pashkevich, A. Kwadrin, R. Khasanov, A. Amato, A.A. Gusev, K.V. Lamonova, D.A. Chervinskii, R. Klingeler, C. Hess, G. Behr, B. Buechner, H.-H. Klauss, *Interplay of rare earth and iron magnetism in RFeAsO (R=La, Ce, Pr, and Sm): Muon-spin relaxation study and symmetry analysis*, Physical Review B 80 (2009) Nr. 9, S. 94524/1-19.

202) A. Malachias, C. Deneke, B. Krause, C. Mocuta, S. Kiravittaya, T.H. Metzger, O.G. Schmidt, *Direct strain and elastic energy evaluation in rolled-up semiconductor tubes by x-ray microdiffraction*, Physical Review B 79 (2009) Nr. 3, S. 35301/1-12.

203) K. Mandal, D. Pal, N. Scheerbaum, J. Lyubina, O. Gutfleisch, *Effect of pressure on the magnetocaloric properties of nickel-rich Ni–Mn–Ga Heusler alloys*, Journal of Applied Physics 105 (2009) Nr. 7, S. 73509/1-6.

204) N. Martin, J. McCord, A. Gerber, T. Strache, T. Gemming, I. Moench, N. Farag, R. Schaefer, J. Fassbender, E. Quandt, L. Schultz, *Local stress engineering of magnetic anisotropy in soft magnetic thin films*, Applied Physics Letters 94 (2009) Nr. 6, S. 62506/1-3.

205) V.V. Maslyuk, V.Y. Aristov, O.V. Molodtsova, D.V. Vyalikh, V.M. Zhilin, Y.A. Ossipyan, T. Bredow, I. Mertig, M. Knupfer, *The electronic structure of cobalt phthalocyanine*, Applied Physics A 94 (2009), S. 485-489.

206) V. Matias, J. Haenisch, E.J. Rowley, K. Gueth, *Very fast biaxial texture evolution using high rate ion-beam-assisted deposition of MgO*, Journal of Materials Research 24 (2009) Nr. 1, S. 125-129.

207) N. Mattern, J. Bednarcik, S. Pauly, G. Wang, J. Das, J. Eckert, *Structural evolution of Cu-Zr metallic glasses under tension*, Acta Materialia 57 (2009) Nr. 14, S. 4133-4139.

208) N. Mattern, G. Goerigk, U. Vainio, M.K. Miller, T. Gemming, J. Eckert, *Spinodal decomposition of Ni-Nb-Y metallic glasses*, Acta Materialia 57 (2009) Nr. 3, S. 903-908.

209) N. Mattern, P. Jovari, I. Kaban, S. Gruner, A. Elsner, V. Kokotin, H. Franz, B. Beuneu, J. Eckert, *Short-range order of Cu-Zr metallic glasses*, Journal of Alloys and Compounds 485 (2009), S. 163-169.

210) C. Mazumdar, L.C. Gupta, K. Nenkov, G. Behr, G. Fuchs, *Effect of Pt on the superconducting and magnetic properties of ErNi2B2C*, Journal of Alloys and Compounds 480 (2009) Nr. 2, S. 190-192.

211) J. McCord, I. Moench, J. Fassbender, A. Gerber, E. Quandt, *Local setting of magnetic anisotropy in amorphous films by Co ion implantation*, Journal of Physics D 42 (2009) Nr. 5, S. 55006/1-6.

212) J. McCord, R. Schaefer, *Domain wall asymmetries in Ni81Fe19/NiO: proof of variable anisotropies in exchange bias systems*, New Journal of Physics 11 (2009) Nr. 8, S. 83016/1-9.

213) Y. Mei, D.J. Thurmer, C. Deneke, S. Kiravittaya, Y.-F. Chen, A. Dadgar, F. Bertram, B. Bastek, A. Krost, J. Christen, T. Reindl, M. Stoffel, E. Coric, O.G. Schmidt, *Fabrication, self-assembly, and properties of ultrathin AlN/GaN porous crystalline nanomembranes: Tubes, spirals, and curved sheets*, ACS Nano 3 (2009) Nr. 7, S. 1663-1668.

214) E. Menendez, M.O. Liedke, J. Fassbender, T. Gemming, A. Weber, L.J. Heyderman, K.V. Rao, S.C. Deevi, S. Surinach, M.D. Baro, J. Sort, J. Nogues, *Direct magnetic patterning due to the generation of ferromagnetism by selective ion irradiation of paramagnetic FeAl alloys*, Small 5 (2009) Nr. 2, S. 229-234.

215) S.B. Menzel, J. Thomas, U. Weissker, F. Schaeffel, C. Hossbach, M. Albert, S. Hampel, T. Gemming, *Preparation of CNT-copper matrix composite films*, Journal of Nanoscience and Nanotechnology 9 (2009), S. 6096-6103.

216) K.E. Metlushka, B.A. Kashemirov, V.F. Zheltukhin, D.N. Sadkova, B. Buechner, C. Hess, O.N. Kataeva, C.E. McKenna, V.A. Alfonsov, *1-(alpha-Aminobenzyl)-2-naphthol: A new chiral auxiliary for the synthesis of enantiopure - aminophosphonic acids*, Chemistry - A European Journal 15 (2009) Nr. 27, S. 6718-6722.

217) W. Miiller, V.H. Tran, M. Richter, *Cancellation of spin and orbital moments in URhGe under pressure: A density-functional prediction*, Physical Review B 80 (2009) Nr. 19, S. 195108/1-6.

218) D. Mikhailova, H. Ehrenberg, S. Oswald, D. Trots, G. Brey, H. Fuess, *Metallic Re-Re bond formation in different MRe2O6 (M=Fe,Co,Ni) rutile-like polymorphs: the role of temperature in high-pressure synthesis*, Journal of Solid State Chemistry 182 (2009) Nr. 2, S. 364-373.

219) D. Mikhailova, H. Ehrenberg, D. Trots, G. Brey, S. Oswald, H. Fuess, *CrxRe1-xO2 oxides with different rutile-like structures: changes in the electronic configuration and resulting physical properties*, Journal of Solid State Chemistry 182 (2009), S. 1506-1514.

220) A. Moebius, P. Karmann, M. Schreiber, *Coulomb gap revisited - a renormalisation approach*, Journal of Physics: Conference Series 150 (2009), S. 22057/1-4.

221) A. Moebius, U.K. Roessler, *Critical behavior of the Coulomb-glass model in the zero-disorder limit: Ising universality in a system with long-range interactions*, Physical Review B 79 (2009) Nr. 17, S. 174206/1-10.

222) A.S. Moskvin, S.-L. Drechsler, *Microscopic mechanisms of spin-dependent electric polarization in 3d oxides*, The European Physical Journal B 71 (2009) Nr. 3, S. 331-338.

223) A.S. Moskvin, Y.D. Panov, S.-L. Drechsler, *Nonrelativistic multiferrocity in the nonstoichiometric spin-1/2 spiral-chain cuprate LiCu2O2*, Physical Review B 79 (2009) Nr. 10, S. 104112/1-5.

224) S. Muehlbauer, C. Pfleiderer, P. Boeni, M. Laver, E.M. Forgan, D. Fort, U. Keiderling, G. Behr, *Morphology of the superconducting vortex lattice in ultrapure niobium*, Physical Review Letters 102 (2009) Nr. 13, S. 136408/1-4.

225) A. Mueller, S. Schippers, M. Habibi, D. Esteves, J.C. Wang, R.A. Phaneuf, A.L.D. Kilcoyne, A. Aguilar, L. Dunsch, *Significant redistribution of Ce 4d oscillator strength observed in photoionization of endohedral Ce@C+82ions*, Physical Review Letters 101 (2008) Nr. 13, S. 133001/1-3.

226) C. Mueller, M.S. Khatri, C. Deneke, S. Faehler, Y.F. Mei, E. E. Bermudez Urena, O.G. Schmidt, *Tuning magnetic properties by roll-up of Au/Co/Au films into microtubes*, Applied Physics Letters 94 (2009) Nr. 10, S. 102510/1-3.

227) C. Mueller, A. Leonhardt, M.C. Kutz, B. Buechner, H. Reuther, *Growth Aspects of Iron-Filled Carbon Nanotubes Obtained by Catalytic Chemical Vapor Deposition of Ferrocene*, Journal of Physical Chemistry C 113 (2009) Nr. 7, S. 2736-2740.

228) S. Myhra, T. Muehl, *Surface patterning of a-C DLC films: aqueous electrochemistry and thermal activation*, Journal of Physics D 42 (2009) Nr. 3, S. 35309/1-8.

229) Y.G. Naidyuk, G. Behr, N.L. Bobrov, V.N. Chernobay, S.-L. Drechsler, G. Fuchs, O.E. Kvitnitskaya, D.G. Naugle, K.D.D. Rathnayaka, I.K. Yanson, *The superconducting gap behavior in the antiferromagnetic nickel-borocarbide compounds RNi2B2C (R=Dy, Ho, Er, Tm) studied by point-contacts spectroscopy*, Journal of Physics: Conference Series 150 (2009) Nr. Part 5, S. 52178/1-4.

230) I.A. Nekrasov, N.S. Pavlov, E.Z. Kuchinskii, M.V. Sadovskii, Z.V. Pchelkina, V.B. Zabolotnyy, J. Geck, B. Buechner, S.V. Borisenko, D.S. Inosov, A.A. Kordyuk, M. Lambacher, A. Erb, *Electronic structure of Pr2-xCexCuO4 studied via ARPES and LDA+DMFT+ sigma k*, Physical Review B 80 (2009) Nr. 14, S. 140510(R)/1-4.

231) T. Niemeier, R. Huehne, A. Koehler, G. Behr, L. Schultz, B. Holzapfel, *Epitaxial c-axis oriented LuNi2B2C thin films on MgO(110)*, Journal of Physics: Conference Series 150 (2009), S. 52185/1-4.

232) K. Nikolowski, S. Scudino, M. Stoica, K.B. Surreddi, J. Das, J. Eckert, *Stress-induced martensitic transformation in a Ti45Zr38Al17 cast rod*, Journal of Physics: Conference Series 144 (2009), S. 12090/1-4.

233) S. Nishimoto, M. Arikawa, *Dynamics in a two-leg spin ladder with a four-spin cyclic interaction*, Physical Review B 79 (2009) Nr. 11, S. 113106/1-4.

234) S. Nishimoto, M. Arikawa, *Basic properties of three-leg Heisenberg tube*, Journal of Physics: Conference Series 145 (2009), S. 12041/1-4.

235) S. Nishimoto, C. Hotta, *Density-matrix renormalization study of frustrated fermions on a triangular lattice*, Physical Review B 79 (2009) Nr. 19, S. 195124/1-6.

236) S. Nishimoto, E. Jeckelmann, D.J. Scalapino, *Current-current correlations in the three-band model for two-leg CuO ladders: Density-matrix renormalization group study*, Physical Review B 79 (2009) Nr. 20, S. 205115/1-5.

237) A. Oesterholm, A. Petr, C. Kvarnstrm, A. Ivaska, L. Dunsch, *The nature of the charge carriers in polyazulene as studied by in situ electron spin resonance-UV-visible-near-infrared spectroscopy*, Journal of Physical Chemistry B 112 (2008), S. 14149-14157.

238) I. Opahle, K. Koepernik, U. Nitzsche, M. Richter, *Jahn-Teller like origin of the tetragonal distortion in disordered Fe-Pd magnetic shape memory alloys*, Applied Physics Letters 94 (2009) Nr. 7, S. 72508/1-3.

239) S. Oswald, R. Hermann, B. Schmidt, *SIMS measurement of oxygen content in y -TiAl single crystals and polycrystalline alloys with Nb addition*, Materials Science and Engineering A 516 (2009) Nr. 1-2, S. 54-57.

240) S. Oswald, K. Nikolowski, H. Ehrenberg, *Quasi in situ XPS investigations on intercalation mechanisms in Li-ion battery materials*, Analytical and Bioanalytical Chemistry 393 (2009) Nr. 8, S. 1871-1877.

241) G. Paasch, B.M. Grafov, *Thermodynamics of interface elasticity*, Russian Journal of Electrochemistry (Elektrokhimiya) 45 (2009) Nr. 1, S. 73-80.

242) G. Paasch, S. Scheinert, *Space-charge-limited currents in organics with trap distributions: Analytical approximations versus numerical simulation*, Journal of Applied Physics 106 (2009) Nr. 8, S. 84502/1-9.

243) J.M. Park, J.H. Han, K.B. Kim, N. Mattern, J. Eckert, D.H. Kim, *Favorable microstructural modulation and enhancement of mechanical properties of Ti–Fe–Nb ultrafine composites*, Philosophical Magazine Letters 89 (2009) Nr. 10, S. 623-632.

244) J.M. Park, N. Mattern, U. Kuehn, J. Eckert, K.B. Kim, W.T. Kim, K. Chattopadhyay, D.H. Kim, *High-strength bulk Al-based bimodal ultrafine eutectic composite with enhanced plasticity*, Journal of Materials Research 24 (2009) Nr. 8, S. 2605-2609.

245) J.T. Park, D.S. Inosov, C. Niedermayer, G.L. Sun, D. Haug, N.B. Christensen, R. Dinnebier, A.V. Boris, A.J. Drew, L. Schulz, T. Shapoval, U. Wolff, V. Neu, X. Yang, C.T. Lin, B. Keimer, V. Hinkov, *Electronic phase separation in the slightly underdoped iron pnictide superconductor Ba1-xKxFe2As2*, Physical Review Letters 102 (2009), S. 117006/1-4.

246) S. Pauly, J. Das, J. Bednarcik, N. Mattern, K.B. Kim, D.H. Kim, J. Eckert, *Deformation-induced martensitic transformation in Cu-Zr-(Al,Ti) bulk metallic glass composites*, Scripta Materialia 60 (2009) Nr. 6, S. 431-434.

247) S. Pauly, J. Das, N. Mattern, D.H. Kim, J. Eckert, *Phase formation and thermal stability in Cu-Zr-Ti(Al) metallic glasses*, Intermetallics 17 (2009) Nr. 6, S. 453-462.

248) S. Pauly, M.H. Lee, D.H. Kim, K.B. Kim, D.J. Sordelet, J. Eckert, *Crack evolution in bulk metallic glasses*, Journal of Applied Physics 106 (2009) Nr. 10, S. 103518/1-7.

249) S. Pauly, G. Liu, G. Wang, J. Das, K.B. Kim, U. Kuehn, D.H. Kim, J. Eckert, *Modeling deformation behavior of Cu–Zr–Al bulk metallic glass matrix composites*, Applied Physics Letters 95 (2009) Nr. 10, S. 101906/1-3.

250) S. Pauly, G. Liu, G. Wang, U. Kuehn, N. Mattern, J. Eckert, *Microstructural heterogeneities governing the deformation of Cu47.5Zr47.5Al5 bulk metallic glass composites*, Acta Materialia 57 (2009) Nr. 18, S. 5445-5453.

251) H. Peisert, I. Biswas, M. Knupfer, T. Chasse, *Orientation and electronic properties of phthalocyanines on polycrystalline substrates*, Physica Status Solidi / B 246 (2009) Nr. 7, S. 1529-1545.

252) H. Peisert, I. Biswas, L. Zhang, B.-E. Schuster, M.B. Casu, A. Haug, D. Batchelor, M. Knupfer, T. Chasse, *Unusual energy shifts in resonant photoemission spectra of organic model molecules*, The Journal of Chemical Physics 130 (2009) Nr. 19, S. 194705/1-7.

253) F. Pezzoli, M. Stoffel, T. Merdzhanova, A. Rastelli, O.G. Schmidt, *Alloying and strain relaxation in SiGe islands grown on pit-patterned Si(001) substrates probed by nanotomography*, Nanoscale Research Letters 4 (2009), S. 1073-1077.

254) D.H. Pi, J.K. Lee, M.H. Lee, S. Yi, J. Eckert, K.B. Kim, *Role of heterogeneity on deformation behavior of bulk metallic glasses*, Journal of Alloys and Compounds 486 (2009), S. 233-236.

255) D. Placha, H. Raclavska, D. Matysek, M.H. Ruemmeli, *The polycyclic aromatic hydrocarbon concentrations in soils in the Region of Valasske Mezirici, the Czech Republic*, Geochemical Transactions 10 (2009) Nr. 12, S. 1-21.

256) M. Pletea, R. Koch, H. Wendrock, R. Kaltofen, O.G. Schmidt, *In situ stress evolution during and after sputter deposition of Al thin films*, Journal of Physics / Condensed Matter 21 (2009) Nr. 22, S. 225008/1-8.

257) B. Podmiljsak, P.J. McGuiness, N. Mattern, H. Ehrenberg, S. Kobe, S. Jozef, S. Ljubljana, *Magnetocaloric properties in the GdSiGeFe system and the magnetic properties of the newly formed Gd(Si,Ge) phase*, IEEE Transactions on Magnetics 45 (2009) Nr. 10, S. 4364-4367.

258) Y.G. Ponomarev, S.A. Kuzmichev, M.G. Mikheev, M.V. Sudakova, S.N. Tchesnokov, O.S. Volkova, A.N. Vasiliev, T. Haenke, C. Hess, G. Behr, R. Klingeler, B. Buechner, *Andreev spectroscopy of LaFeAs00.9F0.1*, Physical Review B 79 (2009) Nr. 22, S. 224517/1-6.

259) A.I. Popa, E. Vavilova, Y.C. Arango, V. Kataev, C. Taeschner, H.-H. Klauss, H. Maeter, H. Luetkens, B. Buechner, R. Klingeler, *High-temperature ferromagnetism of Li-doped vanadium oxide nanotubes*, epl 88 (2009), S. 57002/1-5.

260) A.A. Popov, A.V. Burtsev, V.M. Senyavin, L. Dunsch, S.I. Troyanov, *Spectroscopic and Theoretical Study of the Dimeric Dicationic Fullerene Complex [(C70)2]2+(Ti3Cl13)-2*, Journal of Physical Chemistry A 113 (2009) Nr. 1, S. 263-272.

261) K.G. Prashanth, S. Scudino, B.S. Murty, J. Eckert, *Crystallization kinetics and consolidation of mechanically alloyed Al70Y16Ni10Co4 glassy powders*, Journal of Alloys and Compounds 477 (2009) Nr. 1-2, S. 171-177.

262) K.G. Prashanth, S. Scudino, K.B. Surreddi, M. Sakaliyska, B.S. Murty, J. Eckert, *Crystallization kinetics of Zr65Ag5Cu12.5Ni10Al7.5 glassy powders produced by ball milling of pre-alloyed ingots*, Materials Science and Engineering A 513-514 (2009), S. 279-285.

263) R.-T. Qu, F.-F. Wu, Z.-F. Zhang, J. Eckert, *Direct observations on the evolution of shear bands into cracks in metallic glass*, Journal of Materials Research 24 (2009) Nr. 10, S. 3130-3135.

264) U. Queitsch, C. Hamann, F. Schaeffel, B. Rellinghaus, L. Schultz, A. Blueher, M. Mertig, *Toward dense biotemplated magnetic nanoparticle arrays: Probing the particle-template interaction*, Journal of Physical Chemistry C 113 (2009) Nr. 24, S. 10471-10476.

265) N. Qureshi, M. Zbiri, J. Rodriguez-Carvajal, A. Stunault, E. Ressouche, T.C. Hansen, M.T. Fernandez-Diaz, R. Johnson, H. Fuess, H. Ehrenberg, Y. Sakurai, M. Itou, B. Gillon, T. Wolf, J.A. Rodriguez-Velamazan, J. Sanchez-Montero, *Experimental magnetic form factors in Co3V2O8: A combined study of ab initio calculations, magnetic Compton scattering, and polarized neutron diffraction*, Physical Review B 79 (2009) Nr. 9, S. 94417/1-10.

266 R. Ranjan, R. Garg, A. Senyshyn, M.S. Hegde, H. Ehrenberg, H. Boysen, *Magneto-structural study of a Cr-doped CaRuO3*, Journal of Physics / Condensed Matter 21 (2009) Nr. 32, S. 326001/1-6.

267) P. Rapta, A.A. Popov, S.F. Yang, L. Dunsch, *Charged states of Sc3N@C68: An in situ spectroelectrochemical study of the radical cation and radical anion of a non-IPR fullerene*, Journal of Physical Chemistry A 112 (2008) Nr. 26, S. 5858-5865.

268) S. Rauschenbach, R. Vogelgesang, N. Malinowski, J.W. Gerlach, M. Benyoucef, G. Costantini, Z. Deng, N. Thontasen, K. Kern, *Electrospray ion beam deposition: Soft-landing and fragmentation of functional molecules at solid surfaces*, ACS nano 3 (2009) Nr. 10, S. 2901-2910.

269) E. Reich, T. Thersleff, R. Huehne, K. Iida, L. Schultz, B. Holzapfel, *Structural and pinning properties of Y2Ba4CuM0y (M = Nb,Zr)/YBa2Cu3O7-delta quasi-multilayers fabricated by off-axis pulsed laser deposition*, Superconductor Science and Technology 22 (2009) Nr. 10, S. 105004/1-7.

270) J. Richter, M. Haertel, D. Ihle, S.-L. Drechsler, *Thermodynamics of the frustrated ferromagnetic spin-1/2 Heisenberg chain*, Journal of Physics: Conference Series 145 (2009) Nr. 1, S. 12064/1-4.

271) T. Riedl, T. Gemming, K. Doerr, M. Luysberg, K. Wetzig, *Mn valency at La0.7Sr0.3MnO3/SrTiO3 (0 0 1) thin film interfaces*, Microscopy and Microanalysis 15 (2009), S. 213-221.

272) T. Riedl, T. Gemming, T. Weissbach, G. Seifert, E. Gutmann, M. Zschornack, D.C. Meyer, S. Gemming, *ELNES study of chemical solution deposited Sr0(SrTiO3)n Ruddlesden–Popper films: experiment and simulation*, Ultramicroscopy 110 (2009) Nr. 1, S. 26-32.

273) M.O. Rikel, D. Isfort, M. Klein, J. Ehrenberg, J. Bock, E.D. Specht, M. Sun-Wagener, O. Weber, D. Sporn, S. Engel, O. de Haas, R. Semerad, M. Schubert, B. Holzapfel, *Simplified procedure for estimating epitaxy of La2Zr2O7-buffered NiW RABITS using XRD*, IEEE Transactions on Applied Superconductivity 19 (2009) Nr. 3, S. 3307-3310.

274) M. D. Riktor, S. Deledda, M. Herrich, O. Gutfleisch, H. Fjellvag, B. C. Hauback, *Hydride formation in ball-milled and cryomilled Mg–Fe powder mixtures*, Materials Science and Engineering B 158 (2009) Nr. 1-3, S. 19-25.

275) J.T. Robinson, A. Rastelli, O. Schmidt, O.D. Dubon, *Global faceting behavior of strained Ge islands on Si*, Nanotechnology 20 (2009) Nr. 8, S. 85708/1-6.

276) S. Roessler, S. Harikrishnan, C.M. Naveen Kumar, H.L. Bhat, S. Elizabeth, U.K. Roessler, F. Steglich, S. Wirth, *Phase transition and anomalous low temperature ferromagnetic phase in Pr0.6Sr0.4MnO3 single crystals*, Journal of Superconductivity and Novel Magnetism 22 (2009), S. 205-208.

277) C. Rongeat, C. Geipel, I. Llamas-Jansa, L. Schultz, O. Gutfleisch, *Influence of the dopant during the one step mechano-chemical synthesis of sodium alanate*, Journal of Physics: Conference Series 144 (2009) Nr. 1, S. 12022/1-4.

278) C. Rongeat, I. Llamas Jansa, S. Oswald, L. Schultz, O. Gutfleisch, *Mechanochemical synthesis and XPS analysis of sodium alanate with different additives*, Acta Materialia 57 (2009), S. 5563-5570.

279) H. Rosner, M. Schmitt, D. Kasinathan, A. Ormeci, J. Richter, S.-L. Drechsler, M.D. Johannes, *Comment on "Electronic structure of spin-1/2 Heisenberg antiferromagnetic systems: Ba2Cu(PO4)2 and Sr2Cu(PO4)2"*, Physical Review B 79 (2009) Nr.12, S. 127101/1-3.

280) A. Rother, T. Gemming, H. Lichte, *The statistics of the thermal motion of the atoms during imaging process in transmission electron microscopy and related techniques*, Ultramicroscopy 109 (2009) Nr. 2, S. 139-146.

281) M.H. Ruemmeli, D.B. Adebimpe, E. Borowiak-Palen, T. Gemming, P. Ayala, N. Ioannides, T. Pichler, A. Huczko, S. Cudzilo, M. Knupfer, B. Buechner, *Hydrogen activated axial inter-conversion in SiC nanowires*, Journal of Solid State Chemistry 182 (2009) Nr. 3, S. 602-607.

282) M.H. Ruemmeli, F. Schaeffel, A. Bachmatiuk, G. Trotter, D. Adebimpe, G. Simha-Martynkova, D. Placha, B. Rellinghaus, P.G. McCormick, E. Borowiak-Palen, P. Ayala, T. Pichler, R. Klingeler, M. Knupfer, B. Buechner, *Oxide catalysts for carbon nanotube and few layer graphene formation*, Physica Status Solidi B 246 (2009) Nr. 11-12, S. 2530-2533.

283) M. Samsel-Czekala, *Electronic structure and Fermi surface of strongly ferromagnetic U2N2Z-type (Z=Sb,Te,Bi) compounds from first principles*, Physical Review B 80 (2009) Nr. 4, S. 45121/1-10.

284) A. Sarapulova, D. Mikhailova, A. Senyshyn, H. Ehrenberg, *Crystal structure and magnetic properties of Li,Cr-containing molybdates Li3Cr(MoO4)3, LiCr(MoO4)2 and Li1.8Cr1.2(MoO4)3*, Journal of Solid State Chemistry 182 (2009) Nr. 12, S. 3262-3268.

285) F. Schaeffel, C. Taeschner, M.H. Ruemmeli, V. Neu, U. Wolff, U. Queitsch, D. Pohl, R. Kaltofen, A. Leonhardt, B. Rellinghaus, B. Buechner, L. Schultz, *Carbon nanotubes terminated with hard magnetic FePt nanomagnets*, Applied Physics Letters 94 (2009) Nr. 19, S. 193107/1-3.

286) F. Schaeffel, J.H. Warner, A. Bachmatiuk, B. Rellinghaus, B. Buechner, L. Schultz, M.H. Ruemmeli, *Shedding light on the crystallographic etching of multi-layer graphene at the atomic scale*, Nano Research 2 (2009), S. 695-705.

287) F. Schaeffel, J.H. Warner, A. Bachmatiuk, B. Rellinghaus, B. Buechner, L. Schultz, M.H. Ruemmeli, *On the catalytic hydrogenation of graphite for graphene nanoribbon fabrication*, Physica Status Solidi B 246 (2009) Nr. 11-12, S. 2540-2544.

288) U. Schaufuss, V. Kataev, A.A. Zvyagin, B. Buechner, J. Sichelschmidt, J. Wykhoff, C. Krellner, C. Geibel, F. Steglich, *Evolution of the Kondo State of YbRh2Si2 Probed by High-Field ESR*, Physical Review Letters 102 (2009) Nr. 7, S. 76405/1-3.

289) S. Scheinert, G. Paasch, *Interdependence of contact properties and field- and density-dependent mobility in organic field-effect transistors*, Journal of Applied Physics 105 (2009) Nr. 1, S. 14509/1-9.

290) O.G. Schmidt, *Nanoroehrchen: Von aufgerollten Teppichen und Mikroraketen*, Welt der Physik - Internet-Portal, online only (2009).

291) O.G. Schmidt, *Antrieb fuer Nanoraketen*, Spektrum der Wissenschaft Juli (2009), S. 16-20.

292) M. Schmitt, O. Janson, M. Schmidt, S. Hoffmann, W. Schnelle, S.-L. Drechsler, H. Rosner, *Crystal-water-induced switching of magnetically active orbitals in CuCl2*, Physical Review B 79 (2009) Nr. 24, S. 245119/1-5.

293) M. Schmitt, J. Malek, S.-L. Drechsler, H. Rosner, *Electronic structure and magnetic properties of Li2ZrCuO4: A spin-1/2 Heisenberg system close to a quantum critical point*, Physical Review B 80 (2009) Nr. 20, S. 205111/1-9.

294) M. Schneider, G. Fuchs, K.-H. Mueller, K. Nenkov, G. Behr, D. Souptel, S.-L. Drechsler, *Magnetic pair breaking in superconducting HoNi2B2C studied on a single crystal by thermal conductivity in magnetic fields*, Physical Review B 80 (2009) Nr. 22, S. 224522/1-6.

295) S. Scholz, Q. Huang, M. Thomschke, S. Olthof, P. Sebastian, K. Walzer, K. Leo, S. Oswald, C. Corten, D. Kuckling, *Self-doping and partial oxidation of metal-on-organic interfaces for organic semiconductor devices studied by chemical analysis techniques*, Journal of Applied Physics 104 (2008) Nr. 10, S. 104502/1-10.

296) R. Schuster, R. Kraus, M. Knupfer, H. Berger, B. Buechner, *Negative plasmon dispersion in the transition-metal dichalcogenide 2H-TaSe2*, Physical Review B 79 (2009) Nr. 4, S. 45134/1-5.

297) R. Schuster, S. Pyon, M. Knupfer, J. Fink, M. Azuma, M. Takano, H. Takagi, B. Buechner, *Charge-transfer excitons in underdoped Ca2-xNaxCu02Cl2 studied by electron energy-loss spectroscopy*, Physical Review B 79 (2009) Nr. 21, S. 214517/1-4.

298) S. Scudino, B. Bartusch, J. Eckert, *Viscosity of the supercooled liquid in multi-component Zr-based metallic glasses*, Journal of Physics: Conference Series 144 (2009) Nr. 1, S. 12097/1-4.

299) S. Scudino, P. Donnadieu, K.B. Surreddi, K. Nikolowski, M. Stoica, J. Eckert, *Microstructure and mechanical properties of Laves phase-reinforced Fe-Zr-Cr alloys*, Intermetallics 17 (2009) Nr. 7, S. 532-539.

300) S. Scudino, G. Liu, K.G. Prashanth, B. Bartusch, K.B. Surreddi, B.S. Murty, J. Eckert, *Mechanical properties of Al-based metal matrix composites reinforced with Zr-based glassy particles produced by powder metallurgy*, Acta Materialia 57 (2009) Nr. 6, S. 2029-2039.

301) S. Scudino, G. Liu, M. Sakaliyska, K.B. Surreddi, J. Eckert, *Powder metallurgy of Al-based metal matrix composites reinforced with beta - Al3Mg2 intermetallic particles: Analysis and modeling of mechanical properties*, Acta Materialia 57 (2009), S. 4529-4538.

302) S. Scudino, M. Sakaliyska, K.B. Surreddi, J. Eckert, *Mechanical alloying and milling of Al-Mg alloys*, Journal of Alloys and Compounds 483 (2009) Nr. 1-2, S. 2-7.

303) S. Scudino, M. Sakaliyska, K.B. Surreddi, J. Eckert, *Solid-state processing of Al-Mg alloys*, Journal of Physics: Conference Series 144 (2009), S. 12019/1-4.

304) S. Scudino, K.B. Surreddi, H.V. Nguyen, G. Liu, T. Gemming, M. Sakaliyska, J.S. Kim, J. Vierke, M. Wollgarten, J. Eckert, *High-strength Al87Ni8La5 bulk alloy produced by spark plasma sintering of gas atomized powders*, Journal of Materials Research 24 (2009) Nr. 9, S. 2909-2916.

305) S. Scudino, S. Venkataraman, M. Stoica, K.B. Surreddi, S. Pauly, J. Das, J. Eckert, *Consolidation and mechanical properties of ball milled Zr50Cu50 glassy ribbons*, Journal of Alloys and Compounds 483 (2009) Nr. 1-2, S. 227-230.

306) A. Sebetci, *Does spin - orbit coupling effect favor planar structures for small platinum clusters?*, Physical Chemistry Chemistry Physics 11 (2009), S. 921-925.

307) M. Seifert, V. Neu, L. Schultz, *Epitaxial SmCo5 thin films with perpendicular anisotropy*, Applied Physics Letters 94 (2009) Nr. 2, S. 22501/1-3.

308) M. Seifert, L. Schultz, V. Neu, *Magnetization processes and spin reorientation in epitaxial NdCo5±x thin films*, Journal of Applied Physics 106 (2009) Nr. 7, S. 73915/1-5.

309) A. Senyshyn, D.M. Trots, J.M. Engel, L. Vasylechko, H. Ehrenberg, T. Hansen, M. Berkowski, H. Fuess, *Anomalous thermal expansion in rare-earth gallium perovskites: a comprehensive powder diffraction study*, Journal of Physics / Condensed Matter 21 (2009) Nr. 14, S. 145405/1-4.

310) H. Shiozawa, C. Kramberger, M. Ruemmeli, D. Batchelor, H. Kataura, T. Pichler, S.R.P. Silva, *Electronic properties of single-walled carbon nanotubes encapsulating a cerium organometallic compound*, Physica Status Solidi B 246 (2009) Nr. 11-12, S. 2626-2630.

311) H. Shiozawa, T. Pichler, C. Kramberger, M. Ruemmeli, D. Batchelor, Z. Liu, K. Suenaga, H. Kataura, S.R.P. Silva, *Screening the missing electron: nanochemistry in action*, Physical Review Letters 102 (2009) Nr. 4, S. 46804/1-4.

312) T. Shirakawa, S. Nishimoto, Y. Ohta, H. Fukuyama, *Disorder and superconductivity in doped semiconductor nanotubes*, Journal of Physics: Conference Series 150 (2009), S. 52238/1-4.

313) O. Shuleshova, D. Holland-Moritz, H.G. Lindenkreuz, W. Loeser, B. Buechner, *Phase selection in undercooled Ti-Al-Nb melts*, Journal of Physics: Conference Series 144 (2009) Nr. 1, S. 12118/1-4.

314) O. Shuleshova, D. Holland-Moritz, W. Loeser, H.-G. Lindenkreuz, B. Buechner, *In situ observation of phase selection in undercooled Ni-Al melts*, International Journal of Cast Metals Research 22 (2009) Nr. 1-4, S. 286-289.

315) O. Shuleshova, D. Holland-Moritz, W. Loeser, G. Reinhart, G.N. Iles, B. Buechner, *Metastable formation of decagonal quasicrystals during solidification of undercooled Al-Ni melts: In situ observations by synchrotron radiation*, epl 86 (2009) Nr. 3, S. 36002/1-4.

316) A. Singh, V. Neu, S. Faehler, K. Nenkov, L. Schultz, B. Holzapfel, *Relevance of pinning, nucleation, and interaction in nanograined epitaxial hard magnetic SmCo5 films*, Physical Review B 79 (2009) Nr. 21, S. 214401/1-8.

317) G.P. Singh, S. Ram, J. Eckert, H.-J. Fecht, *Synthesis and morphological stability in Cr02 single crystals of a half-metallic ferromagnetic compound*, Journal of Physics: Conference Series 144 (2009) Nr. 1, S. 12110/1-4.

318) N.K. Singh, P. Kumar, Z. Mao, D. Paudyal, V. Neu, K.G. Suresh, V.K. Pecharsky, K.A. Gschneidner, *Magnetic, magnetocaloric and magnetoresistance properties of Nd7Pd3*, Journal of Physics / Condensed Matter 21 (2009) Nr. 45, S. 4560004/1-5.

319) E.P. Smirnova, A.V. Sotnikov, H. Schmidt, N.V. Zaitseva, M. Weihnacht, *Phase transitions and dielectric relaxation in (1 - x)SrTi03-xBiFe03 (0 = x = 0.04)*, Physics of the Solid State 51 (2009) Nr. 12, S. 2492-2496.

320) E.J. Smith, Z. Liu, Y.F. Mei, O.G. Schmidt, *System investigation of a rolled-up metamaterial optical hyperlens structure*, Applied Physics Letters 95 (2009) Nr. 8, S. 83104/1-3.

321) Z. Sniadecki, U.K. Roessler, B. Idzikowski, *Activation energies of crystallization in amorphous RMn4.5Ge4.5Fe1.5Al1.5 (R = La, Y, Dy) alloys*, Acta Physica Polonica A 115 (2009) Nr. 1, S. 409-412.

322) R. Solc, V. Lukes, P. Rapta, H. Hartmann, L. Dunsch, *Structural changes in 2-diarylthiophene-substituted starburst compounds upon charging: A theoretical and spectroelectrochemical study*, ChemPhysChem 9 (2008) Nr. 17, S. 2501-2509.

323) R. Solc, V. Lukes, M. Ilcin, P. Rapta, M. Zalibera, L. Dunsch, *Semiempirical molecular dynamics study of empty C2(3)-C82 fullerene in neutral and charged forms: Geometrical and spectroscopic characterization*, Journal of Physical Chemistry C 113 (2009) Nr. 45, S. 19658-19663.

324) A.A. Solovev, Y. Mei, E. Bermudez Urena, G. Huang, O.G. Schmidt, *Catalytic microtubular jet engines self-propelled by accumulated gas bubbles*, Small 5 (2009) Nr. 14, S. 1688-1692.

325) A.V. Sotnikov, R. Kunze, H. Schmidt, M. Weihnacht, M. Hengst, J. Goetze, *Piezilectric and elastic properties of Sr3NbGa3Si2O14 (SNGS) single crystals*, Physics of the Solid State 51 (2009) Nr. 2, S. 275-279.

326) V.C. Srivastava, K.B. Surreddi, S. Scudino, M. Schowalter, V. Uhlenwinkel, A. Schulz, A. Rosenauer, H.-W. Zoch, J. Eckert, *Spray forming of bulk Al85Y8Ni5Co2 with co-existing amorphous, nano- and micro-crystalline structures*, Transactions of The Indian Institute of Metals 62 (2009) Nr. 4-5, S. 331-335.

327) V.C. Srivastava, K.B. Surreddi, V. Uhlenwinkel, A. Schulz, J. Eckert, H.-W. Zoch, *Formation of nanocrystalline matrix composite during spray forming of Al83La5Y5Ni5Co2*, Metallurgical and Materials Transactions A 40 (2009) Nr. 2, S. 450-461.

328) M. Stangl, M. Liptak, J. Acker, V. Hoffmann, S. Baunack, K. Wetzig, *Influence of incorporated non-metallic impurities on electromigration in copper damascene interconnect lines*, Thin Solid Films 517 (2009), S. 2687-2690.

329) M. Stoffel, A. Malachias, A. Rastelli, T.H. Metzger, O.G. Schmidt, *Composition and strain in SiGe/Si(001) ìnanoringsî revealed by combined x-ray and selective wet chemical etching methods*, Applied Physics Letters 94 (2009) Nr. 25, S. 253114/1-3.

330) M. Stoica, M. Emmi, S. Ram, A. Wiedenmann, O. Perroud, J. Eckert, *Microstructure and magnetic properties of binary Nd80Fe20 with Ga additions*, Journal of Physics: Conference Series 144 (2009) Nr. 1, S. 12103/1-4.

331) M. Stoica, S. Kumar, S. Roth, S. Ram, J. Eckert, G. Vaughan, A.R. Yavari, *Crystallization kinetics and magnetic properties of Fe66Nb4B30 bulk metallic glass*, Journal of Alloys and Compounds 483 (2009) Nr. 1-2, S. 632-637.

332) S. Strehle, J.W. Bartha, K. Wetzig, *Electrical properties of electroplated Cu(Ag) thin films*, Thin Solid Films 517 (2009) Nr. 11, S. 3320-3325.

333) S. Strehle, S. Menzel, A. Jahn, U. Merkel, J.W. Bartha, K. Wetzig, *Electromigration in electroplated Cu(Ag) alloy thin films investigated by means of single damascene Blech structures*, Microelectronic Engineering 86 (2009) Nr. 12, S. 2396-2403.

334) S.Y. Suck, V. Neu, U. Wolff, S. Bahr, O. Bourgeois, D. Givord, *Magnetic force microscopy analysis of magnetization reversal in exchange-biased Co/CoO nanostructure arrays*, Applied Physics Letters 95 (2009) Nr. 16, S. 162503/1-3.

335) R. Sueptitz, J. Koza, M. Uhlemann, A. Gebert, L. Schultz, *Magnetic field effect on the anodic behaviour of a ferromagnetic electrode in acidic solutions*, Electrochimica Acta 54 (2009) Nr. 8, S. 2229-2233.

336) K.B. Surreddi, S. Scudino, H.V. Nguyen, K. Nikolowski, M. Stoica, M. Sakaliyska, J.S. Kim, T. Gemming, J. Vierke, M. Wollgarten, J. Eckert, *Spark plasma sintering of gas atomized Al87Ni8La5 amorphous powder*, Journal of Physics: Conference Series 144 (2009), S. 12079/1-5.

337) J. Tarabek, L. Kavan, L. Dunsch, M. Kalbac, *Chemical states of electrochemically doped single wall carbon nanotubes as probed by raman spectroelectrochemistry and ex situ x-ray photoelectron spectroscopy*, Journal of Physical Chemistry C 112 (2008) Nr. 36, S. 13856-13861.

338) J. Tarabek, S. Yang, L. Dunsch, *Redox properties of mixed lutetium/ yttrium nitride clusterfullerenes: Endohedral LuxY3xN@C80(I) (x=0–3) compounds*, ChemPhysChem 10 (2009), S. 1037-1043.

339) M. Taut, *Distortion of wigner molecules: a pair function approach*, Journal of Physics : Condensed Matter 21 (2009) Nr. 7, S. 75302/1-10.

340) M. Taut, P. Machon, H. Eschrig, *Violation of noninteracting ypsilon-representability of the exact solutions of the Schrödinger equation for a two-electron quantum dot in a homogeneous magnetic field*, Physical Review A 80 (2009) Nr. 2, S. 22517/1-8.

341) A. Taylor, K. Lipert, K. Kraemer, S. Hampel, S. Fuessel, A. Meye, R. Klingeler, M. Ritschel, A. Leonhardt, B. Buechner, M.P. Wirth, *Biocompatibility of iron filled carbon nanotubes in vitro*, Journal of Nanoscience and Nanotechnology 9 (2009) Nr. 10, S. 5709-5716.

342) A. Teresiak, M. Uhlemann, A. Gebert, J. Thomas, J. Eckert, L. Schultz, *Formation of nanostructured LaMg2Ni by rapid quenching and intensive milling and its hydrogen reactivity*, Journal of Alloys and Compounds 481 (2009) Nr. 1-2, S. 144-151.

343) A. Teresiak, M. Uhlemann, J. Thomas, A. Gebert, *The metastable Mg6Ni phase - Thermal behaviour, crystal structure and hydrogen reactivity of the rapidly quenched alloy*, Journal of Alloys and Compounds 475 (2009) Nr. 1-2, S. 191-197.

344) B. Terziyska, I. Bivas, K. Nenkov, *Modeling of low-temperature specific heat data for Ge27As13S60 and As40S60 glasses by means of the phenomenologically modified soft potential model*, Cryogenics 49 (2009) Nr. 5, S. 171-175.

345) S. Tetali, M. Zaka, R. Schoenfelder, A. Bachmatiuk, F. Boerrnert, I. Ibrahim, J.H. Lin, G. Cuniberti, J.H. Warner, B. Buechner, M.H. Ruemmeli, *Unravelling the mechanisms behind mixed catalysts for the high yield production of single-walled carbon nanotubes*, ACS nano 3 (2009) Nr. 12, S. 3839-3844.

346) J. Thomas, J. Schumann, H. Vinzelberg, E. Arushanov, R. Engelhard, O.G. Schmidt, T. Gemming, *Epitaxial Fe3Si films on GaAs(100) substrates by means of electron beam evaporation*, Nanotechnology 20 (2009) Nr. 23, S. 235604/1-9.

347) M. Thomas, O. Heczko, J. Buschbeck, Y.W. Lai, J. McCord, S. Kaufmann, L. Schultz, S. Faehler, *Stray-field-induced actuation of free-standing magnetic shape-memory films*, Advanced Materials 21 (2009) Nr. 36, S. 3708-3711.

348) F. Thoss, M. Poetschke, U. Gaitzsch, J. Freudenberger, W. Anwand, S. Roth, B. Rellinghaus, L. Schultz, *Grain growth in Ni–Mn–Ga alloys*, Journal of Alloys and Compounds 488 (2009) Nr. 1, S. 420-424.

349) J. Torrens-Serra, P. Bruna, S. Roth, J. Rodriguez-Viejo, M.T. Clavaguera-Mora, *Bulk soft magnetic materials from ball-milled Fe77Nb7B15Cu1 amorphous ribbons*, Intermetallics 17 (2009) Nr. 1, S. 79-85.

350) M. Treier, P. Ruffieux, R. Fasel, F. Nolting, S. Yang, L. Dunsch, T. Greber, *Looking inside an endohedral fullerene: Inter- and intramolecular ordering of Dy3N@C80 (Ih) on Cu(111)*, Physical Review B 80 (2009) Nr. 8, S. 81403/1-4.

351) K. Tschulik, J.A. Koza, M. Uhlemann, A. Gebert, L. Schultz, *Effects of well-defined magnetic field gradients on the electrodeposition of copper and bismuth*, Electrochemistry Communications 11 (2009), S. 2241-2244.

352) G. Urbanik, T. Haenke, C. Hess, B. Buechner, A. Ciszewski, V. Hinkov, C.T. Lin, B. Keimer, *Surface of underdoped YBa2Cu3O7-delta as revealed by STM/STS*, The European Physical Journal B 69 (2009) Nr. 4, S. 483-489.

353) E.B. Urena, Y. Mei, E. Coric, D. Makarov, M. Albrecht, O.G. Schmidt, *Fabrication of ferromagnetic rolled-up microtubes for magnetic sensors on fluids*, Journal of Physics D 42 (2009) Nr. 5, S. 55001/1-8.

354) E. Vavilova, A.S. Moskvin, Y.C. Arango, A. Sotnikov, S.-L. Drechsler, R. Klingeler, O. Volkova, A. Vasiliev, V. Kataev, B. Buechner, *Quantum electric dipole glass and frustrated magnetism near a critical point in Li2ZrCu04*, epl 88 (2009) Nr. 2, S. 27001/1-6.

355) O.S. Volkova, I.GV. Morozov, E.A. Lapsheva, V.V. Shutov, A.N. Vasilev, R. Klingeler, B. Buechner, *Long-range magnetic order in copper nitrate monohydrate Cu(N03)2∑ H20*, JETP Letters 89 (2009) Nr. 2, S. 88-91.

356) T. Waechtler, S. Oswald, N. Roth, A. Jakob, H. Lang, R. Ecke, S.E. Schulz, T. Gessner, A. Moskvinova, S. Schulze, M. Hietschold, *Copper oxide films grown by atomic layer deposition from Bis(tri-n-butylphosphane)copper(I)acetylacetonate on Ta, TaN, Ru, and Si02*, Journal of the Electrochemical Society 156 (2009) Nr. 6, S. H453-H459.

357) G. Wang, N. Mattern, S. Pauly, J. Bednarcik, J. Eckert, *Atomic structure evolution in bulk metallic glass under compressive stress*, Applied Physics Letters 95 (2009) Nr. 25, S. 251906/1-3.

358) L. Wang, U. Koehler, N. Leps, A. Kondrat, M. Nale, A. Gasparini, A. de Visser, G. Behr, C. Hess, R. Klingeler, B. Buechner, *Thermal expansion of LaFeAs01-xFx: Evidence for high-temperature fluctuations*, Physical Review B 80 (2009) Nr. 9, S. 94512/1-5.

359) L. Wang, V. Krapek, F. Ding, F. Horton, A. Schliwa, D. Bimberg, A. Rastelli, O.G. Schmidt, *Self-assembled quantum dots with tunable thickness of the wetting layer: role of vertical confinement on interlevel spacing*, Physical Review B 80 (2009) Nr. 8, S. 85309/1-9.

360) L. Wang, A. Rastelli, S. Kiravittaya, M. Benyoucef, O.G. Schmidt, *Self-assembled quantum dot molecules*, Advanced Materials 21 (2009) Nr. 25-26, S. 2601-2618.

361) W.-M. Wang, W.X. Zhang, A. Gebert, S. Roth, C. Mickel, L. Schultz, *Microstructure and magnetic properties in Fe61Co9xZr8Mo5WxB17 glasses and glass-matrix composites*, Metallurgical and Materials Transactions A 40 (2009) Nr. 3, S. 511-521.

362) J.H. Warner, Y. Ito, M.H. Ruemmeli, B. Buechner, H. Shinohara, G.A.D. Briggs, *Capturing the motion of molecular nanomaterials encapsulated within carbon nanotubes with ultrahigh temporal resolution*, ACS nano 3 (2009) Nr. 10, S. 3037-3044.

363) J.H. Warner, Y. Ito, M.H. Ruemmeli, T. Gemming, B. Buechner, H. Shinohara, G.A.D. Briggs, *One-dimensional confined motion of single metal atoms inside double-walled carbon nanotubes*, Physical Review Letters 102 (2009) Nr. 19, S. 195504/1-4.

364) J.H. Warner, M.H. Ruemmeli, L. Ge, T. Gemming, B. Montanari, N.M. Harrison, B. Buechner, G.A.D. Briggs, *Structural transformations in graphene studied with high spatial and temporal resolution*, Nature naotechnology 4 (2009) Nr. 8, S. 500-504.

365) J.H. Warner, M.H. Ruemmeli, T. Gemming, B. Buechner, G.A.D. Briggs, *Direct imaging of rotational stacking faults in few layer graphene*, Nanoletters 9 (2009) Nr. 1, S. 102-106.

366) J.H. Warner, F. Schaeffel, M.H. Ruemmeli, B. Buechner, *Examining the edges of multi-layer graphene sheets*, Chemistry of Materials 21 (2009) Nr. 12, S. 2418-2421.

367) J.H. Warner, F. Schaeffel, G. Zhong, M.H. Ruemmeli, B. Buechner, J. Robertson, G.A.D. Briggs, *Investigating the diameter-dependent stability of single-walled carbon nanotubes*, ACS Nano 3 (2009) Nr. 6, S. 1557-1563.

368) Y.J. Wei, H. Ehrenberg, K.B. Kim, C.W. Park, Z.F. Huang, C. Baehtz, *Characterizations on the structural and electronic properties of thermal lithiated Li0.33Mn02*, Journal of Alloys and Compounds 470 (2009) Nr. 1-2, S. 273-277.

369) Y.J. Wei, K. Nikolowski, S.Y. Zhan, H. Ehrenberg, S. Oswald, G. Chen, C.Z. Wang, H. Chen, *Electrochemical kinetics and cycling performance of nano Li[Li0.23Co0.3Mn0.47]02 cathode material for lithium ion batteries*, Electrochemistry Communications 11 (2009) Nr. 10, S. 2008-2011.

370) Z. Weiss, E.B.M. Steers, P. Smid, V. Hoffmann, *Towards a catalogue of glow discharge emission spectra*, Journal of Analytical Atomic Spectrometry 24 (2009) Nr. 1, S. 27-33.

371) T. Weissbach, T. Leisegang, A. Kreyssig, M. Frontzek, J.-U. Hoffmann, D. Souptel, A. Koehler, G. Behr, P. Paufler, D.C. Meyer, *Intergrowth of several solid phases from the Y-Ni-B-C system in a large YNi2B2C crystal*, Journal of Applied Crystallography 41 (2008) Nr. 4, S. 738-746.

372) U. Weissker, M. Loeffler, F. Wolny, M.U. Lutz, N. Scheerbaum, R. Klingeler, T. Gemming, T. Muehl, A. Leonhardt, B. Buechner, *Perpendicular magnetization of long iron carbide nanowires inside carbon nanotubes due to magnetocrystalline anisotropy*, Journal of Applied Physics 106 (2009) Nr. 5, S. 54909/1-5.

373) P. Wisniewski, N. Kozlova, J. Freudenberger, Z. Henkie, *High-field magnetisation and magnetoresistance of U3P4 and its solid solution U3(P,As)4*, Acta Physica Polonica A 115 (2009) Nr. 1, S. 254-256.

374) N. Wizent, G. Behr, F. Lipps, I. Hellmann, R. Klingeler, V. Kataev, W. Loeser, N. Sato, B. Buechner, *Single-crystal growth of LiMnPO4 by the floating-zone method*, Journal of Crystal Growth 311 (2009) Nr. 5, S. 1273-1277.

375) N. Wizent, L. Schramm, G. Behr, W. Loeser, W. Gruner, A. Voss, B. Buechner, L. Schultz, *Phase diagram features and solidification behaviour of CoCu203 at elevated oxygen pressure*, Journal of Solid State Chemistry 182 (2009), S. 2036-2040.

376) M. Wolf, R. Schaefer, J. McCord, *Precessional frequency of ferromagnetic elements: influence of magnetic domain width*, Journal of Magnetism and Magnetic Materials 321 (2009) Nr. 18, S. 2920–2924.

377) T.G. Woodcock, K. Khlopkov, A. Walther, N.M. Dempsey, D. Givord, L. Schultz, O. Gutfleisch, *Interaction domains in high-performance NdFeB thick films*, Scripta Materialia 60 (2009), S. 826-829.

378) F.F. Wu, Z.F. Zhang, S.X. Mao, J. Eckert, *Effect of sample size on ductility of metallic glass*, Philosophical Magazine Letters 89 (2009) Nr. 3, S. 178-184.

379) R. Xiao, D. Fritsch, M.D. Kuzmin, K. Koepernik, H. Eschrig, M. Richter, K. Vietze, G. Seifert, *Co dimers on hexagonal carbon rings proposed as subnanometer magnetic storage bits*, Physical Review Letters 103 (2009) Nr. 18, S. 187201/1-4.

380) W. Xu, X. Wu, M. Calin, M. Stoica, J. Eckert, K. Xia, *Formation of an ultrafine-grained structure during equal-channel angular pressing of a beta-titanium alloy with low phase stability*, Scripta Materialia 60 (2009) Nr. 11, S. 1012-1015.

381) W. Xu, X. Wu, R.B. Figueiredo, M. Stoica, M. Calin, J. Eckert, T.G. Langdon, K. Xia, *Nanocrystalline body-centred cubic beta-titanium alloy processed by high-pressure torsion*, International Journal of Materials Research 100 (2009) Nr. 12, S. 1662-1667.

382) Y.D. Yagodkin, J.V. Lyubina, *Hard magnetic materials, Part 2: Structure and properties of oxide containing alloys*, Metallovedenie i Termiceskaja Obrabotka Metallov (2009) Nr. 2, S. 3-9.

383) Y.D. Yagodkin, J.V. Lyubina, *Hard magnetic materials, Part 1: Structure and properties of alloys based on the Nd2Fe14B and FePt compounds*, Metallovedenie i Termiceskaja Obrabotka Metallov (2009) Nr. 1, S. 27-34.

384) S.F. Yang, A.A. Popov, L. Dunsch, *Carbon pyramidalization in fullerene cages induced by the endohedral cluster: Non-scandium mixed metal nitride clusterfullerenes*, Angewandte Chemie - International Edition 47 (2008) Nr. 43, S. 8196-8200.

385) S. Yang, A.A. Popov, L. Dunsch, *Large mixed metal nitride clusters encapsulated in a small cage: the confinement of the C68-based clusterfullerenes*, Chemical Communications 4 (2008) Nr. 25, S. 2885-2887.

386) S. Yang, A.A. Popov, C. Chen, L. Dunsch, *Mixed metal nitride clusterfullerenes in cage isomers: LuxSc3-xN@C80 (x = 1, 2) as compared with MxSc3-xN@C80 (M = Er, Dy, Gd, Nd)*, Journal of Physical Chemistry C 113 (2009) Nr. 18, S. 7616-7623.

387) X. Yang, K. Eckert, S. Muehlenhoff, M. Uhlemann, S. Odenbach, *Pulse magnetoelectrolysis*, Electrochemistry Communications 11 (2009), S. 318-322.

388) L.L. Ying, Z.Y. Liu, Y.M. Lu, B. Gao, F. Fan, J.L. Liu, C.B. Cai, T. Thersleff, S. Engel, R. Huehne, B. Holzapfel, *Epitaxial growth of La2Zr207 buffer layers for YBa2Cu307-delta coated conductors on metallic substrates using pulsed laser deposition*, Physica C 469 (2009), S. 288-292.

389) E.R. Ylvisaker, W.E. Pickett, K. Koepernik, *Anisotropy and magnetism in the LSDA+U method*, Physical Review B 79 (2009) Nr. 3, S. 35103/1-3.

390) Y. Yokoyama, E. Mund, A. Inoue, L. Schultz, *Cap casting and enveloped casting techniques for Zr55Cu30Ni5Al10 glassy alloy rod with 32 mm in diameter*, Journal of Physics: Conference Series 144 (2009) Nr. 1, S. 12043/1-4.

391) V.B. Zabolotnyy, D.V. Evtushinsky, A.A. Kordyuk, D.S. Inosov, A. Koitzsch, A.V. Boris, G.L. Sun, C.T. Lin, M. Knupfer, B. Buechner, A. Varykhalov, R. Follath, S.V. Borisenko, *Fermi surface of Ba1-xKxFe2As2 as probed by angle-resolved photoemission*, Physica C 469 (2009), S. 448-451.

392) V.B. Zabolotnyy, D.S. Inosov, D.V. Evtushinsky, A. Koitzsch, A.A. Kordyuk, G.L. Sun, J.T. Park, D. Haug, V. Hinkov, A.V. Boris, C.T. Lin, M. Knupfer, A.N. Yaresko, B. Buechner, A. Varykhalov, R. Follath, S.V. Borisenko, *(pi, pi) electronic order in iron arsenide superconductors*, Nature 457 (2009), S. 569-572.

393) V.B. Zabolotnyy, A.A. Kordyuk, D.S. Inosov, D.V. Evtushinsky, R. Schuster, B. Buechner, N. Wizent, G. Behr, S. Pyon, T. Takayama, H. Takagi, R. Follath, S.V. Borisenko, *Evidence for fermi surface reconstruction in the static stripe phase of La1.8-xEu0.2SrxCu04, x = 1/8*, epl 86 (2009), S. 47005/1-6.

394) G.S. Zakharova, V.L. Volkov, C. Taeschner, I. Hellmann, A. Leonhardt, R. Klingeler, B. Buechner, *Synthesis and characterization of V307H20 nanobelts*, Solid State Communications 149 (2009) Nr. 19-20, S. 814-817.

395) M. Zalibera, A. A. Popov, M. Kalbac, P. Rapta, D. Dunsch, *The extended view on the empty C2(3)-C82 fullerene: Isolation, spectroscopic, electrochemical, and spectroelectrochemical characterization and DFT calculations*, Chemistry - A European Journal 14 (2008) Nr. 32, S. 9960-9967

396) M. Zalibera, P. Rapta, L. Dunsch, *The power of in situ ESR spectroelectrochemistry in the analysis of a C84 fullerene isomer*, Electrochemistry Communications 10 (2008) Nr. 6, S. 943-946.

397) M. Zalibera, P. Rapta, A.A. Popov, L. Dunsch, *Charged states of four isomers of C84 fullerene: In situ ESR and Vis-NIR spectroelectrochemistry and DFT calculations*, Journal of Physical Chemistry C 113 (2009) Nr. 13, S. 5141-5149.

398) T. Zander, C. Deneke, A. Malachias, C. Mickel, T.H. Metzger, O.G. Schmidt, *Planar hybrid superlattices by compression of rolled-up nanomembranes*, Applied Physics Letters 94 (2009) Nr. 5, S. 53102/1-3.

399) T. Zander, A. Herklotz, S. Kiravittaya, M. Benyoucef, F. Ding, P. Atkinson, S. Kumar, J.D. Plumhof, K. Doerr, A. Rastelli, O.G. Schmidt, *Epitaxial quantum dots in stretchable optical microcavities*, Optics Express 17 (2009) Nr. 25, S. 22452-22461.

400) L.N. Zelenina, T.P. Chusova, N.I. Matskevich, V.N. Naumov, Y.G. Stenin, G. Krabbes, *Thermodynamic properties of Nd1+xBa2-x≠Cu3Oy compounds and their application for optimizing the synthesis of superconducting materials*, European Journal of Inorganic Chemistry (2009) Nr. 8, S. 1096-1102.

401) S.Y. Zhan, C.Z. Wang, K. Nikolowski, H. Ehrenberg, G. Chen, Y.J. Wei, *Electrochemical properties of Cr doped V2O5 between 3.8 V and 2.0 V*, Solid State Ionics 180 (2009), S. 1198-1203.

402) G.J. Zhang, R.H. Wang, S.P. Yuan, G. Liu, S. Scudino, J. Sun, K.H. Chen, *Influence of constituents on the ductile fracture of Al–Cu–Mg alloys: Modulated by the aging treatment*, Materials Science and Engineering: A 526 (2009), S. 171-176.

403) H. Zhang, M. Richter, K. Koepernik, I. Opahle, F. Tasnadi, H. Eschrig, *Electric-field control of surface magnetic anisotropy: a density functional approach*, New Journal of Physics 11 (2009) Nr. 4, S. 43007/1-8.

404) J.J. Zhang, A. Rastelli, H. Groiss, J. Tersoff, F. Schaeffler, O.G. Schmidt, G. Bauer, *Shaping site-controlled uniform arrays of SiGe/Si (001) islands by in situ annealing*, Applied Physics Letters 95 (2009) Nr. 18, S. 183102/1-3.

405) W. Zhang, K. Koepernik, M. Richter, H. Eschrig, *Magnetic phase transition in CoO under high pressure: A challenge for LSDA+U*, Physical Review B 79 (2009) Nr. 15, S. 155123/1-9.

406) J.X. Zhao, R.T. Qu, F.F. Wu, Z.F. Zhang, B.L. Shen, M. Stoica, J. Eckert, *Fracture mechanism of some brittle metallic glasses*, Journal of Applied Physics 105 (2009) Nr. 10, S. 103519/1-6.

407) R. Zinke, S.-L. Drechsler, J. Richter, *Influence of interchain coupling on spiral ground-state correlations in frustrated spin-1/2 J1-J2 Heisenberg chains*, Physical Review B 79 (2009) Nr. 9, S. 94425/1-9.

408) M. Zukalova, J. Tarabek, M. Kalbac, L. Kavan, L. Dunsch, *In situ optical spectroelectrochemistry of single-walled carbon nanotube thin films*, Journal of Solid State Electrochemistry 12 (2008) Nr. 10, S. 1279-1284

409) A.A. Zvyagin, V. Kataev, B. Buechner, *Theory of the electron spin resonance in heavy fermion systems with non-Fermi-liquid behavior*, Physical Review B 80 (2009) Nr. 2, S. 24412/1-7.

Contributions to Conference Proceedings and Monographs

1) M. Azam, N. Ioannides, M.H. Ruemmeli, I. Schagaev, *System software support for router fault tolerance*, in: Preprints of the 30th IFAC Workshop on Real-Time Programming and 4th International Workshop on Real-Time Software, 13-18 (2009).

2) S.V. Biryukov, H. Schmidt, M. Weihnacht, *Gyroscopic effect for SAW in common piezoelectric crystals*, 2009 IEEE International Ultrasonics Symposium, Rom/ Italy, 20.-23.9.09, in: Proceedings, CD-ROM, P2-0-10/1-4 (2009).

3) V. Biryukov, H. Schmidt, M. Weihnacht, *Performance of SAW ring waveguide resonator: 3D FEM and experiments*, 2009 IEEE International Ultrasonics Symposium, Rom/ Italy, 20.-23.9.09, in: Proceedings, CD-ROM, 5B-3/1-4 (2009).

4) A. Boehm, S. Roth, U. Gaitzsch, R. Chulist, W. Skrotzki, H. Kunze, W.-G. Drossel, R. Neugebauer, *Development status of Ni-Mn-Ga ferromagnetic shape memory polycrystals after hot rolling*, 11th International Conference and Exhibition on New Actuators and Drive Systems, Bremen, 9.-11.6.08, in: Proceedings, 742-745 (2008).

5) O.V. Boltalina, A.A. Popov, S.H. Strauss, *Physicochemical properties and the unusual structure of fullerenes: Single-crystal X-ray structures of fullerenes and their derivatives*, in: Strained Hydrocarbons: Beyond the van't Hoff and Le Bel Hypothesis. H. Dodzik (Ed.), Weinheim: Wiley-VCH, 2009, 225-238 (2009).

6) J. Chen, E. Louis, F. Bijkerk, C.J. Lee, H. Wormeester, R. Kunze, H. Schmidt, D. Schneider, R. Moors, W. v. Schaik, M. Lubomska, *Ellipsometric and surface acoustic wave sensing of carbon contamination on EUV optics*, in: Proceedings of SPIE, 7271, 727140 (2009).

7) A. Darinskii, M. Weihnacht, H. Schmidt, *SAW reflection from surface inhomogeneities of isotropic and anisotropic substrates*, 2009 IEEE International Ultrasonics Symposium, Rom/ Italy, 20.-23.9.09, in: Proceedings, CD-ROM, P1-R-01/1-4 (2009).

8) K. Eckert, X. Yang, S. Muehlenhoff, M. Uhlemann, S. Odenbach, *Pulse magnetoelectrolysis. principles and perspectives*, 6th International Conference on Electromagnetic Processing of Materials, EPM 2009, Dresden, 19.-23.10.09, in: Proceedings, 443-446 (2009).

9) J. Freudenberger, J. Goellner, M. Heilmaier, G. Mook, H. Saage, V. Srivastava, U. Wendt, *Materials science and technology*, in: Springer Handbook of Mechanical Engineering, K.-H. Grote; E.K. Antonsson (eds.), Heidelberg: Springer, 2009, 75-222 (2009).

10) U. Gaitzsch, C. Huerrich, M. Poetschke, F. Thoss, A. Boehm, S. Roth, B. Rellinghaus, L. Schultz, *Properties of polycrystalline NiMnGa-alloys for application as magneto-mechanic actuator*, 11th International Conference and Exhibition on New Actuators and Drive Systems, Bremen, 9.-11.6.08, in: Proceedings, 717-720 (2008).

11) A. Gebert, B. Khorkounov, L. Schultz, *Effect of chemical pre-treatments on the stability of melt-spun Mg50Ni30Y20 in extreme alkaline electrolyte*, Reviews on Advanced Materials Science 18 (2008) Nr. 7, S. 639-643.
12) S. Gorantla, F. Boernert, A. Bachmatiuk, R. Schoenfelder, M.H. Ruemmeli, B. Buechner, T. Gemming, J. Eckert, *HRTEM Imaging of Electron Beam Irradiation Defect Dynamics in SWCNTs at 80 kV*, Microscopy Conference 2009 (MC2009), Graz/ Oesterreich, 30.8.-4.9.09, in: Proceedings, W. Grogger, F. Hofer, P. Poelt (eds.) Verlag der TU Graz/ Oesterreich., Vol. 3, 141-142 (2009).
13) G. Guhr, R. Bruenig, H. Schmidt, M. Jaeger, R. Poll, M. Weihnacht, *Combination of surface acoustic wave measurement and impedance spectroscopy for detection of cell adhesion process*, European Frequency and Time Forum - International Frequency Control Symposium, EFTF-IFCS 2009, Besancon/ France, 20.-24.5.09, in: Proceedings, CD-ROM (2009).
14) G. Guhr, R. Bruenig, H. Schmidt, M. Weihnacht, *Acoustoelectronic method for the detection of electrical and mechanical properties of adhering cell cultures*, 2009 IEEE International Ultrasonics Symposium, Rom/ Italy, 20.-23.9.09, in: Proceedings, CD ROM, 4D-6/1-4 (2009).
15) G. Guhr, H. Schmidt, M. Weihnacht, *A new tool to assess mechanical and dielectric properties of tissues*, Engineering in Medicine and Biology Conference - EMBC 2009, Minneapolis/ USA, 2.-6.9.09, in: Proceedings, CD-ROM, 1-4 (2009).
16) O. Gutfleisch, *High-temperature samarium cobalt permanent magnets*, in: Nanoscale magnetic materials and applications, J.P. Liu, E. Fullerton, O. Gutfleisch, D. J. Sellmyer (eds.), Dordrecht: Springer-Verl., 2009, 337-370 (2009).
17) O. Heczko, N. Scheerbaum, O. Gutfleisch, *Magnetic shape memory phenomena*, in: Nanoscale magnetic materials and applications, J.P. Liu, E. Fullerton, O. Gutfleisch, D. J. Sellmyer (eds.), Dordrecht: Springer-Verl., 2009, 399-439 (2009).
18) R. Hermann, G. Behr, G. Gerbeth, J. Priede, C. Guguschev, A. Krauze, B. Buechner, *Single crystal growthof intermetallic compounds by a two-phase RF floating zone method*, 6th International Conference on Electromagnetic Processing of Materials, EPM 2009, Dresden, 19.-23.10.09, in: Proceedings, 849-852 (2009).
19) R. Huehne, K. Gueth, M. Kidszun, R. Kaltofen, V. Matias, J. Rowley, L. Schultz, B Holzapfel, *Development of conducting buffer architectures using cube textured IBAD-TiN layers*, in: Artificially Induced Grain Alignment in Thin Films, V. Matias, R. Hammond, S.-H. Moon, R. Huehne (eds), Warrendale: MRS Proceedings, 1150E, RR04-01 (2009).
20) R. Huehne, M. Kidszun, K. Gueth, F. Thoss, B. Rellinghaus, L. Schultz, B. Holzapfel, *Ion-beam assisted pulsed laser deposition of textured transition-metal nitride films*, in: Artificially Induced Grain Alignment in Thin Films, V. Matias, R. Hammond, S.-H. Moon, R. Huehne (eds), Warrendale: MRS Proceedings, 1150E, RR03-02 (2009).
21) J. Koza, S. Muehlenhoff, M. Uhlemann, K. Tschulik, A. Gebert, K. Eckert, L. Schultz, *Influence of magnetic fields on the hydrogen evolution reaction accompanying the metal electrodeposition*, 6th International Conference on Electromagnetic Processing of Materials, EPM 2009, Dresden, 19.-23.10.09, in: Proceedings, 487-490 (2009).
22) R.Y.W. Lai, R. Schaefer, L. Schultz, J. McCord, *Dynamic observation of AC actuation in bulk magnetic shape memory materials*, Actuator 2008, 11th International Conference on New Actuators, Bremen, 9.-11.6.08, in: Proceedings, 275-278 (2008).
23) J. Liu, N. Scheerbaum, O. Gutfleisch, *Magnetic-field-induced reverse martensitic transformation in Ni-Mn-In-Co ribbons*, 11th International Conference and Exhibition on New Actuators and Drive Systems, Bremen, 9.-11.6.08, in: Proceedings, 721-722 (2008).
24) J. Liu, J. Lyubina, O. Gutfleisch, *Magnetostructural transition and magnetocaloric effect in Ni-Mn-In-(Co) alloys*, 3rd IIF-IIR International Conference on Magnetic Refrigeration at Room Temperature, Des Moines, Iowa/ USA, 11.-15.5.09, in: Proceedings, S. 27-32 (2009).
25) J. Lyubina, O. Gutfleisch, M. Kuzmin, M. Richter, *Refrigeration performance enhancement in the La(Fe,Si)13-based compounds*, 3rd IIF-IIR International Conference on Magnetic Refrigeration at Room Temperature, Des Moines, Iowa/ USA, 11.-15.5.09, in: Proceedings, S. 49-53 (2009).
26) G. Martin, H. Schmidt, S.V. Biryukov, B. Steiner, B. Wall, *New SPUDT cells including fingers and gaps wider than a quarter wavelength*, 2009 IEEE International Ultrasonics Symposium, Rom/ Italy, 20.-23.9.09, in: Proceedings, CD-ROM, 5F-3/1-4 (2009).
27) C. Mickel, C. Deneke, T. Zander, O.G. Schmidt, B. Rellinghaus, *HRTEM - sample preparation for compressed rolled-up-nanomembranes*, MC 2009. Microscopy Conference, Graz/ Austria, 30.8.-4.9.09, in: Proceedings, Volumen 1, Instrumentation and Methodology, G. Kothleitner, M. Leisch (eds.), Graz: Verl. der TU Graz, 2009, Vol. 1, 243-244 (2009).
28) K. Motamedi, N. Ioannides, M.H. Ruemmeli, I. Schagaev, *Reconfigurable network on chip architecture for aerospace applications*, in: Preprints of the 30th IFAC Workshop on Real-Time Programming and 4th International Workshop on Real-Time Software, 131-136 (2009).
29) R. Mueller, M. Bobeth, H. Brumm, G. Gille, W. Pompe, J. Thomas, *Formation of nanostructured tantalum during Mg-vapour reduction of tantalum oxide*, International Conference on Advanced Processing for Novel Functional Materials - APNFM 2008, Dresden, 23.-25.1.08, in: Proceedings, Y. Grin, B. Kieback, J. Schmidt (eds.), 85-90 (2009).
30) G. Paasch, S. Scheinert, A. Herasimovich, I. Hoerselmann, T. Lindner, *Characteristics and mechanisms of hysteresis in polymer field-effect transistors*, in: Organic Electronic - Structural and electronic properties of OFETs, Christof Woell (ed.), Wiley-VCH, 2009, S. 317-346 (2009).

31) A. Pedchenko, A. Bojarevics, J. Priede, G. Gerbeth, R. Hermann, *Model experiments on the melt flow driven by a two-phase inductor*, 6th International Conference on Electromagnetic Processing of Materials, EPM 2009, Dresden, 19.-23.10.09, in: Proceedings, 131-134 (2009).
32) A.A. Popov, *Physicochemical properties and the unusual structure of fullerenes: Vibrational and electronic spectra*, in: Strained Hydrocarbons: Beyond the van't Hoff and Le Bel Hypothesis. H. Dodzik (Ed.), Weinheim: Wiley-VCH, 2009, 238-249 (2009).
33) A. Rastelli, S. Kiravittaya, O.G. Schmidt, *Growth and control of optically active quantum dots*, in: Single Semiconductor Quantum Dots. Series: NanoScience and Technology; Michler, Peter (Ed.) Berlin: Springer-Verl., 31-69 (2009).
34) M. Sakaliyska, S. Scudino, H.V. Nguyen, K.B. Surreddi, B. Bartusch, F. Ali, J.-S. Kim, J. Eckert, *Consolidation and mechanical properties of mechanically alloyed Al-Mg powders*, Advanced Intermetallic-Based Alloys for Extreme Environment and Energy Applications, MRS Symposium 2009, Warrendale/USA, in: MRS Symposium Proceedings, M. Palm; B.P. Bewlay; M. Takeyama; J.M.K. Wiezorek; Y.-H. He (eds), 1128, U05-46 (2009).
35) R. Schaefer, *The magnetic microstructure of nanostructured materials*, in: Nanoscale magnetic materials and applications, J.P. Liu, E. Fullerton, O. Gutfleisch, D. J. Sellmyer (eds.), Dordrecht: Springer-Verl., 2009, 275-307 (2009).
36) K. Skokov, Y.S. Koshkodko, Y.G. Pastushenkov, J. Lyubina, O. Gutfleisch, *The influence of magnetic anisotropy on the magnetocaloric effect in Er2Fe14B single crystal near spin-reorientation transition and Curie temperature*, 3rd IIF-IIR International Conference on Magnetic Refrigeration at Room Temperature, Des Moines, Iowa/ USA, 11.-15.5.09, in: Proceedings, S. 161-165 (2009).
37) A. Sotnikov, H. Schmidt, M. Weihnacht, *Characterization of new promising piezoelectric crystals*, International Mini-Conference on Information Electronics Systems, Sendai/ Japan, 27.-28.10.09, in: Proceedings, 11-14 (2009).
38) A.V. Sotnikov, H. Schmidt, M. Weihnacht, E.P. Smirnova, T.Y. Chemekova, Y.N. Makarov, *Material parameters of AlN and LiAlO2 single crystals*, 2009 IEEE Frequency Control Symposium, Besancon/ France, in: Proceedings, 935-938 (2009).
39) M. Stoica, S. Roth, J. Eckert, G. Vaughan, *Glass-forming Fe-based alloys purified by fluxing techniques*, International Conference on Advanced Processing for Novel Functional Materials - APNFM 2008, Dresden, 23.-25.1.08, in: Proceedings, Y. Grin, B. Kieback, J. Schmidt (eds.), 471- 475 (2009).
40) R. Sueptitz, J. Koza, M. Uhlemann, A. Gebert, L. Schultz, *Magnetic field effect on the anodic behaviour of a ferromagnetic electrode in acidic solutions*, 6th International Conference on Electromagnetic Processing of Materials, EPM 2009, Dresden, 19.-23.10.09, in: Proceedings, 435-438 (2009).
41) T. Thersleff, S. Engel, J. Haenisch, M. Erbe, D. Pohl, R. Huehne, B. Rellinghaus, L. Schultz, B. Holzapfel, *Microstructure and phase evolution of BaHfO3 pinning centers in YBCO thin films fabricated with the TFA-MOD process*, MC 2009. Microscopy Conference, Graz/ Austria, 30.8.-4.9.09, in: Proceedings, Volumen 3, Materials Science, W. Grogger, F. Hofer, P. Poelt (eds.), Graz: Verl. der TU Graz, 2009, Vol. 3, 485-486 (2009).
42) J. Thomas, J. Schumann, T. Gemming, J. Eckert, *TEM investigation of electron beam evaporated epitaxial Fe3Si films on GaAs (100) substrates*, Microscopy Conference 2009 (MC2009), Graz/ Oesterreich, 30.8.-4.9.09, in: Proceedings, W. Grogger, F. Hofer, P. Poelt (eds.) Verlag der TU Graz/ Oesterreich (2009).
43) K. Tschulik, J. Koza, M. Uhlemann, A. Gebert, L. Schultz, *Electrodeposition of copper layers in magnetic gradient fields*, 6th International Conference on Electromagnetic Processing of Materials, EPM 2009, Dresden, 19.-23.10.09, in: Proceedings, 451-454 (2009).
44) M. Uhlemann, J.A. Koza, K. Tschulik, A. Gebert, L. Schultz, *Electrodeposition of Fe and CoFe in superimposed high magnetic fields*, 6th International Conference on Electromagnetic Processing of Materials, EPM 2009, Dresden, 19.-23.10.09, in: Proceedings, 491-494 (2009).
45) A. Winkler, S. Menzel, H. Schmidt, *SAW-grade SiO2 for advanced microfluidic devices*, in: Proceedings of SPIE, 7362, 73621Q (2009).
46) S. Yang, L. Dunsch, *Endohedral Fullerenes*, in: Encyclopedia of Inorganic Chemistry, Verlag John Wiley and Sons 2008, Lukehart, C.M.; Scott, R.A. (eds), online only (2009).
47) X. Yang, K. Eckert, R. Sueptitz, A. Gebert, M. Uhlemann, S. Odenbach, *Potentiostatic current oscillations of iron in sulfuric acid solution in magnetic fields*, 6th International Conference on Electromagnetic Processing of Materials, EPM 2009, Dresden, 19.-23.10.09, in: Proceedings, 495-498 (2009).

Invited Talks

1) M. Benyoucef, Single quantum emitters: Current challenges and potential applications, Seminar, Carl von Ossietzky Universitaet Oldenburg, 16.7.09 (2009).
2) M. Benyoucef, Tunable single-photon source and photonic molecules, Seminar, Universitaet Hamburg, 8.6.09 (2009).
3) M. Benyoucef, Single quantum emitters and optical microcavities, Seminar, Otto-von-Guericke-Universitaet Magdeburg, 11.5.09 (2009).
4) M. Benyoucef, Controlling photons using semiconductor nanostructures, Colloquium, Fraunhofer Center Nanoelectronic Technology, Dresden, 5.5.09 (2009).

5) M. Benyoucef, On the way to quantum interference between two single photons emitted from two independent quantum dots, Seminar, Institute for Quantum Electronics, ETH Zuerich/ Switzerland, 27.10.09 (2009).
6) M. Benyoucef, Nonclassical light from solid-state quantum emitters, Seminar, TU Dresden, 25.8.09 (2009).
7) A.N. Bogdanov, A.A. Leonov, U.K. Roessler, Skyrmion states in chiral magnets, Seminar, Institut fuer Festkoerperforschung, FZ Juelich, 16.12.09 (2009).
8) S. Borisenko, ARPES - a tool to study nature, Solid State Physics Seminar, Vienna University of Technology, Wien/ Oesterreich, 13.5.09 (2009).
9) S. Borisenko, ARPES below 1K, International Workshop on Strong Correlations and Angle-Resolved Photoemission Spectroscopy, Zuerich/ Schweiz, 19.-24.7.09 (2009).
10) S. Borisenko, Highest resolution ARPES today and tomorrow, Kickoff Workshop on Adlershof's Future Light Source, HZ-Berlin, BESSY, Berlin, 18.-19.3.09 (2009).
11) S. Borisenko, Exploring the limits of condensed matter physics with 1-cubed ARPES facility, Invited talk, Scienta Seminar, Moscow/ Russia, 19.-20.10.09 (2009).
12) S. Borisenko, ARPES of superconductors, Seminar Physics Department and INFM Coherentia Laboratory, University of Salerno/ Italy, 11.9.09 (2009).
13) S. Borisenko, High-resolution low-temperature ARPES of the collective quantum phenomena in solids, International Conference on Electronic Spectroscopy and Structure, Nara/ Japan, 6.-10.10.09 (2009).
14) S. Borisenko, High resolution ARPES on superconductors and related compounds, 2nd Workshop LNLS-2 New Source: Scientific Case, Campinas/ Brazil, 27.-28.8.09 (2009).
15) S. Borisenko, ARPES on superconductors, Superconductors by the Mediterranean Sea: Classic and Novel Materials, Electronic States and Critical Properties, Alghero, Sardinia/ Italy, 7.-11.9.09 (2009).
16) S. Borisenko, High resolution ARPES on superconductors and related compounds, 2nd Workshop LNLS-2 New Source: Scientific Case, Campinas/ Brazil, 27.-28.8.09 (2009).
17) B. Buechner, Superconductivity and Magnetism in LaO1-xFxFeAs, APS March Meeting, Pittsburgh/ USA, 16.-20.3.09 (2009).
18) B. Buechner, Magnetic and electronic properties of iron arsenide superconductors, Orbital 2009, Berlin, 7.-8.10.09 (2009).
19) B. Buechner, Supraleitung und Magnetismus in FeAs-Verbindungen, Physikalisches Kolloquium der Universitaet Wuppertal, 5.1.09 (2009).
20) B. Buechner, Magnetism on the nanometer scale: from stripes to magnetic molecules, Seminarvortrag, Saint-Gobain-Recherche, Cedex/ Frankreich, 11.6.09 (2009).
21) B. Buechner, Hochtemperatursupraleitung in Eisen-Arsen-Verbindungen, Physikalisches Kolloquium, Universitaet Wuerzburg, 2.2.09 (2009).
22) B. Buechner, Quantum ground states in low dimensional oxides, European Perspectives of German-Russian Scientific Cooperation, Moskau/ Russland, 25.2.09 (2009).
23) B. Buechner, The iron age of high temperature superconductivity, Festkoerperkolloquium der Fakultaet Physik der TU Muenchen, 4.6.09 (2009).
24) B. Buechner, The iron age of high temperature superconductivity, Physikalisches Kolloquium, TU Chemnitz, 27.5.09 (2009).
25) B. Buechner, Magnetic and electronic properties of iron pnictides, M2S-IX, Tokio/ Japan, 7.-12.9.09 (2009).
26) B. Buechner, Electronic properties of pnictide superconductors, ICMR Summer School on Novel Superconductors, University of California, Santa Barbara/ USA, 2.-15.8.09 (2009).
27) B. Buechner, Magnetism and superconductivity in FeAs-superconductors, Brookhaven National Laboratory, New York / USA, 12.3.09 (2009).
28) B. Buechner, Electronic and magnetic properties of FeAs superconductors, Invited Talk, Universitaet Augsburg, 20.10.09 (2009).
29) B. Buechner, Phase diagram of pnictide superconductors; Interplay between magnetism, structure and superconductivity, ICMR Summer School on Novel Superconductors, University of California, Santa Barbara/ USA, 2.-15.8.09 (2009).
30) B. Buechner, Intrinsische Ladungsinhomogenitaet, Seminar an der Johannes Gutenberg Universitaet Mainz, 18.2.09 (2009).
31) B. Buechner, Iron age of high temperature superconductivity, Condensed Matter Seminar, Universitaet Groningen/ Netherlands, 17.4.09 (2009).
32) B. Buechner, Magnetism on the nanometer scale: From sripes to magnetic molecules, Ohio State University Columbus/ USA, 11.3.09 (2009).
33) M. Calin, J. Das, L.-C. Zhang, C. Ghinea, C. Filipoiu, J. Eckert, Strengthening of multi-component Ti-based glass-forming alloys by microstructure design, WPI-Europe Workshop on Metallic Glasses and Related Materials, Grenoble/ France, 25.-28.8.09 (2009).
34) C. Deneke, Hybrid micro- and nanotubes: How thin membranes form three-dimensional micro- and nanostructures, Seminar, Brazilian Synchrotron Light Laboratory (LNLS), Campinas/ Brazil, 09.11.09 (2009).
35) K. Doerr, Reversible strain experiments on strongly correlated oxide films, Seminarvortrag, (C. Joofl, C. Volkerts), Universitaet Goettingen, 8.1.09 (2009).

36) K. Doerr, Magnetoelectric effect controlled by piezoelectric substrates, 6th International Conference on Magnetoelectric Interaction Phenomena in Crystals (MEIPIC-6), Santa Barbara/ USA, 27.1.09 (2009).
37) K. Doerr, Multi-phase multiferroics, Tutorial zur DPG-Fruehjahrstagung des AK Festkoerperphysik, Dresden, 20.3.09 (2009).
38) K. Doerr, Physics of spin-polarized oxides, Tutorial, W.-E. Heraeus-Seminar "Nanoscale Phenomena in Oxides", Bad Honnef, 3.-6.8.09 (2009).
39) K. Doerr, Multi-phase multiferroics, Workshop, Martin-Luther-Universitaet Halle-Wittenberg, Wittenberg, 16.4.09 (2009).
40) K. Doerr, Dehnungs- und Grenzflaecheneffekte in duennen Schichten hochkorrelierter Oxide, Vortrag an der Universitaet Mainz, 16.2.09 (2009).
41) K. Doerr, Piezoelectric control of epitaxial strain in oxide heterostructures and GaAs quantum dots, Seminarvortrag, (CNMS, H. M. Christen) Oak Ridge National Laboratory, TN/ USA, 29.10.09 (2009).
42) K. Doerr, Reversible strain experiments on strongly correlated oxide films, Seminarvortrag, (H. v. Loehneysen), Forschungszentrum Karlsruhe, 19.2.09 (2009).
43) K. Doerr, Magnetoelectric approaches in spintronics, Tutorial, W.-E. Heraeus-Seminar "Nanoscale Phenomena in Oxides", Bad Honnef, 3.-6.8.09 (2009).
44) L. Dunsch, The nitride cluster fullerenes : Non-IPR cages and beyond, Vortrag am State Key Laboratory for Physical Chemistry of Solid Surfaces, University of Xiamen/ China, 16.8.09 (2009).
45) L. Dunsch, The world of endohedral fullerenes, Vortrag am Dep. of Materials Science and Engineering, University of Science and Technology of China, Hefei/ China, 14.8.09 (2009).
46) L. Dunsch, The world of endohedral fullerenes, Symposium "Le carbon dans sous ses etats", IPCMS, University of Straflburg, Straflbourg/ France, 13.10.09 (2009).
47) L. Dunsch, In situ spectroelectrochemistry - A great challenge for nanostructure studies, Vortrag am Dep. of Materials Science and Engineering, University of Science and Technology of China, Hefei/ China, 15.8.09 (2009).
48) L. Dunsch, Recent advances in endohedral fullerene research, Vortrag am Institute of Chemistry, Chineses Academy of Sciences, Peking/ China, 19.8.09 (2009).
49) J. Eckert, Bulk metallic glasses and composites: The link between structure and deformability, 7th International Conference on Bulk Metallic Glasses (BMG VII), Busan/ Korea, 3.11.09 (2009).
50) J. Eckert, Bulk glassy composites: Phase formation and mechanical properties, Global Research Laboratory Korea - Germany Workshop on Bulk Metallic Glass and Nano-Structured Materials, Seoul/ Korea, 29.4.09 (2009).
51) J. Eckert, Neue Materialien auf der Basis metastabiler Phasen, Materialwissenschaftliches Kolloqium, Universitaet Stuttgart, 21.7.09 (2009).
52) J. Eckert, Heterostructured ultrafine and glassy alloys - Recent results, design strategies and deformation behavior, WPI-AIMR Annual Workshop 2009, Miyagi-Zao/ Japan, 6.3.09 (2009).
53) J. Eckert, Phase formation and properties of nanostructured and glassy metallic materials, Universitaet Wien/ Oesterreich, 16.7.09 (2009).
54) J. Eckert, Structurally inhomogeneous ultrafine and glassy alloys, Department of Materials Science and Engineering, North Carolina State University, Raleigh, NC/ USA, 12.2.09 (2009).
55) J. Eckert, Bulk metallic glasses and composites with different length-scale heterogeneities, Workshop on Future Directions in Bulk Metallic Glasses, Beijing/ China, 3.7.09 (2009).
56) J. Eckert, Amorphe und nanostrukturierte Materialien als Basis fuer neue Hochleistungswerkstoffe, Institut fuer Werkstofftechnik, Universitaet Bremen, 29.1.09 (2009).
57) J. Eckert, High-strength Al-based alloys and composites, 16th International Symposium on Metastable, Amorphous and Nanostructured Materials, (ISMANAM 2009), Beijing/ China, 6.7.09 (2009).
58) J. Eckert, Metallische Werkstoffe der Zukunft - schon heute, Forum Neue Technologien, Voith AG, Heidenheim, 15.1.09 (2009).
59) J. Eckert, From BMGs to composites: The role of heterogeneities on improving the mechanical properties of metastable alloys, Workshop on Amorphous Metals and Composites - Current Status and Future Directions, University of Melbourne/ Australien, 19.11.09 (2009).
60) J. Eckert, Materialdesign fuer innovative Werkstoffe mit erweitertem Eigenschaftsspektrum, 13. Dresdner Leichtbausymposium 2009, Dresden, 18.6.09 (2009).
61) J. Eckert, Metallic glasses and composites - Development of high performance materials based on metastable phases, Seminar am Institut fuer Materialphysik im Weltraum, Deutsches Zentrum fuer Luft- und Raumfahrt e.V. (DLR), Koeln, 28.9.09 (2009).
62) J. Eckert, Current status of research on amorphous metals, Workshop on Amorphous Metals and Composites - Current Status and Future Directions, University of Melbourne/ Australien, 19.11.09 (2009).
63) J. Eckert, Grundlagen und Anwendungen metallischer Glaeser und Komposite, VDMA Arbeitskreis Material Roadmap Expertenworkshop, Frankfurt, 3.4.09 (2009).
64) J. Eckert, How to improve the deformability of bulk metallic glasses, 2009 TMS Annual Meeting and Exhibition, Symposium "Bulk Metallic Glasses (VI)", San Francisco/ USA, 18.2.09 (2009).

65) J. Eckert, Processing, mechanical properties and applications of glassy alloys and composites, European Congress and Exhibition on Advanced Materials and Processes (EUROMAT 2009), Symposium B13 - "Metallic Glasses", Glasgow/ UK, 8.9.09 (2009).
66) J. Eckert, Metastabile Phasen - Von den Grundlagen zu Anwendungen, Werkstoffwissenschaftliches Kolloquium, Universitaet Erlangen-Nuernberg, 27.10.09 (2009).
67) J. Eckert, Ultrafine and glassy alloys with improved deformability, Korea - Germany Joint Workshop on Amorphous - Nanostructured Materials, Ulsan/ Korea, 27.4.09 (2009).
68) J. Eckert, Bulk metallic glasses and composites for engineering applications, Tewkesbury Lecture, University of Melbourne/ Australien, 19.11.09. (2009).
69) J. Eckert, Bulk metallic glasses and hierarchical composites: Tailoring of properties for engineering applications, Global Research Laboratory Korea - Germany Workshop on Bulk Metallic Glass and Nano-Structured Materials, Dresden, 18.12.09 (2009).
70) H. Ehrenberg, Li-Ionenbatterien: Perspektiven und materialwissenschaftliche Herausforderungen, Anorganisch-chemisches Kolloquium, Universitaet zu Koeln, 2.12.09 (2009).
71) H. Ehrenberg, Werkstoffliche Herausforderungen in Li-Batterien, Symposium Hochleistungskeramik 2009 des Gemeinschaftsausschusses der DKG und der DGM, Eurogress Aachen, 26.3.09 (2009).
72) H. Ehrenberg, Li-Ionenbatterien: Perspektiven und materialwissenschaftliche Herausforderungen, Anorganisch-chemisches Kolloquium, TU Berlin, 23.9.09 (2009).
73) H. Ehrenberg, Phosphoolivine LiMPO4 (M=Mn,Fe,Co) cathodes in Li-ion batteries: properties, mechanism and new composite concepts, Vortrag an der Justus-Liebig-Universitaet Giessen, 3.2.09 (2009).
74) H. Ehrenberg, N.N. Bramnik, W. Jaegermann, J.J. Schneider, Fatigue in LiCoPO4 cathodes for Li-ion batteries and new composite concepts, Euromat, Glasgow/ UK, 7.-10.9.09 (2009).
75) H. Eschrig, *The electronic structure of layered iron chalcogenides/ pnictides*, Predictive Capabilities for Strongly Correlated Systems, Oak Ridge/ USA, 14.-16.11.08 (2008).
76) H. Eschrig, The electronic structure of layered iron chalcogenides/pnictides, National Research Laboratory (NRL), Washington DC/ USA, 26.2.09 (2009).
77) H. Eschrig, K. Koepernik, Electronic structure of layered iron chalcogenides/pnictides, Seminar of the Center for Computational Materials Science, Universitaet Wien/ Oesterreich, 22.6.09 (2009).
78) D. Evtushinsky, Bridging angle-resolved photoemission spectroscopy (ARPES) with other experiments: connection to muon spin rotation (muSR) in Ba1-xKxFe2As2, Joint Users' Meeting of PSI 2009, Villigen/ Switzerland, 12.-13.10.09 (2009).
79) D.V. Evtushinsky, D.S. Inosov, V.B. Zabolotnyy, A.A. Kordyuk, T.K. Kim, M. Knupfer, B. Buechner, A.N. Yaresko, G.L. Sun, C.T. Lin, M.S. Viazovska, A. Varykhalov, S.V. Borisenko, Bridging ARPES with other experiments: electronic structure of iron arsenides, Seminar of Keimer's department, MPI-FKF Stuttgart, 3.-5.12.09 (2009).
80) S. Faehler, On the role of interfaces in epitaxial magnetic shape memory film, 2nd International Conference on Ferromagnetic Shape Memory Alloys, Bilbao/ Spain, 1.-3.7.09 (2009).
81) S. Faehler, Magnetism and martensitic transitions in epitaxial magnetic shape memory films, Seminar, Institute of Physics, Czech Academy of Sciences, Prag/ Tschechische Republik, 1.4.09 (2009).
82) S. Faehler, Epitaxial magnetic shape memory films, European Symposia on Martensitic Transformation ESOMAT 2009, Prag/ Tschechische Republik, 8.-11.9.09 (2009).
83) J. Fink, Many-body properties of solids studied by angle-resolved photoemission spectroscopy (ARPES): application to conventional and unconventional superconductors, Kolloquiumsvortrag, Modena/ Italy, 19.3.09 (2009).
84) J. Fink, Stripes in high-Tc superconductors as detected by resonant softx-ray scattering, Seminarvortrag TIFR, Mumbai/ Indien, 19.11.09 (2009).
85) J. Fink, Electronic excitations in correlated systems studied by inelastic electron scattering, Electronic excitations studied by non-resonant inelastic x-ray scattering at PETRA III, Hamburg, 7.-8.5.09 (2009).
86) J. Fink, Many-body properties of solids studied by angle-resolved photoemission spectroscopy:application to conventional anbd unconventional superconductors, Kolloquiumsvortrag TIFR, Mumbai/ Indien, 18.11.09 (2009).
87) J. Fink, Many-body properties of solids studied by (time-dependent) angle-resolved photoemission spectroscopy : application to conventional and unconventional superconductors, MSM 09, Kolkata/ Indien, 11.-14.11.09 (2009).
88) J. Fink, Angular resolved photoemission spectroscopy, a probe for the many-body properties of solids, KKR and Spectroscopy — Hands-on Course 2009, Muenchen, 24.-26.6.09 (2009).
89) U. Gaitzsch, M. Poetschke, S. Roth, L. Schultz, Magnetostrain in polycrystalline Ni-Mn-Ga, ICASM Konferenz, TCE Madurai/ Indien, 7.-9.1.09 (2009).
90) A. Gebert, Effect of surface finishing and mechanically induced defects on the corrosion of bulk metallic glasses, ISMANAM 2009 Conference, Beijing/ China, 5.-9.7.09 (2009).
91) A. Gebert, Effect of structural and mechanical defects on the corrosion behavior of Zr-based bulk metallic glasses and composites, Kolloquium, 1. Physikalisches Institut, Universitaet Goettingen, 12.1.09 (2009).
92) J. Geck, EELS and RIXS studies on doped manganites, Workshop, Stanford/ USA, 29.7.-6.8.09 (2009).

93) H.-J. Grafe, G. Lang, F. Hammerath, K. Manthey, D. Paar, B. Buechner, NMR studies of superconducting LaO1-xFxFeAs, Kick-off meeting of the SOLeNeMaR EU project of the Department of Physics, University of Zagreb/ Croatia, 19.-20.3.09 (2009).
94) M. Grobosch, M. Knupfer, Charge-injection barriers at realistic metal/ organic interfaces: metals become faceless, Printed Electronics Europe 2009, Dresden, 7.-8.4.09 (2009).
95) O. Gutfleisch, Magnetic materials and hydrides for energy efficient technology, Vortrag an der TU Hamburg-Harburg, 29.9.09 (2009).
96) O. Gutfleisch, Solid state energy efficient magnetic cooling and heating, Royal Institution of Great Britain, London/ UK, 7.9.09 (2009).
97) O. Gutfleisch, HDDR processing of NdFeB, International Workshop on Materials for a Sustainable Future, University of Birmingham/ UK, 11.-12.9.09 (2009).
98) O. Gutfleisch, Novel materials for energy efficient technologies, Kolloquium am Instituto de Ciencia de Materiales de Sevilla, Sevilla/ Spanien, 26.5.09 (2009).
99) O. Gutfleisch, J. Lyubina, M. Richter, Novel materials for room temperature magnetic cooling, 1st International Conference on Complex Metallic Alloys and their Complexity (C-MAC-1), Nancy/ France, 4.-7.10.09 (2009).
100) O. Gutfleisch, J. Thielsch, K. Gueth, J. Lyubina, T. Woodcock, B. Rellinghaus, L. Schultz, Advanced permanent magnets, Symposium on Magnetism for Sustainable Energy, Intermag 2009, Sacramento/ USA, 4.-8.5.09 (2009).
101) O. Gutfleisch, J. Thielsch, K. Gueth, J. Lyubina, T. Woodcock, L. Schultz, Advanced permanent magnets for energy applications, UK Magnetics Society, Workshop on Advanced Magnetic Materials and their Applications, Vacuumschmelze GmbH, Hanau, 12.-13.10.09 (2009).
102) V. Haehnel, H. Schloerb, S. Faehler, L. Schultz, Electrodeposition and magnetic properties of nanowire arrays in self-organized aluminum oxide templates, Juelich Centre for Neutron Science JCNS Seminar, Garching bei Muenchen, 21.10.09 (2009).
103) H. Hermann, Modellierung von fulleren-basierten Schichten mit optimierten Eigenschaften, DGM Arbeitskreis-Workshop, Dresden, 24.6.09 (2009).
104) H. Hermann, Theoretische Ansaetze fuer ultralow-k Materialien, Insitutsseminar, Universitaet Cottbus, 6.7.09 (2009).
105) R. Hermann, G. Gerberth, J. Priede, A. Krauze, G. Behr, B. Buechner, Convectional controlled crystal-melt interface using two-phase radio-frequency electromagnetic heating, 6th International Conference HTC 2009, Athen/ Greece, 6.-10.5.09 (2009).
106) C. Hess, The intrinsic electronic phase diagram of iron-pnictide superconductors, SFB-Seminar, II. Physikalisches Institut, Universitaet Koeln, 29.4.09 (2009).
107) C. Hess, The intrinsic electronic phase diagram of iron-pnictide superconductors, Study of Matter at Extreme Conditions - SMEC 2009, Miami/ USA, 28.3.-1.4.09 (2009).
108) C. Hess, Anregungen von Spin und Ladung, Seminarvortrag, Technische Universitaet Wien/ Oesterreich, 6.5.09 (2009).
109) V. Hoffmann, Neue Entwicklungen in der analytischen Glimmentladungsspektrometrie, Institutsseminar, FH Senftenberg, 19.5.09 (2009).
110) V. Hoffmann, V. Efimova, D. Klemm, M. Voronov, J. Eckert, Gepulste Glimmentladungen - von den Grundlagen zu den Anwendungen, 15. Tagung Festkoerperanalytik, Chemnitz, 12.-16.7.09 (2009).
111) R. Huehne, High temperature superconductors: properties and applications, Tutorial auf der "14th International Conference on RF Superconductivity" Dresden und Berlin, 17.-25.10.09 (2009).
112) R. Huehne, J. Eickemeyer, U. Gaitzsch, T. Thersleff, J. Freudenberger, L., Holzapfel, B. Schultz, O. de Haas, V.S. Sarma, M. Weigand, J.H. Durrell, Application of textured highly alloyed Ni-W tapes for coated conductors, International Workshop on Coated Conductors for Applications, CCA 2009, Barcelona/ Spain, 22.-29.11.09 (2009).
113) R. Huehne, J. Eickemeyer, T. Thersleff, R. Haenisch, B. Holzapfel, V.S. Sarma, M. Weigand, J. Durrell, O. de Haas, L. Schultz, Application of textured highly alloyed Ni-W tapes for coated conductor architectures, CEC-ICMC 2009, Tucson, Arizona/ USA, 28.6.-2.7.09 (2009).
114) V. Kataev, Multifrequency ESR spectroscopy of the heavy fermion compound YbRh2Si2 in strong magnetic fields, Seminar at the Molecular Photoscience Research Center, Kobe University, Kobe/ Japan, 4.9.09 (2009).
115) V. Kataev, Disclosing spin polarons in cubic cobaltites by magnetic resonance spectroscopy, International Zavoisky Workshop "Modern Developments of Magnetism", Kazan/ Russia, 28.9.-3.10.09 (2009).
116) V. Khavrus, E. Ibrahim, A. Leonhardt, S. Hampel, S. Oswald, B. Buechner, Separate synthesis of single- and multi-walled carbon nanotubes , Visit to Sohag University (Egypt) for preparation of publications based on the common work performed during stay of E.M.M.Ibrahim at IFW-Dresden, Faculty of Science of Sohag University/ Egypt, 26.6.-4.7.09 (2009).
117) V. Khavrus, E. Ibrahim, M. Ruemmeli, A. Bachmatiuk, S. Hampel, A. Leonhardt, B. Buechner, Application of Raman spectroscopy for investigation properties of carbon nanotubes, Visit to Sohag University (Egypt) for preparation of publications based on the common work performed during stay of E.M.M.Ibrahim at IFW-Dresden, Faculty of Science of Sohag University / Egypt, 26.6.-4.7.09 (2009).

118) A. Kiessling, J. Haenisch, E. Reich, M. Sparing, T.D. Thersleff, B. Holzapfel, L. Schultz, J. Durell, M. Weigand, Deposition temperature dependence on the superconducting properties of YBCO/BZO quasimultilayers, CCA 2009, Barcelona/ Spain, 22.-24.11.09 (2009).
119) R. Klingeler, Konkurrierende Grundzustaende in niedrigdimensionalen Uebergangsmetallverbindungen, Symposium: Physik korrelierter Elektronensysteme in Festkoerpern, Kirchhoff Institut fuer Physik, Universitaet Heidelberg, 22.4.09 (2009).
120) R. Klingeler, Structure, magnetism and giant magnetodielectric coupling in rare earth ferroborates, Seminarvortrag, Institut fuer Festkoerperforschung, FZ Juelich, 3.6.09 (2009).
121) R. Klingeler, Komplexe magnetische Materialien zwischen Molekuel und Festkoerper, Seminar Talk, Universitaet Chemnitz, 14.12.09 (2009).
122) R. Klingeler, Interplay of magnetic, electronic and structural properties of FeAs-based supercoductors, Van der Waals-Zeeman Institute Amsterdam / Netherlands, 6.1.09 (2009).
123) M. Knupfer, Electronic properties of transition metal phthalocyanines: archetypes for organic semiconductors and molecular magnets, Seminar, Max-Planck-Institut fuer Festkoerperforschung, Stuttgart, 15.4.09 (2009).
124) M. Knupfer, Ordered magnetic molecular layers: Fundamentals for molecular magnetism, Russian-German Workshop on the Development and Use of Accelerator driven Photon Sources, Berlin, 17.-18.2.09 (2009).
125) A. Kordyuk, Electrons in cuprates: view by ARPES, I.F. Schegolev Memorial Conference ìLow-Dimensional Metallic and Superconducting Systemsî, Chernogolovka, Moscow/ Russia, 10.-16.10.09 (2009).
126) A. Kordyuk, Electrons in cuprates: view by ARPES, APCTP 2009 Winter Workshop on Frontiers in Electronic Quantum Matter, Korea, 8.-12.2.09 (2009).
127) A. Kordyuk, Does the normal normal state in 2D metals ever set in?, APCTP 2009 Winter Workshop on Frontiers in Electronic Quantum Matter, Korea, 8.-12.2.09 (2009).
128) J. Koza, K. Tschulik, M. Uhlemann, A. Gebert, C. Mickel, S. Baunack, L. Schultz, R. Sueptitz, Electrodeposition of thin magnetic layers under the influence of magnetic fields, MFD-Lehrstuhlkolloqium, TU Dresden, 14.10.09 (2009).
129) U. Kuehn, Herstellung, Eigenschaften und Anwendungen massiver metallischer Gl‰ser und Komposite, Workshop des RGM-Metall-Netzwerkes im Rahmen des BMWi-Impulsprogramms NeMat-Phase2, Technologieorientiertes Gruenderzentrum, TGZ, Glaubitz, 11.3.09 (2009).
130) G. Lang, Local study of the anomalous electronic states of pnictides and cobaltates, Seminar, LPEM, ESPCI-ParisTech, Paris/ France, 30.11.09 (2009).
131) G. Lang, New electronic states and strong correlations: from cobaltates to iron pnictides, CNRS audition, LPS Orsay/ France, 4.3.09 (2009).
132) A. Leonhardt, D. Haase, S. Hampel, Solvothermal decomposition of caspian heavy oil - synthesis of iron/ carbon nanostructures, Meeting im Ministerium fuer Kommunikation- und Informationstechnologien der Aserbaishanischen Republik, Baku/Aserbaishan, 28.8.-1.9.09 (2009).
133) J. Lyubina, O. Gutfleisch, Novel magnetic materials for energy efficient technologies, 11th International Conference on Advanced Materials ICAM 2009, Rio de Janeiro/ Brazil, 20.-25.9.09 (2009).
134) J. Lyubina, O. Gutfleisch, Novel materials for solid state energy efficient magnetic cooling, UK Magnetics Society Seminar Advanced Magnetic Materials and their Applications, Hanau, 12.-13.10.09 (2009).
135) N. Mattern, Heterogeneous metallic glasses by phase separation in the liquid, Korea-Germany Workshop on Bulk Metallic Glasses and Nano-structured Materials, Seoul/ Korea, 29.4.09 (2009).
136) N. Mattern, Phase separation in liqud and amorphous metallic alloys, Korea-Germany Joint Workshop on Amorphous/ Nanostructured Materials, Ulsan/ Korea, 27.4.09 (2009).
137) J. McCord, Magnetische Domaenenbeobachtung mit optischer Mikroskopie, VAC-Kolloquium, Vacuumschmelze Hanau, 26.2.09 (2009).
138) J. McCord, Wide-field magneto-optical microscopy - opportunities and limitations, Physics Seminar University Helsinki, Helsinki, Finnland/ 20.2.09 (2009).
139) J. McCord, Aspects of magnetic heterostructures - statics and dynamics, Institutskolloquium des Instituts fuer Ionenstrahlphysik, FZ Dresden-Rossendorf, 19.11.09 (2009).
140) J. McCord, Preparation and magnetics of magnetic modulated thin films, Seminar Hitachi Global Storage Research Center, San Jose/ USA, 13.5.09 (2009).
141) J. McCord, Magnetische Schichten in der Magnetoelektronik - Status und Entwicklungsmoeglichkeiten, Kolloquium der Mikroproduktionstechnik, Universitaet Hannover, 15.1.09 (2009).
142) J. McCord, Magnetic property modulated films – preparation, magnetic properties and domains, Seminar - Electrical and Computer Engineering, Northeastern University, Boston/ USA, 4.12.09 (2009).
143) J. McCord, Static and dynamic magnetizatio processes in magnetic property patterned thin films, International Seminar and Workshop on Magnonics: From Fundamentals to Applications, Dresden, 2.-7.8.09 (2009).

144) J. McCord, J. Fassbender, Designing soft magnetic materials by ion irradiation, XVIII International Materials Rerearch Congress 2009, Cancun/ Mexico, 16.-21.8.09 (2009).
145) J. McCord, C. Hamann, N. Martin, J.I. Moench, R. Kaltofen, L. Schultz, T. Strache, J. Fassbender, R. Mattheis, Static and dynamic magnetization processes in magnetic property patterned thin films, Intermag 2009, Sacramento/ USA, 4.-8.5.09 (2009).
146) Y.F. Mei, Rolled-up integrative bioanalytic microsystem for a single cell, International Export Symposium, 4th Medical Biotech Forum, Dalian/ China, 7.-9.8.09 (2009).
147) Y.F. Mei, Rolled-up multifunctional nanomembranes towards an integrative bioanalytic microsystem for individual cells, The 1st Sino-German Symposium on Advanced Biomedical Nanostructures, Jena, 27.-30.10.09 (2009).
148) Y.F. Mei, Solid state nanomembranes for nanosciences, Seminar, Shanghai Nanotechnology Promotion Center (SNPC), Shanghai/ China, 20.10.09 (2009).
149) Y.F. Mei, Rolled-up nanomembranes for interdisciplinary research, The 6th Annual International New Exploratory Technologies Conference, Shanghai/ China, 12.-14.10.09 (2009).
150) Y.F. Mei, Thin solid films or nanomembranes?, Seminar, Shanghai Institute of Ceramics, Chinese Academy of Sciences, Shanghai/ China, 12.8.09 (2009).
151) Y.F. Mei, Progress in nanomembrane technology, Seminar, School of Physics and Optoelectronic Technology, Dalian University of Technology, Dalian/ China, 9.8.09 (2009).
152) Y.F. Mei, Strain-engineered nanomembranes, The 2nd Asian Symposium on Advanced Materials, Shanghai/ China, 11.-14.10.09 (2009).
153) Y.F. Mei, Shaping nanomembranes, Seminar, Microsystem Research Center of Chongqing University, Chongqing/ China, 16.10.09 (2009).
154) Y.F. Mei, Solid state nanomembranes for nanosciences, Seminar, Department of Physics, Harbin Institute of Technology, Harbin/ China, 10.8.09 (2009).
155) A. Moebius, Phenomenological aspects of the metal-insulator transition in disordered systems: So, was Mott right after all?, Kolloquium zum SFB/TR49 "Condensed Matter Systems with Variable Many Body Interactions", Physikalisches Institut, Goethe-Universitaet, Frankfurt, 2.7.09 (2009).
156) A. Moebius, Numerical procedures for Coulomb glass simulations, IRTG Workshop, Rackeve/ Hungaria, 31.8.-2.9.09 (2009).
157) T. Muehl, Magnetic nanowires inside carbon nanotubes, Nanotechnologie-Seminar, Nanotech-Messe, Tokyo/ Japan, 19.2.09 (2009).
158) E. Mueller, Organisation von Praeventionstagen in einer Forschungseinrichtung, 34. Jahrestagung der VDSI-Fachgruppe Hochschulen und wissenschaftliche Forschungseinrichtungen, Leipzig, 18.-20.5.09 (2009).
159) V. Neu, Relaxations- und Ummagnetisierungsprozesse in nanoskaligen magnetischen Schichten, Seminar des Instituts fuer Physik, TU Chemnitz, 16.6.09 (2009).
160) R. Niemann, J. Buschbeck, S. Kaufmann, A. Backen, O. Heczko, S. Faehler, L. Schultz, Preparation and characterization of epitaxial magnetic shape memory alloy films, Seminar der Academy of Sciences of the Czech Republic, Institute of Physics, Ostre/ Tschechische Republik, 24.-25.11.09 (2009).
161) G. Paasch, S. Scheinert, M. Grobosch, M. Knupfer, SCLC in organics with distributed traps: analytical approximations vs. numerical simulation and the role of the contacts, International Conference on Organic Electronics 2009, Liverpool/ GB, 15.-17.6.09 (2009).
162) D. Pohl, E. Mohn, U. Wiesenhuetter, J. Barthel, J. Fassbender, K. Albe, L. Schultz, B. Rellinghaus, L10 ordering and surface induced stress in different morphologies of binary nanoparticles from the gas phase, Materials Science and Engineering Departments, UC Berkeley/ USA, 29.1.09 (2009).
163) D. Pohl, E. Mohn, U. Wiesenhuetter, J. Barthel, J. Fassbender, K. Albe, L. Schultz, B. Rellinghaus, L10 ordering and surface induced stress in different morphologies of binary nanoparticles from the gas phase, NCEM, Berkeley/ USA, 28.1.09 (2009).
164) A. Popov, L. Dunsch, I. Kareev, N. Shustova, S. Lebedkin, S. Strauss, O. Boltalina, Spectroelectrochemistry of perfluoroalkylfullerenes: Redox potentials, ESR spectra, and DFT calculations, 19th International Symposium on Fluorine Chemistry, Jackson Hole, Wyoming/ USA, 23.-28.9.09 (2009).
165) A. Rastelli, New approaches for engineering quantum dot light emission properties, Symposium on Optical Spectroscopy on Microstructured Semiconductors, Universitaet Hamburg, 4.3.09 (2009).
166) A. Rastelli, Self-assembled quantum dots: growth phenomena and post-growth tuning, Seminar, School of Physics and Astronomy, University of Nottingham/ UK, 17.11.09 (2009).
167) A. Rastelli, Ultralow thermal conductivity of Si with embedded SiGe nanoclusters, Workshop on Spin Caloritronics, Dresden, 12.-15.5.09 (2009).
168) A. Rastelli, Fabrication and emission energy engineering of self-assembled quantum dot structures, Seminar, Institut fuer Festkoerperphysik Universitaet Bremen, 30.6.09 (2009).
169) A. Rastelli, SiGe/Si and InGaAs/GaAs islands: Shape transitions and 3D composition profiles, European conference on surface science (ECOSS) 26, Parma/ Italy, 30.8-4.9.09 (2009).

170) A. Rastelli, Tuning quantum dot emission and cavity mode energies by stress and heat, Seminar, Lehrstuhl fuer Technische Physik, Universitaet Wuerzburg, 17.12.09 (2009).
171) A. Rastelli, New tools for investigating and modifying the structure of self-assembled quantum dots, SemiconNano 2009, Anan, Tokushima/ Japan, 9.-14.8.09 (2009).
172) A. Rastelli, Alloying and three-dimensional composition profiles of single strained islands, 2nd International Conference on Physics at Surfaces and Interfaces, Puri, Orissa/ India, 23.-27.2.09 (2009).
173) A. Rastelli, F. Pezzoli, Growth and thermal conductivity of self-assembled SiGe/Si(001) nanocrystal multilayers, CECAM Workshop on Thermoelectric Transport: progress in first principles and other approaches and interplay with experiment, Lausanne/Schweiz, 22.-24.7.09 (2009).
174) B. Rellinghaus, Metallische Nanomagnete: Eine "oberflaechliche" Betrachtung, Kolloquiumsvortrag, Institut fuer Festkoerperforschung, FZ Juelich, 23.11.09 (2009).
175) B. Rellinghaus, D. Pohl, U. Wiesenhuetter, J. Barthel, L. Schultz, Surface relaxation in binary metal nanoparticles, Characterisation Seminar, Electron Microscopy Group, Department of Materials, University of Oxford/ UK, 26.1.09 (2009).
176) M. Richter, Tutorial: full-potential local-orbital code (FPLO), European School on Magnetism 2009: Models in Magnetism, Timisoara/ Rumaenien, 31.8.-10.9.09 (2009).
177) M. Richter, Electronic structure: LDA, LSDA, tight binding, DMFT, European School on Magnetism 2009: Models in Magnetism, Timisoara/ Rumaenien, 31.8.-10.9.09 (2009).
178) M. Richter, R. Xiao, D. Fritsch, M. Kuzmin, K. Koepernik, H. Eschrig, K. Vietze, G. Seifert, Subnanometer magnetic storage bits, European Workshop "Self-Organized Nanomagnets 2009", Aussois/ France, 29.3.-3.4.09 (2009).
179) U. Roessler, Skyrmionic textures: chiral mesophases in magnetism and related systems, Seminar am Helmholtz-Zentrum Berlin, 9.3.09 (2009).
180) U.K. Roessler, Skyrmions in chiral magnets, Seminar, Diamond Light Source, Didcot, Oxfordshire/ UK, 21.10.09 (2009).
181) U.K. Roessler, Skyrmions in chiral magnets, Seminar am ILL, Grenoble/ Switzerland, 9.6.09 (2009).
182) M.H. Ruemmeli, Advances in understanding the nucleation and growth of carbon nanotubes, Invited Talk, London Metropolitan University, London/ UK, 27.-29.4.09 (2009).
183) M.H. Ruemmeli, Engineering carbon at the nanoscale, Indiviual Seminar, Sakarya University, Tuerkei, 27.-30.7.09 (2009).
184) M.H. Ruemmeli, Engineering carbon at the nanoscale, Presentation at the Max Bergmann Zentrum, Dresden, 25.6.09 (2009).
185) M.H. Ruemmeli, Rethinking carbon nanotube and graphene growth, Talk, University of the Witswasersrand, Johannesburg/ South Africa, 3.-4.12.09 (2009).
186) M.H. Ruemmeli, Rethinking carbon nanotube and graphene growth, Talk, University of Surrey/ United Kingdom, 17.-18.12.09 (2009).
187) M.H. Ruemmeli, M. Bystrzejewski, R. Schoenfelder, A. Bachmatiuk, I. Ibrahim, C. Schuenemann, A. Balanaga Tetali, F. Boerrnert, B.L. Aryasomayajula, A. Scott, 12 Months growth at the IFW, Vortrag an der Oxford University, Oxford/ UK, 28.-30.1.09 (2009).
188) M.H. Ruemmeli, F. Schaeffel, A. Bachmatiuk, R. Schoenfelder, M. Bystrzewski, F. Boernert, U. Wolff, E. Coric, C. Schuenemann, M. Ulbrich, R. Huebel, M. Knupfer, B. Buechner, Advances in understanding carbon nanotube nucleation and growth, Vortrag an der Oxford University, Oxford/ UK, 28.-30.1.09 (2009).
189) D. Ruiz Romera, N. Van Steenberge, M. Stoica, K. Van Brussel, M. De Wulf, J. Eckert, S. Claessens, Technological applications of bulk metallic glasses: challenges to overcome, IWMG09: International Workshop on Structural and Mechanical Properties of Metallic Glasses, Barcelona/ Spanien, 17.-19.6.09 (2009).
190) S. Sanchez, Nanorobots: the ultimate wireless self-propulsed sensing and actuating devices, Seminar, Chemistry Department, Autonomous University of Barcelona/ Spain, 17.11.09 (2009).
191) R. Schaefer, Magnetische Mikrostrukturen, Schuelervortrag am Annengymnasium in Goerlitz, 16.6.09 (2009).
192) R. Schaefer, Magnetische Domaenen - Daemonische Magnete, Vorlesung, Physik am Samstag, Dresden, 14.11.09 (2009).
193) R. Schaefer, Daemonische Magnete - von der Festplatte zur Diebstahlsicherung, "Physik im Kaufpark", Kaufpark Nickern, Dresden, 17.-20.3.09 (2009).
194) R. Schaefer, Introduction to magnetic microstructures, 6 Doppelstunden Blockvorlesung, Angstroem Laboratory, Uppsala University/ Schweden, 7.-11.12.09 (2009).
195) R. Schaefer, D. Elefant, Giant negative domain wall resistance, Seminar am Helmholtz-Zentrum, BESSY, Berlin, 6.11.09 (2009).
196) F. Schaeffel, M. Ruemmeli, C. Taeschner, B. Rellinghaus, B. Buechner, L. Schultz, Synthesis, characterisation and modification of carbon nanomaterials, Seminar an der FU Berlin, 3.11.09 (2009).
197) N. Scheerbaum, J. Liu, O. Heczko, L. Schultz, O. Gutfleisch, NiMnGa-fibres and NiMnGa-polymer-composites, Department of Physics at the IIT Bombay/ India, 12.1.09 (2009).
198) N. Scheerbaum, J. Liu, L. Schultz, O. Gutfleisch, NiMnGa-fibres and NiMnGa-polymercomposites, International Conference on Active/Smart Materials, Madurai/ India, 7.-9.1.09 (2009).
199) H. Schmidt, Nanobeben auf kleinen Chips - Akustische Oberflaechenwellen, "Physik im Kaufpark", Kaufpark Nickern, Dresden, 17.-20.3.09 (2009).

200) O.G. Schmidt, Rolled-up nanotech: Paradigm shifting approach for integrative, scalable and multifunctional systems, Nanotech Europe 2009, Berlin, 28.-30.9.09 (2009).
201) O.G. Schmidt, Multifunktionale Roehrchen fuer visionaere Anwendungen in der Nanotechnologie, 7. Nanovision, Karlsruhe, 7.12.09 (2009).
202) O.G. Schmidt, Spectral tuning of single quantum dots, Collaborating Conference on Interacting Nanostructures, San Diego/ USA, 10.11.09 (2009).
203) O.G. Schmidt, Smart tubes: New concepts, new materials, new applications, Seminar, Zhjiang University, Hangzhou/ China, 14.5.09 (2009).
204) O.G. Schmidt, Smart tubes, 12th International Conference on the Formation of Semiconductor Interfaces (ICFSI), Weimar, 6.-10.7.09 (2009).
205) O.G. Schmidt, SiGe nanostructures, Growth, properties and potential applications, Seminar, Bilkent University, Ankara/ Turkey, 12.6.09 (2009).
206) O.G. Schmidt, (Plenary) Smart tubes: New concepts, new materials, new applications, Conference on Nanoscience and Nanotechnology, Eskihesir/ Turkey, 8.-12.6.09 (2009).
207) O.G. Schmidt, Multiscale ordering of semiconductor quantum dots, Prominas Workshop on the Convergence of Conventional Microelectronics and Nanotechnology, Grenoble/ France, 15.-17.9.09 (2009).
208) O.G. Schmidt, Material interdiffusion during quantum dot growth, MBE Taiwan 2009, Hualien/ Taiwan, 5.-6.6.09 (2009).
209) O.G. Schmidt, Multifunktionale Mikro- und Nanoroehrchen, Kolloquium, Otto-von-Guericke-Universitaet, Magdeburg, 3.11.09 (2009).
210) O.G. Schmidt, Rolled-up nanotech: Integrative, scalable, and multifunctional, Seminar, National Tung Hwa University, Hsinchu/ Taiwan, 5.6.09 (2009).
211) O.G. Schmidt, Smart tubes, SPIE Europe Microtechnologies for the New Millennium, Dresden, 4.-6.5.09 (2009).
212) O.G. Schmidt, Spatial and spectral control of quantum dot structures by unconventional techniques, SPIE, Photonics West, San Jose, California/ USA, 24.-29.1.09 (2009).
213) O.G. Schmidt, Smart tubes: New concepts, new materials, new applications, Seminar, Institut de Ciencia de Materials de Barcelona (ICMAB), Barcelona/ Spain, 9.2.09 (2009).
214) O.G. Schmidt, Vom Loewenzahn zur Nanorakete, "Physik im Kaufpark", Kaufpark Nickern, Dresden, 17.-20.3.09 (2009).
215) O.G. Schmidt, Surface interdiffusion during strained island growth, Surface Kinetics International Conference, Salt Lake City/ USA, 20.-22.3.09 (2009).
216) O.G. Schmidt, Current challenges for high quality semiconductor quantum emitters, 25 years Omicron, Dresden, 25.3.09 (2009).
217) O.G. Schmidt, Rolled-up nanotech: From basic perception to potential applications, Nanotech Insight 2009, Barcelona/ Spain, 29.3.-2.4.09 (2009).
218) O.G. Schmidt, Deterministic manipulation of quantum dot emission spectra and energy levels, The International Workshop on Quantum Manipulation in Low-Dimensional Semiconductors, Beijing/ China, 28.-30.4.09 (2009).
219) O.G. Schmidt, Strain driven 3D micro- and nanoarchitectures, Kolloquium, Max-Planck Institut fuer Mikrostrukturphysik, Halle, 23.12.09 (2009).
220) O.G. Schmidt, Y.F. Mei, Lab-in-a-tube, The 13th Annual European Conference on Micro and Nanoscale Technologies for the Biosciences, Montreux/ Switzerland, 16.-18.11.09 (2009).
221) L. Schultz, Neue Urban-Maglev Fahrzeuge fuer den Stadtverkehr - passiv stabiles magnetisches Schweben mit Supraleitern, Megapolis - Mobilitaet und Oekologie, Briesen, 11.6.09 (2009).
222) L. Schultz, Nanostructured high temperature superconductors - from coated conductors to levitation systems, Humboldt-Kolleg "Advancements in Nanotechnology and Microelectronics (ANM'09)", El Mouradi, Gammarth/ Tunesien, 13.-14.11.09 (2009).
223) L. Schultz, Riding on magnetic fields - the miraculous world of superconductivity, Public Seminar Lecture, Physics Department, University of St. Andrews/ UK, 3.-4.9.09 (2009).
224) L. Schultz, Vom Schweben auf Magnetfeldern - Die wundersame Welt der Supraleiter, Luescher-Lecture (oeffentlicher Abendvortrag), Klosters/ Schweiz, 13.2.09 (2009).
225) L. Schultz, Vom Schweben auf Magnetfeldern: die wundersame Welt der Supraleitung, Physikalisches Kolloquium TU Chemnitz, 8.7.09 (2009).
226) L. Schultz, Riding on magnetic fields - the miraculous world of superconductivity, DPG SKM Spring Meeting 2009, Dresden, 24.3.09 (2009).
227) L. Schultz, Voellig losgeloest - vom Schweben auf Magneten, Physik im Kaufpark, Dresden, 16.-21.3.09 (2009).
228) L. Schultz, Riding on magnetic fields - the miraculous world of superconductivity, Kolloquiumsvortrag, Department of Engineering, University of Cambridge/ UK, 1.9.09 (2009).
229) L. Schultz, Dreaming of the flying carpet - magnetic levitation using superconductors, German-Middle East International Conference, Amman/ Jordan, 10.-11.5.09 (2009).
230) L. Schultz, Riding on magnetic fields- the miraculous world of superconductivity, Plenary Talk, Euromat 2009, Glasgow/ UK, 7.9.09 (2009).

231) L. Schultz, Riding on magnetic fields - the miraculous world of superconductivity, Seminar Talk, University of Glasgow/ UK, 9.9.09 (2009).
232) L. Schultz, Riding on magnetic fields - the miraculous world of magnetism and superconductivity, Symposium on Materials for a Sustainable Future After Dinner Talk, University of Birmingham/ UK, 11.-12.9.09 (2009).
233) L. Schultz, Schwebesysteme in der bahntechnischen Forschung - passiv stabiles magnetisches Schweben mit Supraleitern, Saechsisch-Russisches Partnerschaftsprogramm: Innovationsmanagement, Dresden, 4.11.09 (2009).
234) L. Schultz, Voellig losgeloest - Vom Schweben auf Magneten, "Physik im Kaufpark", Kaufpark Nickern, Dresden, 17.-20.3.09 (2009).
235) J. Schumann, Duennschicht - Praezisionswiderstaende fuer sensorische und aktorische Anwendungen, VDI - Fachausschuss-Sitzung "Innovative Sensortechnologien und Anwendungen", Leibniz-Universitaet Hannover, 23.9.09 (2009).
236) R. Schuster, Electron energy-loss spectroscopy on underdoped CaNaCuOCl, Arbeitsgruppenseminar, Fribourg/ Schweiz, 8.-9.12.09 (2009).
237) R. Schuster, Inelastic electron scattering on underdoped CaNaCuOCl, Seminar der Abteilung Keimer, MPI Stuttgart , 24.11.09 (2009).
238) M. Seifert, V. Neu, L. Schultz, Magnetization processes and spin reorientation in epitaxial NdCo5 thin films, Seminar ueber Wachstum und Magnetismus von Systemen reduzierter Dimensionen, Universitaet Hamburg, 12.11.09 (2009).
239) A.A. Solovev, Self-assembled microjet engines, DSM Science and Technology Award (South) Vitznau/ Switzerland, 21.-23.6.09 (2009).
240) A. Sotnikov, H. Schmidt, M. Weihnacht, Characterization of new promising piezoelectric crystals, International Mini-Conference on Information Electronics Systems, Sendai/ Japan, 27.-28.10.09 (2009).
241) U. Stockert, Towards Ettingshausen refrigeration: The Nernst effect in CeNiSn, Gemeinsames Seminar des Forschungszentrums Karlsruhe und der Universitaet Karlsruhe, Festkoerperphysik, KIT, Karlsruhe, 2.11.09 (2009).
242) M. Stoica, J. Eckert, D. Ruiz Romera, N. Van Steenberge, G. Vaughan, A.R. Yavari, FeCoBSiNb bulk metallic glasses: thermal stability and magnetic properties, The WPI-Europe Workshop on Metallic Glasses and Related Materials, Grenoble/ France, 25.-28.8.09 (2009).
243) M. Stoica, R. Li, S. Roth, J. Eckert, G. Vaughan, A.R. Yavari, Magnetic properties of FeCoBSiNb BMGs with Cu additions, 11th International Conference on Advanced Materials- ICAM 2009, Rio/ Brazil, 20.-25.9.09 (2009).
244) M. Stoica, R. Li, A.R. Yavari, G. Vaughan, J. Eckert, Thermal stability and magnetic properties of FeCoBSiNb bulk metallic glasses, International Symposium on Metastable, Amorphous and Nanostructured Materials- ISMANAM 2009, Beijing/ China, 5.-9.7.09 (2009).
245) M. Stoica, S. Roth, J., Vaughan, G. Eckert, A.R. Yavari, FeCoBSiNb bulk metallic glasses with Cu additions, E-MRS Fall Meeting 2009, Warshaw/ Poland, 14.-18.9.09 (2009).
246) K. Tschulik, J. Koza, M. Uhlemann, A. Gebert, L. Schultz, Electrodeposition of structured metallic layers in magnetic gradient fields, Group Seminar AK Eychmueller, TU Dresden, 4.11.09 (2009).
247) M. Weihnacht, Materials and material systems for acoustic wave devices, 2009 IEEE International Ultrasonics Symposium, Rom/ Italy, 20.-23.9.09 (2009).
248) N. Wizent, Hochdruckkristallzuechtung ausgewaehlter Oxidverbindungen, Seminarvortrag, Aachen, 14.7.09 (2009).
249) U. Wolff, Investigation of magnetic thin films and nanostructures by in-field magnetic force microscopy, Seminar Microscopy and Microanalysis - Physics Department, Chalmers University, Gothenborg/ Sweden, 5.-6.11.09 (2009).
250) U. Wolff, Magnetic force microscopy of magnetic thin films and nanostructures at different temperatures and applied fields, Seminar am Ris¯ National Laboratory for Sustainable Energy , Technical University of Denmark, Roskilde/ Denmark, 9.-11.11.09 (2009).
251) U. Wolff, In-field magnetic force microscopy of magnetic thin films and nanostructures, Seminar, I. Physikalisches Institut, Georg-August-Universitaet Goettingen, 13.-14.7.09 (2009).
252) F. Wolny, Kohlenstoffnanoroehren - Vielfalt in Form und Funktion, Ausstellung "nano and art", Kugelhaus am Wiener Platz, Dresden, 23.9.09 (2009).
253) A. Wolter, Magnetic carbon nanotubes for biomedical applications, "1ere Ecole Nanomateriaux et Applications biomedicales" Winterschule in Bizerte/ Tunesien, 2.-6.11.09 (2009).
254) T.G. Woodcock, O. Gutfleisch, Multi-phase local texture analysis in NdFeB sintered magnets, Vortrag am Max Planck Institut fuer Eisenforschung, Duesseldorf, 30.11.09 (2009).
255) S. Wurmehl, Nuclear magnetic resonance applied to spin polarized Heusler compounds, DFG-JST Treffen 2009, Kyoto/ Japan, 19.-25.1.09 (2009).
256) S. Wurmehl, Nuclear magnetic resonance applied to spin polarized Heusler compounds, Vortragsbeitrag zum Dreikoenigstreffen der Fachgruppe Magnetismus der DPG, Bad Honnef, 5.-7.1.09 (2009).
257) S. Wurmehl, Spin polarized Heusler compounds, MRS Fall Meeting, Boston/ USA, 30.11.-4.12.09 (2009).

Patents

Issues of Patents 2009

DE 101 63 517 — Resonatorfilterkaskade
Inventors: G. Martin et al.

DE 103 01 722 — Verfahren zur Herstellung endohedraler Fullerene
Inventors: L. Dunsch, P. Georgi, F. Ziegs, H. Zöller

DE 198 37 743 — Akustischer Oberflächenwellenfilter
Inventor: G. Martin

DE 10 2006 027 060 — Oszillatorkreis mit akustischen Eintor-Oberflächenwellenresonatoren
Inventors: G. Martin et al.

DE 10 2008 001 000 — Schichtsystem für Elektroden
Inventor: S. Menzel

Patent Applications 2009

10903 — Isolationsmaterial für integrierte Schaltkreise
Inventors: H. Hermann et al.

10907 — Verfahren zur Steuerung der magnetischen Hyperthermie
Inventors: R. Klingeler, Y. Krupskaya, B. Büchner

10908 — Wandler mit natürlicher Unidirektionalität für akustische Oberflächenwellen
Inventors: G. Martin, M. Weihnacht, S. Biryukov, A. Darinski et al.

10909 — Verfahren und Anordnung zum Anregen von elektro-akustischen Aktuatoren
Inventors: R. Brünig, K. Mensel, H. Schmidt

10910 — Strangförmiges Kompositleitermaterial
Inventor: S. Menzel

10912 — Unidirektionaler Wandler für akustische Oberflächenwellen
Inventor: G. Martin et al.

10913 — Verfahren zur Ermittlung elektrischer und mechanischer Materialeigenschaften
Inventors: G. Guhr, R. Brünig et al.

10914 — Magnetisches Legierungsmaterial und Verfahren zu seiner Herstellung
Inventors: J. Lyubina, O. Gutfleisch

10915 — Bauelement aus einem ferromagnetischen Formgedächtnismaterial und dessen Verwendung
Inventors: S. Fähler, M. Thomas, O. Heczko, J. Buschbeck, J. Mc Cord

10918 — Peltier-Seebeck basiertes thermoelektrisches Bauelement und Verfahren zu seiner Herstellung
Inventors: T. Dienel, J. Schumann, A, Rastelli, O.G. Schmidt

10919 — Thermoionisches Bauelement und Verfahren zu seiner Herstellung
Inventors: T. Dienel, J. Schumann, A, Rastelli, O.G. Schmidt

10924 — Metastabile Legierungen und Verfahren zu ihrer Herstellung
Inventors: J. Eckert, S. Pauly, U. Kühn

PhD Theses 2009

Francesca Cavallo	Strain driven architecture of Si-based nanomembranes
Thomas Dienel	Molekulare Systeme im Wechselspiel von Struktur und Ladung
Fei Ding	Quantum device oriented researches of semiconductor micro-/ nanostructures
Antje Elsner	Computergestützte Simulation und Analyse zufälliger dichter Kugelpackungen
Sebastian Engel	Chemisch deponierte Schichtsysteme zur Realisierung von YBCO-Bandleitern
Mandy Grobosch	Experimentelle Bestimmung der elektronischen Eigenschaften anwendungsrelevanter Grenzflächen organischer Halbleiter mittels Photoelektronenspektroskopie
Ingo Hellmann	Magnetische und elektronische Eigenschaften von Übergangsmetalloxid-Nanostrukturen
Marko Herrmann	Einfluss von Präparation und Dotierung auf die supraleitenden Eigenschaften in mechanisch legierten Magnesium-Diborid
Denis Klemm	Analyse dünner Schichten mit der optischen Glimmentladungs-spektroskopie
Ah-Ram Kwon	Epitaxial Nd-Fe-B films: Growth, texture, magnetism and the influence of mechanical elongation
Ryan Y. W. Lai	Magnetic Microstructure and Actuation Dynamics of NiMnGa Magnetic Shape Memory Materials
Andreas Nilsson	BSCCO superconductors processed by the glass-ceramic route
Anreia Ioana Popa	Electrochemistry and magnetism of Li-doped transition metal oxides
Franziska Schäffel	Synthesis, characterization and modification of carbon nanomaterials
Uwe Schaufuß	Hochfeld/Hochfrequenz-Elektronenspin-Resonanz an Übergangsmetall-verbindungen mit starken elektronischen Resonanzen
Nils Scheerbaum	Magnetische NiMnGa-Komposite
Nadja Wizent	Hochdruckkristallzüchtung ausgewählter Oxidverbindungen
Kostyantyn Zagorodniy	Molekularer Entwurf neuer Isolationsmaterialien für mikroelektronische Anwendungen
Tim Zander	Herstellung und Eigenschaften von Metall/Halbleiter-Übergittern und Mikroringresonatoren
Hongbin Zhang	Relativistic density functional treatment of magnetic anisotropy
Lijuan Wang	Growth and spectroscopic characterization of self-assembled lateral quantum dot molecules
Kim Jong Woo	Multiferroic hexagonal $HoMnO_3$ films

Diploma and Master Theses 2009

Naveen K. Abraham	Experimental Preparation of Theoretically Designed Insulating Materials for Furture Microelectronic Applications
Leif Bader	Mikrostrukturelle und mechanische Charakterisierung von Fe-C-(Cr)-(Mo)-(V)-Legierungen
Dirk Bombor	Konstruktion eines Rastertunnelmikroskops für variable Temperaturen und Oberflächenunter-suchungen an supraleitenden Eisenpniktiden
Maria Dimitrakopoulou	Synthesis and Characterization of Silicon Nanowires
Christian Görner	Konzept zum Umbau einer Walzanlage für das Walzen von Blechen aus amorphen Metalllegierungen (BA)
Veronika Hähnel	Elektrochemisch hergestellte Fe-Nanodrähte: Struktur, Morphologie und magnetische Eigenschaften
Wenbo Han	Functionalisation of carbon nanotubes for application as sensor materials
Alexander Kauffmann	Eisenpniktidsupraleiter in gepulsten Magnetfeldern bis 50 T
Roberto Kraus	Elektronen-Energie-Verlust-Spektroskopie an TiOCl
Maria Krautz	Realstruktur und antiferromagnetische Eigenschaften einer technischen FeMnNiCr-Legierung
Steve Kupke	Elektrischer Transport an freistehenden eisengefüllten, mehrwandigen Kohlenstoffnanoröhren
Jens Liebich	Präparation von Festbett-Katalysatoren auf Basis von Fe, Co, Mo und V für die Herstellung von SWCNTs/DWCNTs
Inge Lindemann	Einfluss eines äußeren Magnetfeldes auf die Anordnung von Cu-Au-Nanopartikeln
Daniel Lorenz	Numerische Simulation der zellularen Erstarrung von Silizium
Tom Marr	Texturentwicklung von Ni-5at%W Rohrmaterial
Rafael Gregorio Mendes	Magnetic Force Microscopy of Nanomagnets
Enrico Mund	Synthese und Charakterisierung von Wolfram- Nanodrähten und deren Verwendung in metallischen Glasmatrix-Kompositen
Friedrich Roth	Untersuchung der optischen Eigenschaften von Supraleitern aus der Gruppe der Eisenarsenide
Christian Schmidt	Photoemissionsspektroskopie an Übergangsmetell-Phthalocyaninen
Tobias Schneider	Entwicklung und Umsetzung einer Herstellungstechnologie für Sensorelemente aus einer amorphen Zirkon-Basislegierung
Sailaja Tetali	Growth enhancement of Carbon Nanotubes using O_2 and H_2 by using Laser Ablation method
Mario Tränkner	Quantitative Bestimmung nanoskaliger $Sr_{n+1}Ti_nO_{3n+1}$-Ruddlesden-Popper Phasen mittels Analyse von TEM-Messungen
Zimo Wang	Functionalisation of carbon nanotubes for biomedical applications

Calls and Awards 2009

Calls on Professorships

Dr. Rüdiger Klingeler	Univ. Heidelberg
Prof. Dr. Bernd Büchner	Univ. Mainz
Prof. Dr. Jürgen Eckert	Univ. Stuttgart

Awards

Prof. Dr. Jürgen Eckert	Gottfried-Wilhelm-Leibniz-Prize 2009 of the DFG
Prof. Dr. Ludwig Schultz	FEMS Gold Medal 2009
Dr. h. c. Rolf Pfrengle	Honorary Doctorate of the Slovakian TU Bratislava
Alexander Solovev	DSM Science and Technology Award 2009
Dr. Christian Kramberger	Prize of the Dresdner Gesprächskreis der Wirtschaft und der Wissenschaft e.V. 2009
Franziska Wolny	First Prize of the Nano&Arts contest
Claudia Hürrich	Second Prize of the Science as Art Competition at the 2009 MRS Fall Meeting in Boston

Publication and Poster Awards

Uta Kühn et al.	Best Poster Award EUROMAT 2009 in Glasgow
Ute Queitsch	Best PhD Poster Award, Trends in Nanotechnology 2009, Barcelona 7-11 September 2009
Jakub Koza	Best Poster Award of the International Conference on Electromagnetic Processing of Materials (EPM 2009)
Ahmed El-Gendy	Best Poster Award of the SFB 491 Summer School on Nanomagnetism
Maria Sparing	Best Poster Award EUCAS 2009 in Dresden

IFW Awards

Dr. Christian Hess	IFW Research Award 2009
Dr.-Ing. Franziska Schäffel	Deutsche Bank Junior Award 2009 for the best PhD thesis
Dr. Mark Rümmeli	IFF Research Award 2009
Dr. Jens Freudenberger	IMW Research Award 2009
Dr. Sergio Scudino	IKM Research Award 2009
Dr. Armando Rastelli	IIN Research Award 2009
Dr. Manuel Richter	ITF Research Award 2009

Conferences and colloquia 2009

Conferences

Kick-Off Meeting of the EU project DIVERSITY
January 16–17, 2009
Chairman: Dr. h.c. R. Pfrengle (IFW Dresden)
30 Participants

Deutsche Kristallzüchtungstagung
March 4 - 6, 2009 in the IFW Dresden, Germany
Chairman: Dr. Behr (IFW Dresden)
100 Participants

DPG Frühjahrstagung der Sektion Kondensierte Materie 2009
March 22 - 27, 2009 in Dresden, Germany
Chairman: Prof. L. Schultz (IFW Dresden)
4500 participants

XXIII International EPR Seminar
April 23 - 25, 2009 in Bad Gottleuba, Germany
Chairman: Prof. L. Dunsch (IFW Dresden), Prof. V. Brezová (SK), Dr.P.Rapta (SK)
50 participants

Spin Caloritronics
Mai 12 - 15, 2009 in the IFW Dresden, Germany
Chairpersons: Prof. B. Büchner (IFW Dresden), Prof. C. Felser (Univ. Mainz)

EUCAS 2009: 9th European Conference on Applied Superconductivity
September 13 - 17, 2009 in Dresden, Germany
Chairman: Prof. L. Schultz (IFW Dresden)
850 participants

Kick-off meeting of the DFG Priority Program1458 "HTS in Fe Pnictides"
July 22, 2009 in the IFW Dresden, Germany
Chairperson: Prof. Dr. B. Büchner (IFW Dresden)

IFW Colloquia

Prof. Albert van den Berg, Univ. of Twente, Netherlands, Lab-on-a-Chip: from micro/nanofluidic research-platform to biomedical applications, 08.01.2009

Prof. Klaus Muellen, Max-Planck Institute for Polymer Research, Mainz

Molecular Electronics, 15.01.2009

Prof. Angel Rubio, Univ. del Pais Vasco, Spain, Excited state dynamics of nanostructures and biomolecules within time-dependent DFT22.01.2009

Prof. Richard Berndt, Univ. Kiel, Conductance of single atoms, clusters and molecules, 26.02.2009

Prof. Jörg J. Schneider, TU Darmstadt, Carbon nanotubes and inorganic oxides: Synthesis and functional material properties, 02.04.2009

Prof. Atac Imamoglu, ETH Zürich, Cavity-QED with a single quantum dot in a nano-cavity, 16.04.2009

Prof. Jürgen Janek, Univ. Gießen, Micro- and Nano-Ionics - Interfaces of solid electrolytes, 23.04.2009

Prof. Ravi Silva, Univ. of Surrey, Carbon Nanotubes: Developing a Platform for Physical and Biological Applications, 30.04.2009

Prof. Klaus Kern, MPI für Festkörperforschung, Stuttgart, Metal-Organic Nanocontacts, 07.05.2009

Prof. Anke Rita Pyzalla, Helmholtz-Zentrum Berlin für Materialien und Energie GmbH

Material characterization using neutrons and synchrotron radiation, 25.06.2009

Prof. Quentin A. Pankhurst, London Centre for Nanotechnology, Univ. College London

Biomedical applications of nanoscale magnetic materials, 02.07.2009

Prof. Peter Littlewood, Cambridge Univ., A new condensate of matter and light: Bose Einstein Condensation of Polaritons, 29.10.2009

Prof. Joachim Spatz, MPI f. Metallforschung Stuttgart, Molecular engineering of cellular environments, 05.11.2009

Prof. John A. Rogers, Univ. of Illinois, Materials for Stretchable Electronics: From Hemispherical Digital Imagers to Devices for Cardiac Electrophysiology, 19.11.2009

Prof. Ferdi Schüth, Max-Planck-Institut für Kohlenforschung, Design von funktionalen Nanomaterialien, 10.12.2009

IFW Winterschool on low dimensions in Oberwiesenthal, January 18-21, 2009

Honorary colloquim on occasion of the award of Prof. Dr. Jürgen Eckert with the Leibniz-Prize 2009, 06.04.2009

Honorary colloquium on the occasion of the 60th anniversary of Dr. h. c. Rolf Pfrengle, 21.04.2009

Opening of the IFW-Colloquium in the winter terms with talks of the prizewinners of the Research-Awards 2009 of the IFW´s Institutes, Oct. 15, 2009

Seminars of the IFW's Institutes

Joint Seminars

Prof. Mostovoy Maxim Vladimirovich Vladimirovich, Univ. of Groningen, Magnetoelectric Coupling in Frustrated Magnets, 15.01.2009, Joint Seminar

Christoph Bruch, Max Planck Digital Library, Will open access change scientific publishing? 27.04.2009, Joint Seminar

Prof. Peter Abbamonte, Univ. of Illinois at Urbana-Champaign, Charge accumulation at La CuO-LaSrCuO4 interfaces observed with resonant soft x-ray scattering, 24.11.2009, ITF-IFF-Seminar

Dr. John Hill, Brookhaven National Laboratory, Hard X-ray RIXS, polarization dependence and orbitons, 02.12.2009, ITF-IFF-Seminar

Dr. Giacomo Ghiringhelli, Politecnico di Milano, Electronic and magnetic excitations studied by high resolution soft x-ray resonant inelastic scattering, 09.12.2009, ITF-IFF-Seminar

Dr. Stephan Roche, TU Dresden & CEA, Institute of Nanosciences and Cryogenics Grenoble, Carbon-based Nanosciences & Nano-technologies: Nanotubes and Graphene at the Heart, 21.07.2009, Joint Seminar IFF and TU Dresden

IFF-Seminars

Prof. Jürgen Schnack, Univ. Bielefeld, Trends in Molecular Magnetism - A Personal Perspective, 22.01.2009

Prof. Bert Koopmans, Eindhoven Univ. of Technology, The Physics of Plastic Spintronics, 26.01.2009

Dr. Alexey Popov, IFW Dresden, Spectroelectrochemistry of fullerene derivatives, 23.02.2009

Prof. Yurii V. Kopaev, Lebedev Physics Institute, Russian Academy of Sciences, Moscow, Biordered superconducting state and the pseudogap, 24.02.2009

Prof. Andreas Hirsch, Univ. Erlangen-Nürnberg, Water-Solubility and Antioxidant Activity of Various Exohedral Fullerene Derivatives, 09.03.2009

Dr. Gerhard Jakob, Univ. Mainz, Thin films of Heusler compounds, 30.03.2009

Dr. Klaus Braun, Deutsches Krebsforschungszentrum Heidelberg, Behandlung von GBM-Zellen mit TMZ-Bioshuttles, 17.04.2009

Dr. John M. Tranquada, Brookhaven National Laboratory, Intertwined Spin, Charge, and Superconducting Orders in Cuprates, 20.04.2009

Prof. Jacques Jupille, Univ. Pierre et Marie Curie Paris, Growth and wetting at a glance, 21.04.2009

Prof. Kurt Westerholt, Ruhr-Univ.t Bochum, Proximity effects in superconductor/ferromagnet thin film heterostructures, 08.06.2009

Dr. Philippe Moreau, Uni. de Nantes, Electron energy-loss spectroscopy to study electronic structures of materials: from lithium battery matarials to perovskites, 15.06.2009

Prof. Andreas Hirsch, Univ. Erlangen-Nürnberg, Water-Solubility and Antioxidant Activity of Various Exohedral Fullerene Derivatives, 22.06.2009

Dr. Thomas Seyller, Univ. Erlangen-Nürnberg, Epitaxial graphene on SiC - a new material for carbon-based electronics, 24.06.2009

Dr. Giuseppe Cirillo, Univ.della Calabria, Functionalized Carbon Nanotubes with antioxidant properties, 29.06.2009

Prof. Dirk Morr, Univ. of Chicago, Pseudo-gap and Coexisting Phases in the Cuprate Superconductors, 24.07.2009

Prof. Wolfgang Windl, Ohio State Univ. Columbus, Electronic Structure Calculations of Materials: From Spin Lifetimes to Bulk Metallic Glasses, 28.07.2009

Prof. Patrick Woodward, Ohio State Univ., Complex Perovskites: Mining the periodic table for new functional materials, 31.07.2009

Dr. Steffen Sykora, TU Dresden, Microscopic approach to high-temperature superconductors within the t-J model, 31.08.2009

Dr. Danny Porath, Hebrew Univ. of Jerusalem, From bio-inspired systems for nanoelectronics to physico-inspired tools to study bio-systems, 08.09.2009

Prof. Junichi Kushibiki, Tokohu Univ. Sendai, Ultrasonic Micro-Spectroscopy Technology and its Recent Applications, 18.09.2009

Dr. Pedro M.F.J. Costa, Univ. of Aveiro, Portugal, In situ characterisation of filled carbon nanotubes: adding a sense of touch to TEM, 23.09.2009

Dr. Wilhelm Auwärter, TU München, Looking at the interior of functional molecules: Tunneling microscopy and spectroscopy on adsorbed porphyrins, 09.10.2009

Prof. Dieter Kölle, Univ. Tübingen, Microscopic Analysis of electric transport and noise in superconductors, 26.10.2009

Dr. Dimitri Argyriou, Helmholtz-Zentrum Berlin, Is there a pseudogap in the Bi-layer manganites? 27.10.2009

Dr. Paola Ayala, Univ. Wien, Substitutionally-Functionalized vs Metallicity-selected Single-Walled Carbon Nanotubes, 06.11.2009

Dr. Sebastian Gönnenwein, Walther-Meißner-Institut, TU München, Magnetoelastic magnetization manipulation in ferromagnet/ferroelectric hybrids, 16.11.2009

Prof. Oleg Sinyashin, A.E. Arbuzov Institute of Organic and Physical Chemistry Kazan, Interplay between structure and molecular interactions in the complexes of phosphorus-sulfur containing compounds, 17.11.2009

Prof. Chun-Ru Wang, Institute of Chemistry, Chinese Academy of Sciences, Several Novel Endohededral Metallofullerenes, 17.11.2009

Dr. Thorsten Schmitt, Swiss Ligth Source, PSI Villingen, Resonant Inelastic Soft X-Ray Scattering in Quasi One Dimensional Cuprates, 26.11.2009

Prof. Carita Kvarnström, Univ. of Turku, Spectroelectrochemistry of conducting polymers, 26.11.2009

Dr. Dmitry Yakhvarov, A.E. Arbuzov Institute of Organic and Physical Chemistry, Russian Academy of Sciences, Kazan, Russia, Electrochemical methods for new chemical technologies and material science, 27.11.2009

Prof. Christopher Brett, Univ. of Coimbra, Portugal, Some recent achievements and future perspectives in electrochemistry,01.12.2009

Prof. Erich Kleinpeter, Univ. Potsdam, Spatial Magnetic Properties of Molecules Subjected to Anisotropic Effects of Functional Groups and Planar/Spherical (Anti)aromaticity, 03.12.2009

Dr. Valentina Bisogni, ESRF Grenoble, Low energy excitations in cuprates: a resonant inelastic X-ray scattering investigation, 04.12.2009

Dr. Katja Weichert, Max-Planck-Institut für Festkörperforschung Stuttgart, LiFePO4 single crystals - electrochemical characterisation and defect chemistry, 07.12.2009

Dr. Björn Bräuer, Stanford Univ. USA, Scanning transmission x-ray microscopy imaging of magnetic nanostructures and organic semiconductor devices, 14.12.2009

Dr. Markus Kriener, Kyoto Univ. Japan, Superconductivity in the charge-carrier doped wide-gap semiconductors diamond, silicon, and silicon carbide,18.12.2009

IMW-Seminars

Prof. Andreas Mortensen, EPFL, Laboratory of Mechanical Metallurgy, Lausanne, Replicated open-pore microcellular aluminium: processing and properties 8.1.2009

Prof. Eberhard Burkel, Univ. Rostock, Neue Materialien für den Cell-Material Dialogue und die Technik, 15.01.2009

Prof. Ralf Wehrspohn, Fraunhofer-Institut für Werkstoffmechanik, Halle, Geordnete poröse Materialien und Anwendungen, 22.01.2009

Jose M. Barandiaran; Volodymyr Chernenko; Jorge Feuchtwanger, Univ. del Pais Vasco, Ferromagnetic Shape Memory Effect, 04.02.2009

Prof. Ibrahim Karaman Karaman, Texas A&M Univ., Recent Advances in Shape Memory Alloys, 20.02.2009

Dr. Johann Schnagl, BMW Group München, Wasserstoff-Tanks, 23.04.2009

Prof. Dietrich Wolf, Univ. Duisburg-Essen, Struktur und Dynamik von Nanopulvern, 04.05.2009

Prof. Robert F. Singer, Univ. Erlangen - Nürnberg, Neue Materialien und Prozesse für Gasturbinen in der Energieerzeugung, 02.07.2009

Prof. Hans-Josef Hug, Univ. of Basel and EMPA, Switzerland, The role of uncompensated spins for the exchange bias effect, 16.07.2009

Dr. Alina Deac, FZ Jülich, Spin-transfer effects in metallic multilayers with in-plane reference and out-of-plane free layer: An analytical model, 05.11.2009

Dr. Martin Wagner, Ruhr-Univ. Bochum, New experimental and theoretical insights into the mechanical behavior of NiTi thermal shape memory alloys, 19.11.2009

Prof. Kazuhiro Hono, Univ. of Tsukuba, Japan, Advances in laser assisted atom probe and its applications to the interface characterizations of permanent magnets, 03.12.2009

Prof. Ophir Auslaender, Technion - Israel Institute of Technology, Using magnetic force microscopy to study superconductors: from vortex manipulation to measuring the magnetic penetration depth, 10.12.2009

IKM-Seminars

Prof. Karl-Ulrich Kainer, GKSS Forschungszentrum Geesthacht, Strategien zur Modifizierung der Zug-Druck-Anisotropie bei Magnesium-Knetlegierungen, 14.01.2009

Dr. Claus Burkhardt, NMI Reutlingen, Analyse an organischen/anorganischen Biomaterialien und Beschichtungen mit FIB-SIMS, 28.01.2009

Henrich Schleifenbaum, FhI für Lasertechnik Aachen, Werkzeug Licht - Werkstoff- und funktionsgerechte Bauteilherstellung mittels Selective Laser Melting, 04.02.2009

Dr. Daniela Zander, Univ. Dortmund, Korrosion von Titanlegierungen in biologischen Ersatzelektrolyten für den Einsatz in der Medizintechnik, 11.02.2009

Dr. Andrés Fabián Lasagni, Fraunhofer IWS Dresden, Surface Functionalization and 2D-3D design using Direct Laser Interference Patterning, 06.05.2009

Dr. Johann Michler, EMPA, Switzerland, In situ Analyse mittels Nanointender, 12.05.2009

Dr. Alexandra Lex, Univ. Münster, The Role of the Electrolyte in Lithium Ion Batteries, 13.05.2009

Dr. Thomas Ebel, GKSS Geesthacht, Metal Injection Moulding von Titan- und Magnesiumlegierungen, 27.05.2009

Prof. Dr. Ludwik Dobrzynski, Andrzej Soltan Institute for Nuclear Studies & Univ. of Bialystock, Warsaw, Poland, Structure, Spin distributions and Spin Dynamics in DO3-type of alloys based on Fe3si and Fe3Al, 03.06.2009

Prof. Dr.-Ing. Christoph Leyens, TU Cottbus, Ti-Legierungen für Anwendungen in der Luft- und Raumfahrt, 24.06.2009

Prof. Robert Glaum, Univ. Bonn, Redox-Verhalten und katalytische Eigenschaften von Phosphaten der Übergangsmetalle, 01.07.2009

Dr. Ahmed Shariq, Fraunhofer Center for Nanoelectronic Technologies, Dresden, Three Dimensional Structural and Compositional Analyses of Semiconducting Materials using Atom Probe Tomography, 02.12.2009

IIN-Seminar

Dr. Anthony J. Bennett, Toshiba Research Europe Ltd., Cambridge, UK, Indistinguishable photons from electrically-driven single quantum dots, 09.01.2009

Dr. Till Hartmut Metzger, ESRF, Grenoble, France, Nanostructures in the light of synchrotronradiation, 16.01.2009

Dr. Alexandre Jacquot, Fraunhofer-Institut für Physikalische Messtechnik, Freibug, Transport properties measurement on problematic samples with the 3Omega-Method, 20.02.2009

Dr. Dmitri Yakovlev, TU Dortmund, Spin coherence of electrons in singly-charged quantum dots, 06.03.2009

Prof. Thomas Heinzel, Univ. Düsseldorf, Transport properties of magnetic barriers, 20.03.2009

Na Liu, Univ. Stuttgart, Three-dimensional metamaterials at optical frequencies, 27.03.2009

Dr. Stefan Mendach, Univ. Hamburg, Spin wave optics in ferromagnetic waveguides and resonators, 03.04.2009

Dr. Ing. Federico Peretti, TU München, Modelling of coplanar devices and equivalent circuit analysis of their interaction with two-level quantum systems, 17.04.2009

Dr. Li Zhang, ETH Zürich, Helical Nanobelts as Motion Converters, 08.05.2009

Dr. Silvano De Franceschi, CEA, Institute for Nanoscience and Cryogenics, Grenoble, France, Quantum transport in self-assembled semiconductor nanostructures, 25.05.2009

Ibraheem A.I. Al-Naib, TU Braunschweig, Microwave and Terahertz Applications of Metamaterials, 28.05.2009

Prof. Carsten Timm, TU Dresden, Molecular Spintronics and the Master Equation, 05.06.2009

Dr. Michal Grochol, Univ. Erlangen, Exitons and photons in cavity-embedded quantum dot lattices, 03.07.2009

Prof. Geoffrey A. Ozin, Univ. of Toronto, P-Ink and Elast-Ink Lab to Market, 13.07.2009

Dr. Kevin A. Prior, Heriot-Watt Univ. Edinburgh, II-VI semiconductors: an overview and MBE Growth at Heriot-Watt Univ., 14.07.2009

Jessica E. Bickel, Univ. of Michigan, The effect of Strain on Surface Reconstructions in Compound Semiconductor Alloys, 17.08.2009

Prof. Guiseppe Grosso, Univ. di Pisa, Tight finding model for the electronic and optical properties of multilayer Silicon/Germanium nanostructures, 11.09.2009

Prof. Hans von Känel, ETH Zürich, Strained Silicon-Germanium Heterostructures, 25.09.2009

Dr. Fei Ding, IFW Dresden, Versatile strain engineering of quantum dots, microrings and grapheme, 09.10.2009

Dr. Marco Schowalter, Univ. Bremen, Quantification of composition in semiconductor heterostructures using TEM, 23.10.2009

Prof. Xingyu Jiang, National Center for Nanoscience + Technology, Beijing, China, Micro/Nano-Scale Tools for Biochemical Analysis, 26.10.2009

Carmine Ortix, Univ. Leiden, Netherlands, Electronic properties of rolled-up materials, 30.10.2009

Prof. Peter Kratzer, Univ. Duisburg-Essen, Theory of the shape evolution of InAs quantum dots on GaAs(001) and In0.5Ga0.5As(001) substrates, 06.11.2009

Dr. Samuel Sanchez, IFW Dresden + WPI, MANA, National Institute for Materials Science, Tsukuba, Ibaraki, Japan, Nanorobots: the ultimate wireless self-propulsed sensing and actuating devices, 20.11.2009

Prof. Dr. Georgeta Salvan, TU Chemnitz, Organic semiconductors for spintronic applications, 27.11.2009

Prof. Dr. David Snoke, Univ. of Pittsburgh, USA, Bose-Einstein Condensation of Polaritons in a Two-Dimensional Trap, 21.12.2009

ITF- Seminars

Dr. Emmanuele Cappelluti, Univ. of Rome "La Sapienza", SMC Research Center, Calculation of Effective Born Charges for Bilayer Graphene, 12.02.2009

Dr. Jan Kunes, Univ. Augsburg, What do the Correlations do? Selected Materials with Dynamical Mean-Field Approximation, 28.05.2009

Prof. Helmut Eschrig, IFW Dresden, The electronic structure of iron-based superconductors revisited, 11.06.2009

Dr. Roman Kuzian, lnstitute for Materials Science, Kiev, A polar state in SrTiO3 induced by manganese impurities, 25.06.2009

Prof. Gernot Paasch, Dr. Susanne Scheinert, IFW Dresden / TU Ilmenau, Space-charge-limited currents in organics with trap distributions: Analytical approximations vs. numerical simulation, 09.07.2009

Dr. Stefaan Cottenier, Center for Molecular Modeling (CMM), Ghent Univ., Belgium, Gamma-Fe4N: facts, hypotheses and open questions, 21.09.2009

Prof. Christian Elsässer, Fraunhofer IWM, Freiburg, First-principles modelling of interfaces in functional metal-oxide devices, 24.09.2009

Prof. Józef Spalek, Marian Smoluchowski Institute of Physics, Jagiellonian Univ., and Univ. of Science and Technology, Krakow, Poland, A quantum critical scaling of the wave function near the Mott-Hubbard transition, 30.10.2009

Dr. Oliver Fruchart, Institut Néel, Grenoble, Magnetization processes within domain walls and control of flux-closure chirality in micron-size self-assembled epitaxial dots, 09.12.2009

Dr. Maurits W. Haverkort, MPI für Festkörperforschung, Stuttgart, Theory of Resonant and non-Resonant Inelastic X-ray Scattering of Orbitons and Magnons, 10.12.2009

Guests and Scholarships

Guest scientists (stay of 4 weeks and more)

Name	Home Institute	Home country
Hanaa Abuzeid	National Research Centre Cairo	Egypt
Prof. Dr. Victor Aristov	Institute of Solid State Physics, Moscow	Russia
Dr. Jhon Bados Ipus	University of Seville, Spain	Columbia
Dr. Nilam Shankarrao Barekar	Indian Institute of Technology Kharagpur	India
Isil Birlik	Dokuz Eylul University Izmir	Turkey
Taufik Aljuhuri Bonaedy	INHA Univ. Inchean, Korea	Indonesia
Christian Bonatto Minella	GKSS FZ Geesthacht	Italy
Michal Bystrzejewski	Univ. Warszawa	Poland
Prof. Dr. Chuanbing Cai	Shanghai University	China
Dr. Ihor Chumak	Univ. Lvov	Ukraine
Dr. Alexander Darinskiy	Institute for Crystallography Moscow	Russia
Dr. Fei Ding	MPI Stuttgart	China
Dr. Evgenia Dmitrieva	Algorithm St. Petersburg	Russia
Hryhoriy Dmytriv	Lvov National University	Ukraine
Roger Domènech Ferrer	Univ. Autonoma de Barcelona	Spain
Feng Fan	Shanghai University	China
Prof. Dr. Ilgiz Garifullin	Zavoisky Phys.-Techn. Institute Kazan	Russia
Dr. Vadim Grinenko	Inst. for supercond. & solid state physics Moscow	Russia
Luminita Harnagea	University Paris	Rumania
Dr. Oleg Heczko	Institute of Physics, Praha	Czech Rep.
Dr. GaoShan Huang	University of Hong Kong	China
Dr. Kazumasa Iida	University of Cambridge, UK	Japan
Dr. Hemchandra Kandpal	Goethe Univ. Frankfurt/Main	India
Dr. Olga Kataeva	Arbuzov Inst. of Organic and Physical Chemistry Kazan	Russia
Dr. Andrea Rozalia Kellenberger	Univ. Politehnica Timisoara	Rumania
Dr. Vyacheslav Khavrus	Pisarzhevsky Inst. of Physical Chemistry Kiev	Ukraine
Prof. Dr. Konstantin Kikoin	Univ. Tel-Aviv, Israel	Russia
Dr. Timur Kim	Paul Scherrer Inst. Villigen, Switzerland	Russia
Dr. Xianghua Kong	Institute of Chemistry, Peking	China
Dr. Vlastimil Krapek	Inst. of Condensed Matter Physics, Brno	Czech Rep.
Natalia Kuratyeva	Nikolaev Inst. of Inorganic Chemistry, Novosibirsk	Russia
Dr. Roman Kuzian	Inst. for Materials Research Kiev	Ukraine
Pavel Leksin	Kazan Physical Technical Institute	Russia
Dr. Irene Lucas del Pozo	Institute of Aerospace Technique Madrid	Spain
Dr. Vladimir Lukes	Slovak. Univ. of Technology Bratislava	Slovakia
Matthias Lutz	University of Southampton, UK	Austria
Dr. Libo Ma	Shandong Normal University Jinan	China
Dr. Jiri Malek	Univ. Praha	Czech Rep.
Dr. Maria Markina	Lomonosov State University Moscow	Russia
Dr. Igor Morozov	Lomonosov State University Moscow	Russia
Prof. Alexander Moskvin	Ural State University, Yekaterinburg	Russia
Dr. Touyana Namsaraeva	Buryat State University, Ulan-Ude	Russia
Dr. Satoshi Nishimoto	MPI PKS Dresden	Japan
Dr. Dalibor Paar	Univ. Zagreb	Croatia
Dr. Jérome Paillier	HEITO Paris	France
Dr. Jin Man Park	Yonsei Univ. Seoul	Korea
Prof. Dr. Volodymyr Pavlyuk	Ivan Franko Lvov National University	Ukraine
Benjamin Podmiljsak	Jozef Stefan Institute Ljubljana	Slovenia

Dr. Ashim Kumar Pramanik	UGC-DAE Consortiu, University Indore	India
Dr. Peter Rapta	Slovak. University of Technology Bratislava	Slovakia
Dr. Samuel Sanchez Ordonez	Intern. Center for Materials Nanoarchitectonics, Tsukuba, Japan	Spain
Angelina Sarapulova	Geological Institute Ulan-Ude	Russia
Mahdi Sargolzaei	Univ. of Sciences and Technology Teheran	Iran
Dr. Chandra Shekhar	Banaras Hindu University	India
Dr. Surjeet Singh	Univ. de Paris-Sud	India
Dr. Konstantin Skokov	Tver State University	Russia
Dr. Elena Smirnova	A.F. Ioffe Physikal. Techn. Inst. St. Petersburg	Russia
Tatyana Vasilchikova	Moscow State University	Russia
Prof. Alexander Vasiliev	Moscow State University	Russia
Dr. Evgeniya Vavilova	Physical Technical Institute Kazan	Russia
Dr. Olga Volkova	Moscow State University	Russia
Lijuan Wang	MPI Stuttgart	China
Dr. Dmitry Yakhvarov	Inst. of Organic and Physical Chemistry Kazan	Russia
Dr. Galina Zakharova	Institute of Solid State Chemistry Yekaterinburg	Russia
Dr. Michal Zalibera	Slovak. TU Bratislava	Slovakia
Yue Zhang	TU Darmstadt	China
Dr. Feng Zhu	Changchun Institute of Applied Chemistry	China
Agnieszka Zlotorowicz	St. Petersburg State University	Poland
Dr. Elena Zvereva	Lomonosov State University, Moscow	Russia

Scholarships

Name	Home country	Donor
Jayaraj Jayamani	India	Alexander von Humboldt-Stiftung
Dr. Hengxing Ji	China	Alexander von Humboldt-Stiftung
Ran Li	China	Alexander von Humboldt-Stiftung
Prof. Dr. Gang Liu	China	Alexander von Humboldt-Stiftung
Dr. Qiang Luo	China	Alexander von Humboldt-Stiftung
Dr. Oksana Kvitnytska	Ukraine	Alexander von Humboldt-Stiftung
Dr. Guillaume Manilal Lang	France	Alexander von Humboldt-Stiftung
Dr. Daoyong Cong	China	Alexander von Humboldt-Stiftung
Ping Feng	China	Alexander von Humboldt-Stiftung
Dr. Alexey Popov	Russia	Alexander von Humboldt-Stiftung
Dr. Gang Wang	China	Alexander von Humboldt-Stiftung
James B. Whitaker	USA	Alexander von Humboldt-Stiftung
Marietta Seifert	Germany	Studienstiftung des deutschen Volkes
Maria Sparing	Germany	Studienstiftung des deutschen Volkes
Franziska Schäffel	Germany	Cusanuswerk
Silvia Vock	Germany	Cusanuswerk
Simon Pauly	Germany	Cusanuswerk
Yulieth Arango	Columbia	EU (AlBan Fellow)
Sebastiano Garroni	Italy	EU
Iwona Dobosz	Poland	EU
Maria Dimitrakopoulou	Greece	DAAD
Mohammed Yehia Taha El Bahrawy	Egypt	DAAD
Fedor Fedorov	Russia	DAAD
Dr. Ahmed Hashem	Egypt	DAAD
Trisha Karan	India	DAAD (IIT-Master-Sandwich-Programm)
Ram Bachchan Kumar	India	DAAD (IIT-Master-Sandwich-Programm)

Daniel Henrique Nogueira Dias	Brazil	DAAD
Roman Rezaev	Russia	DAAD
Kumar Babu Surreddi	India	DAAD
Ivan Tarasiuk	Ukraine	DAAD
Alexey Alfonsov	Russia	Int. Max-Planck Research School
Anupama Parameswaran	India	Int. Max-Planck Research School
Liran Wang	China	Int. Max-Planck Research School
Orkidia Zeneli	Albania	Int. Max-Planck Research School
Grzegorz Parzych	Poland	ECEMP Internat. Graduiertenschule
Dr. Alexander Grüneis	Austria	APART Austria
Fahad Ali	Pakistan	PIEAS Islamabad
Ahmed Aboud Mahmoud lgendy	Egypt	Egypt government
Abdelwahab Hamdy Hassan	Egypt	Egypt government
Dr. Eslam Mohamed Ibrahim	Egypt	Egypt government
Mahmoud Abdel-Hafez Mohamed	Egypt	Egypt government
Dr. Hong Seok Lee	Korea	Korea Res. Foundation / MURI (NATO)
Kaikai Song	China	China Scholarship Council
Jun Tan	China	China Scholarship Council
Yiku Xu	China	China Scholarship Council
Lin Zhang	China	China Scholarship Council
Yang Zhang	China	China Scholarship Council
Na Zheng	China	China Scholarship Council
Franziska Thoss	Germany	Deutsche Bundesstiftung Umwelt

Guest stays of IFW members at other institutes

Dr. Christoph Deneke	Brasil Synchrotron LNLS, Campinas; Oct. 29 – Dec.12, 2009 in the frame of the DFG Project "Combined study of optical active microtubes by photoluminescence and x-ray micro-diffraction"
Thomas Kroll	Centro Atómico Bariloche, Solid State Theory Group, Comisión Nacional de Energía Atómica, Bariloche, Argentinia, Feb. 16 – May 14, 2009 and Oct. 27- Nov. 26, 2009, joint research on FeAs
Martin Philipp	Saint-Gobain Paris, France, 13.09. - 10.10.2009, research stay
Franziska Wolny	Ohio State Univ. Columbus, Ohio, USA, 4.10. - 30.10.2009, guest stay for measurements
Miroslava Sakaliyska	North Carolina State Univ. Raleigh, USA, 01.02.09-30.04.09 research stay on Cu-Zn-Al alloys
Kumar Babu Surreddi	Univ. Ulsan Korea, 01.02.09-31.03.09, research stay on Al-based glassy powder
Prof. Dr. Jürgen Eckert	Univ. Vienna, Austria, 12.07.09 – 26.07.09 and 09.10.09 – 24.10.09, Guest lectures on Metastable Materials
Dr. Bernhard Holzapfel	Physics Dept. Shanghai Univ., China, 03.05.2009 - 26.05.2009, Vorlesung im Rahmen einer Gastprofessur
Dr. Jeffrey McCord	Institut Jean Lamour - Nancy-Univ. -CNRS Nancy, France, Cooperation on magnetic thin film analysis (Three one week stays in Feb., Sept. and Oct. 2009)

The Institute by numbers

Personnel

In 2009 the Leibniz Institute for Solid State and Material Research Dresden employed 523 staff members, including 106 doctorate students, 39 post docs, 21 guest scientists and 18 apprentices. The quote of female staff is 38 %. Furthermore, in 2009, the IFW hosted 49 fellows, that came with their own money to work at the institute. 47 diploma students worked at the IFW and 30 trainees did a practical course at the institute in 2009. The total number of guest scientists, above all was 135.

Financing

Total budget	44,449.7 k€
Thereof	
Federal States of Germany	14,837.4 k€
Free State of Saxony	14,837.4 k€
Third party funding spent	14,518.9 k€
Return on infrastructure, interest, royalties	256.0 k€
Third party funding	
by the DFG	2,724.0 k€
by the EC	3,822.5 k€
by the Federal States of Germany	1,501.6 k€
by Free State of Saxony	4,295.5 k€
by industry	1,358.7 k€
by foundations / others	816.6 k€
Total	14,518.9 k€

Expenditures

Remuneration costs	19,333.8 k€
Equipment, infrastructure and consumables	10,338.8 k€
Investment	14,776.1 k€
Total	44,448.7 k€

Patents

By 31 December 2009 the institute can boast of a total of 119 German and 198 patents registered abroad. In 2009 a total of 12 patent applications were registered.

Personnel according to organisational units 2009

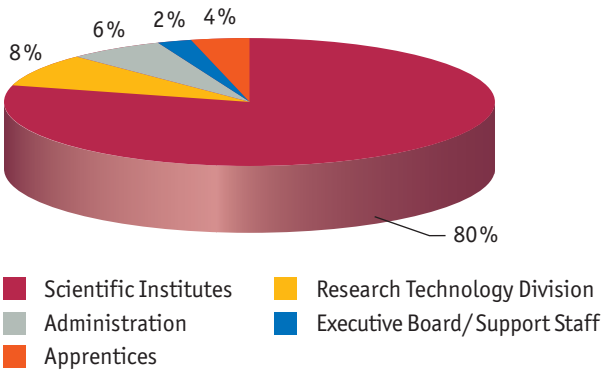

Board of trustees

Dr. Petra Karl, Saxon Ministry of Science and Art - Head -
Liane Horst, Federal Ministry of Education and Research
Prof. Dr. Konrad Samwer, Univ. Göttingen
Dr. Hans Rainer Hilzinger, Vacuumschmelze GmbH & Co Hanau

Scientific Advisory Board

Prof. Dr. Reiner Kirchheim, Univ. Göttingen, Germany -Head-
Prof. Dr. Gertrud Zwicknagl, TU Braunschweig, Germany
Dr. Hans Deppe, AMD Saxony Ltd & Co. KG Dresden, Germany
Prof. Dr. Dominique Givord, Laboratoire Louis Néel, Grenoble, France
Prof. Dr. Alan Lindsay Greer, Univ. of Cambridge, U.K.
Dr. Giselher Herzer, Vacuumschmelze GmbH & Co Hanau, Germany
Prof. Dr. Max Lagally, Univ. of Wisconsin-Madison, U.S.A.
Prof. Dr. Xavier Obradors Berenguer, Univ. Autònoma de Barcelona, Spain
Prof. Dr. George Sawatzky, Univ. of British Columbia Vancouver, Canada

IFW's Research Program 2010

1. Superconductivity and superconductors
1.1 Electronic structure and fundamentals
1.2 Superconducting materials
1 P1 Superconducting transport systems and magnetic bearings
1 P2 YBCO tape conductors
1 P3 Nanoscaled inhomogeneities in superconductors (Pakt 2009)

2. Magnetism and magnetic materials
2.1 Theoretical and experimental fundamentals
2.2 Magnetic materials
2.3 Magnetic microstructures
2.4 Phase equilibria and single crystal growth
2 P1 Pulsed high magnetic fields
2 P2 Magnetic shape memory alloys
2 P3 Energy efficient cooling with magnetocaloric materials (Pakt 2010)

3. Molecular nanostructures and molecular solids
3.1 Nanotubes and fullerenes
3.2 Conducting polymers and organic molecular solids
3.3 Molecular Magnets
3 P1 Manipulation of nanoscaled magnets (Pakt 2007)

4. Metastable alloys
4.1 Solidification and crystallization
4.2 Corrosion and hydrogen
4.3 Materials for sports
4.4 Bulk amorphous metals and composite materials
4.5 Lithium-ion batteries
4 P1 Cluster materials with competing properties (Pakt 2008)

5. Stress-driven architectures and phenomena
5.1 3D micro/nanoarchitectures
5.2 Quantum dots
5.3 Ferroic oxid films
5.4 SAW systems
5 P1 New multiferroic oxides (Pakt 2006)